Geomorphic Assessment of the Santa Clara River Watershed, Synthesis of the Lower and Upper Watershed Studies

Ventura and Los Angeles Counties, California

April 2011

Prepared for

Ventura County Watershed Protection District
Planning and Regulatory Division
800 S. Victoria Avenue
Ventura, CA 93009

Los Angeles County Department of Public Works
900 S. Fremont Avenue
Alhambra, CA 91803

U.S. Army Corps of Engineers
Los Angeles District
915 Wilshire Boulevard, Suite 1101
Los Angeles, CA 90017

Prepared by

Stillwater Sciences
2855 Telegraph Avenue, Suite 400
Berkeley, CA 94705

Stillwater Sciences

Contact:
Derek Booth, Ph.D., P.E., P.G.
Senior Geomorphologist
Stillwater Sciences
2855 Telegraph Avenue, Suite 400
Berkeley, CA 94705
(510) 848-8098
dbooth@stillwatersci.com
www.stillwatersci.com

Sergio Vargas, P.E.
Deputy Director
Ventura County Watershed Protection District
800 S. Victoria Avenue
Ventura, CA 93009
(805) 650-4077
sergio.vargas@ventura.org
www.vcwatershed.org

Cover photography (from top to bottom):

1. Eastward (upstream-facing) view of the upper Santa Clara River through Santa Clarita, January 2005 (courtesy of the California State Coastal Conservancy).
2. Northwestward (downstream-facing) view of eroding uplands in the Santa Susana Mountains (foreground) and floodplain agriculture in the lower Santa Clara River, upstream of Fillmore and near Piru, California, January 2005 (courtesy of the California State Coastal Conservancy) .
3. Westward (downstream-facing) view of the Santa Clara River and Sespe Creek (at right) in flood, January 2005 (courtesy of the California State Coastal Conservancy).
4. Northward (up-coast) view of the Santa Clara River estuary open at flood stage, January 2005 (courtesy of the California State Coastal Conservancy).

Acknowledgements:
This synthesis report draws primarily from two in-depth geomorphology studies we had the opportunity to conduct in the Santa Clara River watershed, for which we are grateful for the support and direction we received from all parties involved. For the lower Santa Clara River study, we acknowledge the California State Coastal Conservancy; for the upper Santa Clara River study and this synthesis report, we acknowledge the Feasibility Study participating agencies (listed alphabetically): Los Angeles County Department of Public Works, U.S. Army Corps of Engineers–Los Angeles District, and Ventura County Watershed Protection District. We also thank RBF Consulting for facilitating the contracting of this project.

This report additionally draws from other relevant studies we have recently conducted that focused on discrete portions of the Santa Clara River watershed. These studies include Santa Paula Creek (*Client: California Department of Fish and Game and Santa Paula Creek Fish Ladder Joint Power Authority*), San Francisquito Creek (*Client: Los Angeles Department of Water and Power*), Sespe Creek (*Client: Ventura County Watershed Protection District*), and the Santa Clara River Estuary (*Client: City of Ventura*).

Project team:
The project team for both the lower and upper watershed studies, including this synthesis report, was led by Drs. Peter Downs and Derek Booth as principal investigators. Technical analysis and written synthesis for this report were provided by geomorphologists Glen Leverich (Project Manager) and Scott Dusterhoff. GIS analyses and map production were performed by Sebastian Araya, Rafael Real de Asua, and Eric Panzer.

Suggested citation:
Stillwater Sciences. 2011. Geomorphic assessment of the Santa Clara River watershed: synthesis of the lower and upper watershed studies, Ventura and Los Angeles counties, California. Prepared by Stillwater Sciences, Berkeley, California for Ventura County Watershed Protection District, Los Angeles County Department of Public Works, and the U.S. Army Corps of Engineers–L.A. District.

Geomorphic Assessment of the Santa Clara River Watershed, Synthesis of the Lower and Upper Watershed Studies, Ventura and Los Angeles Counties, California

Executive Summary

This report presents a geomorphic assessment of key natural and anthropogenically driven processes that have physically shaped and continue to influence the Santa Clara River watershed. The overlying forces controlling geomorphic processes and resulting conditions in the watershed are examined over past, present, and future time frames, and at watershed-wide through sub-reach spatial scales. Detailed assessments of sediment sources and tributary sediment yields based on review of scientific literature and analyses of field data are presented, with an emphasis on the primary controls that have shaped the watershed and drainage network over time. We note how these controls (e.g., wildfire, land-cover/-use) themselves vary through time. An evaluation of mainstem river processes is presented that considered sediment sources, transport capacity, and morphological changes that will assist watershed managers with critical information when planning future management, development, and restoration actions.

This report functions as a synthesis of two comprehensive geomorphology studies recently completed by Stillwater Sciences:

- the *Assessment of Geomorphic Processes for the (lower) Santa Clara River Watershed* (2007a), prepared for the California State Coastal Conservancy as part of the Santa Clara River Parkway, Floodplain Restoration Feasibility Study; and
- the *Assessment of Geomorphic Processes for the Upper Santa Clara River Watershed* (2011a), prepared for the Santa Clara River Feasibility Study agencies.

This report also draws upon information produced from other recently completed studies in specific portions of the watershed, including Santa Paula Creek (Stillwater Sciences 2007b), San Francisquito Creek (Stillwater Sciences 2009), Sespe Creek (Stillwater Sciences 2010), and the Santa Clara River Estuary (Stillwater Sciences 2011b).

Key Findings of the Watershed Geomorphic Assessment

The Santa Clara River (SCR) watershed lies in the tectonically active, semi-arid Transverse Mountain ranges of southern California. As part of this setting, the 4,200 km^2 (1,620 mi^2) watershed is host to a diverse patchwork of landscape types, each composed of a unique suite of geomorphic processes controlled by regional and local forces—tectonics, climate, geology, topography, wildfires, and land use. Where rapid uplift rates, weak lithologies, extreme yet episodic rainfall, steep slopes, and intensive land practices coincide, sediment-production rates can be dramatically high. The variability in sediment-production rates across the watershed has a pronounced effect on the river morphology, which, at the reach scale, is further influenced by the degree of sediment connectivity with specific sediment sources and by the transport capacity along the channel. In general, the highest elevation areas of the watershed are host to the densest vegetation cover (mix of scrub/shrub and forest), receive the most rainfall (greatest average annual precipitation), and are composed of the oldest, most erosion-resistant bedrock lithologies (igneous, meta-igneous rocks [gneiss, granites]). In contrast, the lowland and foothill areas, typically those within and surrounding the Santa Clara River valley and Santa Clarita basin, are much drier, host a sparse vegetation cover (mix of grassland and scrub/shrub), and are composed of the youngest, weakest rock types. Wildfire frequency is greater in the hillslopes immediately

surrounding the Santa Clara River valley and Santa Clarita basin, which can further increase hillslope erosion rates especially when followed closely by large storm events.

Overall, the watershed sediment-production rate is approximately 8.2 million metric tonnes per year (t yr^{-1}), or 2,000 tonnes per square kilometer per year (t km^{-2} yr^{-1}) averaged across the entire watershed area. Because dams on Piru, Castaic, and Bouquet Canyon creeks intercept water and sediment from approximately one-third of the total SCR watershed area, the predicted watershed sediment-production rate is only 5.1 million t yr^{-1}, but accounting for dams only slightly decreases the calculated production rate per unit area to 1,900 t km^{-2} yr^{-1}. This value compares well to production rates estimated independently from rock uplift rates, landscape denudation rates, and our sediment dating analysis. The average annual watershed sediment yield estimated using flow and sediment discharge records at the former Montalvo stream gauge (USGS 11114000) is less than half of the calculated production rate, which is understandable given the substantial volumes of stored sediment in the lower reaches of the major tributaries and in the mainstem itself. Sediment storage in the mainstem SCR and downstream reaches of the major coarse sediment-delivering tributaries is also expressed by the results of the bed level change analysis, which demonstrates long-term aggradation throughout much of the upper Santa Clara River valley and Santa Clarita basin (i.e., reaches located between the Sespe Creek confluence and Soledad Canyon).

Sediment delivery from hillslopes and tributaries to the mainstem river are dominated by extreme events associated with large, infrequent storms. The episodic and extreme nature of discharge in the watershed results in the majority of sediment transport occurring in very short periods of time. For example, annual sediment discharge over the past several decades at the County line, Sespe Creek, and Montalvo stream gauges (i.e., representing the upper SCR, Sespe Creek, and lower SCR watersheds) is estimated to have varied by a factor of more than 50,000. The three water years that contain the highest annual maximum instantaneous discharge at the Montalvo gauge account for nearly half of the total sediment yield out of the SCR. In contrast, most years have an annual total sediment yield less than 10% of the average annual total sediment yield. Unlike humid-region rivers, moderate discharges of intermediate recurrence thus do not carry the majority of the sediment load—the "dominant discharge" for the SCR is the largest discharge on record.

Due to the episodic nature of the system, the active river channel has adjusted primarily in response to the largest flood events (as observed over the past century). Channel boundaries have only significantly expanded during the largest flows on record (e.g., 1928 St. Francis Dam failure, and the 1938, 1969, and 2005 floods). Of these events, the dam-break flood released down San Francisquito Canyon caused a massive scouring of the mainstem river and valley floor and, therefore, this event represents the most recent and significant channel-forming flow in those impacted reaches.

Throughout much of the river, active channel widths have been further reduced by floodplain encroachment and even river channel encroachment over the past several decades. These developments have stabilized channel boundaries along most of the channel reaches situated near the cities of Ventura and Santa Clarita. The flow constrictions associated with the width reductions have the potential to create an unstable condition in the river's morphology, which could result in accelerated channel bed level changes and/or bank failure and create additional hazards to the population and infrastructure. Partly in response to this dynamic, some lower tributary reaches have now been completely lined with concrete (e.g., Santa Paula, Bouquet Canyon), essentially locking those channels in place but impacting a range of natural geomorphic and ecological processes.

The long-term trends in the level of the channel bed indicate a general incisional pattern in the lowermost reaches (i.e., downstream of the Sespe Creek confluence) and an aggradational pattern in the reaches situated between the Sespe Creek confluence and Soledad Canyon, punctuated by notable occurrences of localized incision at the major tributary confluences (Sespe and Castaic Creeks, San Francisquito Canyon, South Fork SCR, and Bouquet Canyon). The greatest degree of incision is associated with those reaches having experienced instream aggregate mining activities within the past several decades. The overall aggradational and narrowing trends observed in the river's morphology suggest four possible influences: (1) recovery following the scouring flows released during the St. Francis Dam failure event (i.e., recovery to a quasi-equilibrium condition); (2) flow reductions from dam regulated subwatersheds; (3) increased sediment yields from past land-use activities, such as early settlement and ranching/agriculture activities, but not related to the urban developments that pave over land surfaces and intercept water and sediment delivered from upstream sources; and (4) floodplain and active channel encroachments by the growing urban footprint.

Historically, significant geomorphic change has also occurred within the Santa Clara River estuary, where the river discharges to the Santa Barbara Littoral Cell in the Pacific Ocean. Currently, flood flows within much of the lower river are constrained compared with historical conditions due to the network of flood-control levees. Overall, the high, episodic storm flows in the river will maintain a river mouth and estuary that will: (1) remain in a fixed location on the Oxnard Plain in comparison with historical conditions; (2) migrate within the current constrained active channel during high discharge events; and (3) supply sediment for mouth closure (near-shore deposition) and down-coast beach building (near-shore and offshore deposition). Although sediment loading to the SCR mouth is reduced compared with historical levels and sea level will continue to rise, hyperpycnal flow events—flows in which the river discharge is denser than ocean water due to high suspended sediment concentration, thereby causing the suspended sediment to pass through the estuary and nearshore zone, and be deposited on the offshore delta—still occur with sufficient frequency to maintain the mouth/estuary.

The growing urban footprints of Ventura, Oxnard, Santa Paula, Fillmore, Piru, Santa Clarita, and Acton are projected to further reduce sediment-production rates (and associated tributary sediment yields to the river channel) in the watershed and narrow the active river channel. However, this result does not indicate that continued development in the watershed will lessen the likelihood of geomorphic hazards from occurring (e.g., debris flows, landslides, flash floods, river bank erosion). These events have widely distributed sources, commonly with a watershed or subwatershed extent, that are unlikely to be significantly affected by human development in the watershed for the foreseeable future. Further expansion of the urban footprint (particularly in steep upland areas) will also place a greater proportion of the population and infrastructure closer to the sources and consequences of these hazards. Additionally, continued expansion and construction of hazard-mitigating infrastructure have the potential to result in understandable but largely unpredictable responses by the river and tributary morphology during large flood events. The ongoing acquisition and restoration of the river corridor, primarily along the lower river in Ventura County, should limit future growth upon the floodplain in those reaches, which will ideally provide: adequate space for the river to safely migrate; floodplain connectivity with the active river channel to attenuate flood flows; and conservation and/or recovery of the river's ecological functions.

Table of Contents

List of Tables

List of Figures

List of Appendices

LIST OF ACRONYMS AND ABBREVIATIONS

Acronym or abbreviation	Definition
ac	acres
CDF FRAP	California Department of Forestry and Fire Protection – Fire and Resource Assessment Program
CDFG	California Department of Fish and Game
CDP	Census Designated Place
CDWR	California Department of Water Resources
cfs	cubic feet per second
CGS	California Geological Survey
cm	centimeter
CNRA	California Natural Resources Agency
D_{16}	grain diameter at which 16% of the particle size distribution lies below; represents the "finer fraction"
D_{50}	median grain diameter, where 50% of the particle size distribution lies above and below
D_{84}	grain diameter at which 84% of the particle size distribution lies below; represents the "coarser fraction"
DEM	digital elevation model
ENSO	El Niño–Southern Oscillation
est.	established
FEMA	Federal Emergency Management Agency
ft	feet
g	grams
GIS	geographic information system
GLU	Geomorphic Landscape Unit
HEC-RAS	Hydrologic Engineering Center's River Analysis System
HSPF	Hydrologic Simulation Program–Fortran
I-5	Interstate 5
IfSAR	Interferometric Synthetic Aperture Radar
in	inch
kg	kilogram
km	kilometer
L	liter
LADPW	Los Angeles County Department of Public Works
LADWP	Los Angeles Department of Water and Power
LiDAR	Light Detection and Ranging
LSCR	Lower Santa Clara River
m	meter
M	(earthquake) Magnitude
mi	mile

Acronym or abbreviation	Definition
mm	millimeter
MSL	mean sea level
NAIP	National Agriculture Imagery Program
Q_2	2-year flow
Q_{100}	100-year flow
s	second
SAF	San Andreas Fault
SCR	Santa Clara River
SCRE	Santa Clara River Estuary
SNPCR	Saugus-Newhall Production-Consumption Region
t	tonnes (metric)
UCSB	University of California at Santa Barbara
USACE (Corps)	United States Army Corps of Engineers
USCR	Upper Santa Clara River
USFS	United States Forest Service
USGS	United States Geological Survey
VCWPD	Ventura County Watershed Protection District
WY	water year
yd	yard
yr	year

Notes:
[1] Geologic rock unit symbology is defined in Appendix A.
[2] Symbology used in mathematical equations is defined in the text adjacent to the associated equation(s).

GLOSSARY OF KEY TERMS

Keyword	Definition
abrasion	The process of mechanical wearing, grinding, scraping, or rubbing away of rock (or sediment) surfaces by friction or impact, typically in a stream channel as sediment transport is occurring.
aggradation	The process involving the deposition of sediment on the landscape, but most commonly in a stream channel.
alluvial	Having originated through the transport by and deposition from running water.
bedload	Sediment transporting along the streambed by rolling, sliding, and saltating (jumping). Includes coarser grains larger than 0.0625 mm in diameter, such as sand, gravel, cobbles, and boulders; however, sand-sized particles can often be transported as suspended bed material load in higher energy flows, thus making them part of the bed material load.
bed material load	Composed of sediments transported by the river that contains material derived from the channel bed; all bedload and the proportion of the suspended load that is represented in the bed sediments.
boulders	Substrate particles greater than 256 mm in diameter. Often subclassified as small (256-1,024 mm) and large (>1,024 mm) boulders.
bulk density	The mass of a material (rock or sediments) divided by the total volume they occupy [in units of mass per length cubed, i.e., M/L^3].
channel	Natural or artificial waterway of perceptible extent that periodically or continuously contains moving water.
channel migration	Lateral movement of the active channel, usually in response to large flow events.
bankfull discharge	Discharge that just overtops a river or stream channel banks onto the adjacent floodplain. Bankfull discharges commonly occur approximately every 1 to 2 years for most humid-region rivers of the world, with a median recurrence interval of about 1.5 years (~Q_2) and is generally considered to be the primary channel-forming discharge in humid environments. This common assumption does not apply in the semi-arid SCR watershed.
cobble	Substrate particles 64–256 mm in diameter. Often subclassified as small (64–128 mm) and large (128–256 mm) cobble.
cosmogenic nuclides	Characteristic atomic isotopes produced in the minerals (i.e., quartz) of soil and rock materials at the landscape's surface that can be measured to estimate landscape erosion rates.
denudation	The sum of the processes that result in the wearing away or the progressive lowering of the Earth's surface by various natural agencies, including weathering, erosion, mass wasting, and transportation.
deposition	The process whereby Earth materials accumulate, which is commonly achieved by the mechanical settling of sediment from suspension in water or the accumulation of coarse materials as delivered by ice, water, or wind.
discharge (stream)	The volume of flow passing a stream cross section in a unit of time [unit of L^3/T].
erosion	The process whereby Earth materials are loosened, dissolved, or worn away, and simultaneously transported away from the material source by natural agencies, such as abrasion, solution, transportation, and weathering, but is most commonly achieved mechanically by ice, water, or wind, or even biogenic agents (e.g., tree throw, gopher burrowing).
geographic information system (GIS)	A computer system capable of storing and manipulating spatial data. A geographic information system has four major components: a data input subsystem, a data storage and retrieval subsystem, a data manipulation and analysis subsystem, and a data reporting subsystem.
gravel	Substrate particles 2–64 mm in diameter.

Keyword	Definition
hyperpycnal flows	Flows in which the river discharge is denser than ocean water due to high suspended sediment concentration, thereby causing the suspended sediment to pass through the river's mouth and be deposited on the offshore delta.
hypopycnal flows	Flows in which the river discharge is less dense than ocean water, thereby causing the formation of near-shore deltas.
incision	The process whereby a channel (stream or trench) vertically erodes downward resulting in a lower bed elevation.
littoral cell	Discrete coastal regions that can be considered closed systems within which sediment is transported.
riparian vegetation	Vegetation growing on or near the banks of a stream or other body of water in soils that exhibit some wetness characteristics during some portion of the growing season.
sand	Substrate particles 0.062–2 mm in diameter.
sediment	Fragments of rock, soil, and organic material transported and deposited in beds by wind, water, or other natural phenomena.
sediment delivery	The process whereby sediment is transported from a production source to a given location in the drainage network. The *sediment delivery rate* is the total delivery over a given time period; usually reported in mass per year [*M/T*].
sediment delivery ratio	Ratio of sediment production rate to sediment delivery rate. High delivery ratios indicate that production closely equals delivery, and low delivery ratios indicate that production is much lower than delivery, usually due to storage.
sediment discharge	The quantity of sediment passing a stream cross section in a unit of time (i.e., volume or mass per unit of time).
sediment production rate	The total amount of sediment eroded from the landscape surface over a given time period; usually reported in mass per year [*M/T*].
sediment storage	The process by which sediment is delivered to a location and is then stored there for a period of time (e.g., days to millennium, or even beyond).
sediment transport	The process involving the movement of sediment.
sediment transport capacity	The maximum load a stream channel can transport.
sediment yield	The total amount of sediment transported past a point over a given time period; usually reported in mass per year [*M/T*].
silt	Substrate particles 0.004–0.062 mm in diameter.
stream power	The measure of the river's ability to transport sediment. *Unit stream power*, or stream power per unit area of the channel, is the product of the shear stress and flow velocity.
suspended load	Sediment that transports continuously in suspension within the water column. Under most flow conditions, commonly comprises particles finer than about 0.0625 mm (i.e., silt and clay-sized particles), but can also include coarser sediment (e.g., sand) in higher energy flows.
thalweg	A longitudinal line following the deepest points along the steambed.
water surface slope	The ratio of vertical drop of the water surface per longitudinal distance, as measured along the thalweg at any given discharge.
water year (WY)	The 12-month period for any given year from October 1 through September 30.

General information sources used here:

Bagnold 1966
MacArthur and Hall 2008
Neuendorf et al. 2005
Ritter et al. 2002
Selby 1993

UNIT CONVERSION FACTORS

Most values presented in this report are reported in the metric system. This table presents conversion factors of the commonly used metric units to English system units.

Metric	Multiply by	English
mm (millimeters)	3.937×10^{-2}	in (inches)
m (meters)	3.281	ft (feet)
km (kilometers)	6.214×10^{-1}	mi (mile)
km^2 (square kilometers)	3.861×10^{-1}	mi^2 (square miles)
m^3 (cubic meters)	3.531×10^{1}	ft^3 (cubic feet)
t (tonnes)	1.102	tn (tons)
t km^{-2} (tonnes per square kilometer)	2.855	tn mi^{-2} (tons per square mile)

1 INTRODUCTION

Geomorphology is the study of landforms and the processes that modify them over time, encompassing spatial and temporal scales that range from the instantaneous motion of individual sand grains in rivers during floods to the uplift of entire mountain ranges over millions of years. It synthesizes information about the internal geologic processes that create topography and the external surface processes that erode and move material across the landscape.

The goals and objectives of this project, and the background conditions of the Santa Clara River watershed, are presented in this chapter as an introduction to this watershed assessment of geomorphic processes.

1.1 Project Goals and Objectives

This geomorphic assessment investigates the key natural and anthropogenically driven processes that have physically shaped and continue to influence the Santa Clara River (SCR) watershed. The watershed is nearly evenly contained within the counties of Ventura and Los Angeles (Figure 1-1). Because the river flows east to west toward the Pacific Ocean through these two counties, the watershed is separated into two politically designated halves that coincide with the two counties:

- the upper Santa Clara River (USCR) watershed, which represents the eastern half of the entire watershed and is contained within Los Angeles County, from the County line (between the town of Piru and city of Santa Clarita) up towards the town of Acton; and
- the lower Santa Clara River (LSCR) watershed, which represents the western half of the entire watershed and is contained within Ventura County, from the coast near the city of Ventura up to the County line.

This report functions as a synthesis of two comprehensive geomorphology studies recently completed by Stillwater Sciences:

- the *Assessment of Geomorphic Processes for the (lower) Santa Clara River Watershed* (2007a), prepared for the California State Coastal Conservancy as part of the Santa Clara River Parkway, Floodplain Restoration Feasibility Study; and
- the *Assessment of Geomorphic Processes for the Upper Santa Clara River Watershed* (2011a), prepared for the Santa Clara River Feasibility Study agencies.

This report also draws upon information produced from other recently completed studies in specific portions of the watershed, including Santa Paula Creek (Stillwater Sciences 2007b), San Francisquito Creek (Stillwater Sciences 2009), Sespe Creek (Stillwater Sciences 2010), and the Santa Clara River Estuary (Stillwater Sciences 2011b).

Overall, this synthesis report has been developed to assist the Santa Clara River Feasibility Study agencies—Ventura County Watershed Protection District (VCWPD), Los Angeles County Department of Public Works (LADPW), and the U. S. Army Corps of Engineers–Los Angeles District (USACE-LA)—in identifying opportunities and constraints associated with protecting, managing, and restoring lands as part of the Feasibility Study's overall efforts. A comprehensive overview of current and historical watershed-wide geomorphic processes, both natural and anthropogenically altered, and their links to in-channel and floodplain factors are presented here. Evaluation and summary of expected future geomorphology conditions within the developed and currently undeveloped areas of the watershed are also presented.

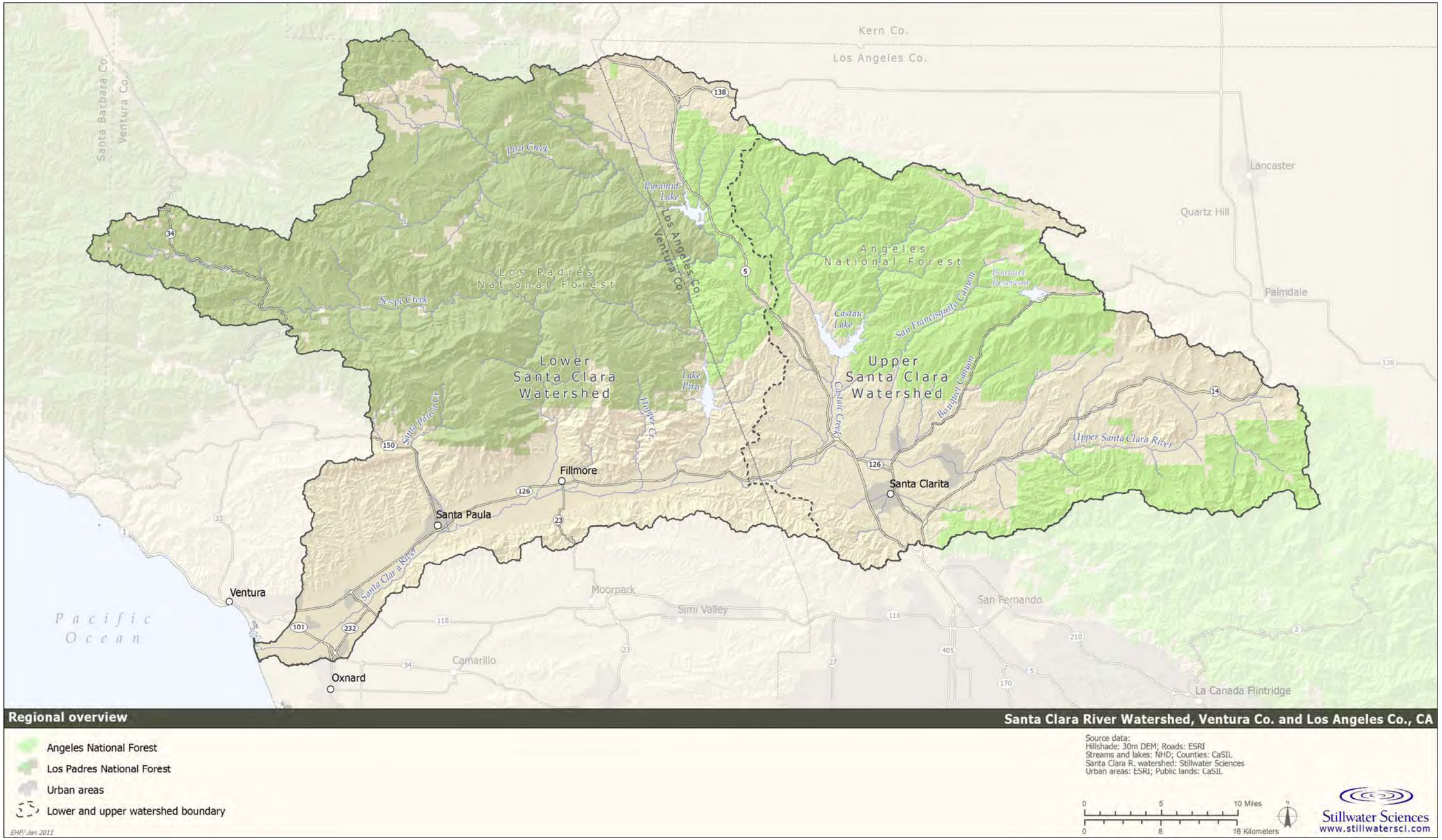

Figure 1-1. The Santa Clara River watershed and vicinity.

Although the specific study questions of the two previously completed geomorphology studies were slightly different, both studies were developed with similar goals in mind:

1. Provide a synthesis of existing and recently collected data to describe channel morphologic change and watershed sediment transport dynamics under current conditions, driven by both natural and anthropogenic controls (e.g., storm events and land-use change, respectively); and
2. Forecast probable future geomorphic conditions within the mainstem and tributary channels throughout the watershed to the extent permitted by available data.

Specific objectives of both studies were:

1. Characterization of geomorphic processes and channel response along the river, relating observations to the dynamics of channel change in a dryland river setting, including the impact of tectonic activity, storm events, and wildfire;
2. Characterization of sediment delivery and channel adjustment attributable to past and present human activities, including channel modification associated with urban development; and
3. Assessment of probable future hazards and assets related to geomorphology in the watershed, to better understand the challenges and opportunities facing sustainable approaches to river management.

For both studies, and again presented here, watershed geomorphic processes in tributaries and along the mainstem of the SCR have been examined from both a current and a historic perspective to produce a comprehensive understanding of the geomorphic processes controlling channel migration and the production, delivery, storage, and transport of sediment within the watershed. Ultimately this work will assist the Feasibility Study project partners to identify management strategies that meet the goal of maintaining and restoring geomorphic processes to protect vulnerable floodplain infrastructure and sustain desired ecologic functions throughout the watershed.

In geographic scope, the assessment presented here encompasses the entire SCR watershed. The Feasibility Study area similarly includes the entire watershed, but with greater focus on the mainstem river and its major tributaries. Specifically, the area of interest of the Feasibility Study includes the developed, downstream reaches of major tributaries designated by the USACE and Federal Emergency Management Agency (FEMA), which are listed in Table 1-1 and shown in Figure 1-2. Although this synthesis report does not make an attempt to present information on each of these reaches, they are considered cumulatively from a watershed-wide perspective. Particular attention, however, is paid towards the mainstem river reaches and to the more significant tributaries, such as Santa Paula, Sespe, Hopper, Piru, Castaic creeks; San Franciscquito and Bouquet canyons; and the South Fork Santa Clara River.

Table 1-1. Feasibility Study reaches of the Santa Clara River (SCR) watershed. [a]

Feasibility Study stream name [a]	Feasibility Study reach system [b]		Total drainage area (total area below dams) [c]		Total stream length (total length below dams, if present) [d]	
	USACE study reach	FEMA study reach	km^2	mi^2	km	mi
Soledad Canyon	X		23.2	9.0	8.8	5.5
Kentucky Springs	X		23.5	9.1	11.6	7.3
Aliso Canyon	X		63.2	24.4	15.5	9.7
Gleason Canyon			15.5	6.0	9.5	5.9
Trade Post Canyon	X		6.7	2.6	5.0	3.6
Acton Canyon	X	X	54.4	21.0	9.3	5.8
Escondido Creek	X	X	24.6	9.5	10.2	6.4
Red Rover Mine	X		5.7	2.2	5.7	3.5
Acton Canyon 2	X		6.5	2.5	5.0	3.1
Hughes Canyon			8.0	3.1	4.2	2.7
Young Canyon			7.3	2.8	5.1	3.2
Agua Dulce Canyon	X	X	76.1	29.4	12.4	7.7
Bear Canyon			15.1	5.8	8.0	5.0
Tick Canyon	X		14.8	5.7	8.8	5.5
Oak Springs Canyon	X		14.6	5.7	8.7	5.4
Sand Canyon	X		33.0	12.7	13.8	8.6
Iron Canyon	X		6.9	2.7	7.9	4.9
Mint Canyon	X		75.8	29.3	22.4	14.0
Bouquet Canyon	X	X	180.4 (145.2)	69.7 (56.0)	34.6 (26.1)	21.6 (16.3)
Dry Canyon	X		19.7	7.6	16.5	10.3
Haskell Canyon	X	X	28.4	11.0	14.4	9.0
Plum Canyon	X		8.2	3.2	6.5	4.1
Vasquez Canyon	X		11.1	4.3	7.9	4.9
Texas Canyon	X		28.2	10.9	12.8	8.0
So. Fork SCR	X	X	116.2	44.9	7.3	4.6
Pico Canyon	X	X	17.6	6.8	8.4	5.3
Lyon Canyon	X		3.6	1.4	5.3	3.3
Gavin Canyon	X		29.4	11.4	5.5	3.5
Towsley Canyon	X		14.9	5.8	5.8	3.6
Placerita Creek	X		23.1	8.9	11.8	7.4
Newhall Creek		X	21.3	8.2	4.8	3.0
San Francisquito Cyn	X	X	134.6	52.0	34.9	21.8
Lion Canyon	X		2.2	0.8	2.5	1.5

Feasibility Study stream name [a]	Feasibility Study reach system [b]		Total drainage area (total area below dams) [c]		Total stream length (total length below dams, if present) [d]	
	USACE study reach	FEMA study reach	km^2	mi^2	km	mi
Castaic Creek	x		524.6 (122.6)	202.5 (47.3)	39.5 (12.5)	24.7 (7.8)
Hasley Canyon	x		20.7	8.0	9.4	5.9
Violin Canyon 1	x		15.1	5.8	14.2	8.9
Violin Canyon 2 (Marple Canyon)	x		9.6	3.7	8.3	5.2
Long Canyon	x		4.0	1.5	5.9	3.7
S. M. Chiquito Cyn	x		12.4	4.8	7.9	5.0
S. M. Grande Canyon	x		8.6	3.3	4.6	2.9
Potrero Canyon	x		11.6	4.5	8.6	5.4
Upper Santa Clara River [e]	**x**	**x**	**1,679 (1,242)**	**648 (479)**	**62.4**	**39.1**
Piru Creek	x		1,132 (39.3)	437 (15.2)	108 (11.4)	67.2 (7.1)
Real Wash	x		3.8	1.5	2.8	1.8
Edwards Canyon	x		1.2	0.5	2.9	1.8
Hopper Canyon		x	62.0	23.9	19.3	12.0
Pole Creek		x	27.7	10.7	10.6	6.6
Sespe Creek		x	673	260	97.0	60.3
Bardsdale Ditch	x		11.2	4.3	2.5	1.6
Bear Creek	x		3.6	1.4	3.8	2.4
Reimer Ditch	x		9.9	3.8	4.7	2.9
O'Leary Creek	x		4.6	1.8	3.6	2.3
Balcom Creek	x		9.2	3.6	3.5	2.2
Timber Canyon	x		4.5	1.8	6.2	3.8
Santa Paula Creek	x		117.1	45.2	22.4	13.9
Sisar Creek	x		29.7	11.5	8.7	5.4
Fagan Barranca	x		9.0	3.5	7.1	4.4
Peck Road Drain	x		2.5	1.0	2.6	1.6
Adams Barranca	x		22.9	8.9	12.2	7.6
Haines Barranca	x		9.1	3.5	6.2	3.8
Briggs / Cummings Road Drains	x		8.7	3.4	4.0	2.5
Todd Baranca	x		24.6	9.5	14.0	8.7
Ellsworth Barranca	x		37.1	14.3	12.7	7.9
Wason (Franklin) Barranca	x		9.7	3.7	5.1	3.2
Brown Barranca	x		12.0	4.6	6.3	3.9
Sudden Barranca	x		3.8	1.5	4.3	2.7
Clark Barranca	x		3.4	1.3	4.8	3.0
Harmon Barranca	x		11.6	4.5	6.7	4.2

Feasibility Study stream name [a]	Feasibility Study reach system [b]		Total drainage area (total area below dams) [c]		Total stream length (total length below dams, if present) [d]	
	USACE study reach	FEMA study reach	km^2	mi^2	km	mi
Lower Santa Clara River [f, g]	X	X	**2,526 (1,433)**	**975 (553)**	**69.9**	**43.4**
Entire Santa Clara River	**X**	**X**	**4,204 (2,675)**	**1,623 (1,033)**	**132.3**	**82.5**

[a] Streams listed in order of upstream to downstream position along the SCR starting at the headwaters in the eastern end of the watershed. Stream names that are indented and printed in italics are tributaries to the stream listed above (e.g., Escondido Creek is a tributary to Acton Canyon). "S.M." is abbreviated for San Martinez. "So. Fork SCR" is abbreviated for South Fork Santa Clara River.

[b] Checkmark indicates that the stream is part of the respective USACE and/or FEMA Feasibility Study reach system.

[c] Drainage area derived in a GIS using a USGS 10m Digital Elevation Model (DEM). Area includes the total drainage area of any listed stream watershed.

[d] Stream length derived in a GIS using a USGS 10m DEM-generated stream network with a contributing area threshold of 0.04 km^2.

[e] As measured along the USCR course between the retired USGS stream gauge station (11108500) at the Los Angeles-Ventura County line and the confluence with Kentucky Springs Canyon.

[f] As measured along the LSCR course between the river mouth on the coast and the retired USGS stream gauge station (11108500) at the Los Angeles-Ventura County line.

[g] The following Feasibility Study reaches in the LSCR watershed are not listed here because generation of their drainage area in a GIS did not yield reliable results given their relatively small size and unusual function (e.g., drainage ditches): Fairview Road Drain, Basolo Ditch, Grimes Canyon Wash, Orcutt Canyon, El Rio Drain, and Victoria/Patterson Drain.

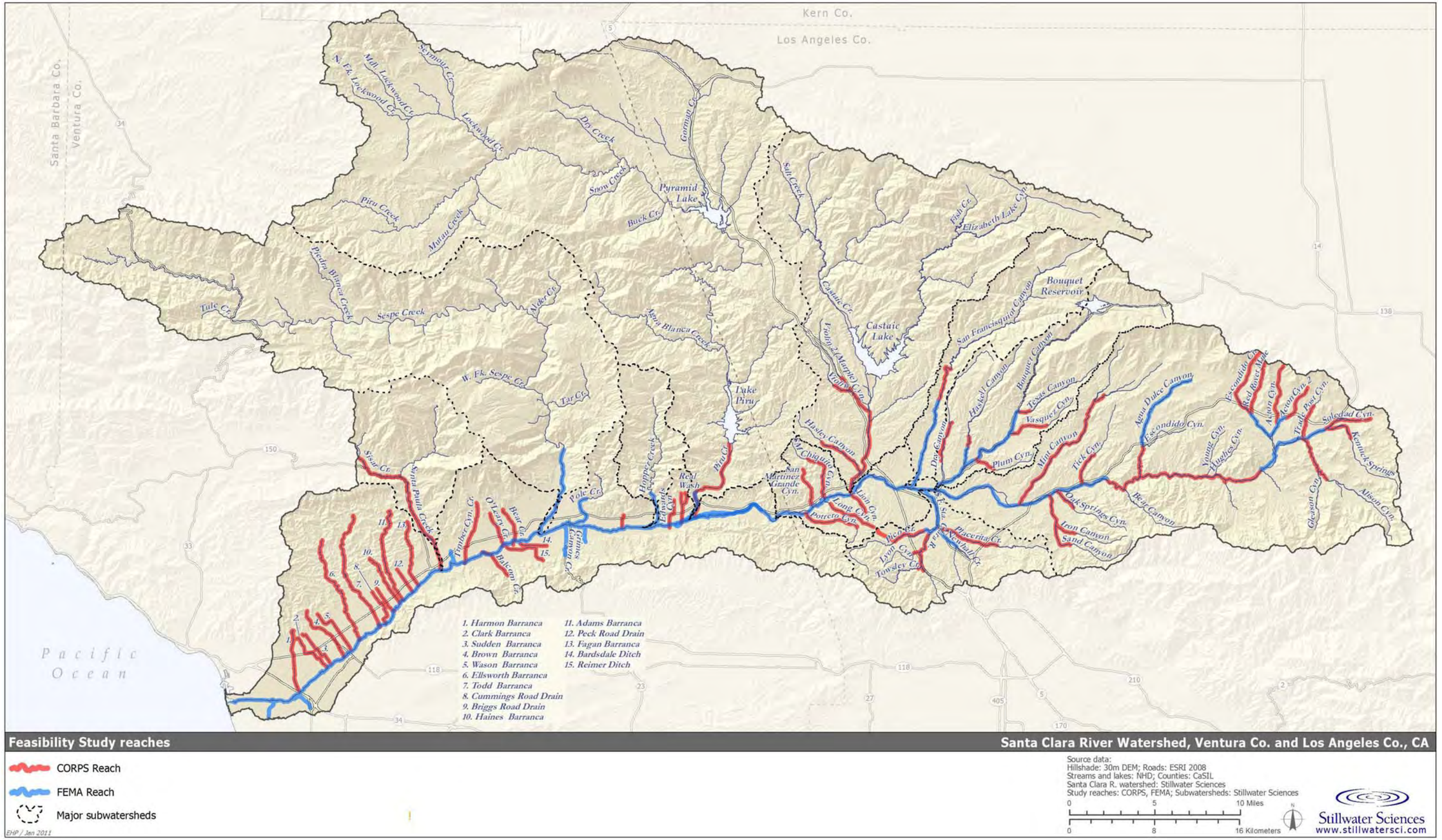

Figure 1-2. Feasibility Study and other mainstem river and tributary reaches and their contributing areas in the SCR watershed.

1.2 Regional Setting and Watershed Characteristics

Flowing 132 km (83 mi) from the northwestern San Gabriel Mountains to the coast, the entire Santa Clara River drains approximately 4,204 km^2 (1,623 mi^2)—one of the largest watersheds on the southern California coast. Elevations here range from sea level to about 2,700 m (8,900 ft) (Figure 1-3). The river is fed by numerous named stream tributaries as it flows westward from the broad Acton Basin, through a confined canyon (Soledad Canyon), through the broad Santa Clarita Valley (the Santa Clarita Basin), and finally through the Santa Clara River Valley that eventually opens out across the expansive Oxnard Plain before flowing into the Pacific Ocean.

The SCR as a whole remains in a relatively natural state in comparison with other large, coastal southern California rivers (e.g., Simons, Li & Associates 1983, 1987; AMEC 2005; Kennedy/Jenks 2008). For example, on the Los Angeles, Santa Ana, and San Gabriel rivers, flood protection and urban development modifications have been so extensive that natural physical processes have become largely ineffective at maintaining a dynamic river system. Although recent developments near the urban centers of Ventura, Oxnard, Santa Paula, Fillmore, Santa Clarita, and Acton have encroached upon the river's floodplain, and even on the active channel bed in some instances, the mainstem SCR retains many of the attributes of more natural coastal southern California rivers, including a sand-gravel-bedded, braided channel (in most areas) and broad floodplain terraces. The downstream reaches of several major tributaries, however, have been highly modified by channelization efforts where these water courses flow through the urban areas (e.g., Santa Paula Creek, South Fork SCR, and Bouquet and Mint canyons). The river and its tributaries experience high annual flow variability, multi-year droughts, and extreme seasonal flooding, which together result in a highly dynamic alluvial system.

For this assessment, the SCR watershed is divided into four morphologically similar areas. The geomorphic regions are distinguished primarily by valley width and, accordingly, general sediment delivery and transport characteristics inherent within them. Starting in the headwaters of the watershed, the *Acton Basin* region encompasses the Acton depositional basin and includes all areas of the upper watershed draining to the river downstream to a point just above the river's transition to the canyon reaches. This region includes the tributary streams of Acton and Aliso canyons. The *Soledad Canyon* region is essentially defined by those areas of the watershed that drain to the highly confined canyon reaches, or Soledad Canyon. Agua Dulce Canyon is the primary tributary flowing to the river in this region. The *Santa Clarita Basin* region is larger as it includes the drainages of all USCR tributaries feeding the river in the Santa Clarita Valley, or Santa Clarita Basin as is referred to herein. The USCR watershed's largest tributaries, including Castaic Creek, South Fork Santa Clara River (South Fork SCR), and San Francisquito, Bouquet, and Mint canyons, all join the river in this broad depositional basin.

The *Santa Clara River Valley* region is the largest as it essentially constitutes the entire LSCR watershed along its valley floor and downstream across the Oxnard Plain. This region can be further subdivided into two hydrogeomorphic-specific halves that are separated at the confluence with Sespe Creek—the largest, un-regulated tributary—at the town of Fillmore, where the upstream half is referred to here as the *Upper Santa Clara River Valley* and the downstream half is referred to as the *Lower Santa Clara River Valley*.

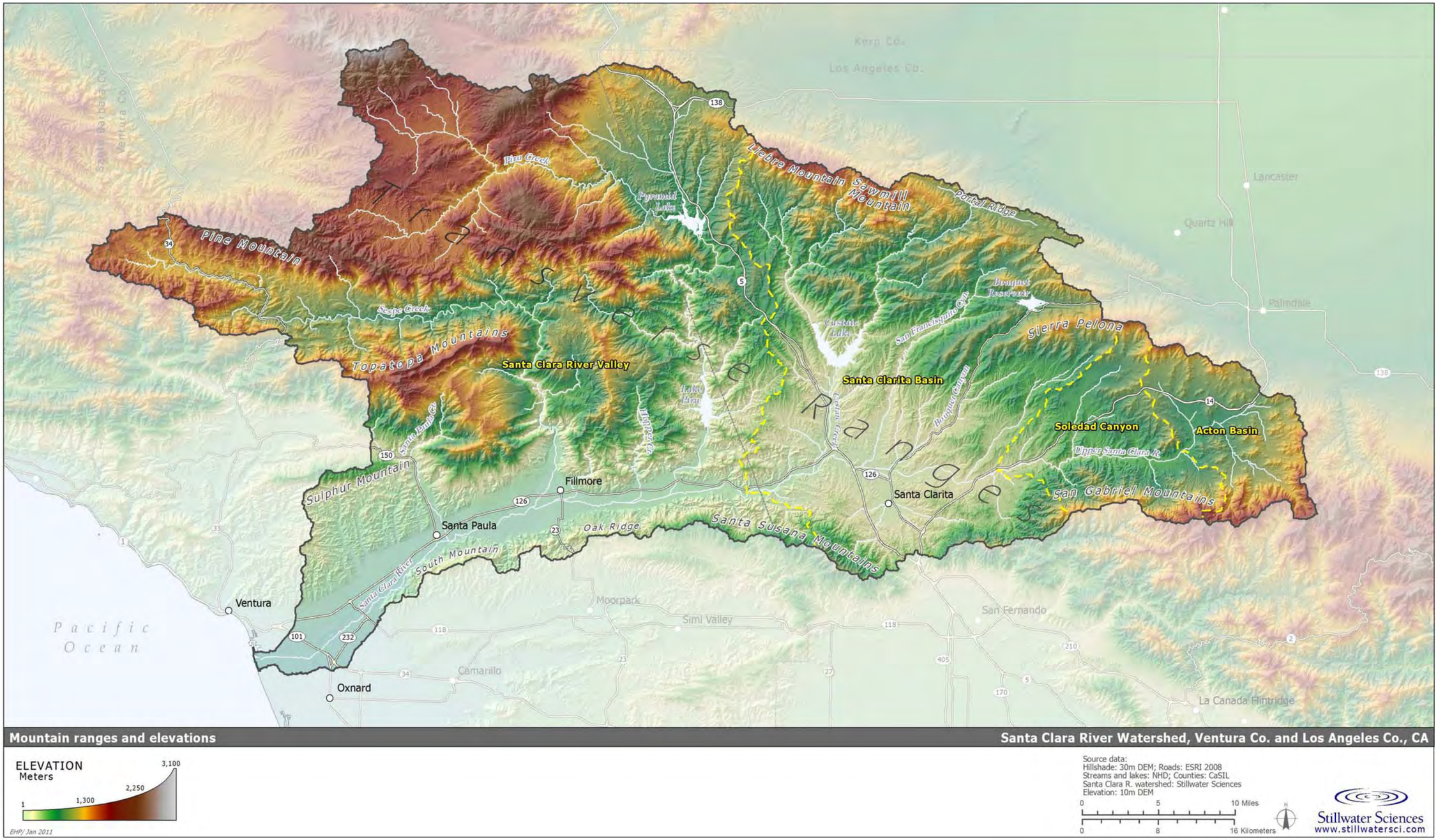

Figure 1-3. Mountain ranges and elevations of the SCR watershed.

1.2.1 Geology and tectonic setting

The SCR watershed is located within a distinctive geologic province of California known as the Transverse Ranges. Unlike the Coast Ranges to the north and the Peninsular Ranges to the south, both of whose major ridges and intervening valleys trend generally northwest–southeast, the Transverse Ranges are oriented almost exactly east–west and form a marked disruption to the overall grain of California topography. The SCR flows between the east–west trending mountains of this province: the Transverse Mountains on the north and San Gabriel and Santa Susana mountains (and South Mountain) on the south.

The regional tectonic activity of California over the last 6 million years has created this unusual topographic and tectonic setting. Positioned immediately adjacent to the northeastern boundary of the watershed (near the towns of Lake Hughes and Elizabeth Lake), the 1,000-km-long (600-mi-long) San Andreas Fault (SAF) separates the northwest-moving Pacific plate from the (relatively) stationary North American plate (Figure 1-4). Where the SAF is straight, these plates slide past each other as a "transform plate boundary," with either continuous motion (at rates of a few centimeters per year) or stick–slip motion where movement is episodic (and often expressed as earthquakes when it occurs) (Shen et al. 1996). The SAF is deflected from its straight trend, however, at its intersection with a northeast–southwest trending cross-cutting fault—the Garlock Fault—about 50 km south of Bakersfield. Where the SAF is bent, the Pacific and North American plates cannot simply slip past each other. Because the underlying plate motion continues, the north-migrating rocks of the Pacific plate (which include those of the USCR watershed) "pile up" in the region south of the San Andreas Fault's bend. The crustal shortening that results from this underlying plate movement provides an ideal setting for rapid rates of landscape uplift.

The drainage network pattern exhibited in the watershed is strongly influenced by geologic structure and the location of active faults. Through the reaches of Soledad Canyon, the river follows the axis of the west-trending Soledad Fault before eventually following the San Gabriel (in part) and Holser faults in the Santa Clarita Basin. The river then flows parallel to and between the San Cayetano and Oak Ridge faults through the Santa Clara River Valley. Several of the watershed's major tributaries follow (and whose valleys were likely formed by) significant faults, such as Mint, Pelona (Bouquet), and San Francisquito (not shown in Figure 1-4, but this fault is mapped by Dibblee [1997: Green Valley quadrangle] as following middle San Francisquito Canyon along the north side of the Pelona Schist unit), San Gabriel (upper Piru), and Pine Mtn/Santa Ynez (upper Sespe).

Persistent regional geologic instability over the last 28 million years has exposed a wide variety of highly deformed, fractured, and faulted rock types across the entire SCR watershed (Yeats 1981, Rockwell et al. 1984, Rockwell 1988). The watershed is dominated by a mixture of geologically old igneous and metamorphic rocks, including granite (units "Kg" and "Pzg3" in Figure 1-4), anorthosite ("Ya"), and schist ("uMze"), and younger sedimentary rocks, ranging from claystone to sandstone and conglomerate. The former (older) bedrock group is primarily situated in the high-relief uplands of the northern and eastern portions of the watershed, while the latter (younger) group is concentrated in and around the Santa Clarita Basin and the Santa Clara River Valley, which is understandable considering that several of these sedimentary units have recently formed in these depositional basins over the past several million years.

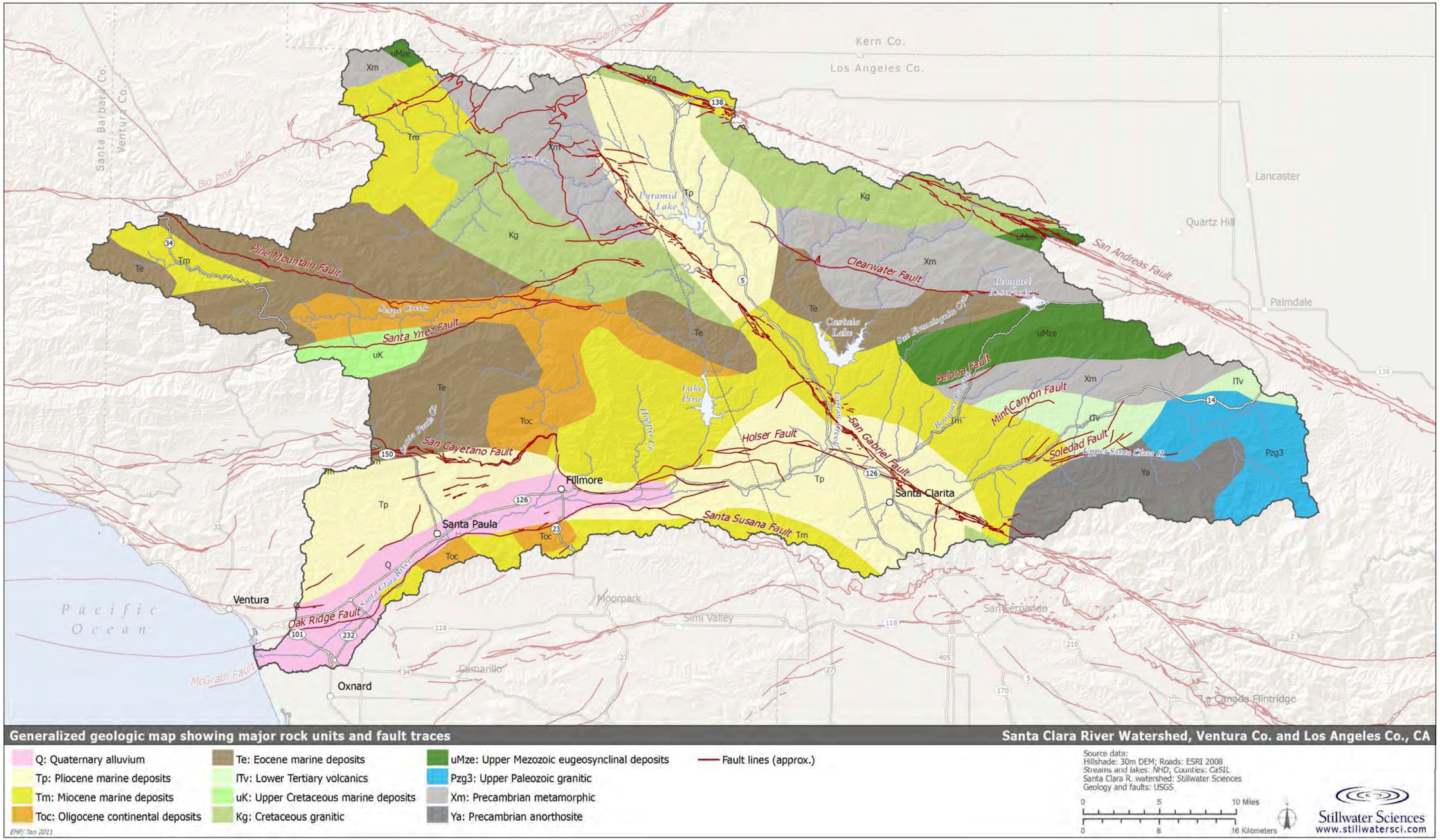

Figure 1-4. Generalized geologic map showing major rock units and fault traces in the SCR watershed.

Fractures, deformation, and faulting contribute to high bedrock erodibility throughout the SCR watershed. For example, the sedimentary bedrock units immediately bordering the Santa Clarita Basin and Santa Clara River Valley are often poorly consolidated, intensely folded, and have steeply tilted beds, making them susceptible to landsliding (e.g., Harp and Jibson 1996) and erosion by dry raveling (Scott and Williams 1978). For example, the Pico Formation siltstone has been found to have considerably high erosion rates (Stillwater Sciences 2011a; mapped here in Figure 1-4 as part of unit "Tm"). Even areas underlain by granite, gneiss, and schist (which are normally relatively resistant to erosion) have been described as being highly erodible (e.g., Scott and Williams 1978, Wells et al. 1987) due to extensive deformation and fracturing, which is especially true of the Pelona Schist bedrock unit ("ps") that trends across much of the USCR through San Francisquito and Bouquet canyons (Spotila et al. 2002).

Additional explanation of tectonic activity and uplift rates are presented in Section 3.3.1. More detailed geologic maps (i.e., 1:24,000 scale) with comprehensive explanations are presented in the other SCR watershed reports (e.g., Stillwater Sciences 2007b, 2009, 2010, and 2011a).

1.2.2 Climate and hydrology

Coastal watersheds of southern California function according to a semi-arid, two-season Mediterranean-type climate, with cool wet winters and dry warm-to-hot summers. Rainfall and air moisture both tend to decrease with increasing distance from the coast. Within the SCR watershed, proximity to the Pacific Ocean moderates both seasonal and diurnal temperatures. Most precipitation occurs between November and March, with precipitation varying significantly throughout the watershed and most strongly influenced by elevation and distance from the Pacific Ocean (Figure 1-5). That is, the wettest areas are found along the high-relief mountain ranges on the west, north, and south sides of the watershed, while the driest areas are found in the lowlands of the Santa Clarita and Acton basins. Overall, average annual precipitation in the watershed has ranged between 9 and 45 inches (23–114 mm) during the years 1971–2000; the wettest areas are in the headwaters of Sespe Creek. At higher elevations, some winter precipitation occasionally falls as snow.

Periodicity in the pattern of the wet/dry years in southern California is correlated to the El Niño–Southern Oscillation (ENSO) climatic phenomenon. ENSO is characterized by warming and cooling cycles in the waters of the eastern equatorial Pacific Ocean, which typically have a 1–1.5 year duration and a 3–8 year recurrence interval (NWS CPC 2010). In southern California, ENSO years are characterized by relatively high rainfall intensities, with rivers and streams (such as those in the SCR watershed) exhibiting higher annual peak flow magnitudes than they do in non-ENSO years. The most recent ENSO event occurred in water year (WY) 2010 (NWS CPC 2010). Additional details on the effects of ENSO events on flow magnitude and sediment delivery rates are discussed in Section 4.1.3.

The climatic and hydrologic characteristics of the SCR watershed generally produce an intermittent flow regime along the majority of the mainstem USCR and its tributaries; ephemeral streams are also common throughout the drainage network. Consistent with other rivers in the region, the watershed experiences highly variable annual rainfall and peak flows. During the rainy season, flows can increase, peak, and subside rapidly in response to high intensity rainfall (the term "flashy" is commonly used to describe this characteristic), with the potential for severe flooding under saturated or near-saturated watershed conditions. Between winter rainfall events in wet years, the river may exhibit continuous baseflow to the ocean from residual watershed discharge; in dry years, flow may be intermittent. Generally, flows in the river are relatively small: 75% of the time flows are less than 4.2 cubic meters per second ($m^3 s^{-1}$) (150 cubic feet per

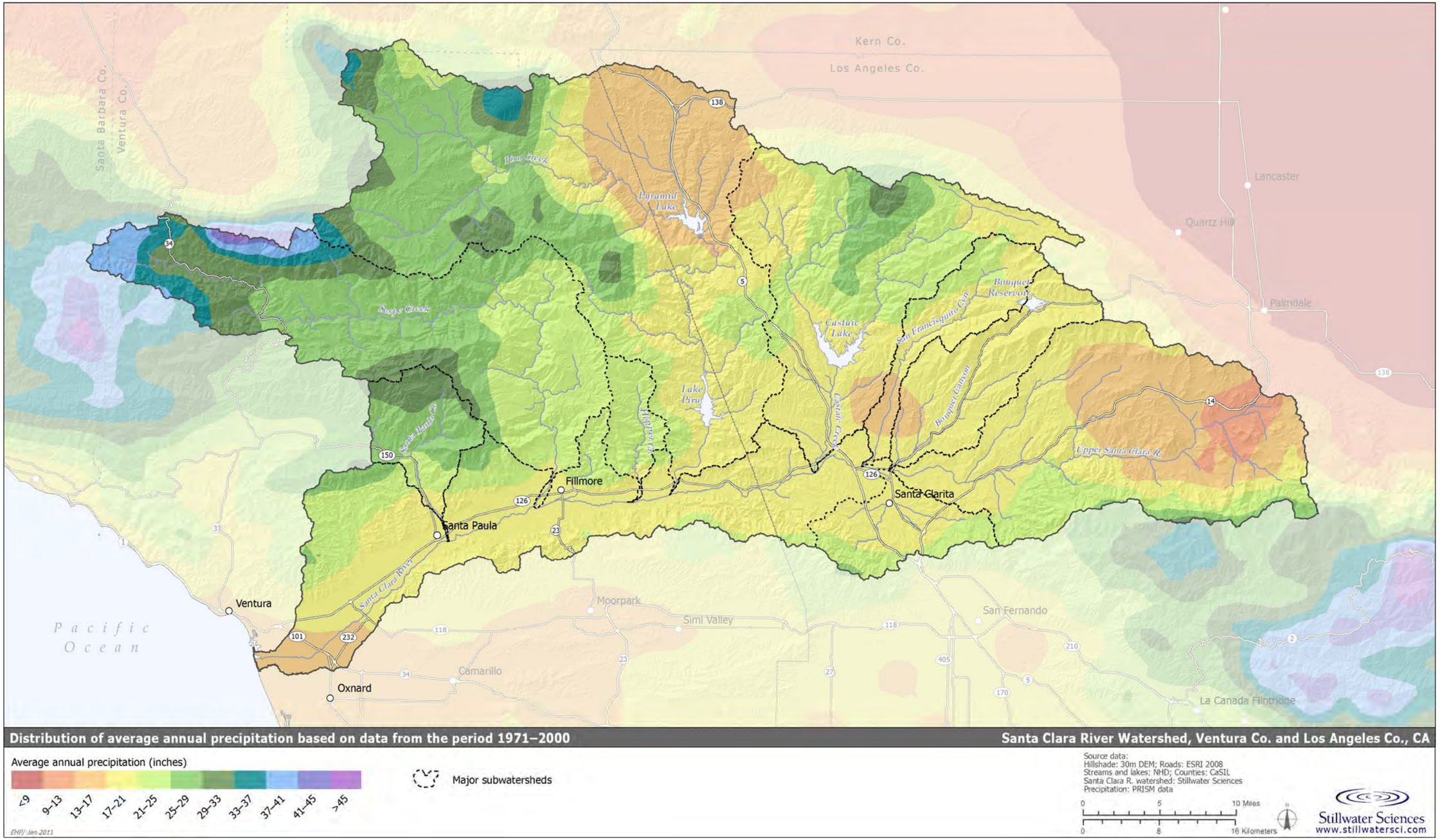

Figure 1-5. Distribution of average annual precipitation across the SCR watershed based on data from the period 1971-2000.

second [cfs]) at Montalvo and 50% of the time flows are less than 0.3 $m^3 s^{-1}$ (10 cfs) (URS 2005). However, large peak flows associated with winter storm events cause flows to exceed about 2,800 $m^3 s^{-1}$ (100,000 cfs) once every 10 years on average (see Section 4.1).

During the dry summer season, flows in the mainstem are intermittent or non-existent, depending primarily on areas of rising groundwater or inflows from dam releases or other anthropogenic sources. Reaches of lower Piru and Castaic creeks and Bouquet Canyon typically support a low flow even during dry summer months, insofar as they receive flow from their respective water storage reservoirs upstream. Groundwater discharges to the mainstem river occur when groundwater levels are high and the water table is close to the surface. Three geologic features are important to surface water–groundwater interactions on the mainstem—Soledad Canyon and the Piru and Fillmore narrows. In these locations, constrictions in the width of unconsolidated deposits combined with subsurface bedrock controls cause groundwater to rise and discharge to the river, depending on groundwater levels and surface flow conditions (URS 2005, Kennedy/Jenks 2008). In areas away from the bedrock controls, surface flow is lost through the highly permeable bed materials to groundwater.

The watershed also supports a highly developed groundwater pumping infrastructure used to supply water for agricultural, domestic, and industrial purposes, primarily in the Santa Clarita Basin and the Santa Clara River Valley. As a consequence, summer baseflow in certain river and lower tributary reaches through these regions is undoubtedly diminished as compared to historical, pre-pumping conditions (see Chapter 2). Detailed accounts of the groundwater–surface water interactions in the USCR watershed is presented in the *Upper Santa Clara River Integrated Regional Water Management Plan* report (Kennedy/Jenks 2008) and in the LSCR watershed is presented in the *Santa Clara River Parkway Floodplain Restoration Feasibility Study—Water Resources Investigations* report (URS 2005).

As introduced above, the major tributaries of the SCR include Santa Paula, Sespe, Hopper, Piru, Castaic, San Francisquito Canyon, and Bouquet Canyon creeks, and South Fork Santa Clara River (Figure 1-6). Other tributaries, including numerous barrancas (small, generally incised tributary streams) and unnamed ephemeral creeks empty into the mainstem river along its course. More than one-third of the watershed area lies upstream of dams and debris basins that regulate water and/or sediment discharge to the river corridor. Major dams include Santa Felicia and Pyramid dams on Piru Creek, Castaic Dam on Castaic Creek, and Bouquet Canyon Dam on Bouquet Canyon (Table 1-1 and Figure 1-6). Throughout the year, controlled releases of water from Lake Piru and Castaic Lake reservoirs supplement surface flows in the river reaches in the Santa Clarita Basin and the Santa Clara River Valley.

1.2.3 Land use/Land cover

The SCR watershed remains relatively undeveloped in comparison to many of the coastal watersheds to the south, such as the Los Angeles, Santa Ana, and San Gabriel rivers, but the population in the watershed has risen from about 60,000 to 600,000 since 1950. Large expanses of the mountainous northern portions of the watershed are part of the Angeles and Los Padres National Forests (see Figure 1-1). Land development is generally concentrated within the lowlands and surrounding foothills on the Santa Clara River Valley and Santa Clarita and Acton basins, with several other unincorporated towns and low-density settlements scattered throughout. Infrastructure in support of water supply storage and conveyance, power transmission, natural resource extraction and distribution (e.g., oil and natural gas), and transportation (e.g., highways) is present throughout much of the watershed, except in the more remote, higher elevation areas.

Additional details on historic and present-day land use activities and their effects on the watershed's geomorphic processes are presented in Chapter 2 and Section 4.2.

Land cover in the upland areas predominantly comprises scrub/shrub (chaparral) vegetation (Figure 1-7). Higher density vegetation cover and larger trees generally concentrate on north-facing slopes, but particularly so in the wetter and higher elevation areas of the watershed (e.g., Sespe Creek, Piru Creek, and Castaic Creek/Elizabeth Lake Canyon headwaters and the north side of the San Gabriel Mountains). Despite the mostly semi-arid climate, the vegetation cover in the watershed effectively hinders erosion of land surfaces by providing: (1) a continuous surface cover that intercepts rainfall and prevents rainsplash erosion, and (2) roughness to the landscape surface that slow sheetwash upon the land surface. Conversely, burning of the watershed's vegetation cover by frequent wildfires often results in increased surface erosion and pulses of fine sediment into the drainage network (see Section 3.2.3.3). Along floodplain and valley bottom areas of the Santa Clara River Valley, orchard and row crop agriculture is the dominant land use, with significant urban areas in Ventura, Oxnard, Santa Paula, Fillmore, and Santa Clarita (Figure 1-7).

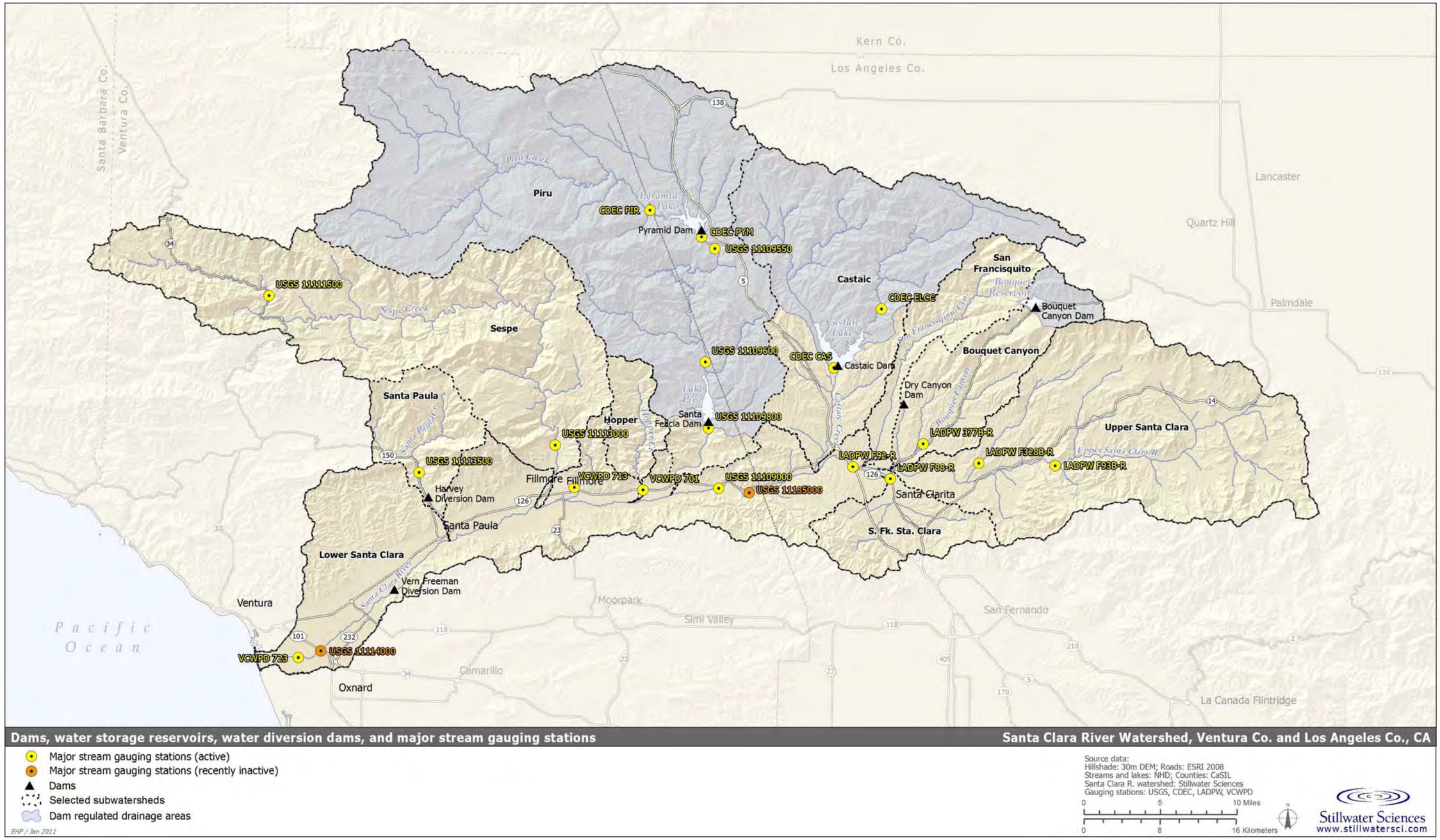

Figure 1-6. Dams, water supply reservoirs, regulated drainages, diversions, and stream gauges in the SCR watershed.

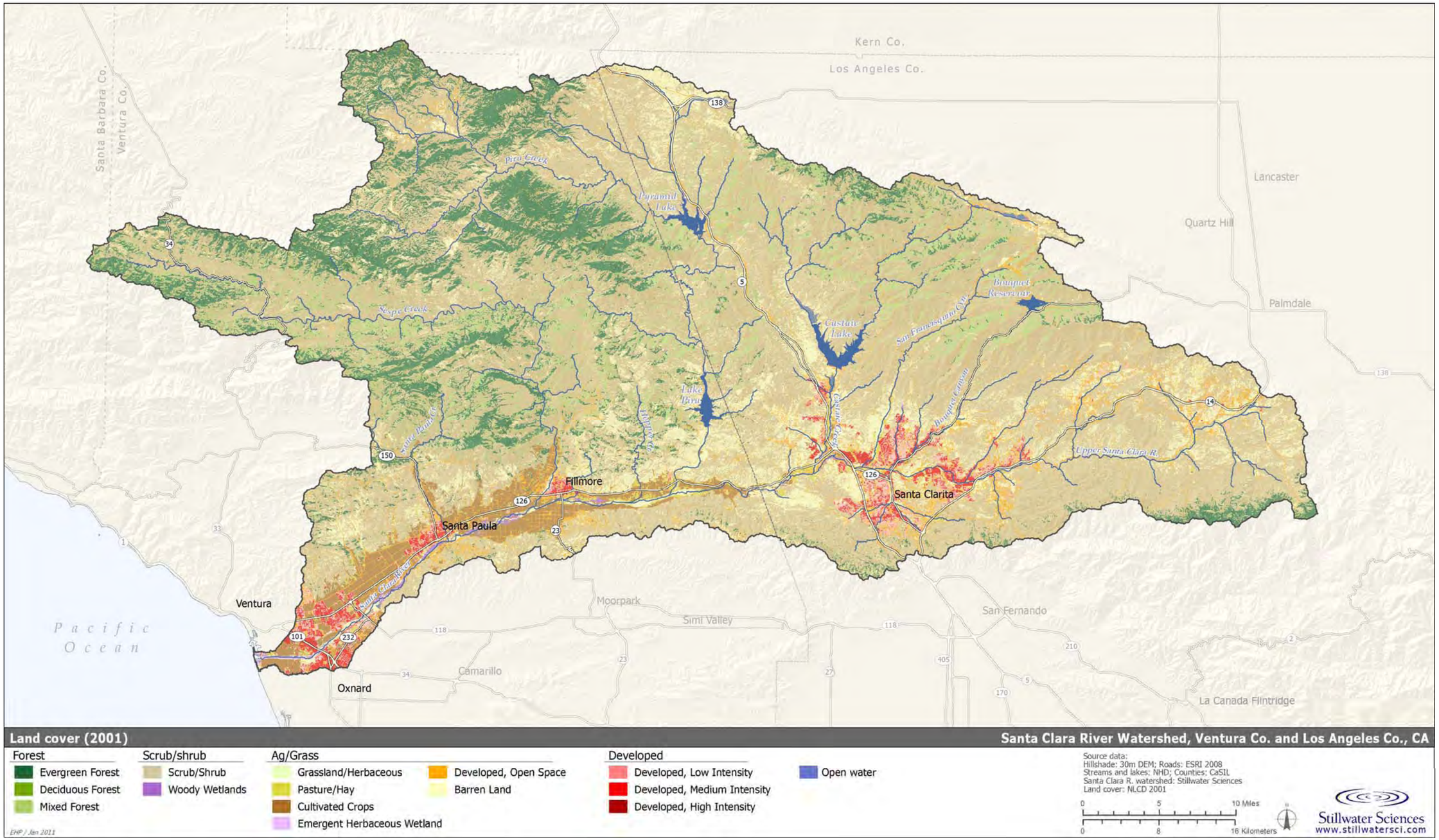

Figure 1-7. Land cover (2001) within the SCR watershed.

2 HISTORICAL PERIODS OF CHANGES TO WATERSHED GEOMORPHIC PROCESSES

A conceptual understanding of past periods is critical in determining how the physical watershed and river corridor used to function, and it helps form the foundation for determining how changes in watershed and river function have occurred. Understanding these elements makes it possible to hypothesize the potential future trajectory of channel conditions and thus helps to guide sustainable river management strategies. Information from a variety of sources (Table 2-1) has been distilled into a time chart of historical events that have had an effect on water and sediment discharge throughout the entire SCR watershed, and therefore that have influenced geomorphic processes and channel morphological responses within the river corridor (Figure 2-1 and Appendix A).

The history of land-use changes and the evolution of water and river management practices within the entire Santa Clara River watershed have been comprehensively documented by Schwartzberg and Moore (1995) and AMEC (2005). These authors subdivided the history of the entire watershed into four distinct phases based primarily upon cultural and land developmental considerations: pre-European settlement (pre-1872), the Agrarian Era (1782–1870), the Commercial Era (1870–1920), and the Industrial Era (1920–present).

From a geomorphological perspective, however, the data in Figure 2-1 and Appendix A suggest that five historical periods have likely altered the response of channel morphology to natural extremes in water and sediment discharge. These periods are as follows:

- Pre-1760: “Pre-European Colonization”
- 1760–1820: “European Arrival”
- 1820–1910: “Settlement & Ranching”
- 1910–1980: “Irrigation, Diversions, Dams, & River Modifications”
- 1980–2010 (present): “Urbanization”

This section provides a broad overview of the anthropogenic activities associated with these five periods and discusses their potential influence on geomorphologic processes in the SCR watershed over time. Expected future conditions for many, but not all, of the watershed impacts considered in Figure 2-1 have been included based upon forecasts made by others (e.g., AMEC 2005, Kennedy/Jenks 2008, County of Ventura 2008, LACDRP 2009, CNRA 2010). This time period is simply referred to as “future” here and extends out to the year 2050, which was selected because minimal information was available beyond this year. Additional details regarding specific events that occurred during these historical periods and regarding expected future conditions beyond 2010 are presented in Section 4.2 and Appendix A. A description of the method utilized to determine “wet” and “dry” periods in the watershed, which follows the method initially developed by Freeman (1968) for use with the long-term Santa Paula precipitation data, are also described in this appendix. A more detailed discussion on wildfires and their effects is presented in Section 3.2.3.3.

Table 2-1. Historical sources for the SCR watershed.

Data	Source	Dates	Notes
Aerial photography	LADPW, UCSB, USGS, VCWPD	1928 to present	Photo coverage is not synchronous between the LSCR and USCR. First suitable coverage for the LSCR is from 1938, while excellent 1928 coverage is available for the USCR, likely commissioned in response to the 1928 St. Francis Dam failure. Full coverage exists for numerous years after 1938 for the LSCR. Photo coverage and availability is sparse in the USCR after 1928 until the 1960s; much improved after 1980.
Topographic maps, longitudinal profiles, and digital data	Intermap, USACE, LADPW, USGS, UWCD, VCWPD	1920s to 2005	In the LSCR, several excellent longitudinal profile datasets from USACE and UWCD. In the USCR, excellent topographic coverage from historical 24:000 scale USGS maps (1930s; 5-ft contour spacing along river channel), 1:1200 scale LADPW maps (1964; 2-ft contour spacing), and high resolution Intermap IfSAR data (2001; 5-m resolution). In both LSCR and USCR, high-resolution VCWPD and LADPW LiDAR data.
Precipitation and streamflow	LADPW, LADWP, USGS, VCWPD	various	Historical precipitation data from Santa Paula in the LSCR watershed extended back in time by Freeman (1968). Various rain and stream gauge records throughout the SCR watershed with varying durations, from early or mid-20th century.
Wildfires	CDF FRAP	1878 to present	Comprehensive database of documented wildfire events throughout California, including the SCR watershed.
Miscellaneous ground-based photography	LADPW, VCWPD	1900s and later	Excellent panoramic photos of the river following the 1928 St. Francis Dam failure and low-elevation. In USCR, oblique-angle aerial photographs of the river during the 1969 floods.
Textual accounts	Report: Schwartzberg and Moore (1995), *Santa Clara River Enhancement and Management Plan: A History of the Santa Clara River* Book: Freeman (1968). *People-Land-Water: Santa Clara Valley and Oxnard Plain, Ventura County, California*	1700s and later	Excellent summary of the history of the entire Santa Clara River Valley (Ventura and Los Angeles counties). Includes accounts of the river's historical condition, especially during flood events.
Textual accounts and ground-based photography	Santa Clarita Valley Historical Socity http://www.scvhs.org/	Pre-history and later	Online compilation of newspaper articles, research, photographs, and accounts of historical conditions in the USCR Valley.
Vegetation plot and mad data	UC Berkeley Wieslander Vegetation Type Mapping http://vtm.berkeley.edu	Early 1900s	Online compilation of detailed vegetation mapping of the Santa Clara River Valley on USGS topos.

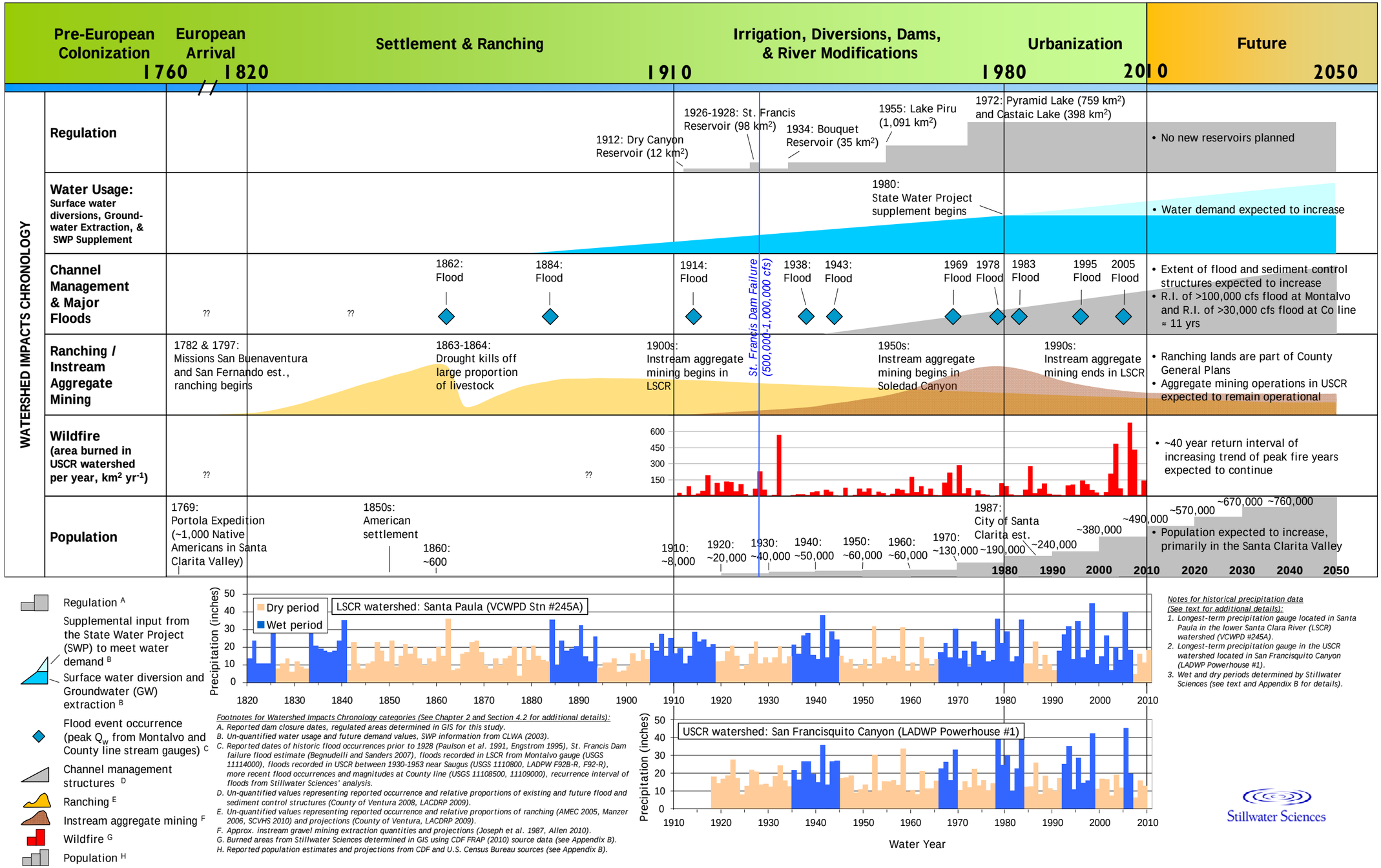

Figure 2-1. Chronology of potential watershed impacts and events. Precipitation records indicate periods of cumulatively wetter and drier periods in the watershed. See text and Appendix B for additional details.

2.1 Pre-European Colonization (pre-1760) and European Arrival (1760–1820)

In the period prior to widespread European ranching and colonization (approximately prior to 1820, following establishment of Mission San Buenaventura in 1782 and Mission San Fernando in 1797), the SCR watershed presumably was in a relatively pristine state, responding only to fluctuating flood, drought, and fire sequences with relatively minor impacts associated with the agricultural practices of the indigenous Chumash and Tataviam peoples, which were culturally similar to one another (Schwartzberg and Moore 1995; W&S Consultants 1995, as cited by USACE and CDFG 2009; Szabolcsi 2000). There are historical reports that describe perennial stream flow for several southern California rivers, including the Santa Ana, Santa Margarita, and San Luis Rey, that are now intermittent largely as a result of water impoundment, diversion, and groundwater pumping (Boughten et al. 2006). As summarized by Schwartzberg and Moore (1995), Father Juan Crespi (of the Portola Expedition that traveled along the California coast) noted a mature riparian forest along the river near Castaic Creek in 1769: "tall thick cottonwoods and oaks" and an "arroyo with a great deal of water which runs in a moderately wide valley, well grown with willows and cottonwoods." It is therefore likely that the USCR (and the entire SCR course through the Santa Clara River Valley, as well) experienced perennial stream flow and supported a more-or-less continuous and broad riparian forest in all reaches, with the possible exception of those located farther upstream in the Acton Basin which ran through (and continue to run through) a considerably more arid terrain.

2.2 Settlement & Ranching (1820–1910)

Beginning in the 1820s, establishment of large-scale ranching activity throughout the SCR watershed and other coastal California watersheds is likely to have caused significant changes to rainfall-runoff relationships as deep-rooted native perennial grasses in the valleys and foothills were degraded and replaced by shallow-rooted non-native annual grass species, which are less able to resist soil erosion (Rice and Foggin 1971, Gabet and Dunne 2002). Drought in the mid-1860s caused a shift from traditional cattle grazing to sheep, potentially accelerating the removal of vegetation and subsequent erosion (Freeman 1968, Manzer 2006). Timber-harvesting activities were generally limited in the watershed due to the lack of easily accessible conifer stands; however, logging activities did occur in the region including the upland areas of the watershed (Blakley and Barnette 1985, USFS 2010). The expansion of farming in the Santa Clara River Valley during the 1870s probably further contributed to erosion and changes in runoff characteristics. Overall, it is likely that greater volumes of hillslope runoff were generated per unit rainfall as a result of land-use change during this period, with far greater volumes of fine sediment production throughout the watershed and increased shallow landslide potential on the hillslopes (Rice and Foggin 1971, Gabet and Dunne 2002). Historical accounts describe the extensive effort undertaken to clear riparian forests throughout central and southern California watersheds (Gordan 1996, as cited in Boughton et al. 2006). Floodplain forests were first cleared for fuel supply, then to prepare the land for grazing and farming, and finally to increase flood conveyance. These land uses and climatic events resulted in decreased stream bank stability and increased stream power, allowing high flows to entrench the channel. Prior to incision, the river channel would have supported higher groundwater elevations and more frequent floodplain inundation under lower flows. These channel conditions would have facilitated the recruitment and establishment of large tracts of riparian vegetation. In addition, prior to incision and the increased supply of fine sediment that channel incision causes, rivers like the Santa Clara likely supported gravel and cobble substrates in the lower reaches (Boughton et al. 2006).

By the end of this period, public concern over land-use effects on the region's landscape fueled the creation of the Angeles National Forest in 1892 (originally designated as the San Gabriel Timberland Reserve) (USFS 2010) and the national forestland predecessors to the Los Padres National Forest (formerly designated in 1936 with the assemblage of Santa Barbara National Forest, San Gabriel National Forest [portion], Pine Mountain and Zaca Lake reserves, and Santa Ynez Reserve). Presently, the national forests include over one half of the SCR watershed's total area.

2.3 Irrigation, Diversions, Dams, & River Modifications (1910–1980)

The period starting in the 1910s is characterized primarily by large-scale development of water supply infrastructure to serve the growing demand for water with the increase in agricultural use and settlement along the Santa Clara River Valley (including the Santa Clarita Basin, particularly on the Newhall Ranch property which was formerly part of the immense Rancho San Francisco) (Freeman 1968, Schwartzberg and Moore 1995). Other land uses that became established in the watershed during this time period included mining and oil drilling, both of which involved land clearing, road and railway construction, town establishment, and water use. In this period, irrigation using surface flow from the river was supplemented by pumped groundwater supplies. Following the formation of the Santa Clara River Protective Association (now United Water Conservation District) in 1925, diversions began first from Piru Creek (1930) and then Santa Paula Creek (1931). Irrigated acreage in Ventura County increased from 128 km^2 (31,700 ac) in 1919 to 436 km^2 (107,700 ac) in 1949. The first public water utility in the Santa Clarita Basin, the Newhall Water System (now the Newhall County Water District), was formed in 1913 and provided groundwater to 125 connections; by 1953 this had expanded to six wells serving 870 connections with a combined production of 725 gallons per minute (Hamilton 1999). A 1933 map prepared by the California Department of Water Resources (CDWR) depicting land use types in the Santa Clarita Basin shows that much of the river valley up to Soledad Canyon in the east, including the lower reaches of the major tributaries (e.g., South Fork SCR, Castaic Creek, and San Francisquito and Bouquet canyons), was supporting the production of water-intensive crops (e.g., citrus and alfalfa) but that most farmed lands were unirrigated (see Figure 3-1 in Schwartzberg and Moore 1985).

Impacts of groundwater extraction in the watershed, specifically in the Santa Clara River Valley, likely included an initial reduction in baseflow within the river followed by a lowering of the groundwater table due to pumping. Groundwater subsidence in particular may have led to further degradation of mature riparian vegetation (in areas where riparian vegetation was not replaced by orchards), which is reliant primarily on groundwater during the summer dry season. Large floodplain areas with extensive riparian vegetation may have attenuated floods within the SCR; the removal and degradation of large riparian stands would have therefore increased the "flashy" response of the river during flood events. The removal of riparian vegetation would also have resulted in decreased complexity of floodplain habitat and increased river water temperature. Prior to disturbance, the riparian area likely supported dense, multi-stored stands of broadleaf trees, including cottonwood, sycamore, and various willows, that extended from a few to several miles wide (Boughton et al. 2006).

By 1912, the first large dam in the watershed had been constructed in Dry Canyon, a tributary to lower Bouquet Canyon (the dam was subsequently decommissioned in the 1960s due to leakage); in 1913 the Owens Valley–Los Angeles aqueduct, which cut through Soledad, Bouquet, and San Francisquito canyons, was completed. In 1926, St. Francis Dam was completed on San

Francisquito Canyon; however, the dam failed catastrophically in March 1928, resulting in one of the largest and most tragic dam failures in United States history. The long-term effects of the St. Francis Dam disaster on the morphology of the entire SCR are not fully known but are potentially significant and ongoing (see Section 4.2). Bouquet Dam was completed in 1934 to impound imported water in Bouquet Reservoir, in the relatively dry northeastern corner of the watershed. After 1955, with the completion of the 61 m (200 ft) high Santa Felicia Dam on Piru Creek (regulating 1,090 km^2 [421 mi^2]) the watershed began to be subjected to an increasing amount of direct flow regulation and channel manipulation. Pyramid and Castaic dams, completed in 1972, retain water imported from northern California. Today, these dams intercept runoff and sediment from approximately 34% of the watershed area (see Sections 3.4 and 4.2). Further, the floodplain and channel along the Santa Clara River Valley and Santa Clarita Basin were increasingly modified, beginning in the 1950s with the dredging of pilot channels, in the 1960s with the construction of the extensive levee system from South Mountain to Highway 101 and, following the flood of 1969, construction of various additional levees, groins, and bank protection projects that continue to the present day.

2.4 Urbanization (1980-2010)

More recent, and perhaps the most significant, influences on the evolutionary history of the SCR are associated with the increasing rate of urban development in Ventura and Los Angeles counties, with the greatest proportion of the growth occurring in the Santa Clarita Basin. Although only recently incorporated in 1987, the City of Santa Clarita (which includes Canyon Country, Newhall, Saugus, and Valencia) is now the second-largest city in Los Angeles County based on size (approximately 170 km^2) and the fourth-largest based on population (CDF 2010). Between 2000 and 2008 the City of Santa Clarita's population growth rate was almost twice that of all of Los Angeles County (see Section 4.2). Other urban centers have experienced growth as well, including Ventura, Oxnard, Santa Paula, and Fillmore, albeit at a much reduced rate as compared with Santa Clarita (see Table A-2 in Appendix A).

During this growth period, the SCR floodplain and channel near these urban centers were increasingly modified for the purpose of providing for development, along with associated infrastructure for flood control and debris-flow protection. Urban growth throughout the watershed, and southern California as a whole, is also linked to demand for aggregate materials needed to improve and expand existing infrastructure. Thus during the 1960s through the 1980s, the pace of mining activity in the watershed escalated dramatically (Joseph et al. 1987) and appears to coincide with increased rates of channel incision upstream of aggregate mining pits in this period (see Sections 4.2.2 and 4.3.3). In 1986, the creation of the Ventura County "red line", restricting the depth of instream aggregate extraction, marked the beginning of the decline in instream mining within the LSCR watershed. The construction of a permanent Vern-Freeman Diversion Dam in 1992 likely aided the stabilization of the mainstem river bed elevation and halted incision resulting from the aggregate mining operations.

The geomorphic impact of such direct modifications to water and sediment discharge, and to the channel perimeter, is likely to have been significant but difficult to disentangle from the impact of previous watershed land-use changes and natural flood events (Simons, Li & Associates 1987, Chang 1990). For example, the reduction in sediment discharge caused by dam construction may have reversed some of the increase in sediment load that likely followed land clearing and subsequent changes in upland vegetation. Clear-water discharge from dams may have also led to channel incision, such as below Castaic Dam on lower Castaic Creek (Simons, Li & Associates 1987). Bank protection in the Lower Santa Clara River Valley and the Santa Clarita Basin may

have changed instream flow patterns, deflecting erosional energy to new locations. Levees and hardened banks may also be increasing rates of channel incision by confining flood events to the floodway and thus increasing flow depths rather than allowing overbank flooding to occur (Simons, Li & Associates 1987) (see Section 4.2).

2.5 Future (2010-2050)

Beyond the present day, it is predicted that the populations of Ventura and Los Angeles counties will continue to increase at current growth rates, particularly within the Santa Clarita Basin and surrounding areas (Kennedy/Jenks 2008). As such, the urban footprint of the main populated centers will continue to expand within the watershed, resulting in an increased demand for water, flood and debris protection, and construction materials (i.e., aggregate) (see Section 4.2.4). Growth trends forecasted to occur within the watershed through 2050 are displayed in Figure 2-1 and summarized in Tables A-1 and A-2 of Appendix A.

The subsequent sections in this report further investigate the geomorphic conditions and processes in the SCR mainstem following almost two centuries of European colonization, land-use changes, and direct modification of water and sediment discharges and channel morphology in the watershed. It is important to note that, first, the periods outlined above are separated for convenience and that their impacts on the watershed are both gradational and cumulative over time. Because the cumulative impact is difficult to quantify, however, this report has compiled a large number of both quantitative and qualitative studies as the basis for a preliminary understanding of the evolutionary trajectory of the river channel. Second, sediment transport and morphological changes in the entire SCR occur only in brief periods during flood events, and especially when flood events follow large fires (Lavé and Burbank 2004, Warrick et al. in prep). As such, both a natural component to channel morphology changes and a confounding factor of human impacts in the watershed are expressed during major flood (and especially fire–flood) events. This makes disentangling comprehensive human impacts from natural events one of the most challenging arenas in geomorphology (Downs and Gregory 2004).

3 HILLSLOPE AND TRIBUTARY SEDIMENT PRODUCTION AND DELIVERY

3.1 Overview

This chapter evaluates the hillslope processes that control the production of sediment across the watershed, and the subsequent delivery of that sediment into the channel network. Overall, rates of hillslope sediment production in the watershed are driven by tectonics, geology, climate, and land uses. In detail, sediment is released from hillsides via several discrete processes, including dry ravel, soil creep, gullying, and landsliding.

Representative rates of soil production and hillslope sediment transport are difficult to quantify because they are driven by the episodic and commonly transient effects of rainstorms, windstorms, fires, earthquakes, and human and other disturbances (Benda and Dunne 1997, Gabet and Dunne 2003). The inherently episodic nature of erosional processes results in substantial year-to-year variability and makes any assessment of sediment-production and transport rates sensitive to the timescales over which they are averaged (Kirchner et al. 2001). For example, if the basin-wide erosion rate is averaged over a relatively dry 10-year period it will be considerably lower than if it were averaged over a 10-year period that included several wet years. Although long-term averages cannot predict the sediment load for any given year, they nevertheless are useful in assessing the long-term consequences of alternative management actions.

As the first step in understanding and quantifying the magnitude of sediment flux down the channel of the SCR, this section evaluates the production of hillslope sediment across the watershed and the delivery of that sediment into the channel network. These rates have been estimated using a variety of techniques, over a variety of temporal and spatial scales, because multiple scales of analysis can provide more robust and reliable estimates than any single method alone. Over a millennial timeframe, long-term erosion rates can be estimated using sediment dating techniques (i.e., measurement of cosmogenic nuclide concentrations in eroded sediments), which we have employed as part of the USCR study (Stillwater Sciences 2011a). Results of this investigation are referenced below where applicable. Over the longest time scales, best represented by the geologic record of the past several million years, the likely magnitude of sediment production should approximate the rate of overall landscape uplift (Burbank et al. 1996). This provides a coarse indication of the likely range of average sediment-delivery rates across the watershed as a whole, and one that is completely independent of other methods.

Over shorter, more human timescales, rates of sediment production can be assessed using a "geomorphic landscape unit" (GLU) approach, in which different parts of the watershed are recognized to erode at different rates due to differences in their physical characteristics, and to which representative erosion rates can be assigned and then summed over the watershed area as a whole. The degree to which these long-term and short-term estimates agree, not only with each other but also with additional data on the rate of in-channel sediment transport directly, provides a measure of the reliability of these results.

3.2 Dominant Sediment Production and Delivery Processes

Upland topography reflects the interplay of uplift due to tectonic processes and the wearing away of slopes by erosion. In general, high, steep mountains occur in areas that have been subjected to

sustained, rapid uplift, whereas low, gently sloping mountains occur in areas where uplift is slow or has been followed by long periods of denudation. Steeper areas generally have higher erosion rates (e.g., Ahnert 1970), because erosion is typically more effective on steeper slopes and because steep slopes are prone to mass movement, which can enhance erosion. Hence, faster tectonic uplift rates are generally associated with steeper mountains and faster erosion rates. In general, the linkages between uplift, slope steepness, and erosion imply that slopes should tend to contribute sediment in proportion to their uplift rates over the long term.

Slopes throughout the SCR watershed are steep (see Figure 3-1), with long-term uplift rates that are among the fastest in the continental United States (see Section 3.3.1). Erosion rates are likewise rapid but are not so fast that soils are completely stripped everywhere from slopes.

Soil moves downslope toward channels and unchanneled valleys, transported incrementally by hillslope sediment transport processes, such as mass wasting, overland flow, and biogenic disturbances. These processes deliver sediment directly to channels from slopes, or bring it to unchanneled valleys where it may first collect before being delivered to channels by channel-head erosion and landsliding. After entering channels, sediment is transported downstream by stream flow or in concentrated debris flows. Sediment transport by the SCR and its major tributaries is discussed in Chapter 4. In this chapter, the focus is on the upslope processes that ultimately deliver that sediment to the drainage network.

3.2.1 Discrete hillslope processes

Evaluation of active hillslope processes in the watershed was accomplished by reviewing other geology and geomorphology studies previously conducted in the watershed, and then performing ground-based field surveys as part of various studies (LSCR [Stillwater Sciences 2007a], Santa Paula Creek [Stillwater Sciences 2007b], San Francisquito Canyon [Stillwater Sciences 2009], Sespe Creek [Stillwater Sciences 2010], and USCR [Stillwater Sciences 2011a]). These field surveys served to identify and characterize active geomorphic processes in viewable and/or accessible areas, with a focus on areas representative of general landscape types (e.g., consisting of distinct combinations of geology, land cover, and hillslope gradient) (see Section 3.3.2). Active hillslope processes in the watershed, as identified during the field surveys and supported by information presented in other published accounts, are summarized in Table 3-1.

Table 3-1. Active hillslope processes in the USCR watershed.

Category	Hillslope process	Process description [A]
Natural processes		
Sediment production	Conversion of bedrock to soil mantle	Physical, chemical, and biotic-breakdown of bedrock material into friable weathered rock and then physically disrupted into soil. [a]
	Rockfall	Mass failure of mostly rock that has separated from its parent bedrock surface (typically along vertical cliff). [a]
Mass-wasting processes	Soil creep	Slow, often indiscernible downslope movement of surface soils or rock debris. [a]
	Dry ravel	Downslope transport of individual particles under power of gravity (or bioturbation) rather than water; mostly occurring where vegetation cover is non-existent. [b]
	Rain impact	Erosion of soil surface through the impact of rain drops that effectively detach and transport sediment particles; rain impact energy diffused or altogether blocked by ground cover vegetation. [a]

Category	Hillslope process	Process description [A]
Mass-wasting processes (cont.)	Biogenic transport	Exhumation and down-slope transport of soil and rock fragments by biological forces, including tree-throw and burrowing animals. [a]
	Shallow landsliding	Mass failures that have a composition mostly of colluvial sediments, a failure plane above the soil-bedrock interface, and a relatively long travel distance through the low order channel network. [c]
	Deep-seated landsliding	Mass failures that have a composition mostly of bedrock (parent material), a failure plane below the soil-bedrock interface, and a surface area >0.1 km^2. [d]
Overland flow erosion	Sheetwash	Downslope transport of fine particles (<2 mm) driven by concentrated surface runoff. [a]
	Rilling	Formation of generally discontinuous, small channels less than several cm deep and wide that develop on slopes composed of fine-grained sediments where surface runoff has concentrated. Typically occurs in areas of land disturbance and/or vegetation clearing. [a]
Tributary connection with hillslope processes	Gullying	Formation often driven by the coalescence of several rills into an enlarged master rill, which can further extend the drainage network upslope. Often occurs in areas of land disturbance and/or vegetation clearing. [a]
	Channel head advance	Upslope migration of a stream channel into hillslope colluvium, usually due to gully incision and/or channel head-cutting. [a]
Human disturbances		
Agriculture and rangeland	Surface wash, rilling, and gullying	(see description above)
	Shallow landsliding	(see description above)
Road-related	Cut and fill failures	Erosion by sheetwash, rilling, gullying, or shallow landslides into road cuts or road fill material. [e]
	Surface erosion	Erosion of fine sediments from unpaved road surfaces. [e]
	Gully formation associated with inboard ditch relief	Occurs when road runoff concentrates into an inboard ditch that then incises the ditch and/or adjacent surfaces where the routed flows have been discharged. [e]
	Gully formation and mass failure on the outboard side	Occurs when road runoff concentrates on the outboard side of the road and erodes/destabilizes road fill material and/or hillside soils. [e]
Urban	Construction phase sediment pulse	Release of fine sediment downslope and into the drainage network during the disturbance of the landscape.
	Slope destabilization	Surface erosion and mass failures can occur on slopes that have been over steepened and/or undercut.

[A] Sources: [a] Selby 1993; [b] Gabet 2003; Roering et al. 2003; [d] Roering et al. 2005; [e] Reid and Dunne 1984

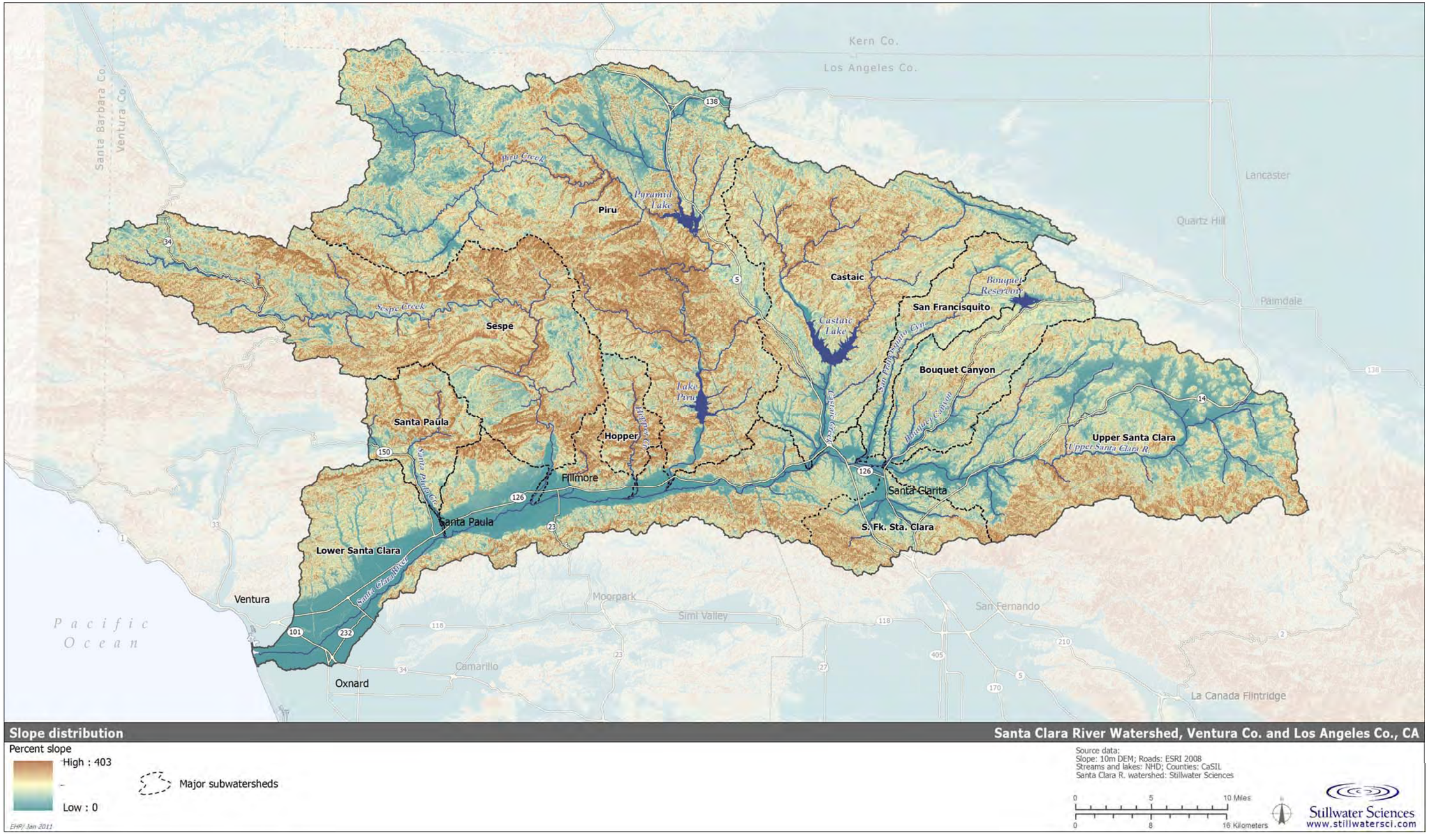

Figure 3-1. Slope distribution in the SCR watershed.

3.2.2 Production and delivery of fine and coarse sediment

With continuous landscape uplift to drive hillslope processes and large areas of highly sheared and/or fractured igneous, metamorphic, and sedimentary rock units now hundreds of meters above the valley bottoms, the SCR watershed's geologic characteristics have a strong influence on erosion rates and spatial distribution. The eroded sediment is derived from four distinct sources, categorized as follows:

1. Older, relatively durable and moderately fractured igneous (e.g., granite), meta-igneous (e.g., gneiss), and sandstone, chiefly found in the higher elevation and headwater areas of the watershed and primary producer of coarse-grained materials (generally, units "Toc", "Kg", "Pzg3", "Xm", and "Ya" in Figure 1-4);
2. Moderately erodible and highly sheared/fractured rocks that erode into abundant sand, gravel, and cobble-sized clasts, primarily the Pelona Schist (unit "uMze" in Figure 1-4) traversing San Francisquito and Bouquet canyons; and the geologically young, poorly consolidated sandstones/conglomerates flanking the Santa Clara River Valley and Santa Clarita Basin (generally, unit "Te" in Figure 1-4);
3. Easily erodible, fine-grained siltstone, mudstone, and claystone of the geologically young Pico and Castaic formations, primarily found interbedded with sandstone units in the western portions of the watershed (e.g., Pico Canyon and lower Castaic Creek) (generally, units "Tp", "Tm", and "Te" in Figure 1-4); and
4. Easily erodible, mostly coarse-grained alluvial and colluvial material that deposited relatively recently along river valleys and as part of large paleo-landslides (generally, unit "Q" in Figure 1-4).

This four-part division into relative grain size and erodibility components is central in understanding the present behavior, and predicting the future behavior, of river channels such as the SCR. By analogy to other rivers world-wide, the fine-grained sediment load (i.e., the clay and silt-sized material) represents the majority of sediment that is delivered by hillslopes into the channel and that is subsequently transported by the channel to the ocean. Field observations indicate that areas displaying relatively high hillslope erosion are chiefly underlain by the geologically younger sandstone/conglomerate and shale units, along with the highly sheared/fractured Pelona Schist. Although coarse-grained sediments are produced in much less voluminous quantities by the other geologic source terrains, these larger particles are particularly important to stabilizing channel bed morphology and, thus, supporting favorable aquatic habitat conditions and minimizing the need for channel management.

The processes and rates by which sediment is eroded off of hillslopes, and subsequently delivered to the channel network, vary substantially across the watershed. All rock units in the watershed produce some fraction of fine-grained sediments, although their relative proportion of fine to coarse particle sizes depend on the specific material properties and the local conditions (e.g., vegetation cover, land uses, and hillslope gradient). Coarse-bearing bedrock can produce fine-grained sediments when the rock already contains a fine matrix component or when biotic (e.g., tree throw or gopher burrowing) or abiotic (e.g., bedrock dissolution or abrasion during transport) processes occur. Fine sediment production from predominately coarse-bearing bedrock is evident by the presence of a mixed-size soil mantle throughout the watershed, not just in those areas underlain by fine-grained rock units.

Overall, the fine-grained rocks are generally very susceptible to erosion, especially in the absence of vegetation, whereas the coarse-grained rocks are generally less so. By analogy to other studies, rates of sediment delivery from the fine-grained rocks (and rocks having a mix of grain sizes)

should vary most directly with hillslope gradient and vegetation cover (Reid and Dunne 1996). Observations throughout the watershed affirm this principle, recognizing that vegetation cover is both a cause and an effect of relative hillslope stability. Lack of vegetation cover enhances the rate of sediment delivery; but where the ground is unstable or eroding rapidly, vegetation does not grow well.

3.2.3 Factors affecting hillslope sediment production

In the SCR watershed and elsewhere in southern California, there are several dominant forces that directly affect hillslope sediment production and, thus, sediment delivery to the drainage network. This section discusses these natural and man-made forces: storms, earthquakes, wildfire, and human-induced land cover change.

3.2.3.1 Large storms

Slope failures, whether shallow or deep-seated, are usually associated with a triggering event, particularly a storm of prolonged duration or high intensity. Heavy rains brought by the El Niño event of 1997–1998 triggered thousands of shallow landslides throughout California; in nearby Sedgwick Reserve, for example, more than 150 slides occurred in a scant 9.5 km^2 (Gabet and Dunne 2002). Slope failures are more likely to be triggered in areas that have recently been destabilized by human or natural disturbances, such as fire, which destroys vegetation and roots and thus reduces soil cohesion. A discussion on El Niño events as they relate to peak streamflow events in the SCR is presented below in Section 4.1.3.

3.2.3.2 Earthquakes

Ground motions during earthquakes can also trigger landslides. The watershed's location within the seismically-active San Andreas Fault system (Figure 1-4), makes its slopes especially prone to earthquake-induced landsliding—a potentially significant source of both coarse and fine sediment for the river corridor. The low tensile strength and high relief of bedrock in the watershed generally results in steep, easily eroded canyon walls that are susceptible to failure during seismic events.

In 1994, the Magnitude 6.7 Northridge earthquake triggered nearly 7,400 landslides across the watershed (Figure 3-2) (Harp and Jibson 1996). The most intense area of landslide activity occurred in the Santa Susana Mountains bordering the south-central portion of the watershed, in deformed siltstone and sandstone of the Pico and Castaic formations having little cementation and thus low tensile strength. Most of the earthquake-induced slides were shallow, with depths less than 5 m and an average volume of less than 1,000 m^3. However, some individual slides had volumes exceeding 100,000 m^3. Several tens to possibly hundreds of slides were deep (>5 m) slumps, including the previously noted San Martinez Grande deep-seated slide (Harp and Jibson 1996).

Although the shallow landslides typically traveled considerable distances (>50 m) downslope from their source areas (Harp and Jibson 1996), not all of the material that was mobilized during the Northridge earthquake was immediately transported downstream to the mainstem river. Numerous landslide deposits remained intact in tributary channels where they came to rest immediately after being triggered by the earthquake (A. Orme, pers. comm., 2005). Our examination of recent aerial photographs taken at the location of the large San Martinez Grande landslide noted that this large deposit has remained largely intact since 1994. Even so, subsequent storms have likely led to the erosion of stored materials at most or all of the landslide locations;

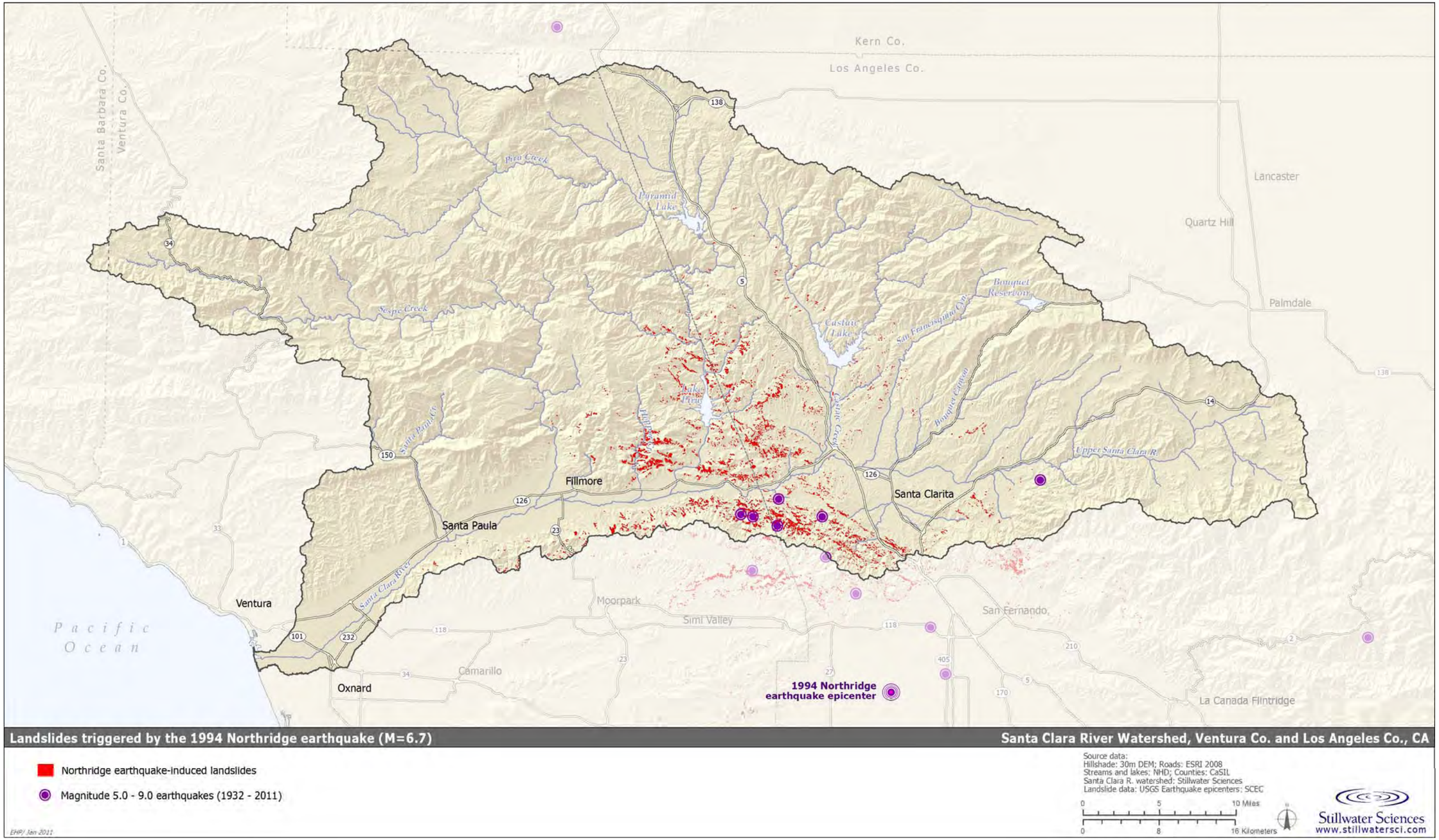

Figure 3-2. Landslides triggered by the 1994 Northridge earthquake (M=6.7). Nearly 7,400 landslides occurred in the SCR watershed. Epicenters of other earthquakes of M 5.0–9.0 recorded since 1932 are also shown.

exactly how much of the sediment remains in the watershed is unknown. Transport of that material could be reactivated by future earthquakes or intense storms and thus add significantly to the sediment load of the SCR. Given that the majority of these landslides were concentrated in the south-central part of the watershed, any increase in sediment delivery from the continued erosion of these features would result primarily in increased sediment delivery to the mainstem LSCR, rather than the USCR.

3.2.3.3 Wildfire

Wildfires have always been a significant contributor to hillslope erosion throughout the entire SCR watershed. Wildfires often contribute to drastically accelerated rates of sediment supply in subsequent years: recently burned hillslopes in steep, semi-arid to arid lands can respond to winter rains with increased runoff and accelerated erosion, which results in debris flows, landslides, and floods—thus completing what has been dubbed the "fire–flood" sequence (USFS 1954).

The watershed's landscape is dominated by large areas of contiguous chaparral vegetation, which is fire-dependent for germination and regeneration and thus has a proclivity to burn (Keeley et al. 1981, Keeley 1987). In addition to the type of vegetation, the combination of climate, soil type, and fire history all play primary roles in controlling fuel conditions for fires within the watershed. Currently, most of the watershed is designated as open space, of which much is within (and surrounded by) the Angeles and Los Padres National Forests (Figure 1-1). As these areas are generally undeveloped with nominal fuel-control efforts and large stands of older chaparral vegetation, wildfires continue to control vegetation generation as well as affect hydrologic and geomorphic dynamics within the watershed at varying spatial and temporal scales (Bendix and Cowell 2010).

Historical trends in the SCR watershed

Over the past century, the majority of the SCR watershed has been burned by wildfire (Figure 3-3). Most of the watershed has been burned at least once in the last century, with many areas of the watershed that are characterized by scrub/shrub vegetation burning up to eight times since 1878 (CDF FRAP 2010). Fire frequency is highest in the upland areas immediately surrounding the Santa Clara River Valley and Santa Clarita Basin, with the highest burn frequency occurring along South Mountain and along lower Castaic Creek near Hasley Canyon—an area also heavily impacted by landslides triggered during the 1994 Northridge earthquake (see above). Further, the areas burned more frequently also overlie the generally weaker rock units that are more prone to erosion in comparison with the more competent rock units located in the headwaters of most of the major tributaries (see Figures 1-4 and 3-3).

Examination of the historical wildfire records (CDF FRAP 2010) reveals that, between the years of 1911 and 2009[1], the average annual burned area within the SCR watershed is approximately 70 km^2 (17,300 ac), with a slight increase in the average amount of burned watershed area over this duration. As Figure 3-4 shows, a cyclical pattern emerges that is characterized by an approximate 40-year return period of peak maximum burned areas. Studies in the surrounding region have found similar patterns and return intervals in peak events (e.g., Mensing et al. 1999). For the SCR-specific data, there are three periods represented—pre-1911–1932, 1933–1970, and 1971 to approximately present day—each with similar trends whereby the peak events progressively increase over the period and then re-set to much lower magnitudes, upon which a new period has been initiated. Also observable in this plot is that two of the largest fire peaks in the data closely

[1] There is a continuous series of wildfire event records between these years.

follow two of the largest flood seasons (see Figure 2-1). That is, the peak burn years of 1970 and 2006 respectively follow the flood seasons of 1969 and 2005. Mensing et al. (1999) and Kelley and Zedler (2009) found that large fires in the region consistently occur at the end of wet periods and the beginning of droughts, which is consistent with our findings for the SCR watershed (see Figure 2-1). Wildfire occurrence, intensity, and areal extent in any given year, however, are locally influenced by summer/fall temperatures, presence and strength of Santa Ana winds, available fuel supply, natural fire ignition events (e.g., lightning), and human actions (Keeley and Zedler 2009). This indicates that small and large fires in the future have the potential to occur during any given year in the SCR watershed, but that the largest ones (in terms of most watershed area burned in a given year) will likely continue to follow the flood-drought climatic cycle of the region. Additional discussion on fire management effects is presented below.

The ten largest fires, in terms of areal extent, are summarized in Table 3-2; the largest of these fires—the Day Fire of 2006—burned 16% of the SCR watershed area. Additionally, five of the ten largest fires occurred within the past 10 years.

Table 3-2. Ten largest documented fires in the SCR watershed for the period (1878–2009) in rank order of their area of influence across the watershed.

Fire name [a]	Portion of watershed	Year [a]	Total burn area [a]		Burn area within SCR watershed [b]		% of SCR watershed burned [b]
			km^2	ac	km^2	ac	
Day	Sespe and upper Piru creeks	2006	655	161,815	652	161,148	16%
Matilija	Sespe and upper Santa Paula creeks	1932	890	219,998	548	135,358	13%
Piru	Piru Creek	2003	258	63,726	258	63,726	6%
Ranch	Piru Creek	2007	236	58,410	236	58,410	6%
Liebre	Upper Castaic Creek	1968	197	48,564	196	48,523	5%
Simi	Santa Susana Mtns	2003	435	107,570	178	44,064	4%
Unnamed	Sespe and Piru creeks	1917	178	44,009	178	44,009	4%
Ridge #98	Piru Creek	1928	176	43,472	176	43,472	4%
Ferndale	Santa Paula Creek	1985	189	46,805	174	42,980	4%
Buckweed	Bouquet, Mint, and San Francisquito canyons	2007	155	38,347	155	38,347	4%

[a] Source: CDF FRAP (2010).
[b] Proportion of fire extent within the total watershed area determined in GIS.

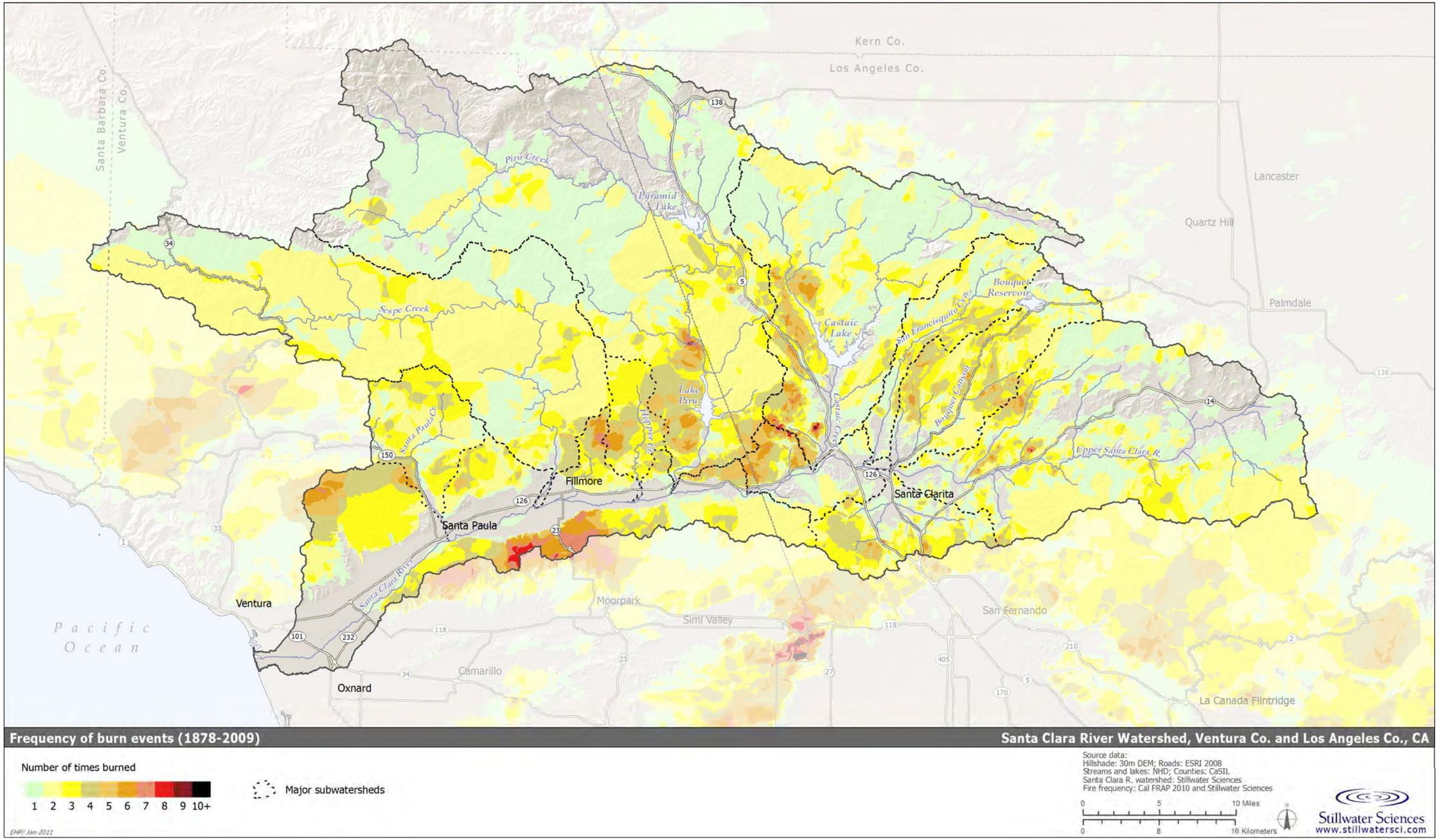

Figure 3-3. Frequency of burn events in the SCR watershed (1878–2009).

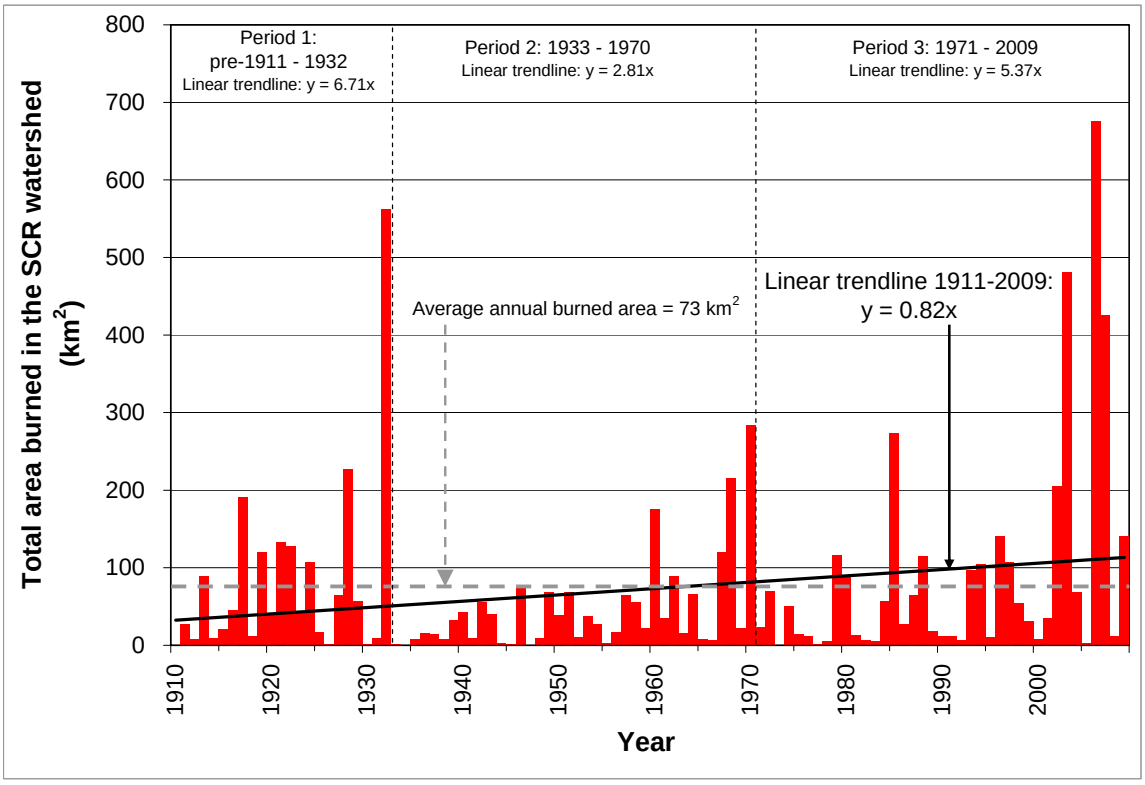

Figure 3-4. Total area of the SCR watershed burned annually from 1911–2009 and the three periods of increasing peak magnitudes contained therein (source: CDF FRAP 2010).

Impacts of wildfire on sediment dynamics in chaparral environments

Wildfire can cause significant physical changes to watershed ground surfaces, thereby affecting geomorphic and hydrologic processes responsible for the production and delivery of sediment to adjacent channels. Impacts include both direct changes to the physical properties of rocks and soil, and changes to geomorphic and hydrologic process rates until pre-fire conditions are reestablished (Shakesby and Doerr 2006). These changes can reduce the infiltration rate by an order of magnitude, shift the dominant runoff process from subsurface storm flow to overland flow, and increase peak flows and sediment yield by more than two orders of magnitude (see Larsen and MacDonald 2007 and citations therein). The primary changes to watershed ground surfaces induced by wildfires include removal of vegetation, alteration to soil physical and chemical structure, and changes to rates of bedrock and *in situ* coarse sediment erosion.

Impacts on rates of sediment production and delivery

Most studies of fire effects cannot directly calculate increase in sediment production because data on pre-fire sediment rates are typically lacking, but they do quantify post-fire rates in detail. From a compilation of 25 measured post-fire rates (Shakesby and Doerr 2006, their Table 3), first-year post-fire erosion measurements for watersheds from <0.001 km^2 to >5 km^2 in area range between 0–41,400 tonnes per square kilometer (t km^{-2}) with a median value of about 6,000 t km^{-2}. The lone San Gabriel Mountain study reported in this compilation (from Krammes and Osborne 1969) measured 19,700 t km^{-2} from three small plots with a combined area of less than 100 m^2.

Those studies that do quantify the changes in runoff and sediment yield following fire have been concentrated in semi-arid regions of the world with vegetative and climatic characteristics similar to southern California, and so many of the results should have broad applicability to the SCR watershed. From local studies, De Koff et al. (2006) measured a 6.6-fold increase in sediment yield from a prescribed burn in chaparral-covered southern California; Wells (1981) documented ten- to hundred-fold increases in sediment transport rates in woodlands of the San Gabriel Mountains. Other short-term increases in erosion rates following wildfires in chaparral-dominated southern California watersheds include factors ranging between 18-fold (Wohlgemuth 2003) and 35-fold (Rowe et al. 1954) increases over long-term pre-fire values. Most of these increases can be attributed to increases in dry raveling rates, both during and immediately after fires, and increases in sediment delivery along post-fire rills (Wells et al. 1987, Wells 1987).

Reported erosion rates tend to decline rapidly following the first year of post-fire rains, which leads to a so-called "window of disturbance" (Prosser and Williams 1998) that begins immediately after a wildfire and can vary in length from several seconds to a decade, depending on fire and watershed characteristics (Figure 3-5). For instance, Doerr et al. (2000) showed that wildfire can affect soil infiltration characteristics and sediment production and delivery dynamics for periods ranging up to several months, depending on fire duration and intensity. Other research has shown that the overall cumulative impact of fire on sediment production and delivery dynamics can be on the order of years, with impact durations ranging from 2–4 years (Wohlgemuth et al. 1998) to up to 10 years after the fire (LACFCD 1959, USFS 1997). One study that specifically assessed coarse sediment production separately found elevated rates for at least five years following a burn (Reneau et al. 2007). The five years following a fire has been suggested to be the most critical for fire-induced sediment production (Lavé and Burbank 2004). Because of very high rates immediately post-fire, however, wildfire still may account for 50% (Davis et al. 1989) to 80% (Lavé and Burbank 2004) of the total long-term sediment production and subsequent delivery within chaparral-dominated southern California watersheds.

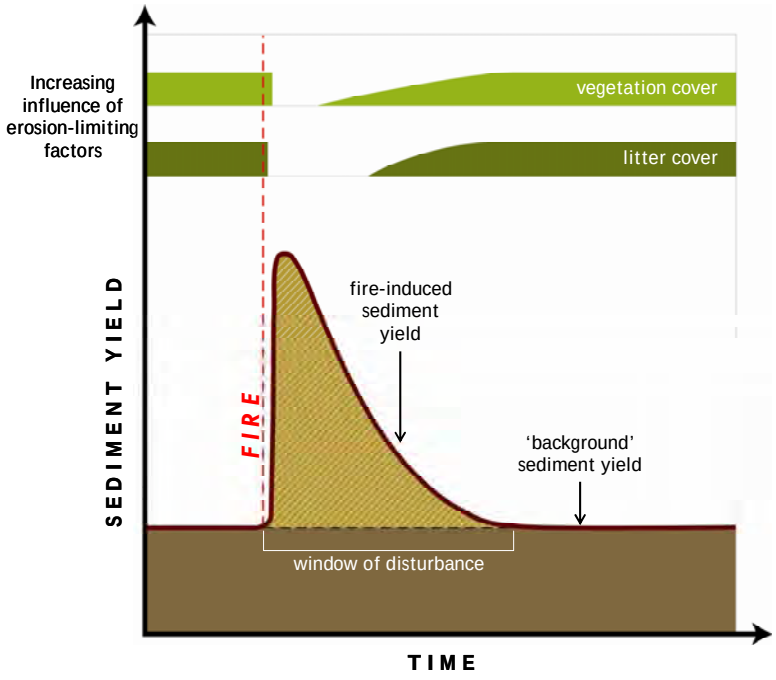

Figure 3-5. Conceptualization of sediment yield and associated vegetation and litter recovery during the fire-induced "window of disturbance" (based on Shakesby and Doerr 2006).

3.2.3.4 Human-induced land cover change

Rates of sediment production and transport on slopes can be significantly altered by human disturbance and changes in land management practices. This most certainly has been the case in the SCR watershed as a whole.

Today, significant changes in the watershed are due to expanding urbanization and changes in the way lands are managed for fire suppression. Historically, major changes followed the arrival of Europeans, the onset of extensive grazing, the California Gold Rush (which accelerated range degradation), agricultural development in the early 1900s, and the population boom that followed World War II (Willis and Griggs 2003).

Effects of European settlement on sediment transport rates

Records indicate that European settlement of coastal southern California led to the degradation of native grasses on slopes starting in the early 1800s, the appearance of widespread barren lands by the mid- to late 1800s, and domination by non-native animals of rangelands by the late 1800s (Pulling 1944). This has led to significant increases in sediment yields in modern times; rates of offshore sedimentation along coastal southern California during the 20th century are many times more than they were in pre-colonial times (Sommerfield and Lee 2003). Moreover, peak rates of sedimentation in estuaries along the California coast appear to have occurred in mid- to late 19th century, coinciding with the peak degradation of rangelands (Willis and Griggs 2003, Warrick and Farnsworth 2009). Conversely, the construction of dams has served to reduce the accentuated sediment yields. In the entire SCR watershed, it has been estimated that dams have reduced the suspended-sediment flux by about 45% since the construction of the watershed's dams (Warrick and Farnsworth 2009).

Effects of conversion to non-native grasses on landslide frequency

The non-native annual grasslands of the Transverse Ranges have been shown to be three times more susceptible to mass wasting than native brush and chaparral (Rice and Foggin 1971). Analysis of 150 landslides at Sedgwick Ranch, north of Santa Barbara, confirms that conversion of native scrub/shrub to exotic-dominated grassland can lead to an increase in landsliding frequency (Gabet and Dunne 2002) and, presumably, sediment yield. When scrub/shrub cover was converted to grassland, soils became unstable (Rice et al. 1969, Orme and Bailey 1971) because the effective cohesion imparted by the shallow-rooted grass was lower than it had been for the deeper-rooted scrub. This instability led to progressive thinning of soils over time by landsliding, which will presumably continue until soils become thin enough that the shallow-rooted grass can stabilize them against failure. There is some indication that slopes may never stabilize under the new land cover, due to the high moisture-holding capacity of root masses (A. Orme, pers. comm., 2005). In any case, sediment yields under non-native grasses are likely to stay higher than they were under natural conditions (unless soil depth eventually adjusts to the new root cohesion). This is an example of a land-use "legacy" on geomorphic processes: the conversion to grassland from native scrub/shrub continues to affect sediment yields long after the land-use change was initiated. Such legacies are important throughout the SCR watershed.

Fire management

Given the dramatic, accelerating effects of fire on hillslope sediment transport (discussed above), it is worth considering whether land management practices have affected fire frequency and thus contributed indirectly to increased sediment production in the watershed.

These considerations were the focus of a recent study of the frequency of big fires parts of the Los Padres National Forest (Santa Barbara and Ventura counties; Mensing et al. 1999). Charcoal

layers in sediment from the offshore Santa Barbara Basin, fed predominately by the SCR, were used to derive a 560-year record of fires with area greater than 200 km^2, revealing that the recurrence interval has remained constant at 20–30 years over the period of record despite substantial changes in management practice. Historical records indicate that the Chumash (coastal and Santa Clara River Valley) and Tantaviam (Santa Clarita Basin) Indians managed vegetation for thousands of years by burning slopes until the late 1700s, when European settlers began practicing fire prevention by, for example, outlawing fires in wildfire-prone areas (Mensing et al. 1999). A more active approach, emphasizing quick-response fire suppression, was adopted in about 1900 and continues to be used today. The unchanging frequency of big fires over a 560-year period that was marked by changing fire management suggests that big fires are a natural part of the environment, occurring regardless of what coastal residents have been doing to suppress or prevent them (Mensing et al. 1999; Keeley and Zedler 2009). This challenges previous interpretations, from analysis of a time series of LANDSAT imagery (Minnich 1983), that big fires are an artifact of changes in vegetation distributions due to increased fire suppression.

Conversely, smaller fires, which may affect sediment yields locally, may be much more closely related to changes in land management practices and the growing urban footprint that has effectively placed people closer to fire-susceptible landscapes. Analysis of data from the Los Angeles County debris basins suggests that encroaching urbanization in southern California wilderness has increased overall fire frequency (Lavé and Burbank 2004), a finding supported regionally by Keeley and Zedler (2009) who concluded that the frequency (not areal extent) of small fires has increased in recent years due to human ignitions. Sediment yields and fire history from the small watersheds that feed the debris basins, considered together, suggest that anthropogenic fires (i.e., fires caused by human inhabitants rather than natural causes) have augmented sediment yields by as much as 400% in particular watersheds, with an average increase using all data equal to 60% (Lavé and Burbank 2004). An earlier analysis of the same debris basin data, however, yielded inclusive results about the effects of fire frequency on sediment yield (Brozovic et al. 1997, Booker 1998), which is also consistent with the findings of Mensing et al. (1999) and Keeley and Zedler (2009) that both found that the incidence of large fires in the region has not increased over time.

Taken together, these disparate results suggest that although the frequency of fire may have increased with human encroachment into fire-susceptible regions, their effects on long-term sediment yield are difficult to quantify precisely. Discussion on sediment yields measured in the debris basins of the SCR watershed is presented below in Section 3.3.2.

3.3 Rates of Hillslope Processes

Watershed topography reflects the interplay between uplift (if any) due to tectonic processes and the sculpting and wearing away of slopes by erosion. In general, high steep mountains occur in areas that have been subjected to sustained rapid uplift, whereas gently sloping terrain is found where uplift is slow or has been followed by long periods of denudation. The linkages between uplift, slope steepness, and erosion imply that slopes should tend to contribute sediment in proportion to their uplift rates over the long term (Burbank et al. 1996). Uplift rates, in turn, are directly related to the tectonic setting and deformation history of the landscape (see Section 1.2.1).

3.3.1 Rates of rock uplift

The mountains of the region have been uplifted over millions of years by a complex series of processes at the boundary between two tectonic plates (Blythe et al. 2000, Meigs et al. 2003). Long-term average uplift rates from the region's mountain ranges are among the fastest on record for the continental United States. In the San Gabriel Mountains, Blythe et al. (2000) looked at the cooling history of mineral grains, which can indicate the age at which rocks now at the surface were buried at least several kilometers deep in the crust. The younger that age, the more rapid has been the exhumation of the overlying material. Based on such data, Blythe et al. (2000) determined likely uplift rates averaging as high as about 1 millimeter per year (mm yr^{-1}) in the eastern San Gabriel Mountains, with less well-determined but significantly lower rates in the western San Gabriel Mountains (Table 3-3). These rates are somewhat lower than the 0.75 to >5 mm yr^{-1} range of uplift rates that has been reported for the Santa Ynez Mountains, which rise along the coast west of the SCR watershed (Metcalf 1994, Trecker et al. 1998, Duvall et al. 2004). A summary of coastal uplift rates for the Transverse Ranges region reports an even broader range of 0.05 to 9 mm yr^{-1} (Orme 1998).

Within the boundaries of the SCR watershed, the San Cayetano and Holser reverse faults have been estimated to have experienced displacement rates of up to 8.8 and 0.4 mm yr^{-1}, respectively (Rockwell 1988, Peterson et al. 1996). Another thrust fault with reported dip-slip estimates is the Santa Susana Fault, which parallels the Holser Fault to the south and trends close to the south-central side of the watershed. Peterson and Wesnousky (1994) and Wills et al. (2008) predicted a relatively high slip rate of up to 5 and 8 mm yr^{-1}, respectively, along this thrust fault, which is in the same order of magnitude of estimates along the San Cayetano Fault to the west.

Table 3-3. Summary of rates of uplift, displacement, sediment production, and sediment yield.

Location	Rate expressed as landscape denudation rate (mm yr^{-1})			Rate expressed in sediment production units (t km^{-2} yr^{-1}) [a]			Reference
	Low	High	Average	Low	High	Average	
Rates of Uplift and Dip-displacement							
San Gabriel Mts.	<0.1	1.0	—	<260	2,600	—	Blythe et al. 2000
Santa Ynez Mts.	0.75	>5.0	—	1,950	13,000	—	Metcalf 1994, Trecker et al. 1998, Duvall et al. 2004
Transverse Ranges (all)	0.05	9.0	—	130	23,400	—	Orme 1998
San Cayetano Fault	1.1	8.8	—	2,900	22,900	—	Rockwell 1988
Holser Fault	>0	0.4	—	>0	1,040	—	Peterson et al. 1996
Santa Susana Fault	>2	>8	—	>5,200	>20,800	—	Peterson and Wesnousky 1994, Wills et al. 2008
Regional Rates of Sediment Production from the Transverse Ranges							
San Gabriel Granite	0.05	0.46	0.29	130	1,200	750	Heimsath 1998, Appendix 2

[a] Uplift rates are converted to sediment production units under the hypothetical assumption that rates of mountain uplift are roughly balanced by rates of hillslope erosion (such that topography does not change over time); conversions from length per unit time into sediment production rate units use bedrock density = 2.6 tonnes m^{-3}. Blank entries indicate rates were not reported or are not applicable.

Rates of bedrock denudation from granitic slopes in the San Dimas Experimental Forest (southern San Gabriel Mountains) have been reported to range from 0.05 to 0.46 mm yr^{-1} (average = 0.29 mm yr^{-1}), based on methods that average denudation rates over 1,000-year time scales (Heimsath 1998). These averages are at the low end of the range of rates implied by the long-term, million-year average uplift rates of the San Gabriel Mountains. Assuming a bedrock density of 2.6 tonnes per cubic meter (t m^{-3}) (typical for granite, which underlies much of the higher relief portions of the watershed), the average bedrock denudation rate corresponds to equivalent soil production rate of 750 tonnes per square kilometer per year (t km^{-2} yr^{-1}).

In summary, published rates of crustal uplift surrounding and within the SCR watershed range by two orders of magnitude from about 0.1 mm yr^{-1} up to 9 mm yr^{-1}, with the fastest rates to the west along the Transverse Mountains and the slowest rates to the south along the San Gabriel Mountains. Based on overall watershed physiography and the limited degree of deformation observed in the sedimentary rocks here (with some notable exceptions in the Pico Formation near the active Santa Susana Fault), we infer that uplift rates in the watershed are at most one to a few mm per year. "Uplift rates," however, do not directly translate into erosion rates or sediment production rates, particularly in still-active mountain belts, and so long-term sediment production averaged across the SCR watershed is probably somewhat less than this range.

To move beyond this broad constraint on predicted sediment production using evidence from tectonic uplift, however, requires a more refined assessment. This geologic-based assessment, however, provides a useful constraint for evaluating the predicted magnitude of sediment production derived using other, independent approaches.

3.3.2 Rates from debris basins and reservoir sedimentation yields

Regional sediment yield data are available from debris basins and some water storage reservoirs in Ventura and Los Angeles counties. These data sources provide a range of sediment yields for the region that can be corroborated by other regional metrics such as tectonic uplift and fault displacement.

For several decades, VCWPD and LADPW have monitored debris basins throughout their respective counties, including the Santa Clara River watershed, in order to protect inhabitants and property from high-energy debris flows. As developments within the counties have expanded, the number of debris basins has expanded. For example, today there are over 100 debris basins in Los Angeles County alone (Lavé and Burbank 2004, LADPW-provided data 2010 [M. Araiza, pers. comm., 2010]). After each major winter storm the debris basins are inspected, and whenever needed, the basins are excavated. Using either a rapid geodetic survey or weighing by truck, volumes of sediment deposition are tracked, which can then be converted to annual and unit-area sediment yields. The counties also maintains over 20 smaller debris retention structures that similarly intercept debris flows; however, sediment removal records are not kept for these structures and therefore they were not considered further in our analysis.

Regional sediment yields were previously estimated by Lavé and Burbank (2004) using sediment removal records from approximately 115 debris basins in Los Angeles County. A majority of those basins are located outside of the SCR watershed in the southern foothills of the San Gabriel Mountains (i.e., the Los Angeles River watershed). Sediments deposited in the debris basins range in size from silts and clays up to boulders; however, because the debris basins are designed to intercept sediment-laden debris flows yet continue to convey water during storm events (in order to avoid having flows overtop the debris basin dams), they preferentially trap the coarser sediments (i.e., sand and gravel, with some silt and likely little clay) (LADPW 2006). Sediment

yields from the debris basins imply 200 to 14,700 t km^{-2} yr^{-1} of sediment production from the watersheds that feed them, with equivalent landscape denudation rates of 0.1 to 5.7 mm yr^{-1} (Lavé and Burbank 2004). As stated above, Lavé and Burbank note that anthropogenic fires have led to 60–400% increase in sediment production rates in the drainage areas contributing to the debris basins compared with the background, "natural" production rates in those drainage areas.

We have used the sedimentation records from seven of the VCWPD-maintained and eleven of the LADPW-maintained debris basins located within the SCR watershed (Table 3-4, Figure 3-6). Of these, two were considered by Lavé and Burbank in their study: Wildwood and William S. Hart debris basins, located near one another in the upper South Fork SCR watershed. All debris basins have variable periods of operation over the past decades. In addition to the VCWPD and LADPW debris basins, sedimentation data from a series of three in-line debris basins situated along upper Castaic Creek at the Castaic Powerplant was used in this analysis (G. Wu, pers. comm., 2010). For the past 35 years, the Los Angeles Department of Water and Power (LADWP) has maintained these three debris basins for the purpose of preventing debris flows from upper Castaic Creek interrupting operations at the Castaic Powerplant, which is positioned along the upstream end of the Castaic Creek arm of Castaic Lake (i.e., Elderberry Forebay). Copies of sedimentation records at the VCWPD, LADPW, and LADWP debris basins are included in Appendix B. An evaluation of the impacts of debris basins on watershed sediment yields and river morphology is presented in Section 4.2.1.7. Finally, sedimentation data from Bouquet, Castaic Lake, and Lake Piru reservoirs were also utilized in our analysis.

Sedimentation in Bouquet Reservoir and Lake Piru were recorded for a relatively short time period just after the closure of those two dams (Appendix B). Minear and Kondolf (2009) compiled these two datasets, adjusted the sediment mass value with measured values in nearby reservoirs, and estimated that the areas contributing to Bouquet Reservoir and Lake Piru had annual sediment yields of approximately 450 t km^{-2} yr^{-1} and 2,400 t km^{-2} yr^{-1}, respectively. Unfortunately, sedimentation rates have not been recorded in either reservoir since these early surveys were conducted (M. Sirakie, pers. comm., 2010). For Castaic Lake, Warrick (2002) estimated long-term suspended sediment yields intercepted by the reservoir by calculating the difference in average annual suspended sediment yield at the County line stream gauge (USGS 11108500) before and after closure of the dam. Warrick's estimate of suspended sediment yield (only) from the areas draining into Castaic Lake was approximately 1,000 t km^{-2} yr^{-1} for the time period of 1972–1996 (with an assumption of the total load being 10-20% higher).

Prior to construction of Castaic Lake Dam, a USGS study (Lustig 1965) estimated the total sediment yield in the area above the un-built dam to be approximately 1,500 t km^{-2} yr^{-1}, which is similar to Warrick's (2002) estimate for the same contributing area. The approach followed by the USGS involved compiling known sediment yields from neighboring watersheds in the San Gabriel Mountains (e.g., Pacoima and Big Tujunga reservoirs), comparing geomorphic parameters in those watersheds to Castaic Creek, plotting a best-fit regression through these data (sediment yield versus watershed area), and then interpreting a sediment yield value for upper Castaic Creek watershed by relating its watershed area to the regression equation (i.e., scaled by its watershed area).

Table 3-4. Debris basin and reservoir sedimentation data used to quantify rates of sediment production in the SCR watershed.

Name	Contributing area (km^2) [a]	Years evaluated (water years)	Annual average sediment yield ($m^3\ yr^{-1}$)	Sediment yield per unit area ($t\ km^{-2}\ yr^{-1}$) [b]	Equivalent denudation rate ($mm\ yr^{-1}$)
Debris basins—Ventura County (LSCR) [c]					
Adams Barranca	21.8	14 (1994–2008)	15,218	1,326	0.70
Arundell Barranca	7.1	39 (1969–2008)	8,392	2,246	1.18
Cavin Road	0.4	39 (1969–2008)	425	2,215	1.17
Fagan Canyon	7.5	14 (1994–2008)	10,378	2,625	1.38
Jepson Wash	3.5	39 (1969–2008)	8,173	4,472	2.35
Real Wash	0.6	41 (1967–2008)	8,031	23,567	12.4
Warring Canyon	2.8	41 (1967–2008)	9,294	6,279	3.30
Debris basins—Los Angeles County (USCR) [c]					
Crocker	1.75	26 (1983–2008)	407	442	0.23
Marston-Paragon	0.49	20 (1989–2008)	75	287	0.15
Oakdale	3.58	5 (2005–2009)	12,293	6,520	3.43
Saddleback #3	0.39	18 (1991–2008)	192	926	0.49
Shadow	2.45	11 (1995–2005)	1,216	942	0.50
Victoria	0.70	7 (2003–2009)	3,812	10,325	5.43
Wedgewood	2.41	5 (2002–2005)	246	194	0.10
Whitney	0.40	5 (2001–2004)	236	1,126	0.59
Wildwood	1.68	41 (1968–2008)	2,311	2,614	1.38
William S. Hart	0.23	25 (1984–2008)	15	124	0.07
Yucca	0.39	9 (1997–2005)	604	2,922	1.54
Castaic Powerplant [d]	173	35 (1975–2009)	74,703 (52,846)	822 (581)	0.43 (0.31)
Reservoirs					
Bouquet Reservoir [e]	35.2	5 (1934–1939)	15,814	449	0.45
Castaic Lake [f]	402	25 (1972–1996)	470,000	1,200	1.2
Castaic Creek watershed above the proposed dam [g]	402	36 (1927–1962)	310,000	1,500	0.8
Lake Piru [e]	1,091	10 (1955–1965)	2,590,000	2,373	2.37

[a] Determined in GIS using USGS 10m DEM.

[b] Assumed bulk density of 1.9 t m^{-3} (after Lavé and Burbank 2004), except for Bouquet, Castaic Lake, and Lake Piru reservoirs (see footnotes [e] and [f] below).

[c] All debris basin sediment removal data provided by VCWPD and LADPW, except for removal records from Castaic Powerplant.

[d] Sediment removal data for the series of three debris basins along Castaic Creek at the Castaic Powerplant was provided by LADWP. The power plant is part of the West Branch of the California Aqueduct and is situated at the upstream end of the Elderberry Forebay of Castaic Lake reservoir. Sediment yield and denudation rate values presented in parenthesis exclude an estimate of ~1 million yds^3 (765,000 m^3) made by LADWP in the reservoir immediately below the debris basins.

[e] Source data: Minear and Kondolf (2009). The assumed bulk density used in the conversion from volume to mass is 1.0 t m^{-3}, based on an average of estimates of 0.96 t m^{-3} and 1.04 t m^{-3} made by Minear and Kondolf (2009) and Warrick (2002), respectively. The estimate from the former were based on all sedimentation data considered in the authors' analysis of California reservoirs, while the estimate from the latter was derived by the author from sedimentation data collected by the USGS in Lake Piru reservoir between 1955–1965 (i.e., Scott et al. 1968).

[f] Source data: Warrick (2002). Method used to determine natural suspended sediment yields from upper Castaic Creek watershed into the reservoir was based on quantifying a reduction factor in suspended sediment discharge at the County line stream gauge (USGS 11108500) for periods before (1956–1971) and after (1972–1996) dam closure. The total sediment yield estimate reported here assumes that the bed material load fraction accounts for 17% of the total load, following assumptions made by Williams (1979) for the USCR at the County line stream gauge. The assumed bulk density used in the conversion from mass back to volume is 1.0 t m^{-3} (see footnote e above for details).

[g] Source data: Lustig (1965). Method used to determine long-term sediment yields from upper Castaic Creek watershed into the proposed reservoir area was based on a comparison of geomorphic parameters for watersheds in the San Gabriel Mountains, for which there was long-term sediment yield data records, and for the Castaic Creek watershed.

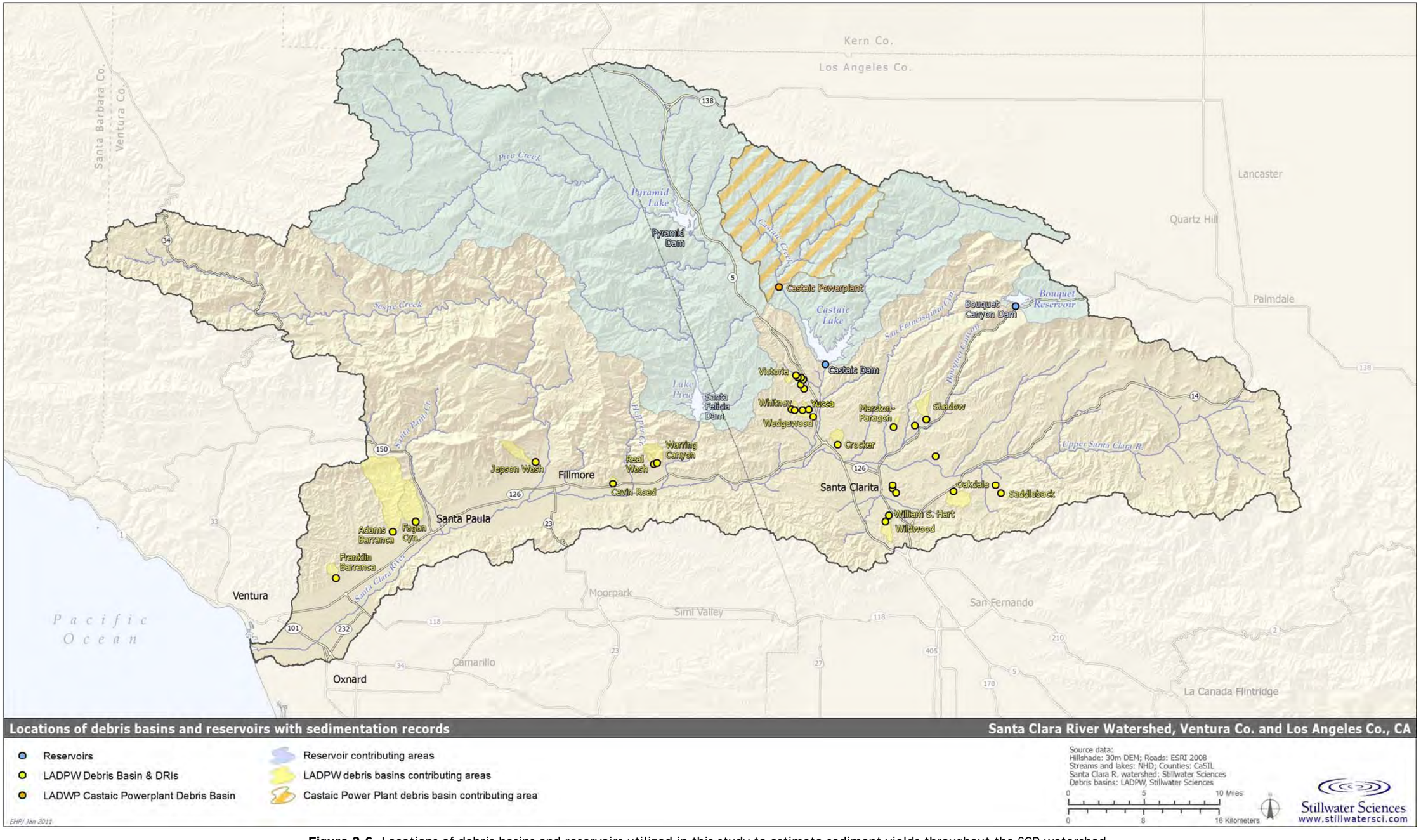

Figure 3-6. Locations of debris basins and reservoirs utilized in this study to estimate sediment yields throughout the SCR watershed.

Annual average total sediment yields, as estimated at the debris basins and reservoirs, range between 30 and 2,600,000 tonnes per year (t yr^{-1}). Figure 3-7 displays the data normalized for watershed size, producing a log-linear regression equivalent to the average per unit area sediment yield. This regression can be refined slightly by excluding the sedimentation records having less than 5 years of data. Converting the volume to mass using a bulk density of 1.9 t m^{-3} for debris-basin sediments (Lavé and Burbank 2004), the slope of the best-fit line indicates an annual average sediment yield of approximately 11.4 million t yr^{-1} for the entire SCR watershed, equivalent to a sediment yield per unit area of **2,700 t km^{-2} yr^{-1}**. This value equates to a landscape denudation rate of about 1.4 mm yr^{-1}, which is within the range estimated by Lavé and Burbank (2004) for the San Gabriel Mountains. This denudation rate is also within the (admittedly broad) range of nearby, localized uplift rates reported above (0.1–9.0 mm yr^{-1}).

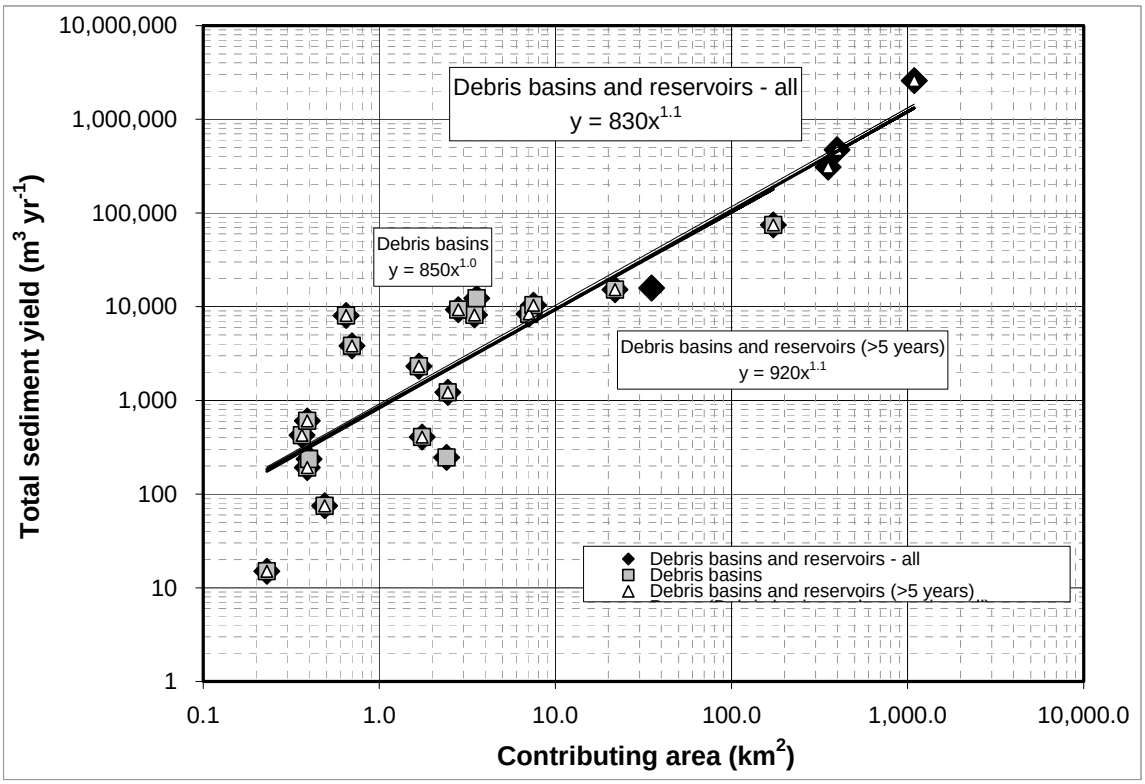

Figure 3-7. Relationship of estimated sediment yields from debris basins and reservoirs in the SCR watershed to their contributing watershed area. Original sediment yield values given volumetrically as reported in the debris basin and reservoir sedimentation data sources.

As can be seen in Table 3-4 and Figure 3-7, there is significant variability in the debris basin and reservoir derived sediment yields, especially in those basins of less than 10 km^2, which is likely due to environmental controls unique to the drainage areas above their structures. From an examination of several potential factors, the primary ones appear to be drainage area size, sediment connectivity, dominant lithology, and hillslope gradient. To a lesser extent, other factors include vegetation cover and land use. Storm events and wildfires are major factors influencing sediment yields at the watershed scale, but likely do not affect the variations seen between the VCWPD and LADPW debris basins because all were operational during the 2005 storm events and have experienced no more than one fire since they began operation. The three exceptions are

at Real Wash, Warring Canyon, and Wildwood debris basins, which also have the longest periods of record and were operational during the 1969 and 2005 storm events and during several wildfires.

3.4 Sediment Delivery from Tributaries to the Upper Santa Clara River Valley

3.4.1 Episodic sediment delivery from tributaries

Over the short term, sediment delivery to the mainstem SCR from its tributaries is likely to be much more episodic than the rate of supply from hillslopes directly adjacent to the river. Storms of all sizes help move sediment down slopes and into channels by rain impact, overland flow, and mass wasting, leading to nearly continuous inputs to tributaries from slopes during the wet season. In the dry season, hillslope sediment production continues via dry raveling (Scott and Williams 1978). In contrast, sediment is delivered from tributaries to the mainstem more episodically, in flows associated with big storms and also in moderate storms that follow fires (Wells 1981; Florsheim et al. 1991).

Sediment transport along the mainstem SCR is even more episodic than delivery of sediment from tributaries. Extreme events associated with major storms are the primary movers of sediment in the watershed, as discussed in greater detail in Section 4.1 below.

3.4.2 Contributions from tributaries along the river corridor

3.4.2.1 Quantification of sediment-production rates in the Feasibility Study subwatersheds

In order to provide an estimate of sediment delivery rates from the Feasibility Study tributaries to the mainstem river corridor, we have quantified sediment-production rates for the tributary drainage areas using sedimentation data from compilation of debris basin and reservoir sedimentation data, as introduced above. For tributaries of the USCR watershed, in addition to Santa Paula and Sespe creeks, we previously derived their sediment-production rates using our Geomorphic Landscape Unit (GLU) approach, which also utilized debris basin and reservoir sedimentation data to calibrate relative rates of sediment production estimated through GIS analysis and field-based observations of hillslope erosion determinants (Stillwater Sciences 2007b, 2010, and 2011a).

Table 3-5 summarizes our sediment-production estimates for each of the Feasibility Study subwatersheds, listed in order of greatest to lowest sediment-production rate per unit area. The total production rate for the entire SCR watershed (ignoring influence of dams) is estimated to be 8.2 million t yr^{-1}, or **2,000 t km^{-2} yr^{-1}**, which was derived by summing production rates from all contributing subwatersheds. This value compares modestly well to the total watershed production rate extrapolated from the debris basin and reservoir sedimentation rating curve (2,700 t km^{-2} yr^{-1}; Figure 3-7).

Figure 3-8 graphically represents the relative differences in sediment production from the majority of these subwatersheds. For Bouquet Canyon, Castaic Creek, and Piru Creek, we split their watersheds into upper and lower portions, divided at their respective (lowermost) dams. As represented in this figure, the subwatersheds predicted to exhibit the greatest sediment-production rates per unit area (>3,000 t km^{-2} yr^{-1}) are located near the western side of the Santa Clarita Basin

where landscapes are characterized by sparse vegetation cover, weak lithologies, and moderate to steep slopes (rainfall is also greater in this part of the watershed). Specifically, these subwatersheds are lower Castaic Creek, and Gavin, Lyon, Pico, Portrero, San Martinez Grande, San Martinez Chiquito, Towsley, and Violin canyons. Most of these tributaries have direct connectivity with the mainstem river as they are positioned close to the river in the Santa Clarita Basin. The presence of debris basins and debris retention inlets in portions of lower Castaic Creek (e.g., Hasley Canyon area) and the South Fork SCR do, however, effectively reduce the total sediment-production rates (particularly coarse-grained material) from these subwatersheds.

In contrast, the subwatersheds predicted to exhibit the lowest sediment-production rates per unit area (<1,000 t km^{-2} yr^{-1}) are located in the eastern portions of the USCR watershed: Acton, Aliso, Bear, Kentucky Springs, Soledad (eastern-most end of USCR watershed), Trade Post, and upper Bouquet canyons. These landscapes are also characterized by less erodible bedrock types (more competent igneous and sandstone rocks).

Overall, the major subwatersheds with the greatest sediment-production rates in terms of tonnes per year are (listed in order of greatest to lowest) are Sespe Creek, the remainder of the LSCR watershed, lower Castaic Creek (below Castaic Dam), South Fork SCR, Bouquet Canyon, Santa Paula Creek, and San Francisquito Canyon. These production rates approximately represent the sediment contribution from these subwatersheds, insofar as each have direct connection with the mainstem river and have been found to have relatively minimal sediment storage potential along their respective channels.

Discussion on the effects of infrastructure on sediment delivery processes is presented below in Section 4.2.

Table 3-5. Predicted sediment production results for the SCR Feasibility Study subwatersheds. [a]

Watershed	Major stream name	Area (km^2) [b, c]	Average annual sediment production ($t\ yr^{-1}$) [b, c]	Sediment production per unit area ($t\ km^{-2}\ yr^{-1}$) [b, c]
USCR	Towsley Canyon	14.9	69,000	4,600
	S. M. Grande Canyon	8.6	38,000	4,400
	Lyon Canyon	3.6	15,000	4,200
	Gavin Canyon	29.4	120,000	4,200
	Potrero Canyon	11.6	47,000	4,100
	Violin Canyon 2	9.6	37,000	3,900
	S. M. Chiquito Canyon	12.4	49,000	3,900
	Pico Canyon	17.6	67,000	3,800
	Violin Canyon 1	15.1	57,000	3,800
	So. Fork SCR	116.2	320,000	2,800
	Long Canyon	4.0	10,000	2,600
	Lion Canyon	2.2	5,600	2,600
	Hasley Canyon	20.7	50,000	2,400
	Vasquez Canyon	11.1	26,000	2,400
LSCR	LSCR (remainder) [d]	529.7	1,200,000	2,200
	Santa Paula Creek	117.1	250,000	2,200

Watershed	Major stream name	Area (km^2) [b, c]	Average annual sediment production ($t\ yr^{-1}$) [b, c]	Sediment production per unit area ($t\ km^{-2}\ yr^{-1}$) [b, c]
USCR	Haskell Canyon	28.4	60,000	2,100
	Plum Canyon	8.2	17,000	2,100
	Newhall Creek	21.3	44,000	2,100
LSCR	Piru Creek	1,132.2 (39.3)	2,700,000 (76,000)	2,400 (1,900)
USCR	Tick Canyon	14.8	30,000	2,000
	Placerita Creek	23.1	44,000	1,900
	Dry Canyon	19.7	35,000	1,800
LSCR	Sespe Creek	673.0	1,200,000	1,800
	Harmon Barranca	11.6	21,000	1,800
USCR	Bouquet Canyon [c]	180.4 (145.2)	310,000 (280,000)	1,700 (1,900)
	USCR (remainder) [d]	268.6	460,000	1,700
	Castaic Creek [c]	524.6 (122.6)	860,000 (370,000)	1,600 (3,000)
	Mint Canyon	75.8	120,000	1,600
	Texas Canyon	28.2	46,000	1,600
	San Francisquito Canyon	134.6	220,000	1,600
	Young Canyon	7.3	10,000	1,400
	Escondido Creek	24.6	32,000	1,300
	Agua Dulce Canyon	76.1	98,000	1,300
	Red Rover Mine	5.7	7,100	1,200
	Sand Canyon	33.0	41,000	1,200
	Hughes Canyon	8.0	9,400	1,200
	Acton Canyon	54.4	64,000	1,200
	Oak Springs Canyon	14.6	17,000	1,200
	Kentucky Springs	23.5	27,000	1,100
	Soledad Canyon	23.2	25,000	1,100
	Iron Canyon	6.9	7,500	1,100
	Bear Canyon	15.1	16,100	1,000
	Aliso Canyon	63.2	64,000	1,000
	Trade Post	6.7	6,600	980
	Acton Canyon 2	6.5	6,300	980
	Gleason Canyon	15.5	12,000	780
Total SCR watershed		***4,204 (2,674)***	***8,200,000 (5,100,000)***	***2,000 (1,900)***

[a] Locations of the subwatersheds with their relative sediment production values are shown in Figure 3-8.
[b] Values given for the major streams with a direct connection with the SCR include the total area and sediment-production rate for that subwatershed (i.e., includes values from any tributary subwatersheds).
[c] Areas and sediment-production rates for regulated areas below dams are given in parenthesis.
[d] Portion of the LSCR and USCR watersheds excluding the major stream watersheds listed in this table.

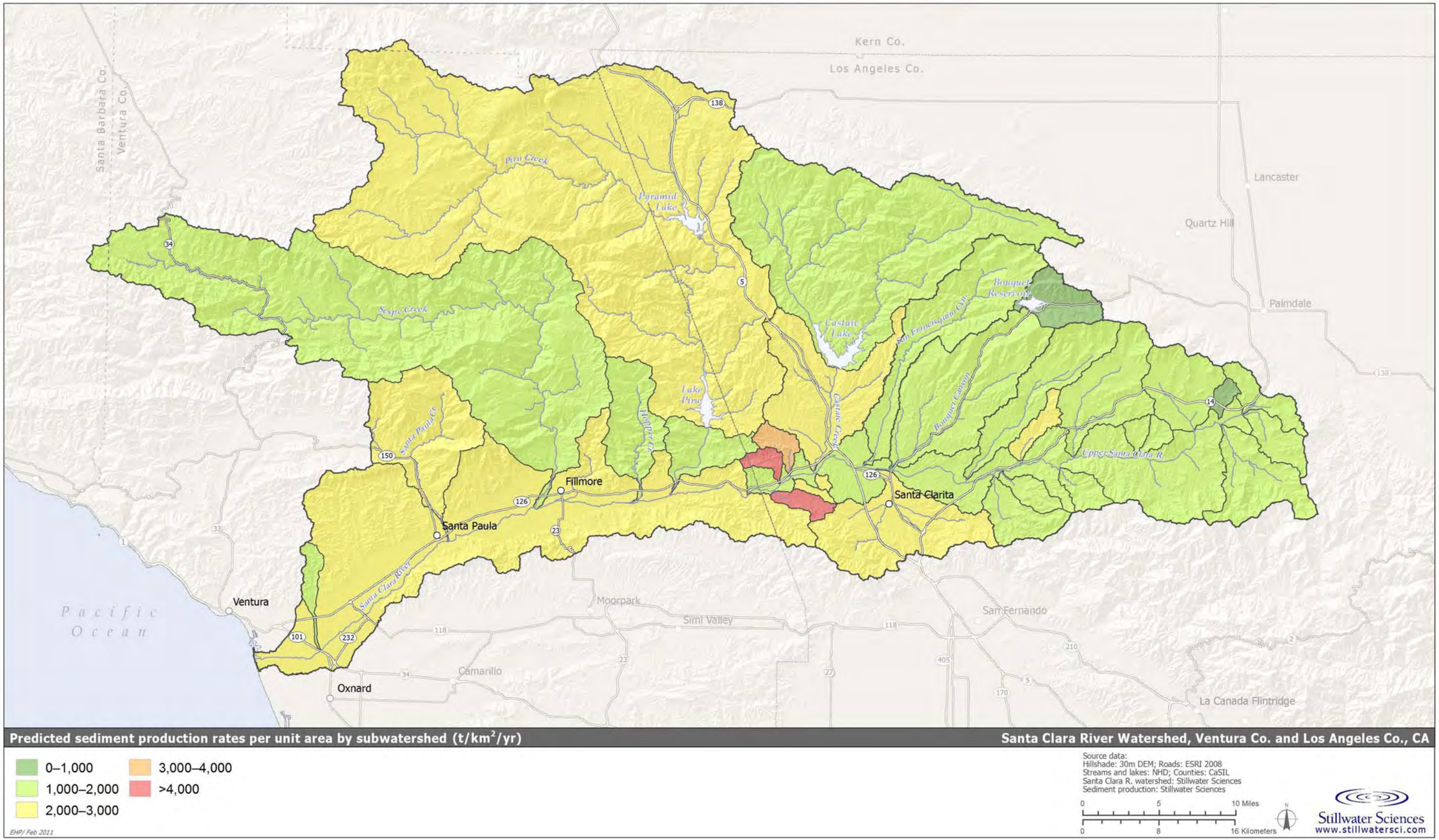

Figure 3-8. Predicted sediment-production rates per unit area by Feasibility Study subwatershed in the SCR watershed.

3.4.2.2 Tributary sediment yields from sediment gauging data

Hillslope sediment delivery to streams is ultimately reflected, to some degree, in the load that actually gets transported by the streams. Rating curves, which relate suspended sediment concentration to discharge, can be used in conjunction with discharge records to calculate an estimate of what suspended sediment discharge has been over the period of the discharge record, which in this case dates back to 1928 (see Section 4.1 for additional details on sediment discharge).

Suspended sediment yields for the major subwatersheds of the SCR are summarized in Figure 3-9 (after Warrick and Mertes 2009)[2]. An estimated 910 t km^{-2} yr^{-1} and 1,600 t km^{-2} yr^{-1} of suspended sediment are generated in the areas upstream of the Santa Felicia and Castaic dams, respectively, with essentially all of it being impounded upstream of the river corridor. The authors estimated that roughly 740 t km^{-2} yr^{-1} of suspended sediment originates from the area upstream of the gauge at the County line, which is comparable to our estimate of total load at the gauge (see Section 4.1 below). Sespe and Hopper creeks were found to contribute similarly high rates of 2,300 t km^{-2} yr^{-1} and 2,700 t km^{-2} yr^{-1}, respectively, at their junctions with the SCR. The highest suspended sediment yield—5,300 t km^{-2} yr^{-1}—is observed in the LSCR subwatershed, where weak Plio-Pleistocene siltstones predominate, and presumably contribute to enhanced erosion. This hypothesis is corroborated by the fact that suspended sediment concentrations within the nearby Santa Ynez Mountains correlate strongly with percent of contributing area underlain by Plio-Pleistocene rocks (Warrick and Mertes 2009).

In terms of total suspended yield in tonnes per year, the areas with the greatest contributions to the SCR were found to be the remaining portions of the LSCR watershed (which includes Santa Paula Creek [4.3 million t yr-1]) and Sespe Creek (1.5 million) (Warrick and Mertes 2009).

3.4.3 Summary of rates of hillslope processes

The rates of hillslope sediment production and transport in the SCR watershed, along with its major subwatersheds, are summarized in Table 3-6. The debris basin data from Los Angeles and Ventura counties and reservoir sedimentation data from Bouquet, Castaic Lake, and Lake Piru reservoirs, taken together, imply bedrock lowering rates of 0.1 to 12 mm yr^{-1}, which are quite consistent with the range of long-term rates of uplift (0.1–9 mm yr^{-1}) that have been inferred for the region's mountain ranges (see above).

The suspended sediment yields imply sediment-production rates that are roughly consistent with those implied by the debris basin and reservoir data.

As part of our USCR study (Stillwater Sciences 2011a), we determined landscape erosion rates from cosmogenic nuclide sediment dating analyses in select subwatersheds, including one sample at the County line to get a USCR watershed-wide estimate. This sample's result agreed remarkably well with the sediment-production rate estimate derived from our GLU approach—1,900 t km^{-2} yr^{-1} in both cases. A parallel sediment dating study being conducted by others in the LSCR watershed also determined landscape erosion rates again very similar to our sediment-production estimates made in that part of the SCR watershed (B. Romans, pers. comm., 2011).

[2] Subwatersheds delineated in the Warrick and Mertes (2009) analysis differ slightly from those presented elsewhere ("Feasibility Study subwatersheds") in this report, based on the availability of suspended sediment data.

Perhaps the most significant result in Table 3-6 is the substantial variability in rates implied by each of the datasets. For example, long-term uplift rates vary by two orders of magnitude, as do the dip-displacement rates for the San Cayetano Fault. The upper end of the range of debris basin data (Table 3-4 and Figure 3-7) implies sediment-production rates that are among the fastest ever recorded, consistent with rates that have been reported for rapidly uplifting mountains in Taiwan, New Zealand, and Tibet. In comparison, rates from the nearby Sierra Nevada are ten to one hundred times slower; rates from the Appalachian Mountains are more than one thousand times slower (Bierman 2004). Hence, sediment production on slopes in the SCR watershed appears by all accounts to be enormous, at least in the context of the sediment-production rates from other watersheds in less tectonically active areas in California and around the world.

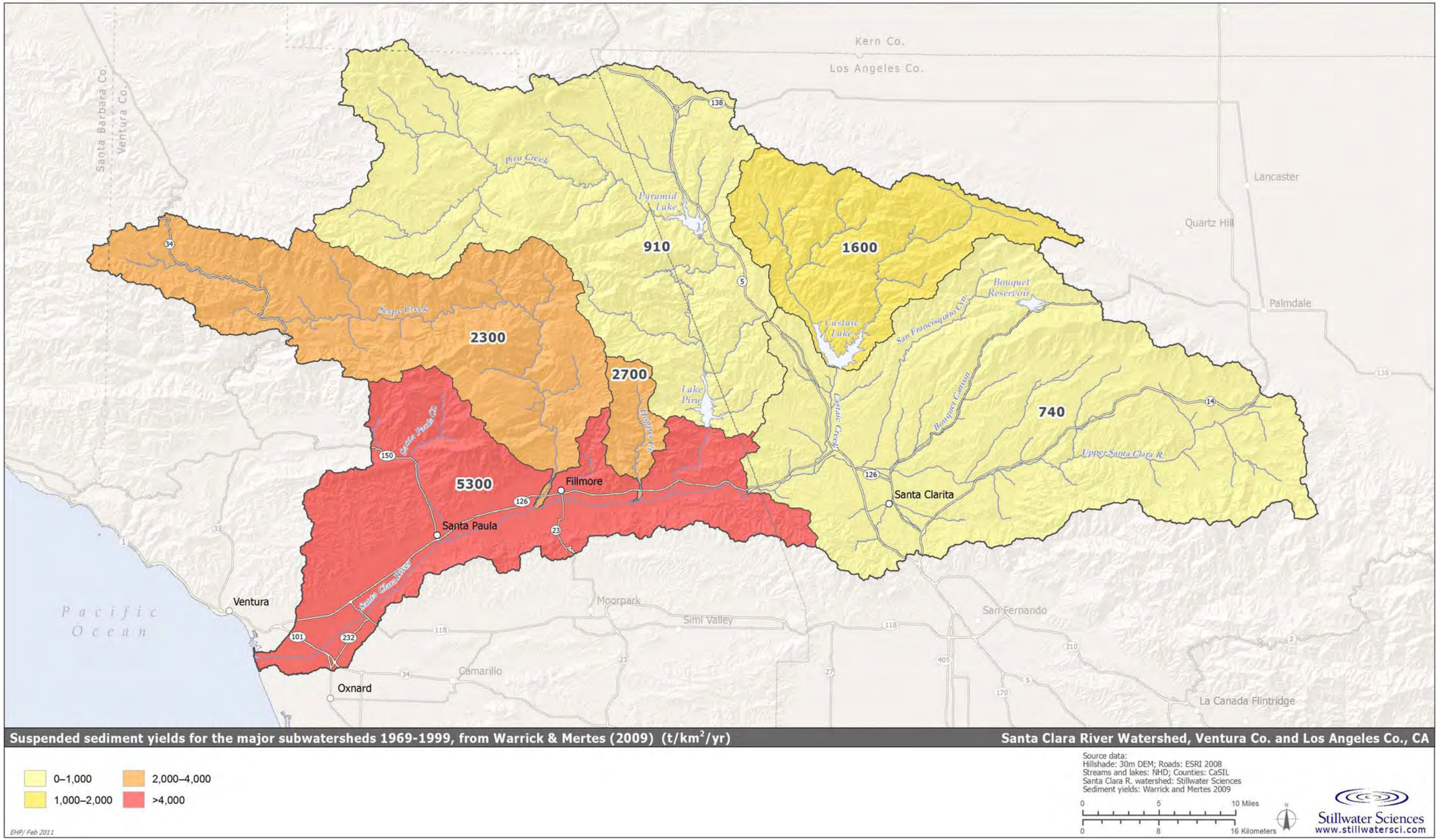

Figure 3-9. Suspended sediment yield by major subwatershed for the period 1969-2009 (modified from Warrick and Mertes 2009). [Note: subwatersheds delineated by the authors differ slightly from those presented in this report.]

Table 3-6. Comparison of sediment yields in the Santa Clara River watershed as derived from various approaches.

Major Subwatershed [a]	Drainage area (km^2)	Sediment production rate per unit area ($t\ km^{-2}\ yr^{-1}$)							Sediment yield per unit area ($t\ km^{-2}\ yr^{-1}$)		
		Stillwater Sciences estimate [b]	Regional rates of sediment production [c]						Cosmogenic nuclide sediment dating [d]	Sediment discharge records [e]	
			Rock uplift and dip-displacement					Landscape denudation		Full hydrologic record	1969–2009
			San Gabriel Mtns [i]	Santa Ynez Mtns [ii]	Transverse Ranges [iii]	San Cayetano Fault [iv]	Holser Fault [v]	Santa Susana Fault [vi]	San Gabriel Granite [vii]	Stillwater Sciences' estimate	Warrick and Mertes (2009)
Upper Castaic Creek (above Castaic Dam)	402	1,200	<260–2,600	1,950–13,000	130–23,400	2,900–22,900	0–1,040	5,200–20,800	130–1,200	na	na	1,600
USCR (below dams) [f]	1,240	1,900								1,900 ±200	720 (1953-2009)	740
Upper Piru Creek (above Santa Felicia Dam)	1,093	2,400								na	na	910
Hopper Creek	62	2,000									na	2,700
Sespe Creek	673	1,800									1,520 (1928-2009)	2,300
Santa Paula Creek	117	2,200									na	5,300
LSCR (below dams) [g] (not including Upper Piru, Hopper, Sespe, and Santa Paula)	698	2,200									na	
Total (below dams)	2,674	1,900								1,900 ±300	660 (1950-2004)	1,675

a. See Figure 3-9 for subwatershed locations; average annual sediment yields adapted from Warrick and Mertes (2009) are presented therein.
b. Derived from either our Geomorphic Landscape Unit (GLU) approach (i.e., Upper Castaic Creek, USCR, Sespe Creek, and Santa Paula Creek) or from our regression analysis that estimated sediment production rates based on a subwatershed's given drainage area (i.e., Upper Piru Creek, Hopper Creek, and LSCR).
c. Uplift and dip-displacement rates are converted to sediment production units under the hypothetical assumption that rates of mountain uplift are roughly balanced by rates of hillslope erosion (such that topography does not change over time); conversions from length per unit time into sediment production rate use bedrock density = 2.6 tonnes m^{-3}. Information sources are:
   i. Blythe et al. 2000
   ii. Metcalf 1994, Trecker et al. 1998, Duvall et al. 2004
   iii. Orme 1998
   iv. Rockwell 1988
   v. Peterson et al. 1996
   vi. Peterson and Wesnousky 1994, Wills et al. 2008
   vii. Heimsath 1998 (Appendix 2)
d. Cosmogenic nuclide sediment dating results for the USCR from Stillwater Sciences (2011a). Preliminary results for the entire SCR watershed from an ongoing, independent study (B. Romans, pers. comm., 2011).
e. Calculated from stream gauge data using established sediment discharge rating curve; Stillwater Sciences' estimates utilized entire available hydrologic record, while Warrick and Mertes (2009) focused on period that encapsulated the sediment discharge measurements. Warrick and Mertes combined Santa Paula Creek with the remainder of the LSCR watershed.
f. Includes all of the USCR watershed, except for upper Castaic Creek (i.e., above Castaic Lake and Bouquet Canyon dams).
g. Includes all of the LSCR watershed, except for upper Piru Creek (i.e., above Santa Felicia Dam), Hopper, Sespe, and Santa Paula creeks.

na = indicates rates were not derived or are not applicable.

3.5 Conceptual Model of Hillslope Processes and Implications for the Santa Clara River Geomorphology

Observations highlighted above, synthesized in Figure 3-10, have important implications for the morphologic evolution of the SCR. Foremost is the fact that sediment delivery rates to the mainstem are inferred to be extremely rapid are among the fastest on record for the world, due to rapid uplift, episodic earthquakes, seasonally intense rainfall, and frequent fires. By extension, the sediment load delivered to the mainstem is likewise enormous, with significant repercussions for fluvial processes in the river corridor (see also Chapter 4 for further details).

Another implication is that sediment loading from tributaries, while apparently quite rapid, is inherently difficult to precisely predict. This is because it depends on numerous factors besides the rate of supply of sediment from hillslope erosion. Prediction of average annual sediment loading is further complicated by the fact that sediment delivery is episodic, depending on the frequency, magnitude, and timing of stochastic events such as storms, fires, landslides, and earthquakes. Of critical importance, in particular, is how (and whether) these events coincide with one another. Big fires followed by droughts, for example, probably contribute less sediment to the mainstem than they would if they were followed by big storms. Similarly, earthquake-induced landslides in a dry year might become stabilized where they initially come to rest, contributing minimally to sediment delivery; there is some indication that this occurred after the 1994 Northridge earthquake (Orme, pers. comm., 2005). Hence, rates of sediment supply to the river, as well as the relative contributions from the various subwatersheds, are reflections of the complex interactions of probabilistic processes.

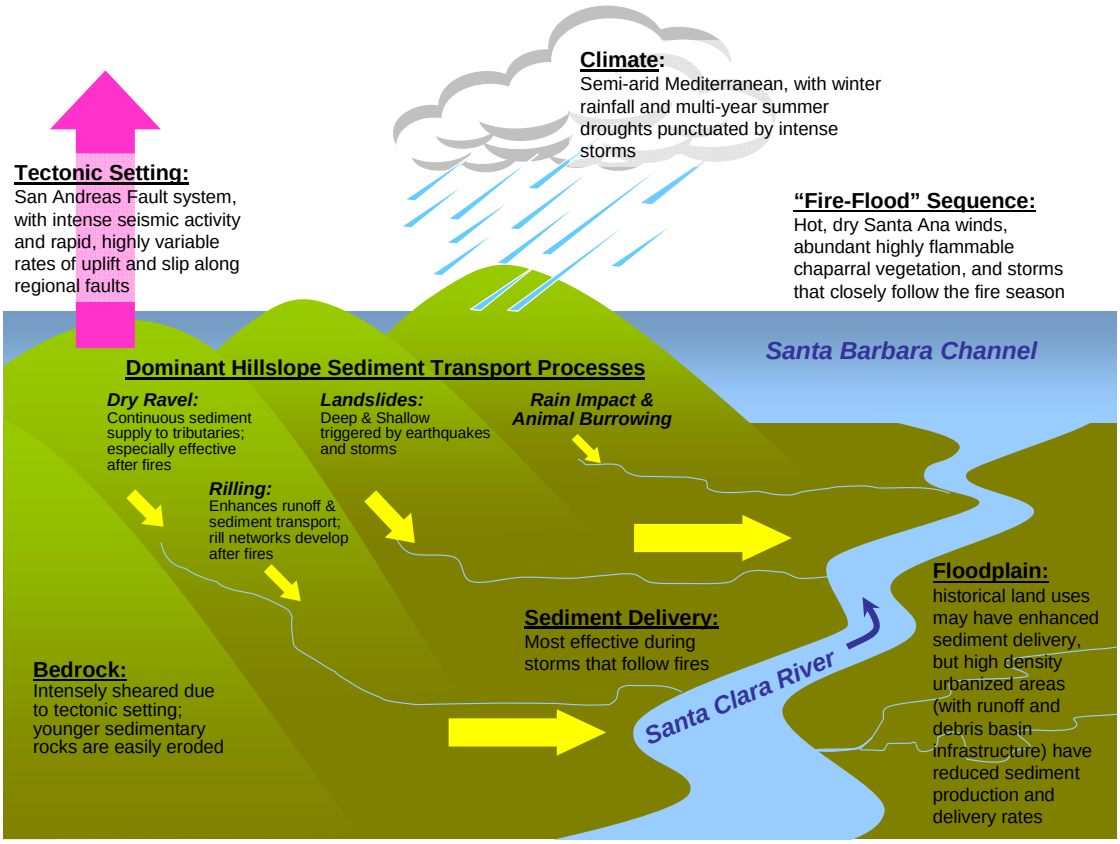

Figure 3-10. Illustration of conceptual model of hillslope processes in the SCR watershed.

4 TRIBUTARY AND MAINSTEM SEDIMENT TRANSPORT AND MAINSTEM MORPHOLOGICAL CHANGE

This chapter focuses on the factors affecting the morphology of the mainstem SCR and its major tributaries. First, we present a summary on the characteristics of sediment transport and the episodic events that convey the vast majority of sediment through the drainage network and river channel. Specific elements of water system and urban infrastructure and their potential effects on the river's morphology and sediment transport rates are discussed next. In the following section, we present detailed descriptions of the geomorphically-based river reaches and the major tributaries. In support of these descriptions are the results of historical changes in the active channel widths and the bed levels of the mainstem river reaches over the past 80 years. The chapter concludes with a comprehensive summary of the reach-level dynamics and overall fluvial geomorphic processes along the SCR.

4.1 Frequency and Magnitude of Sediment Transport

Sediment transport processes throughout the SCR and its major tributaries, such as the unregulated and relatively undeveloped Sespe Creek, are dominated by extreme events associated with their highest flows (Table 4-1). These events transfer water and sediment from the hillslopes to the drainage network, and they are integral to changes in form of the mainstem SCR and its floodplain over time. The exchange of sediment between the river channel and floodplain during flood events (i.e., episodes of erosion and deposition) determines both the "hazards" and the "assets" of the river corridor. In an apparent contradiction, the hydrologic and geomorphic processes that create hazards (such as flooding, unwanted bed and bank erosion, and deposition) are the same processes that help sustain river ecosystems by creating assets (such as aquatic and riparian habitat diversity). Hence, understanding the fluvial geomorphic processes in the watershed is a necessary precursor for understanding both the risks and the opportunities of the river corridor.

This assessment of frequency and magnitude of sediment transport in the watershed focuses on three points of interest: USCR at the County line, Sespe Creek near Fillmore, and LSCR at Montalvo, where each corresponds with a long-term USGS stream gauge location that additionally includes sediment discharge measurements. Additionally, Sespe Creek was chosen here to represent a major tributary in the system that could be likened to the other large tributaries. It can also be considered to potentially represent historical conditions in the now regulated drainages of Piru and Castaic creeks, two other major tributaries with large drainage areas and high elevation relief.

Table 4-1. Flow discharge and recurrence intervals (RI) for the largest recorded floods on the USCR at the County line gauge, Sespe Creek at the Fillmore gauge, and LSCR at the former Montalvo gauge.

Date	USCR at the County line [a]			Sespe Creek near Fillmore [b]			LSCR at Montalvo [c]		
	Flow		RI (years)	Flow		RI (years)	Flow		RI (years)
	($m^3 s^{-1}$)	(cfs)		($m^3 s^{-1}$)	(cfs)		($m^3 s^{-1}$)	(cfs)	
Mar. 2, 1938	765 [d]	27,296 [d]		1,590	56,000	12.0	630	120,000	18.0
Jan. 23, 1943	*no data*	*no data*		1,250	44,000	8.0	2,300	80,000 [d]	-
Apr. 3, 1958	200	7,070	3.6	804	28,400	4.8	1,480	52,200	4.9
Feb.10–11, 1962	260	9,100	4.1	720	25,600	4.2	1,350	47,700	4.2
Dec. 29, 1965	910	32,000	29.0	610	21,600	3.6	1,470	51,900	4.5
Dec. 6, 1966	*no data*	*no data*		610	21,600	3.4	990	35,000	3.2
Jan. 25, 1969	**1,950**	**68,800**	**58.0**	1,700	60,000	14.4	**4,670**	**165,000**	**54.0**
Feb. 25, 1969	1,770	62,500	-	1,270	45,000	-	4,300	152,000	-
Feb. 11, 1973	360	12,800	7.3	1,080	38,300	6.0	1,650	58,200	5.4
Feb. 9–10, 1978	650	22,800	11.6	2,070	73,000	36.0	2,790	98,610	-
Mar. 4, 1978	470	16,600	-	1,410	49,800	-	2,890	102,200	9.0
Feb. 16, 1980	390	13,900	8.3	1,150	40,700	6.5	2,300	81,400	6.0
Mar. 1, 1983	870	30,600	14.5	1,590	56,000	12.0	2,830	100,000	7.7
Feb. 14–15, 1986	350	12,300	5.8	*no data*	*no data*		1,240	43,700	3.4
Feb. 12, 1992	350	12,300	5.8	1,250	44,000	8.0	2,940	104,000	10.8
Jan. 10, 1995	480	17,100	9.7	1,840	65,000	24.0	3,110	110,000	13.5
Feb. 3, 1998	280	9,990	4.5	1,770	62,500	18.0	*data gap*	*data gap*	
Feb. 23, 1998	*no data*	*no data*		*data gap*	*data gap*		2,380	84,000	6.8
Jan. 10, 2005	910	32,000	29.0	**2,420**	**85,300**	**72.0**	3,850	136,000 [e]	27.0
Feb. 24, 2005	*data gap*	*data gap*		*data gap*	*data gap*		2,330	82,200 [e]	-
Apr. 4, 2006	*data gap*	*data gap*		1,260	44,600	9.0	*no data*	*no data*	
Jan. 25-27, 2008	90	3,100	2.4	870	30,800	5.1	*no data*	*no data*	

[a] Source: USGS 11108500 (WY 1953-1996) and USGS 11109000 (WY 1928-1932, 1997-present; RI base don available peak discharge record: WY 1953-2009)
[b] Source: USGS 11113000 (complete gauge record : WY 1912-1913, 1928-1985, 1991-1992, 1993-present; RI based on available peak discharge record : WY 1933-2009)
[c] Source: USGS 11114000 (WY 1928-2004; decommissioned; RI based on available peak discharge record: WY 1932-2004, with 2005 estimate at Freeman Diversion)
[d] Estimated value (no gauging information available)
[e] Estimated at Freeman Diversion [source: VCWPD]
no data = gauge malfunction or outside of years of gauge operation
data gap = currently unable to access the data
- = RI not calculated for second greatest peak discharge in a single year
Largest peak flows for a given stream gauge are presented in bold

4.1.1 Sediment discharge

Sediment discharge dynamics in the SCR and Sespe Creek—the largest, unregulated drainage with relatively minimal development-related impacts—were examined in two ways. First, the daily mean flow records for the USCR, Sespe Creek, and the LSCR (i.e., entire SCR watershed) were each combined with their associated gauge-specific sediment-rating curves to determine sediment yields both for individual flood events and on an annual basis. Secondly, the sediment-rating curves were each combined with the associated distribution of daily mean flows (i.e., flow frequency) to determine the magnitude and frequency of sediment transporting flows within each portion of the watershed and to investigate their respective "dominant discharges" (i.e., the range of discharges that transports the most sediment over time).

Flow and sediment discharge data used in the analysis were from the following three locations in the watershed and spanned the following years of record:

- USCR—downstream end near the County line (USGS 11108500 and 11109000) between WY 1953–2009 (Figure 4-1);
- Sespe Creek—downstream end near Fillmore (USGS 11113000) between WY 1928–2009; and
- LSCR—downstream end of entire SCR watershed at Montalvo and the Highway 101 bridge (USGS 11114000) between 1928–2004 (gauge decommissioned thereafter).

The locations of the USCR and Sespe Creek gauges are shown on Figure 1-6. The location of the former Montalvo gauge is not shown here (only active gauges are shown); it was situated on the LSCR at the Highway 101 bridge crossing, just upstream of the active LSCR gauge currently operated by VCWPD (VCWPD #723).

The daily mean flow data from the three gauges were compiled for the available years of record (Figures 4-1a, 4-2a, and 4-3a) and flow frequency was determined by dividing the daily mean flow into log-based bins (i.e., bins were defined by increasing the exponent by 0.1) ranging from 10^{-2} (0.01) $m^3 s^{-1}$ to 10^3 (1,000) $m^3 s^{-1}$ and fitting a regression through the relationship (Figures 4-1b, 4-2b, and 43b).

The sediment discharge rating curves for each gauge were calculated as a combination of the suspended sediment load and bedload, using the measurements at each gauge by the USGS during the 1960s and 1970s (Williams 1979). The (measured) suspended sediment discharge data (and the associated flow data) for each gauge was compiled and a regression was fitted through the associated relationship. Bedload discharge at the USCR/LSCR and Sespe Creek gauges, not directly measured, was assumed to be 6% and 10%, respectively, of the total suspended load. For the LSCR gauge, the bedload-to-total-load fraction data was based on Williams (1979) measurements and calculations (from a modified Einstein sediment transport equation). For the USCR and Sespe Creek gauges, the bedload-to-total-load fractions were based in part on Williams' (1979) initial values for those two gauges (from 17% and 33%, respectively) but further refined using more recently collected sediment discharge measurements (e.g., 2005 measurements at USCR gauge and late-1970s measurements at Sespe Creek gauge) and other published estimates made in the SCR and other southern California coastal watersheds (e.g., Simons, Li & Associates 1987, Brownlie and Taylor 1981, Willis and Griggs 2003). In combination, these additional data support the use of smaller fractions than Williams' original recommendation at both gauges. Combining the suspended load and bedload rating curves gives overall total sediment rating curves for the USCR, Sespe Creek, and the LSCR (Figure 4.1c, 4.2c, and 4.3c).

a)

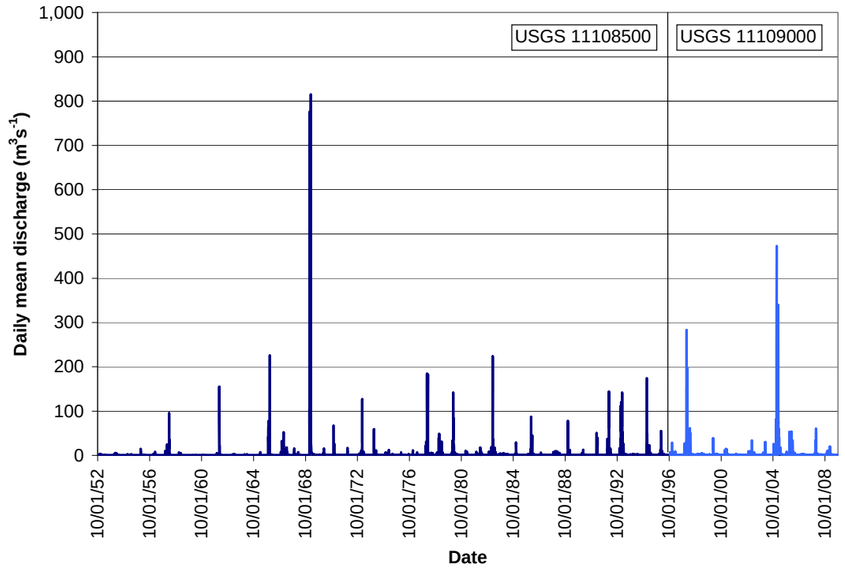

Figure 4-1a. Daily mean discharge for the USCR at the County line (USGS 1118500 and 11109000) between WY 1953 and 2009.

b)

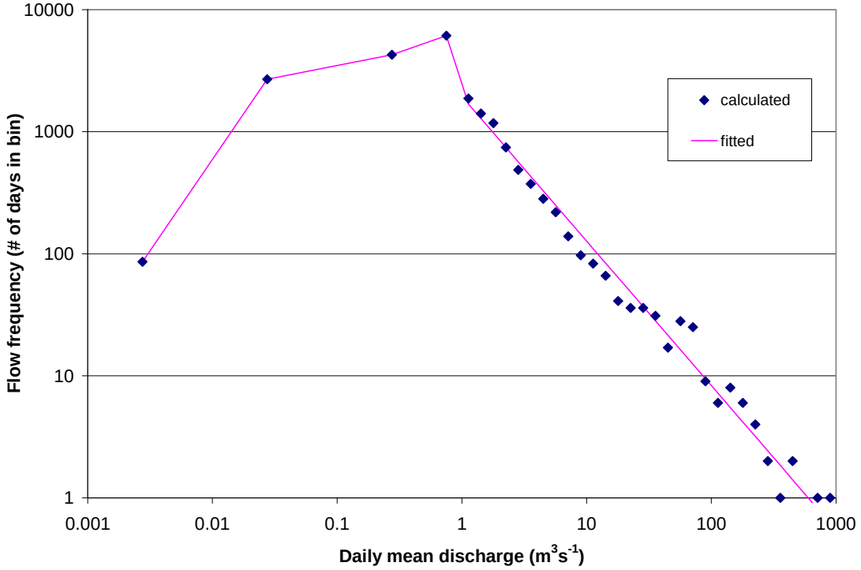

Figure 4-1b. Daily mean flow frequency distribution for the USCR at the County line (USGS 1118500 and 11109000) between WY 1953 and 2009.

c)

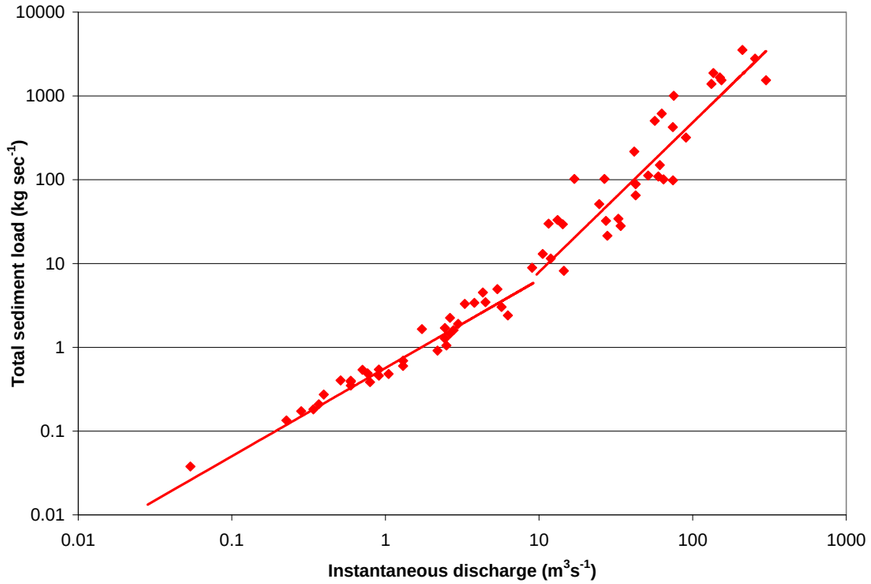

Figure 4-1c. Total sediment load (suspended load + bedload) rating curve for the USCR at the County line (USGS 11108500 and 11109000).

d)

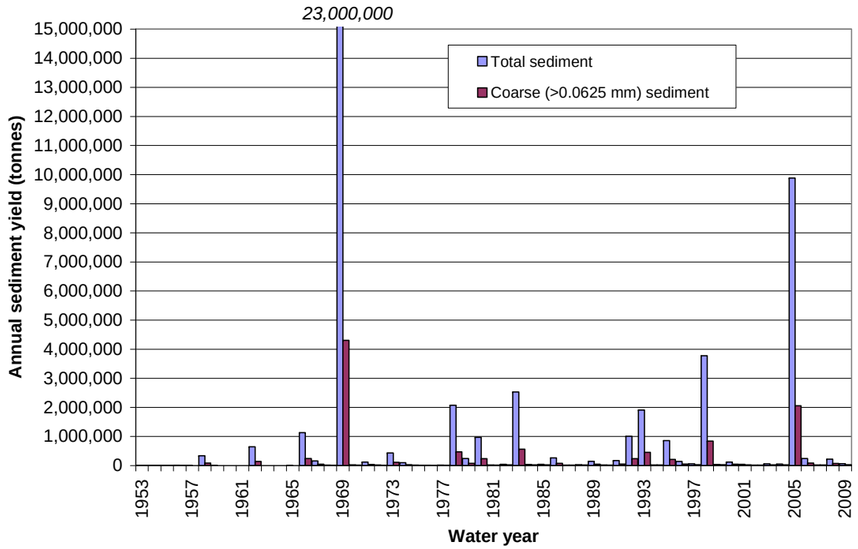

Figure 4-1d. Calculated total sediment yield (suspended load + bedload) and coarse (>0.0625 mm) sediment yield for the USCR at the County line between 1953 and 2009 (USGS 1118500 and 11109000).

a)

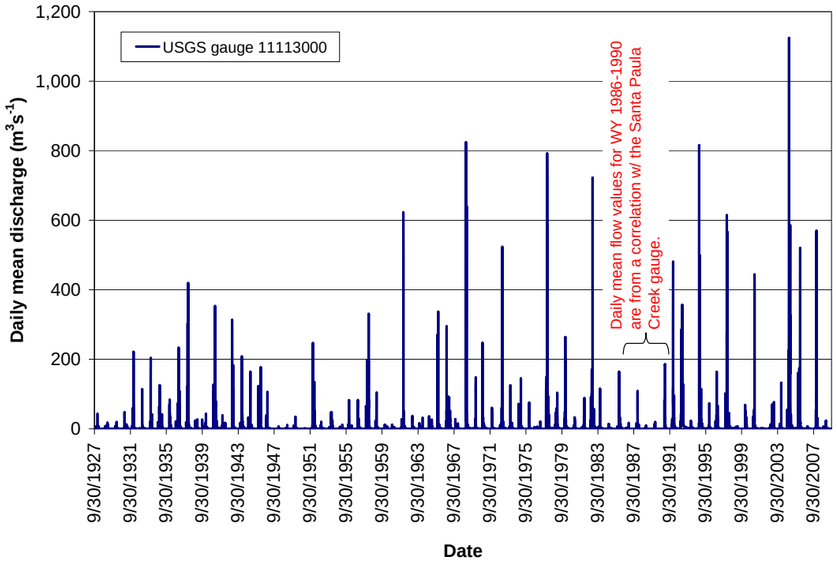

Figure 4-2a. Daily mean discharge for Sespe Creek near Fillmore (USGS 11113000) between WY 1928 and 2009. Daily mean flow values for WY 1986-1990 were absent for this gauge and were derived based on a correlation (R^2=0.86) with the Santa Paula Creek gauge (USGS 11113500).

b)

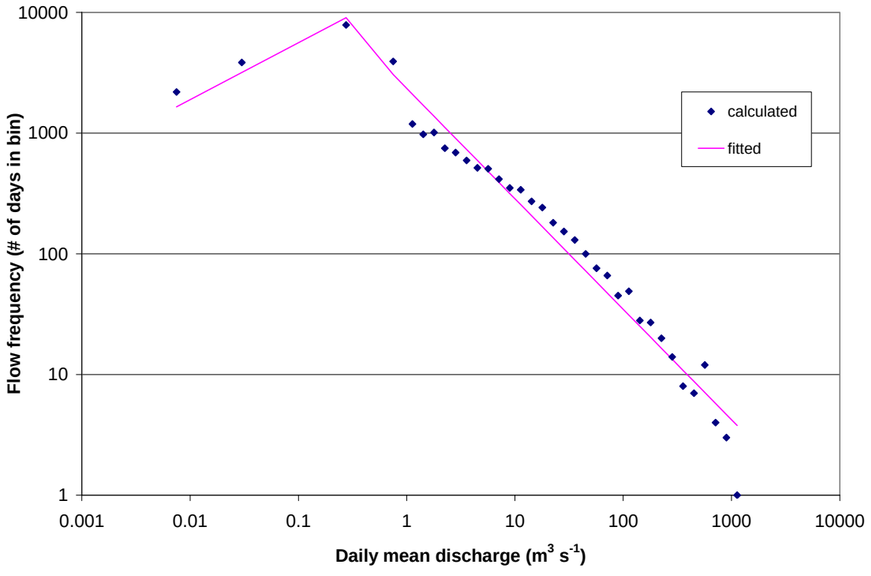

Figure 4-2b. Daily mean flow frequency distribution for Sespe Creek near Fillmore (USGS 1111300 and 11109000) between WY 1928 and 2009.

c)

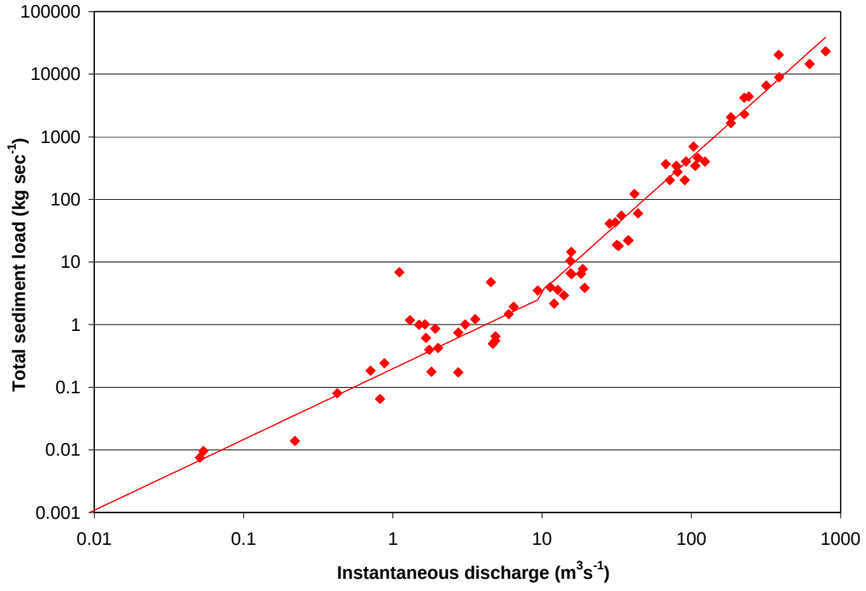

Figure 4-2c. Total sediment load (suspended load + bedload) rating curve for Sespe Creek near Fillmore (USGS 11113000).

d)

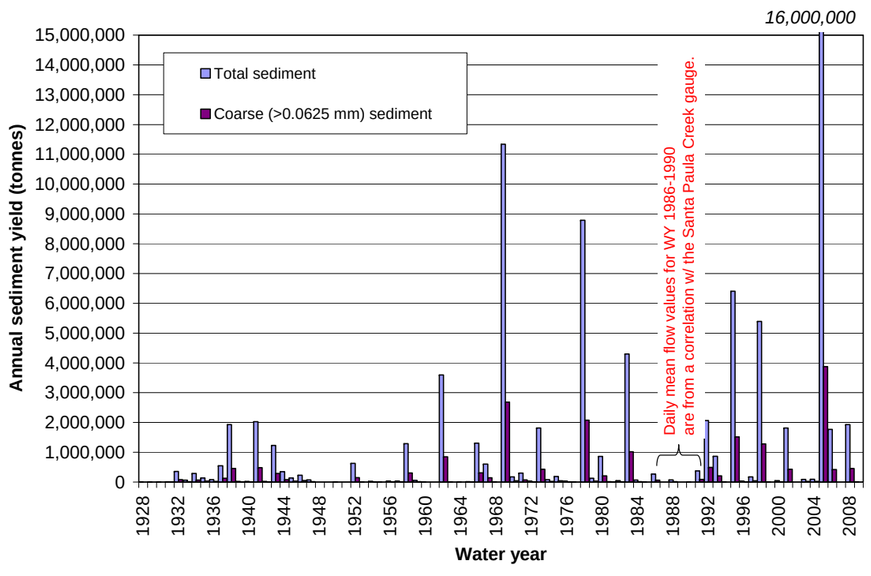

Figure 4-2d. Calculated total sediment yield (suspended load + bedload) and coarse (>0.0625 mm) sediment yield for Sespe Creek near Fillmore between 1928 and 2009 (USGS 11113000).

a)

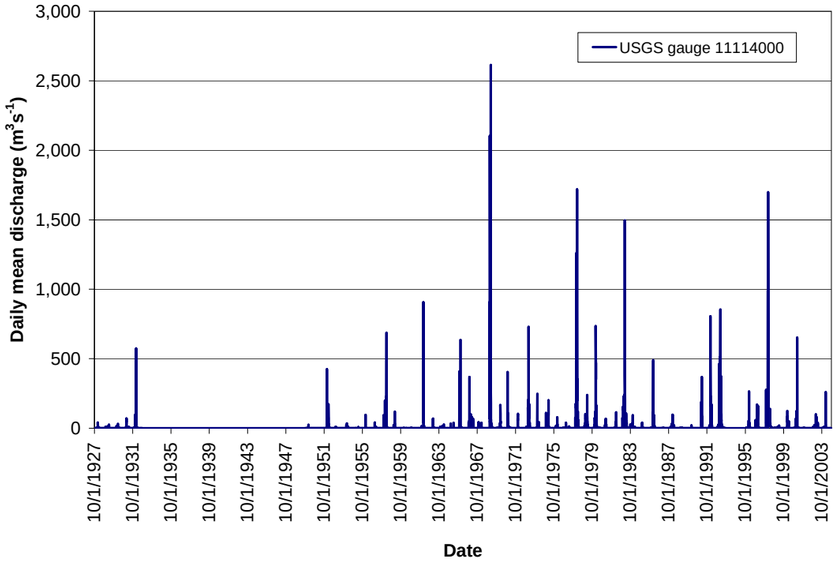

Figure 4-3a. Daily mean discharge for LSCR at Montalvo (USGS 11114000) between WY 1928 and 2004 [gauge decommissioned thereafter].

b)

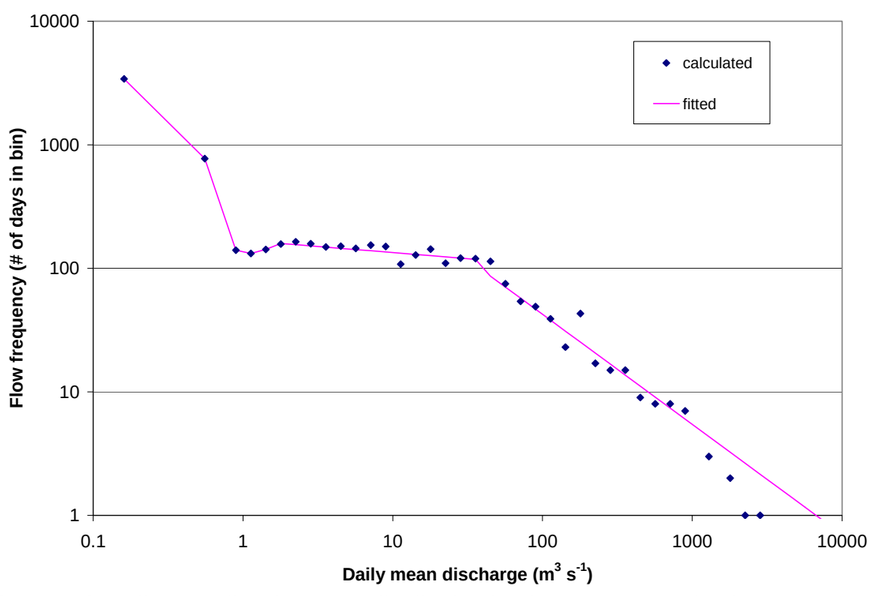

Figure 4-3b. Daily mean flow frequency distribution for the LSCR at Montalvo (USGS 11114000) between WY 1928 and 2004.

c)

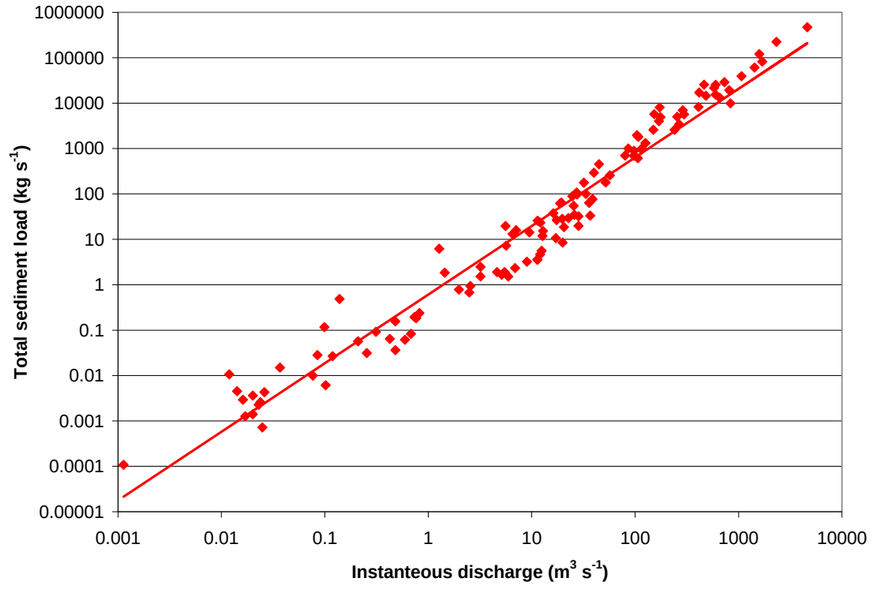

Figure 4-3c. Total sediment load (suspended load + bedload) rating curve for the LSCR at Montalvo (USGS 11114000).

d)

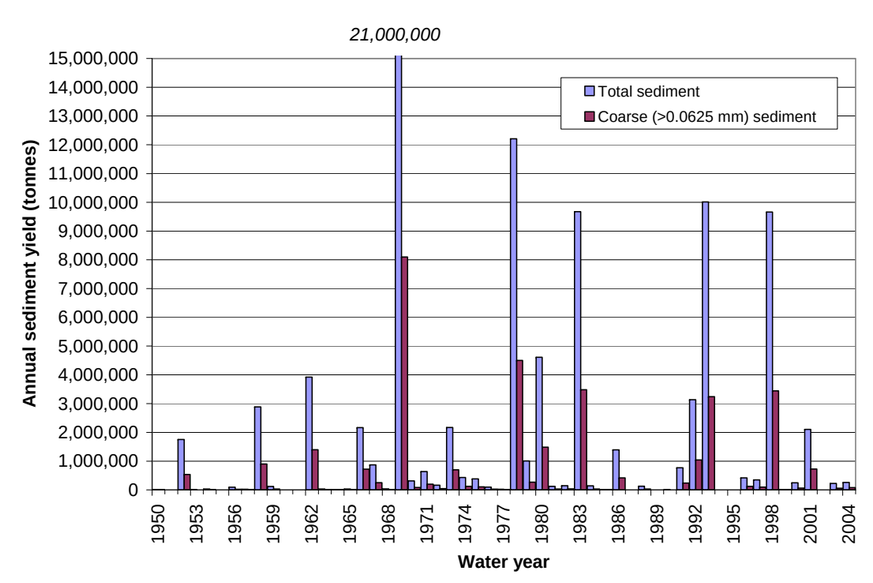

Figure 4-3d. Calculated total sediment yield (suspended load + bedload) and coarse (>0.0625 mm) sediment yield for the LSCR at Montalvo between 1950 and 2004 (USGS 11114000).

The average annual total sediment yield estimates for USCR, Sespe Creek, and LSCR during their respective periods of record are as follows (Table 4-2):

- USCR—WY 1953 to 2009 is approximately 900,000 t yr^{-1}, or a yield per unit area of 720 t km^{-2} yr^{-1} from the effective contributing area (i.e., downstream of Bouquet and Castaic dams) of 1,242 km^2 (Figure 4-1d). Annual sediment discharge over the past 57 years, however, is estimated to have varied by a factor of more than **50,000**—from a low of approximately 410 tonnes (WY 1961) to more than 23 million tonnes (WY 1969, which contains the flood of record). The two water years that contain the highest annual maximum instantaneous discharge (1969 and 2005) account for over half of the total sediment yield out of the USCR. In contrast, over one-half of all years have an annual total sediment yield less than 10% of the average annual total sediment yield. The coarse fraction (>0.0625 mm) of the total average annual sediment yield is approximately 190,000 t yr^{-1}, or a unit area contribution of 155 t km^{-2} yr^{-1} (from areas downstream of Bouquet and Castaic dams).
- Sespe Creek—WY 1928 to 2009 is approximately 990,000 t yr^{-1}, or a yield per unit area of 1,500 t km^{-2} yr^{-1} (Figure 4-2d). Annual sediment discharge over the past 82 years is estimated to have varied by a factor of more than **60,000**—from a low of approximately 250 tonnes (WY 1951) to more than 16 million tones (WY 2005, which contains the flood of record for Sespe Creek but not for either USCR or LSCR). Four water years (1969, 1978, 1995, and 2005) account for over half of the total sediment yield out of Sespe Creek. The coarse fraction (>0.0625 mm) of the total average annual sediment yield is approximately 230,000 t yr^{-1}, or a per unit area contribution of 360 t km^{-2} yr^{-1}.
- LSCR—WY 1950 to 2004 is approximately 1.8 million t yr^{-1}, or a yield per unit area of 660 t km^{-2} yr^{-1}, from the effective contributing area (i.e., downstream of Bouquet, Castaic, and Piru dams) of 2,675 km^2 (Figure 4-3d). Annual sediment discharge over the period of record is estimated to have varied by a factor of nearly **90,000**—from a low of approximately 230 tonnes (WY 1960) to more than 20 million tonnes (WY 1969, which contains the flood of record). Three water years (1969, 1978, and 1993) account for nearly half of the total sediment yield out of the watershed. The coarse fraction (>0.0625 mm) of the total average sediment yield is approximately 620,000 t yr^{-1}, or a per unit area contribution of 230 t km^{-2} yr^{-1} (from areas downstream of Bouquet, Castaic, and Piru dams). Although the period of record ends at WY 2004, it can be reasonably assumed that the total sediment yield during WY 2005 would have been comparable to the yield of WY 1969 based on similarities in their estimated discharge (instantaneous peak discharge in 2005 in the LSCR was made at the nearby Freeman Diversion Dam [see Table 4-1]).

The "coarse" sediment sizes referenced above included suspended sediment and bedload greater than 0.0625 mm, or bed-material load, which excludes silt and clay sized particles as they will transport as suspended or dissolved load even in low flow conditions, and are therefore frequently carried into the mainstem SCR and beyond (Simons, Li & Associates 1983). As such, these particles have little influence on the channel morphology and the dynamics of morphological change.

Table 4-2. Average annual sediment yields of the USCR, Sespe Creek, and LSCR watersheds, as calculated at stream gauges with long-term sediment discharge measurements.

Watershed	Effective contributing area (km^2) [a]	Period of record (water years)	Average annual total sediment yield ($t\ yr^{-1}$)	Average annual total sediment yield per unit area ($t\ km^{-2}\ yr^{-1}$)	Average annual coarse sediment yield ($t\ yr^{-1}$)	Average annual coarse sediment yield per unit area ($t\ km^{-2}\ yr^{-1}$)
USCR	1,242	1953–2009	900,000	720	190,000	155
Sespe Creek	650	1928–2009	990,000	1,500	230,000	360
LSCR (SCR watershed)	**2,675**	**1950–2004**	**1,800,000**	**660**	**620,000**	**230**

[a] Area contributing to the respective stream gauges below dams.

4.1.2 Characteristics of the "dominant discharge"

The majority of sediment transport throughout the SCR occurs during very short periods of time. For instance, in the USCR, an estimated 50% of the roughly 51.2 million tonnes (56.4 million tons) of sediment that passed the County line stream gauge (USGS 11108500 and 11109000) between 1953 and 2009 was transported during high flows in just five days. Warrick (2002) concluded that 25% of the total sediment discharge out of the entire SCR watershed for the period 1928–2000 occurred in four days.

These results contrast sharply with the observations of alluvial rivers in humid environments, which have provided the historic basis for many of the classic generalizations of fluvial geomorphology, including the concept of "dominant discharge"—presumed to be the flow that, over the long term, performs the most work in terms of sediment transport (Wolman and Miller 1960, Emmett and Wolman 2001). In humid rivers, that dominant flow is most commonly associated with an *intermediate* discharge: increasing sediment transport with increasing flow, coupled with the rapidly decreasing durations of large (and thus uncommon) flows, produce a maximum total sediment load (calculated as the product of the sediment transport rate and flow frequency) at flows neither very small (because little sediment is moved) nor very large (because they occur so rarely and so briefly)—thus, "intermediate." Figure 4-4a illustrates the dominant discharge concept in a hypothetical example for an idealized alluvial river.

For the SCR and its major tributaries, a very different picture emerges from the data (Figure 4-4 b–d). The flow frequency (blue line) shows the typical pattern of discharges over several orders of magnitude—the larger the flow, the less commonly does it occur. Similary, the sediment load increases monotonically with increasing flows—big flows move more sediment. Yet the *total* sediment loads, calculated as the product of flow frequency and sediment transport rate, do not follow the trend suggested by the "classic" dominant-discharge model over the range of historic floods. Instead, the total loads increase with discharges across the entire range of each dataset, with the greatest total loads occurring at the highest projected flows. Hence the "dominant discharge" for the entire SCR and its major tributaries is the largest discharge on record. There is, surely, *some* large discharge that is so infrequent that the contribution to total sediment movement is smaller than a discharge of lesser magnitude but greater frequency—but unlike humid-region rivers, the range of discharges over which this occurs must have a recurrence much longer than that of a 100-year flood. For purposes of river management at human time scales, this is intriguing but not terribly relevant.

Correspondence of the dominant discharge with the largest flow on record has important implications for channel-forming processes. Dominant discharge is often described as the "channel-forming" flow, at the center of a range of flows that are most directly responsible for shaping and maintaining the channel in its characteristic "equilibrium" morphology (e.g., Wolman and Leopold 1957). The fact that the dominant, channel-forming flow is the largest flow on record implies that these systems do not behave like a classic humid-region, alluvial river system, but instead like arid channels. This was theorized (absent data) over thirty years ago by Wolman and Gerson (1978). Thus, there is no reason to expect that the channels will overflow their banks every 1 or 2 years, or maintain well-defined, regularly spaced riffle-pool sequences. We expect alluvial river morphology to exhibit equilibrium tendencies, with small, year-to-year fluctuations around a long-term "average" condition; in contrast, our results lead to the inescapable conclusion that the Santa Clara River will experience dramatic changes due to episodically high flows that change the dynamics of the entire system, altering roughness and channel shape, and potentially leading to significant fluctuations in local channel bed elevation that persist for years, decades, or longer. A "classical" interpretation of this river will yield fundamentally flawed expectations and, ultimately, deeply misguided management decisions.

a)

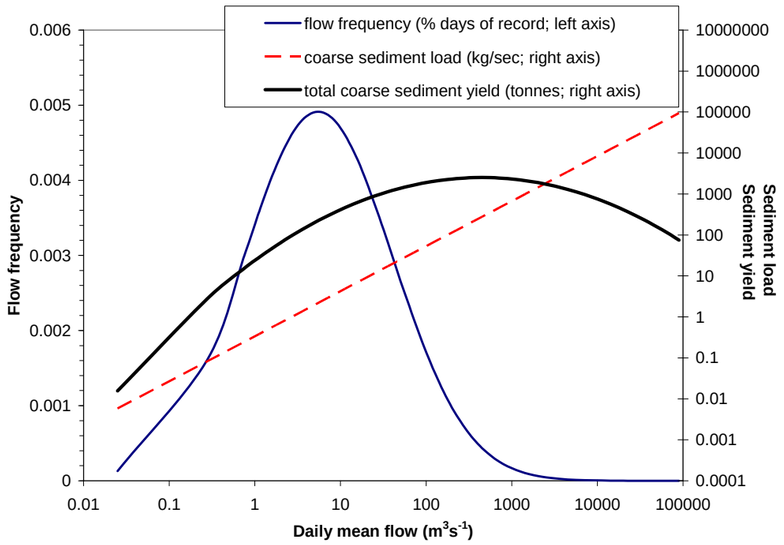

Figure 4-4a. Flow frequency (left axis, scaled to 1) and sediment load (right axis) plotted against flow, showing conceptual, dominant discharge model of an idealized alluvial river by Wolman and Miller (1960). Blue line tracks flow frequency (for mean daily flow), red line tracks sediment transport rate (in tonnes/day) and black line tracks total sediment load (in tonnes). Sediment load increases to a maximum at an intermediate flow.

b)

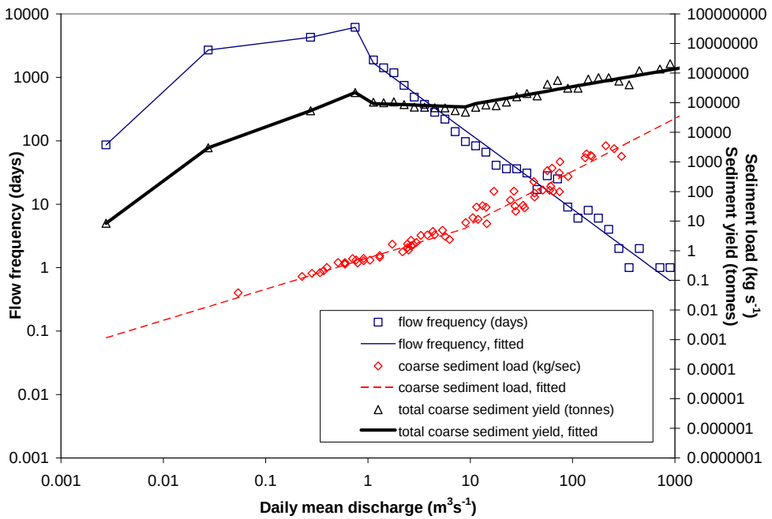

Figure 4-4b. Flow frequency and coarse (>0.0625 mm) sediment load for long-term daily mean flow record for USCR at the County line (USGS 1118500 and 11109000). Unlike classic alluvial rivers, the variation of sediment yield with flow does not exhibit a peak at "intermediate" discharges (as defined by the range of flows seen over the last century), but increases with increasing flood frequency without (heretofore observed) bounds.

c)

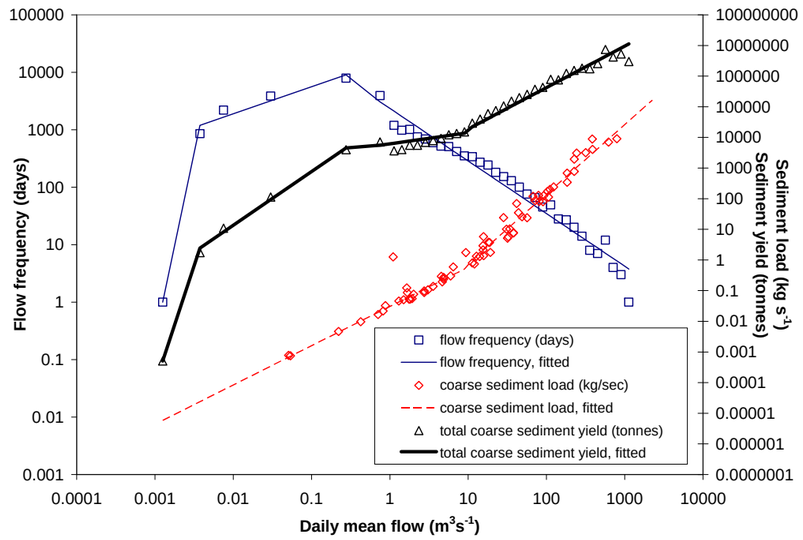

Figure 4-4c. Flow frequency and coarse (>0.0625 mm) sediment load for long-term daily mean flow record for Sespe Creek near Fillmore (USGS 11113000). Note: the daily mean flow values for WY 1986-1990 were absent for this gauge, but were derived here based on a correlation (R^2=0.86) with the Santa Paula Creek gauge (USGS 11113500). Unlike classic alluvial rivers, the variation of sediment yield with flow does not exhibit a peak at "intermediate" discharges (as defined by the range of flows seen over the last century).

d)

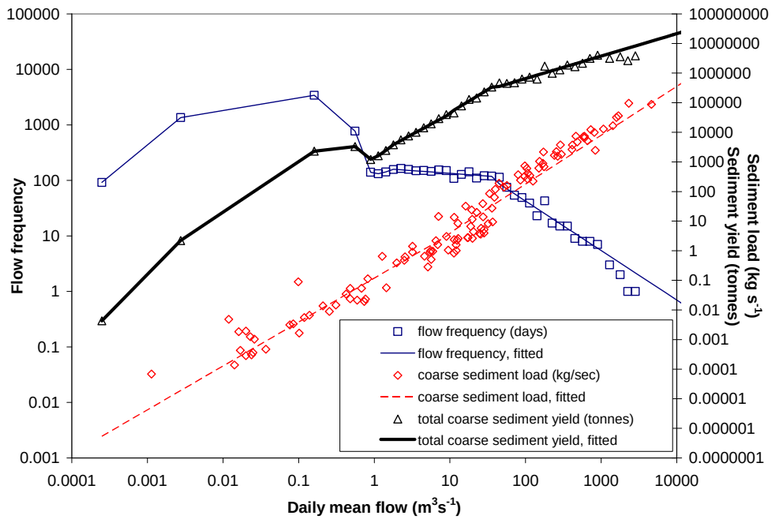

Figure 4-4d. Flow frequency and coarse (>0.0625 mm) sediment load for long-term daily mean flow record for LSCR at Montalvo (USGS 11114000). Unlike classic alluvial rivers, the variation of sediment yield with flow does not exhibit a peak at "intermediate" discharges (as defined by the range of flows seen over the last century).

4.1.3 Effects of the El Niño–Southern Oscillation on flow magnitude and sediment delivery

The El Niño–Southern Oscillation (ENSO) is a climatic phenomenon that is characterized by warming and cooling cycles (oscillations) in the waters of the eastern equatorial Pacific Ocean. ENSO cycles have a 1–1.5 year duration and a 3–8 year recurrence interval, and they are related to changes in atmospheric circulation, rainfall, and upper ocean heat content (see Deser et al. 2004 and references contained therein). In southern California, ENSO years are normally characterized by relatively high rainfall intensities, with rivers and streams exhibiting higher annual peak flows than they do in non-ENSO years (Cayan et al. 1999, Andrews et al. 2004). This difference in flow magnitude is shown quantitatively in an analysis of the instantaneous peak flow record for the USCR and LSCR (County line gauges and Montalvo gauge) for ENSO and non-ENSO years over their respective periods of record. For ENSO years there is nearly a 50% probability of peak flows exceeding 280 $m^3 s^{-1}$ (10,000 cfs) in the USCR and 2,300 $m^3 s^{-1}$ (81,400 cfs) in the LSCR (Figure 4-5a, b: open symbols) whereas a non-ENSO year has less than a 10% probability of peak flows exceeding that same value (Figure 4-5a, b: closed symbols). This relationship is more pronounced in the LSCR because it is more directly under the influence of coastal conditions.

The frequency of ENSO-induced climate fluctuations vary on a multi-decadal time scale that is consistent with the observed shift from a relatively dry climate (averaged over the period 1944–1968) to a relatively wet climate (averaged over the period 1969–1995) in North America's Pacific region (Inman and Jenkins 1999). The wet-period ENSO cycle, which existed to the end of the Inman and Jenkins study (1995) and has likely continued to the present, has been marked by strong ENSO years every 3–7 years and mean sediment fluxes for southern California rivers (from the Pajaro River south to the Tijuana River) that have been approximately 5 times greater than during the preceding dry period (1944–1968) (Inman and Jenkins 1999). For the entire SCR, the annual net sediment yield during the recent wet period was approximately 8 times greater than it was during the preceding dry period (Inman and Jenkins 1999). Within the period of 1950 to 1999, Warrick and Milliman (2003) found that almost 90% of the historical suspended sediment flux from the SCR (as measured at the Montalvo gauge) has occurred during ENSO winters. The characteristic episodic delivery of sediment from southern California watersheds in general, and the entire SCR watershed in particular, is thus strongly linked to ENSO-induced precipitation events with high daily or multi-day rainfall totals. A good example of this phenomenon in the USCR is a 10-day period during and directly after the January 2005 storm event, which accounted for approximately 10% of the total sediment delivered from 1953–2009 (i.e., 10% of the total sediment was delivered in 0.05% of the total time). In summary, sediment transport throughout the SCR drainage network, and particularly in the mainstem river, is highly concentrated in very brief periods of time.

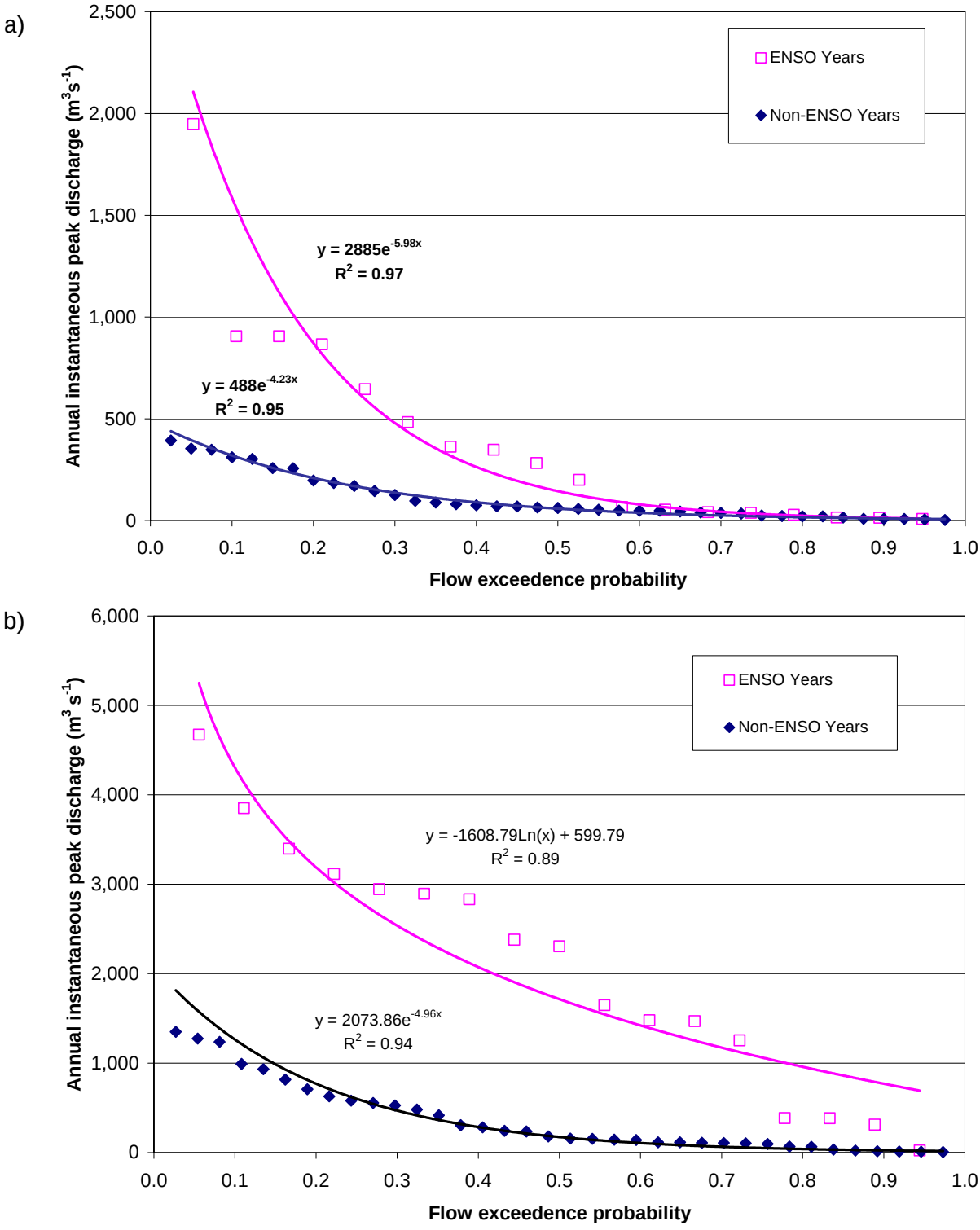

Figure 4-5. Flow exceedance for ENSO/non-ENSO years for the USCR at the County line (USGS 1118500 and 11109000) from WY 1953-2009 (a), and for the LSCR at Montalvo (USGS 11114000) from WY 1950-2005 (b). Instantaneous peak discharge from 2005 for the LSCR is from an estimated value at the Freeman Diversion Dam.

4.1.4 Bed material and bedload particle sizes

The coarse sediment load of the river is a primary factor in the geomorphology of the mainstem channel and in controlling the river's ability to change over time (i.e., the channel morphodynamics). Bed particle sizes along the SCR channel network range from very fine sand (0.0625–1.25 mm in diameter) to large boulders (>256 mm), with dominant sizes along the mainstem river bed ranging from medium sand to fine gravel[3]. Particles-size distributions derived from recently collected bulk sediment samples throughout the SCR drainage network are depicted in Figure 4-6 (relative size of circles corresponds to particle size category). Also considered in this section are bedload data derived from repeat sediment discharge samples collected by the USGS at three key points in the watershed: the County line stream gauge (i.e., export from the USCR watershed and input to the LSCR), the Sespe Creek gauge near Fillmore (i.e., export from a major tributary and input to the LSCR), and the Montalvo gauge (i.e., export from the entire SCR to the ocean).

Within the mainstem SCR at the County line, the D_{16} is sand-sized, D_{50} ranges in size from sand to very fine gravel, and D_{84} ranges from sand to medium gravel (Table 4-3). Within the coarse-sediment bearing Sespe Creek, the finer fraction (D_{16}) is typically sand-sized, with median particle sizes (D_{50}) range from very fine to medium gravel; the coarse fraction (D_{84}) ranges from medium to coarse gravel (Table 4-4). The particle-size distribution within the mainstem SCR at Montalvo is most similar to the County line values (Table 4-5), indicating that the relatively coarse load delivered by Sespe Creek is effectively diluted with finer particles at this point along the river.

Temporally, bed sediments (e.g., D_{50}) at Sespe Creek and the LSCR at Montalvo have become finer through the respective periods of record, 1969-1971 and 1971-1984, but this may be an artifact of bed sediments coarsening during large floods (i.e., 1969), and becoming finer following smaller floods in the intervening period. Bed sediments at the County line have become progressively coarser through its longer period of record, 1968-1977 and more recently in 2004, which may be related to the increased frequency of larger flood events in the recent, wetter period (i.e., since the 1960s) (see Section 4.1.3 above).

[3] Sediment particle size categories referenced here: very fine sand = 0.0625–0.125 mm, fine sand = 0.125–0.25 mm, medium sand = 0.25–0.5 mm, coarse sand = 0.5–1 mm, very coarse sand = 1–2 mm, very fine gravel = 2–4 mm, fine gravel = 4–8 mm, medium gravel = 8–16 mm, coarse gravel = 16–32 mm.

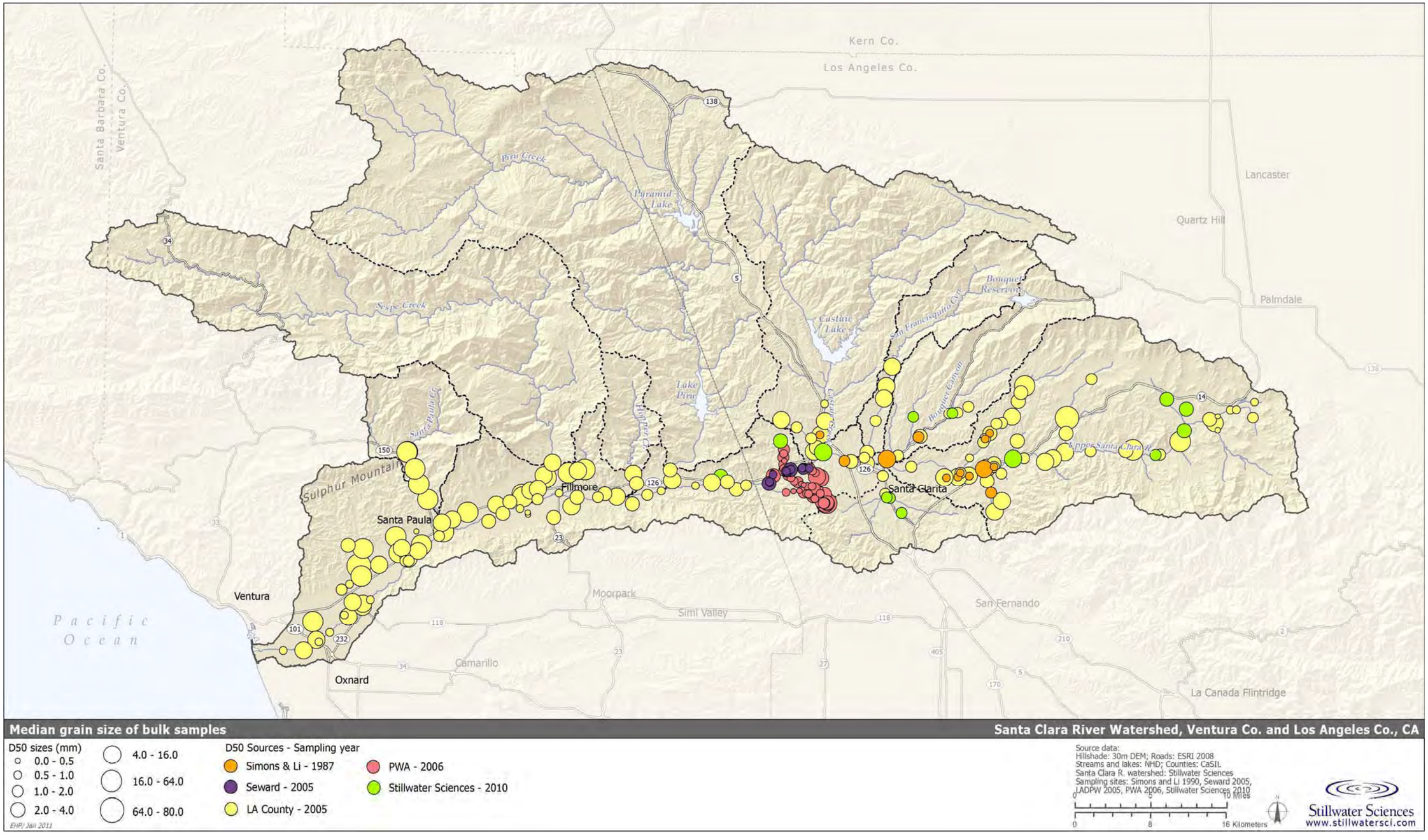

Figure 4-6. Median grain size (D_{50}) of bulk sediment samples collected throughout the SCR watershed.

Table 4-3. Characteristics of channel bed sediment for the USCR at the County line.

Sample date	Particle size (nth percentile) [mm]		
	D_{16}	D_{50}	D_{84}
10/21/1968	0.19	0.46	1.90
11/5/1968	0.31	0.61	1.24
2/10/1969	0.24	0.59	**7.20**
8/27/1969	0.20	0.52	1.53
11/4/1969	0.36	0.71	1.56
9/14/1970	0.37	0.76	1.63
9/30/1975	0.32	0.93	**8.00**
9/15/1977	0.38	**2.67**	**13.33**
9/20/1978 (5 counts)	0.22	1.74	**7.78**
10/7/2004 (3 counts)	0.47	1.32	**4.10**
10/16/2004 (3 counts)	0.51	1.53	**6.13**
10/21/2004 (3 counts)	0.48	1.46	**5.12**
12/17/2004 (2 counts)	0.42	0.99	**3.03**
12/30/2004 (2 counts)	0.40	1.36	**8.54**

Source: USGS, National Water Information System, "Santa Clara River at the Los Angeles-Ventura County line, CA" (USGS 11108500) [1968-1978] and the "Santa Clara River near Piru, CA" (USGS 11109000) [2004].
Bold values indicate gravel-size sediment.

Table 4-4. Characteristics of channel bed sediments for Sespe Creek near Fillmore.

Sample date	Particle size (nth percentile) [mm]		
	D_{16}	D_{50}	D_{84}
1/14/1969	1.26	**3.38**	**9.07**
2/19/1969	0.63	**9.60**	**31.30**
8/3/1971	0.21	**2.22**	**24.00**

Source: USGS, National Water Information System, "Sespe Creek near Fillmore, CA" (USGS 11113000).
Bold values indicate gravel-size sediment.

Table 4-5. Characteristics of channel bed sediments for LSCR at Montalvo.

Sample date	Particle size (nth percentile) [mm]		
	D_{16}	D_{50}	D_{84}
8/2/1971	0.50	**2.25**	**10.46**
8/10/1973	0.20	0.65	**2.86**
3/18/1975	0.42	0.87	**3.40**
4/30/1975	0.44	0.91	**3.82**
9/30/1975	0.28	0.65	**4.00**
9/16/1977	0.25	0.69	**8.57**
9/20/1978 (7 counts)	0.22	0.55 (+1 @ **21.58 mm**)	2.5 (+1 @ 40.73 mm)
8/22/1979 (19 counts)	0.28	0.45 – finest 14 **20.43 – coarsest 5**	**2.35** – finest 14 **36.81** – coarsest 5
8/14/1980 (13 counts)	0.16	0.44	1.676 (+1 @ **9.14 mm**)
9/30/1981	0.21	0.58	**5.33**
8/5/1983	0.15	0.38	1.14
11/3/1983	0.16	0.40	**2.40**
12/12/1984	0.26	0.44	0.92

Source: USGS, National Water Information System, "Santa Clara River at Montalvo, CA" (USGS 11114000).
Bold values indicate gravel-size sediment.

Bedload particle size at the County Line and Montalvo gages measured during low to moderate flow has been shown to consist mainly of fine and coarse sand, with fine gravel-sized particles also being represented in the coarser bedload fraction at higher flows (Tables 4-6 and 4-8). Bedload particle sizes in Sespe Creek near Fillmore are generally coarser than the sediment in the mainstem Santa Clara River, ranging from coarse sand to medium gravel (Table 4-7). The channel bed at Montalvo is characterized by medium to coarse gravel, whereas bedload samples (collected during moderate flood events) contain mostly sand and fine gravel (Tables 4-5 and 4-8). Taken together, these observations suggest that the coarser material is mobilized and deposited during relatively large floods which are not represented in the bedload sampling data. For reference, the highest flow sampled for bedload was 112 $m^3 s^{-1}$ (3,970 cfs), which has a recurrence interval of 1.3 years. Similarly, the County line and Sespe Creek gauges were also only sampled at relatively low flows (Tables 4-6 and 4-7).

Simons, Li & Associates (1983) calculated that a flow of 57 $m^3 s^{-1}$ (2,000 cfs) at the Montalvo gauge is sufficient to mobilize 907 tonnes day^{-1} (1,000 tons day^{-1}) of very fine gravel, 113 $m^3 s^{-1}$ (4,000 cfs) is sufficient to mobilize 907 tonnes day^{-1} of fine gravel, 255 $m^3 s^{-1}$ (9,000 cfs) is sufficient to mobilize 907 tonnes day^{-1} of medium gravel, and 850 $m^3 s^{-1}$ (30,000 cfs) is sufficient to mobilize 907 tonnes day^{-1} of coarse gravel. Previous studies of sediment transport dynamics within the watershed (e.g., Williams 1979, Noble Consultants 1989, Warrick 2002) have concentrated on characterizing the transport of fine sediment through the mainstem and out to the Santa Barbara Channel. The coarse sediment load has been less intensively studied, but will receive considerable attention as part of a sediment transport modeling effort to be conducted under the next phase of the SCR Feasibility Study.

Table 4-6. Characteristics of bedload sediment samples for the USCR at the County line.

River discharge		Bedload discharge		Particle size (nth percentile) [mm]		
$m^3 s^{-1}$	cfs	tonnes day^{-1}	tons day^{-1}	D_{16}	D_{50}	D_{84}
0.09	3.2	3.2	3.5	0.54	1.57	1.60
0.19	6.6	6.1	6.7	0.63	1.35	**3.09**
0.20	6.9	17	19	0.47	1.58	**2.31**
0.21	7.4	16	18	0.43	1.52	1.81
0.21	7.4	1.4	1.5	0.38	1.47	1.91
0.22	7.9	13	14	0.47	1.55	1.93
0.25	8.9	22	24	0.48	1.56	**2.29**
0.26	9.3	1.5	1.6	0.54	1.56	1.97
0.28	10	15	16	0.50	1.58	**2.57**
0.31	11	15	16	0.45	1.54	1.85
0.31	11	6.2	6.8	0.42	1.49	1.90
0.40	14	23	25	0.50	1.57	1.79
0.40	14	10	11	0.36	1.40	1.92
0.45	16	49	54	0.44	1.55	1.81
0.51	18	31	34	0.41	1.50	1.85
0.59	21	44	48	0.40	1.52	1.78
0.62	22	34	38	0.51	1.56	1.93
0.79	28	19	21	0.47	1.04	**3.00**
1.47	52	54	60	0.41	1.57	**2.91**
1.90	67	66	73	0.20	1.72	1.00
2.04	72	47	52	0.17	1.62	1.45
2.69	95	83	92	0.40	1.61	1.73
2.78	98	155	171	0.40	1.20	**10.13**
2.80	99	266	293	0.66	**2.75**	**8.62**
2.89	102	101	111	0.53	1.60	**5.50**
5.30	187	200	221	0.20	1.74	1.38
5.32	188	380	419	0.30	1.35	**2.80**
6.91	244	117	129	0.48	1.18	**4.00**
9.17	324	118	130	0.19	1.08	1.00

Source: USGS, National Water Information System, "Santa Clara River at the Los Angeles-Ventura County line, CA" (USGS 11108500).
Bold values indicate gravel-size sediment.

Table 4-7. Characteristics of bedload sediment samples for Sespe Creek near Fillmore.

River discharge		Bedload discharge		Particle size (nth percentile) [mm]		
$m^3 s^{-1}$	cfs	tonnes day^{-1}	tons day^{-1}	D_{16}	D_{50}	D_{84}
0.8	30	5.0	5.5	0.73	**2.23**	**6.75**
1.1	39	21	23	0.95	**2.83**	**7.24**
1.1	39	25	28	0.75	**2.48**	**6.00**
1.2	43	0.8	0.9	0.40	0.98	**6.77**
1.3	45	5.8	6.4	0.79	**2.13**	**5.43**
2.1	73	16	18	1.41	**3.45**	**7.57**
2.1	74	5.4	6.0	0.83	1.91	**4.50**
3.6	126	15	16	0.35	0.76	**2.00**
5.7	201	44	48	1.04	**2.58**	**6.18**
10.4	366	29	32	1.86	**7.57**	**14.36**
43.9	1,550	836	921	1.29	**9.10**	**22.26**

Source: USGS, National Water Information System, "Sespe Creek near Fillmore, CA" (USGS 11113000).
Bold values indicate gravel-size sediment.

Table 4-8. Characteristics of bedload sediment samples from the LSCR at Montalvo.

River discharge		Bedload discharge		Particle size (nth percentile) [mm]		
$m^3 s^{-1}$	cfs	tonnes day^{-1}	tons day^{-1}	D_{16}	D_{50}	D_{84}
0.96	34	56	63	0.27	0.42	0.82
0.99	35	29	32	0.27	0.44	0.87
2	70	132	146	0.35	0.61	0.93
8.4	297	396	437	0.39	0.82	1.95
14.5	512	661	729	0.31	0.57	1.62
15.5	549	324	358	0.34	0.70	1.93
15.6	550	299	330	0.37	0.79	**2.44**
19.5	689	224	247	0.30	0.49	1.18
19.7	695	282	311	0.33	0.63	1.57
20	714	585	645	0.34	0.66	**2.00**
21	740	1,170	1,290	0.34	0.62	1.50
22	786	478	527	0.18	0.38	0.90
24.7	872	228	251	0.34	0.62	1.09
40	1,410	971	1,070	0.23	0.42	0.93
44	1,560	1,243	1,370	0.54	1.41	**5.78**
47.6	1,680	651	718	0.18	0.44	1.33
112.4	3,970	unknown	unknown	0.29	0.85	**4.44**

Source: USGS, National Water Information System, "Santa Clara River at Montalvo, CA" (USGS 11114000).
Bold values indicate gravel-size sediment.

4.2 Impacts of Infrastructure and Anthropogenic Channel Modifications

Channel-related infrastructure, channel modifications, and land-use changes within the watershed since the arrival of European settlers (see Chapter 2) have all affected fluvial geomorphology throughout the entire SCR, and they have contributed to several contemporary challenges for river management in both Los Angeles and Ventura counties. Infrastructure changes include dams constructed during the twentieth century, the failure of the St. Francis Dam in 1928, water diversions, instream aggregate mining, and the construction of roads, bridges, and levees. The most direct and substantive channel modifications are expressed by the armored and/or concrete-lined lower reaches of many tributaries to the SCR, with associated reductions in channel width and loss of sediment storage. Other direct impacts have included agricultural and, increasingly, urban occupation of the floodplain; levee construction to protect the increasing development of areas adjacent to the river; and the lowering of the channel bed that accompanied instream aggregate mining and cross-channel structures that block downstream sediment movement.

4.2.1 Dams and debris basins

Along tributaries to the SCR, dams on Piru Creek, Castaic Creek, and Bouquet Canyon regulate roughly 36% of the drainage area of the SCR watershed (Figures 1-6 and 3-6), impounding water for consumptive use and effectively reducing both downstream flow and downstream sediment delivery compared with what it would have been in the absence of the dams.

4.2.1.1 Santa Felicia Dam and Lake Piru

Santa Felicia Dam on Piru Creek was completed in 1955 and operations began the following year. Lake Piru has a reservoir capacity of approximately 109 million m^3 (88,340 ac-ft). Inflow from the floods of January and February 1969 exceeded the reservoir capacity and forced the release of roughly 140 million m^3 (113,500 ac-ft) of water (Simons, Li & Associates, 1983). The intense rainfall during this period contributed to the eventual release of 816 m^3s^{-1} (28,800 cfs) on February 25, 1969, which is the largest recorded peak flow measured downstream of Santa Felicia Dam (USGS 11110000, inactive). Spill or release events exceeding daily mean flows of 28 $m^3 s^{-1}$ (1,000 cfs) have reportedly also occurred during 1978, 1980, 1983, 1993, 1995, 1998, 2005, and 2006 (UWCD 2010). With exception to these events, flows in Piru Creek have been regulated to below 28 $m^3 s^{-1}$ (1,000 cfs) since the completion of the dam.

4.2.1.2 Pyramid Dam and Lake

In 1971, a second facility was completed in the Piru Creek drainage, upstream of Lake Piru, with the goal of impounding water from northern California under the California Water Project. Reservoir capacity is 211 million m^3 (171,200 ac-ft). This facility was constructed in concert with Castaic Lake (see below) by the California Department of Water Resources. Together, these two reservoirs function as a hydroelectric pumped storage project, where Pyramid Lake serves as the upper reservoir and Castaic Lake (i.e., Elderberry Forebay) serves as the lower reservoir.

4.2.1.3 Castaic Dam and Lake

Castaic Dam, completed in 1972, is a State Water Project facility located on Castaic Creek, far upstream of its confluence with the USCR. The facility (capacity 401 million m^3 [325,000 ac-ft]) is designed to contain water imported from northern California. It also blocks all but the largest flows from its contributing 397 km^2 (153 mi^2) watershed.

4.2.1.4 Bouquet Dam and Reservoir

Bouquet Dam impounds imported water in Bouquet Reservoir, in the moderately dry north-central portion of the watershed. Completed in 1934, the facility has a capacity of 42 million m^3 (34,000 ac-ft) and affects less than 1% of the SCR watershed area. Its effects on watershed hydrology are probably not great, due to its location and small regulated watershed area, although it does intercept the influx of water and sediment from the upstream contributing area. Most of the impounded water, however, arrives from the Los Angeles Aqueduct (State Water Project waters); the dam performs much the same functions of regulating releases and storing water in the case of an interruption upstream as did the ill-fated St. Francis Dam.

4.2.1.5 St. Francis Dam

In 1924, construction began on the St. Francis Dam, near Saugus in San Francisquito Canyon. Its reservoir was to serve as a backup water supply for local farmers in the event that supply from Owens Valley was interrupted. The dam was finished to a height of 57 m (187 ft) in 1926 and eventually filled with nearly 50 million m^3 (41,000 ac-ft) of water. Just before midnight on March 12, 1928, a large section of the dam suddenly collapsed, sending a wall of water down the valley towards the Pacific Ocean, 87 km (54 mi) away. The peak water depth has been estimated at 24 m (78 ft), and peak flow between the dam failure and the County line on the SCR was probably between 15,000 and 30,000 m^3s^{-1} (500,000 and 1,000,000 cfs) (Simons, Li & Associates 1983; Begnudelli and Sanders 2007). Large volumes of mud and debris were entrained in the flow as it rushed first down San Francisquito Canyon, and then down the SCR Valley, affecting the established communities along the way out to the ocean (Figure 4-7; see flood scour path on Figure 4-17 a–c and Figure 4-19 a, b).

The reservoir contents emptied into the ocean less than six hours after the dam broke, but the effects of the flood were far more long-lasting. Nearly 500 people died in the disaster, and parts of Ventura lay under 20 m (70 ft) of mud; total property damage was approximately $5.5 million in 1928 dollars (University of Southern California 2004; equivalent to $70 million in 2010 dollars). The St. Francis Dam failure changed perceptions about dam safety and water projects in California and was the impetus for the creation of the California Division of Safety of Dams, which now regulates non-federal dams in the state (CDSD 2005).

Figure 4-7. The remains of the St. Francis Dam after collapsing just before midnight on March 12, 1928, in the San Francisquito Canyon subwatershed (top). Middle, a downstream view of the mainstem Santa Clara River near the County line, five days after the dam break flood. Below, a downstream view of the mainstem SCR near Santa Paula Creek, the day after the dam break flood. Photos courtesy of the VCWPD.

4.2.1.6 Effects of dams on the delivery of water and sediment to the USCR

The four major dams on tributaries of the SCR watershed (Piru and Castaic creeks and Bouquet Canyon) control the discharge from nearly 36% of the watershed. Analysis of suspended-sediment concentrations and flow from the river and its tributaries suggest that the dams have reduced suspended sediment delivery to the mainstem by roughly 21% (Warrick 2002), assuming 100% sediment trapping efficiency (Williams 1979). Bedload delivery to the mainstem is also estimated to have been reduced by approximately 20%, due to the influence of dams (Brownlie and Taylor 1981), but this assessment is not entirely independent because bedload is estimated partly as a function of suspended load.

The consequences of reduced sediment loads are generally most severe immediately downstream of dams, where channel incision is commonly observed due to more effective erosion of the channel bed by sediment-starved water (e.g., Williams and Wolman 1984). The effect diminishes with increasing distance downstream as sediment-laden water from tributaries is added to the flow (Petts 1984). For example, Simons, Li & Associates (1987) compared pre- and post-dam profiles of Castaic Creek and found an average of about 1 m (3.9 ft) of degradation (6 ft maximum) between 1964 and 1980, which they attribute to the blockage of sediment from the dam. Our own field reconnaissance in 2010 supports these findings. Overall, the impact of dams on river channel morphology is probably greatest in the reaches downstream of both Castaic and Piru creeks (i.e., the Upper Santa Clara River Valley), with impacts presumed to decrease downstream of Fillmore following flow and sediment contributions from Sespe Creek (i.e., the Lower Santa Clara River Valley).

St. Francis Dam had persistent effects on river morphology as a result of the dam break, not only in San Francisquito Creek but throughout the entire SCR downstream of the tributary confluence. The estimated peak flow is 8–15 times greater than any subsequent peak flow that has occurred at the County line, and 3–5 times greater than at the Montalvo stream gauge (recognizing that neither gauge was operational during the event). URS (2005) estimated that the dam-break flow had a hydrological return period equivalent to a 200–1,000 year flood in the LSCR. The relationship between magnitude and frequency implied by data presented in Section 4.1 indicates that the dominant, channel-forming discharge on the SCR is the largest flood on record. Hence, it can be argued that the St. Francis dam failure is the most recent "channel-forming" flow, and thus the present-day channel morphology continues to reflect (at least in part) the effects of this event.

The lower reaches of the USCR and upper reaches of the LSCR (i.e., Reaches 7–13, or the Santa Clarita Basin and Upper Santa Clara River Valley) have been progressively narrowing and aggrading over the last 80 years, suggesting that the flood's primary morphological impact was extensive broadening and incision of the channel and floodway (see Sections 4.3.2 and 4.3.3 below). These morphological changes since the dam failure event have likely been amplified in part by other factors, including reduction of flow caused by Santa Felicia and Castaic dams and urban growth of Santa Clarita with associated encroachment on the floodplain. However, we judge that the dam break was the most recent and significant "channel-forming" flow by virtue of its sheer magnitude, and so many of the large-scale characteristics of the mainstem river channel and floodway, from the confluence and downstream through the SCR to the ocean, are likely relict effects of the dam-break flood.

4.2.1.7 Effects of debris basins on watershed sediment yields and river morphology

A detailed background on debris basins operated by VCWPD and LADPW to protect urban infrastructure from debris flows in and around the SCR Valley, in addition to the debris basins

operated by LADWP at the Castaic Powerplant, was presented earlier in Section 3.3.2. Because the Castaic Powerplant debris basins are positioned upstream of Castaic Dam, these debris basins do not impact the SCR's contemporary sediment yield or morphology.

The VCWPD and LADPW debris basins and debris retention inlets collectively cut off only 1.4% of the total SCR watershed area (60 km^2 of 4,202 km^2). As a result, they reduce watershed sediment yields and impact tributary and river morphology to a much lesser extent than the large water-storage dams and reservoirs. The debris basins annually intercept approximately 150,000 t of sediment in total. The approximate amounts intercepted by the debris basins below large dams (2,674 km^2) account for 8% of our estimated average annual total sediment load calculated at the Montalvo stream gauge (1.8 million t yr^{-1}) and 3% of our estimated average annual total sediment-production rate for the entire watershed (5.1 million t yr^{-1}) (see Table 3-6).

Downstream effects of these structures on the tributary channel morphology is generally minimal because most are situated above completely channelized reaches that lock the channel geometry in place. For this reason, it is difficult to directly assess the isolated effects of the debris basins on mainstem river-channel morphology. Our field observations made throughout the watershed did not note any obvious channel instabilities in the river directly below the confluence of any tributaries with debris basins. Therefore, it appears that the most significant effect of these structures on the river is their trapping of sediment.

4.2.2 Instream aggregate mining

Large volumes of aggregate resources designated by the California Geological Survey (CGS) in both the USCR (in the Saugus-Newhall Production-Consumption Region [SNPCR] of Los Angeles County) and LSCR (in the Western Ventura Production-Consumption Region [WVPCR] of Ventura County) have attracted long-standing interest in aggregate mining (Figure 4-8). Small-scale operations began in the early 1900s, often using riverbed lands leased from farmers; operations grew larger during and after World War II (Schwartzberg and Moore 1995).

Overall, aggregate mining has been the greatest single anthropogenic factor in the form of the LSCR. In the USCR, effects of aggregate mining are less broadly significant than those of dam construction (and failure), channelization, and urban development, but their effects are nonetheless apparent. Because aggregate mining effects in the LSCR and USCR have been markedly different, this section presents background information and discusses the effects to each part of the watershed separately.

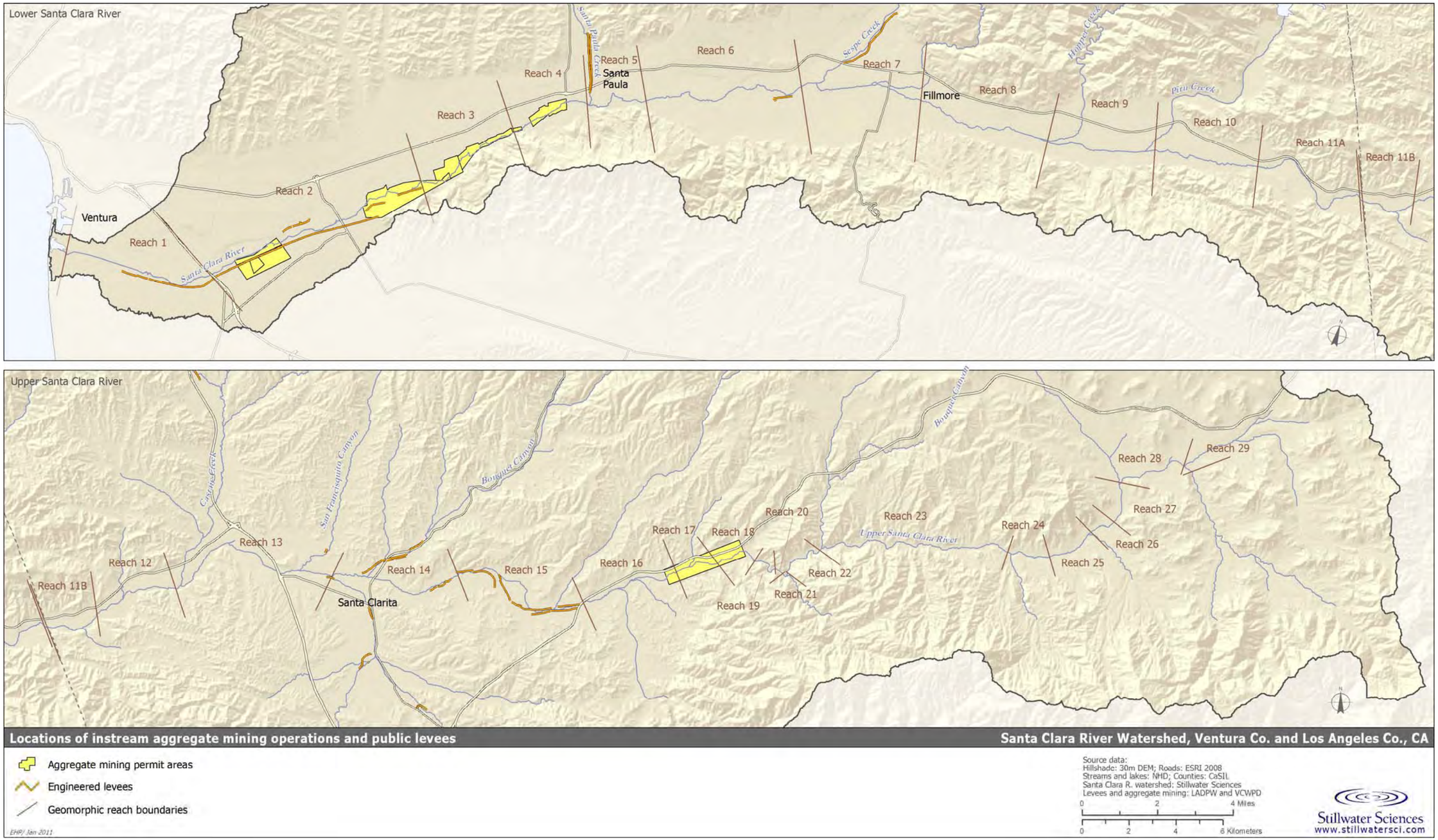

Figure 4-8. Instream aggregate mining and public levee locations along the mainstem SCR. Geomorphic reaches referenced throughout this study are also shown.

4.2.2.1 Effects of aggregate mining to the LSCR

Aggregate mining was largely unregulated until the early 1970s when county permitting requirements were introduced. This was followed by State regulations, including the Surface Mining and Reclamation Act (1975). Years that followed were marked by growing interest in the environmental and economic impacts of mining, especially those related to channel incision. By 1979, the Ventura County Environmental Resource Agency stated "…the loss of riverbed materials and accompanying channel degradation is primarily, if not totally, the result of gravel mining from the channel" (Schwartzberg and Moore 1995). Of particular concern was the prospect that channel incision would undermine bridges and other infrastructure. For example, the demise of Saticoy Bridge in the 1969 floods had been blamed on erosion of the bridge's pilings due to channel incision (Schwartzberg and Moore 1995), as was undercutting of the Highway 118 bridge over the river (Simons, Li & Associates 1983) (Figure 4-9). Other effects of channel incision included the repeated need for the United Water Conservation District to move its earthen dam at Saticoy progressively upstream to retain sufficient gravity flow for water diversion until, in 1991, a permanent concrete diversion—the Vern Freeman Diversion Dam—was constructed to anchor the point of water diversion.

Figure 4-9. Undercutting of the Highway 118 bridge over the SCR as a result of incision following the 1969 floods. (Photo courtesy of the VCWPD.)

Instream aggregate mining is reported to have peaked between 1981 and 1986 (Noble Consultants 1989). In 1985, the Board of Supervisors of Ventura County and the Ventura County Flood Control District jointly issued a revised "red line" restriction on the depth of permissible gravel mining, where the red line defines a grade that is deemed to reduce the risk of upstream erosion. The new red line reduced available resources in the WVPCR to 128 million tonnes (141 million tons)—some 91 million tonnes (100 million tons) short of the CGS 1993 estimate of the 50-year aggregate demand for the WVPCR (CDMG 1993, as cited in AMEC 2005)—and led to the cessation of instream aggregate operations in Ventura County by 1989 (SCREMP 1996, as cited in AMEC 2005). In Sespe Creek, mining has not reportedly occurred since 1992 but, in 2006, permits from various state and federal agencies (e.g., USACE) were granted to mining operators to resume instream extraction activities through 2015 (see Stillwater Sciences 2010).

There are few published rates of aggregate extraction for the LSCR. Simons, Li & Associates (1983) estimated annual aggregate extraction rates for the LSCR (WVPCR) for the period 1960–1977, of which an estimated 63% occurred directly from the mainstem channel. Table 4-9 lists the extraction rates by year from instream sites. The average annual rate of extraction for the period of record is 1.71 million tonnes (1.89 million tons). More recent reports (i.e., Noble Consultants 1989, SCREMP 1996, AMEC 2005) discuss aggregate mining but do not contain any updates on extraction rates.

Table 4-9. Instream aggregate production from the LSCR 1960–1977.*

Year	Instream aggregate production	
	(thousands of tonnes)	(thousands of tons)
1960	1,260	1,389
1961	1,783	1,965
1962	2,523	2,781
1963	1,278	1,409
1964	1,242	1,370
1965	2,039	2,247
1966	1,857	2,047
1967	1,647	1,815
1968	1,606	1,770
1969	2,061	2,272
1970	1,849	2,038
1971	2,178	2,401
1972	1,908	2,104
1973	2,155	2,376
1974	1,453	1,602
1975	1,347	1,485
1976	837	922
1977	1,626	1,792
Mean	1,710	1,890

* Note: The figure given is 63.3% of the estimated total production, estimated as the direct proportion mined from the channel.
Source: CDMG (1977) in Simons, Li & Associates (1983, p 2.41).

Aggregate mining has been identified as the primary cause of continual river bed lowering in the LSCR:

> "*Preliminary studies indicated that sand/gravel mining was the dominant factor causing continuous lowering of the river bed. Mining has affected not only*

> *degradation and general river morphology, but also groundwater recharges, riparian habitat, beach sand supply and the stability of bridges, flow diversion work and pipeline crossing"* (Simons, Li & Associates 1983, p.xiii)

The potential effect of mining activity is readily apparent when the average annual extraction rate (1.71 million tonnes yr^{-1}) is compared to Brownlie and Taylor's (1981) estimated annual sand and gravel yield (1.08 million tonnes yr^{-1} for the period 1956–1975, which post-dates dam construction) (Brownlie and Taylor 1981) and their estimated "natural" yield (1.35 million tonnes yr^{-1}) for the entire watershed (i.e., including areas regulated by dams). Extraction activities thus were removing sand and gravel faster than it was being replenished. However, comparisons between annual extraction and replenishment rates are complicated by the highly episodic nature of sediment transport in the river.

Instream mining has the potential indirect effect of causing knickpoint erosion, if the thalweg of the stream manages to connect with the mining pit. Mining pits beside the channel on the floodplain (i.e., from out-of-stream mining) can be "captured" as well (Collins and Dunne 1990, Kondolf 1994a, b) when levees are breached in large flood events. For a river like the Santa Clara, which is prone to large floods, pit captures are virtually unavoidable. "Channel piloting", which involves dredging a low-flow channel to guide flow away from the pits, was practiced on the river but probably did not reduce the likelihood of pit captures during high-flow events, when water levels far exceed the height of low-flow channel banks. Once a river is connected to a deep pit, the headwall of the pit acts as a significant step (or knickpoint) in the channel profile. If the headwall erodes, the knickpoint may migrate upstream until such a time that the channel returns to an equilibrium long profile (e.g., Parker and Andres 1976). The distance of upstream migration will depend on: (1) the ability of channel bed material to hold up as a headwall before becoming "smoothed out"; and (2) on the original depth of the pit (which may also control the depth of channel bed lowering). As knickpoints migrate upstream, mass failures of river banks become likely due to an increased tendency for the channel to widen (Harvey and Watson 1986, Simon 1989). Erosion and undermining of bridge supports and other in-channel infrastructure may also occur (see Figure 4-9). To explore this phenomenon on the SCR mainstem, repeat bed elevation surveys from 1949 and 2005 were used to analyze channel bed-level changes in Section 4.3.3.

4.2.2.2 Effects of aggregate mining to the USCR

In the USCR, one large-scale in-channel operation continues to extract aggregate resources from the bed and adjacent floodplain of the river, east of Santa Clarita near the mouth of Soledad Canyon (Figures 4-8 and 4-10). Total aggregate production here between 1960 and 1980—a boom period for urban development in the greater Los Angeles area—was estimated by the CGS to range between 200,000–1,000,000 t yr^{-1}, with the peak value being reached in the early 1970s (Joseph et al. 1987). This estimate does not discriminate between in-channel and off-channel aggregate production rates; however, information provided by the USACE suggests that the 30-year average annual extraction rate as reported from the only instream operation was approximately 270,000 tonnes (300,000 tons), with a maximum of about 450,000 tonnes (500,000 tons) per year (A. Allen, pers. comm., 2010). This average annual extraction rate accounts for approximately one-third of the average annual total sediment yield of the USCR watershed as calculated at the County line stream gauge (900,000 t yr^{-1}; see Section 4.1), and almost surely exceeded the average coarse-sediment flux in the river. Because the stream gauge record overlaps much of this aggregate mining period, this finding implies that the watershed's average annual sediment yield at the County line would have been greater when including this difference (in the absence of the instream mining activities). Instream aggregate extraction has reportedly

diminished somewhat in the years since Los Angeles County re-authorized the mining permit in 1994, but the exact extraction quantities are not known (A. Allen, pers. comm., 2010).

Figure 4-10. Lang Station Road and location of ongoing instream aggregate mining on the USCR near the mouth of Soledad Canyon. As visible in the NAIP 2006 aerial photograph (above), sediment is impounded on the upstream side of the 75-m (250-ft) long grade-control structure. Active floodplain and instream aggregate mining is visible downstream. The bottom photo taken during our spring 2010 field surveys shows a profile view of the 5–6 m (15–20 ft) high crossing with the river's flow being routed through large culverts (flow direction is to the left).

Determining the degree of recent channel degradation in the USCR resulting from aggregate mining is hampered by limited data and by channel-spanning grade controls, which not only anchors the bed elevation but also disrupts downstream sediment transport. The area of most prominent change is at Lang Station Road (Figure 4-10), within the area of most active ongoing aggregate extraction and itself a significant impediment to downstream sediment movement. Interruption of sediment movement is evident from the visible change in river morphology up- and downstream of this location.

The dynamic nature of this reach of the USCR was also highlighted by Simons, Li & Associates (1987), who reported up to 8 m (26 ft) of degradation between 1964 and 1977. They also noted that the bed recovered about one-half of this downcutting between 1977 and 1981 (the last reported measurement in their report). They ascribed the aggregated mining here as the most likely cause of the bed-elevation changes (p. 6.28). Our own analysis of bed level changes between the years 1928 and 2005 supports this finding for the reaches immediately upstream and downstream of the Lang Station Road crossing; the reach-average change in thalweg elevation for the two reaches is, respectively, -2 m (-7 ft) and -6 m (-20 ft) (see Section 4.3.3 and Figure 4-20 presented therein).

4.2.3 Levees, bank protection, and channelization

Flood flows from the LSCR historically spilled onto the Oxnard Plain and flowed towards the Pacific Ocean. However, since the 1950s, a series of 53 levees (both public and private) have been constructed along nearly 40 km (130,000 ft) of river bank length (Table 2-5 in URS 2005), amounting to approximately one-third of the total LSCR bank length in Ventura County. Throughout the USCR, levees and bank protection structures are common, but they are primarily concentrated along the Santa Clarita Basin reaches to provide flood control and channel stability. Many of the USCR's major tributaries have been channelized along their downstream reaches where they traverse dense developments. The locations of public levees mapped along the entire SCR are shown in Figure 4-8; locations of private levees are not available for the entire SCR.

Levees along the SCR include both public and private structures, constructed independently on left and right banks, and designed variously to protect agricultural lands, urban development, and floodplain mining pits. Many of the private levees are composed of riverbed materials and are designed to protect agricultural land from flooding; these typically have to be repaired or re-constructed after large floods (URS 2005). Several of these structures are themselves protected by earthen or stone groins projecting perpendicular from the levee and designed to reduce the velocity of near-bank flood flows that might otherwise undermine the levee.

AMEC (2005, Table 5.7-1) listed flood-protection features along the SCR based on their review of the 1996 Flood Protection Report (VCWPD and LADPW 1996)[4]. The reach descriptions are listed in upstream to downstream order; the reach numbers provided parenthetically are from this study (see Figure 4-8):

[4] The AMEC (2005) report additionally tabularizes information on existing flood protection facilities, including levees, bank protection, and groins that were initially summarized by VCWPD and LADPW in their 1996 report. Comparison of this comprehensive summary with the spatial data contained in Figure 4-8 of this report points out key differences between the two datasets used for each analysis and, further, highlights the need for a comprehensive spatial database of all flood protection facilities along the entire SCR and its tributaries.

Acton Basin (Reach 28): *"In the Acton area, the floodplain changes to a broad shallow plain varying in width from 1000 to 2000 feet. Private property owners have built some levees to protect recreational areas."*

Lang gauging station to Interstate 5 (Reaches 14–13): *"The floodplain varies in width from 500 feet at the 1-5 Freeway to 2000 feet near Bouquet Canyon Road. West of Whites Canyon Road to the 14 Freeway, the 100-year floodplain is contained with levees on either one side or both sides of the river. East of the 14 Freeway, the flood plain widens to an average of 1000 to 1500 feet. At Lang Station, it narrows down to less than 500 feet. Between Oak Springs Canyon and Sand Canyon, there are some permitted levees on the south bank of the river"*

Interstate 5 to County line (Reach 11-B): *"The Santa Clara River passes primarily through privately owned land. Property owners have built some levees to protect farming areas. Newhall Land and Farming Company is proposing a 'Natural River Concept', currently under review by the Los Angeles County, for the portion of the river within their property"*

Highway 23 to Sespe Creek (lower part of Reach 7): *"Severe erosion along the north bank has necessitated construction of groins"*

Sespe Creek to Willard Road (Reach 6): *"This is the widest flood plain area of the river, where the width varies from 3000' to about 7000'. The small berms and levees constructed by property owners and the Flood Control District … are of an interim nature and do not provide even 25-year protection particularly since they are flooded from the upstream end"*

12th Street to Adams Barranca (Reach 4): *"There are numerous equalizers through the freeway for the passage of flood flows from the north side of the freeway to the south side. However, the extent of flooding of the City of Santa Paula north of the freeway due to Santa Clara River has not been analyzed or identified … Except when protected by groins, the south bank is susceptible to severe erosion. On the other hand, most of the north bank is highly subject to deposition"*

Freeman Diversion to Highway 118 (upper part of Reach 2): *"All of the flood flows are contained in this subreach of the river. The USACE levee ends about 0.6 miles upstream of Highway 118 on the right bank. However, there is potential for extensive bank erosion, particularly on the north bank"*

Highway 118 to Highway 101 (lower part of Reach 2): *"USACE levee on the south bank provides flood protection for the entire Oxnard plain area. However, the flooding on the south bank between the Highway 101 and the Southern Pacific Railroad bridges, results in minor flooding behind the USACE levee. The entire south bank area below the bluff is in the 100-year flood plain"*

Levees confine high discharges that would otherwise spill onto neighboring floodplains, reduce the effective flow width during floods, and are frequently intended to stabilize the river's planform. However, because they exceed the natural elevation of the floodplain, the contained flood flows run deeper and generate increased shear stresses on the channel bed compared to the conditions if the flow was able to spill over the banks. Increased shear stresses increase the

chance of channel bed incision but, because flood sediments are also confined within the channel rather than being deposited onto the floodplain, large amounts of sediment may be deposited instream as the flood recedes. Hence, the net change in bed elevation along reaches that are bounded by levees depends on multiple competing factors and is difficult to predict.

Where levees are used in conjunction with bank protection to "train" the channel to a particular planform there is the risk that, if the imposed channel planform does not align with the natural planform tendency during flood events (or if the channel is simply too narrow), the flood thalweg will flow directly towards the levee in certain locations. This will lead to high near-bank flow velocities and the potential for levee erosion and an increased risk of bank erosion. An additional impact of protected levees is that flood flows can be reflected towards an opposing, unprotected bank that would not otherwise be prone to substantial erosion.

Damage to levees along the SCR has been noted during flood events, such as during 1969 floods caused a 610 m (2,000 ft) reach of the South Mountain–Highway 101 levee to fail. Further flood damage to the downstream levee and to the Saticoy "dike" (which protects Cabrillo village) occurred during the 1978 events (Simons, Li & Associates 1983). The damage was attributed primarily to undercutting brought about by channel incision associated with the effects of aggregate mining.

4.2.4 Urban growth

4.2.4.1 Existing urban growth

Population in the watershed has increased approximately 8-fold since the 1950s (Figure 4-11), with much of the growth occurring along the mainstem corridor and particularly in the vicinity of the present-day cities of Ventura, Oxnard, Santa Paula, Fillmore, and Santa Clarita (see Table A-2 in Appendix A). The greatest amount of growth has been occurring in Santa Clarita, which was only recently established in 1987 with the joining of four unincorporated towns: Canyon Country, Newhall, Saugus, and Valencia.

Increases in population and urbanization throughout the watershed (and greater vicinity) will undoubtedly continue into the foreseeable future and are likely to have increasing effects on geomorphic processes in the river corridor. Figure 4-12 shows three simplified stages of urban development growth in the watershed that have occurred to date since pre-European settlement times, and that are predicted to occur in the near future. These stages are: pre-settlement (absence of development), present (i.e., 2001 National Land Cover Database [Homer et al. 2004]), and future (CNRA 2010).

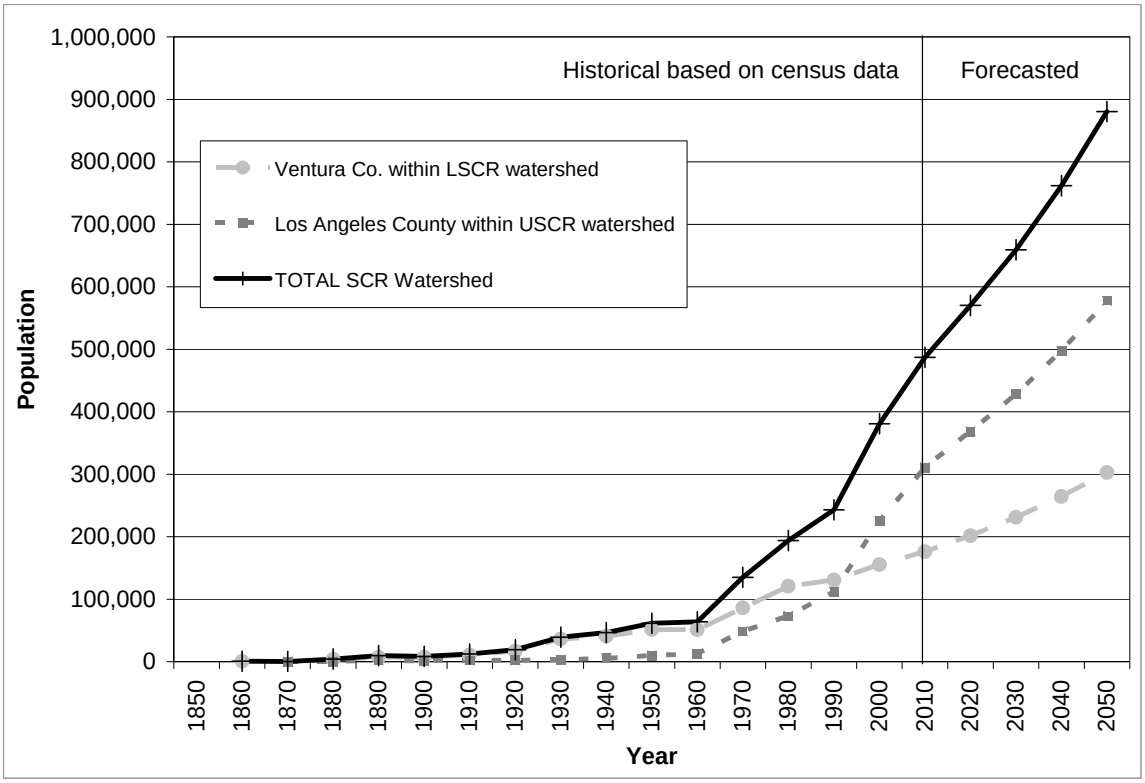

Figure 4-11. Historical and forecasted population of Ventura and Los Angeles counties within the SCR watershed (see Table A-2 in Appendix A for data sources).

There are two major geomorphic effects on the SCR related to urbanization. The first arises where construction occurs close to the river and requires levees or channelization for flood protection and enhanced flow conveyance. Where the levees constrain the width of the river, accelerated erosion can result (see Section 4.2.3 above). The second impact may be of greater regional consequence, and it arises from the increasing area of impermeable surface that accompanies population growth and urban expansion. The most widely recognized of these impacts, the hydrological changes that are expressed by higher peak flows and a more rapidly experienced peak flood flow, have been analyzed for nearly half a century (e.g., Leopold 1968). A less commonly recognized change in watershed conditions that can accompany urbanization, however, is the reduction in sediment delivery to stream channels in proportion to flow discharge (e.g., study of increased flow discharge with relative decrease in sediment discharge along the Santa Ana River by Warrick and Rubin [2007]). For erodible channels, such as the Santa Clara and Santa Ana rivers, this imbalance can be as destabilizing as an increase in discharge. This is because the condition of "stable stream channels" reflects a balance between the capacity of the flow to transport sediment and the availability of sediment for transport. Under the broad geomorphic concept of dynamic equilibrium, this balance is not necessarily achieved at every moment in time or at every point along the stream channel. Over a period of time, however, an observed condition of equilibrium is commonly presumed to express such a water–sediment balance. Conversely, the balance of these components is normally considered to be the defining precondition for stability in adjustable, alluvial streams. Thus a change in either component of the river's load, namely water or sediment (and urbanization commonly results in changes to both), can lead to a state of channel dis-equilibrium. In most cases within the SCR watershed, this has been (or is anticipated to be) expressed by channel incision or degradation (see Section 4.3.3).

Given the multiple confounding influences on the mainstem SCR (i.e., channelization, instream aggregate mining, St. Francis dam failure), tributary channels are most likely to first express urban-related impacts. A review of existing and likely future development patterns, relative to the present (and potential future) condition of the channel, is therefore instructive (see Figure 4-12, bottom panel).

Future land use as predicted by the regional zoning map (CNRA 2010; Figure 4-12, bottom panel) reveals that urban growth will be most concentrated within the Santa Clarita Basin. Further densification and infilling is anticipated, with significant expansions of development into the lower areas of several major tributaries including Castaic Creek (below Castaic dam), San Francisquito Canyon, Placerita Creek, Newhall Creek, and Railroad Canyon. The lower reaches of these streams would normally, therefore, be the first anticipated to display the combined effects of increased discharge and decreased sediment loading as a result of future urbanization. However, of this list only San Francisquito Canyon and Castaic Creek have not already been confined into concrete channels over much of their lower reaches, and the latter is already displaying the effects of a depleted sediment load from the effects of the upstream dam (see Section 4.3.4). Thus the effects of future urbanization are likely to be transmitted downstream to the mainstem USCR, with presumably less direct expression in these already severely impacted lateral tributaries. Of the major USCR tributaries, therefore, San Francisquito Canyon is poised to respond most freely to any significant future changes in watershed land use.

In the LSCR, urban expansion will be concentrated around the city centers of Ventura, Oxnard, Santa Paula, Fillmore, and Piru, albeit at a substantially smaller magnitude than in the Santa Clarita Basin. Several conservation projects are currently planned for the majority of the LSCR corridor that would involve acquisition and restoration of floodplain land, which would likely limit future urban growth along much of the active river corridor. One large-scale effort currently underway is the Santa Clara River Parkway project, which is being implemented by the California State Coastal Conservancy, in collaboration with the Nature Conservancy's LA-Ventura Project, Friends of the Santa Clara River, private landowners, and local governments (http://www.santaclarariverparkway.org/).

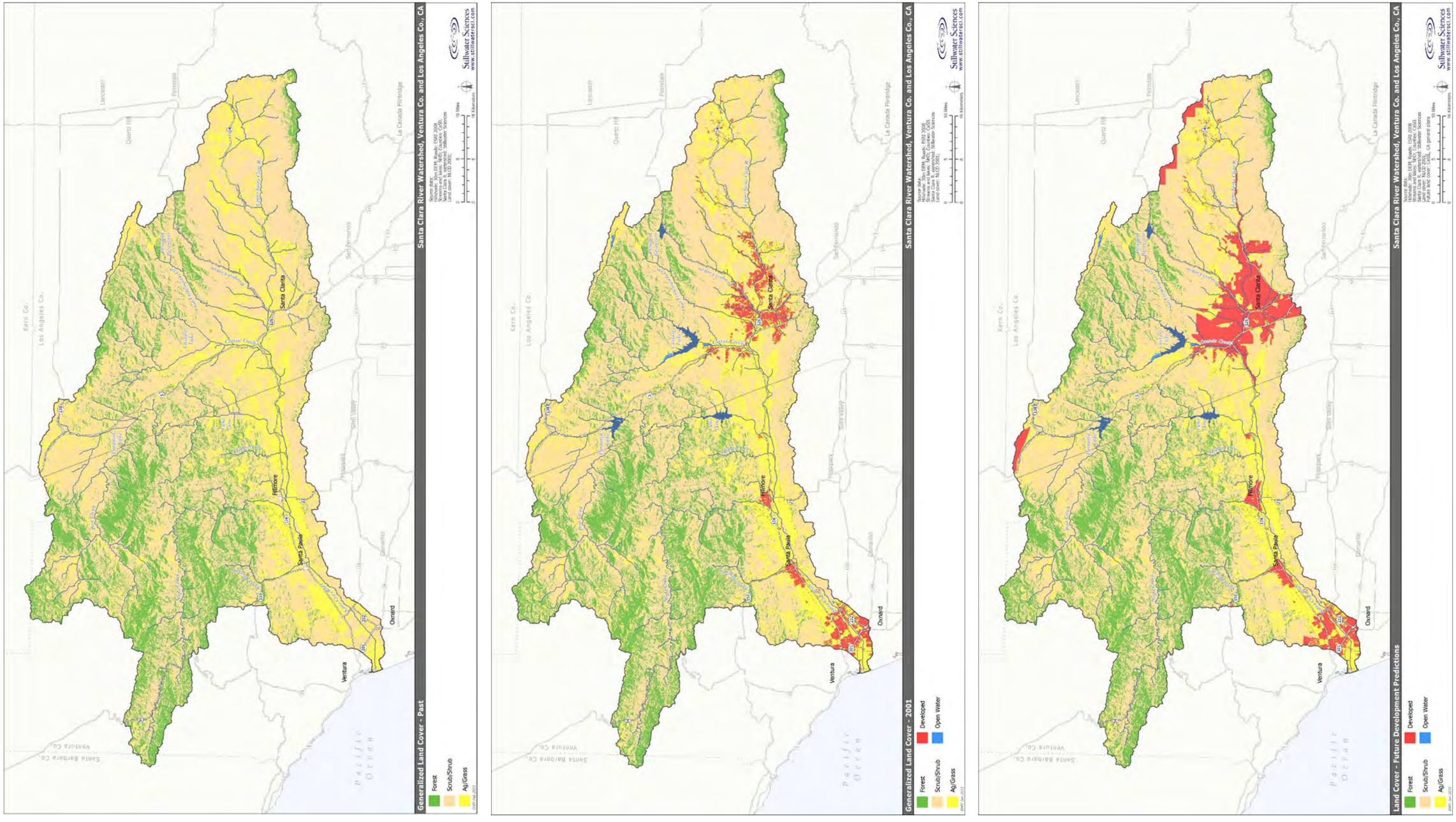

Figure 4-12. Generalized past (upper figure), present (middle figure), and future (lower figure) land-cover/-use categories depicting growth of urban footprints in the SCR watershed.

4.3 Morphology and Channel Dynamics

Understanding river morphologic and sediment character is a fundamental component in understanding the interplay between natural and anthropogenic impacts on the entire SCR drainage network, but particularly on the mainstem river. This understanding is key to identifying appropriate management actions into the future (e.g., Downs and Gregory 2004). Accordingly, this section describes current dominant processes and trends along the mainstem river channel. The summary presented here, however, does not provide a comprehensive catalog of all channel conditions throughout the watershed. More detailed river and tributary reach descriptions are presented elsewhere (e.g., Stillwater Sciences 2007a, 2007b, 2009, 2010, and 2011a).

Preexisting data sources used in the analyses discussed here include river bed sediment data, historical aerial photographs, and historical topographic data. The analyses also draw upon field observations made during our various reconnaissance efforts conducted as part of our LSCR and USCR geomorphology studies (Stillwater Sciences 2007a and 2011a). The bed sediment particle-size distribution data were collected in 1987 by Simons, Li & Associates, in 2005 by Seward, in 2006 by PWA, and in 2005 by LADPW, which were compiled in the 2008 LADPW field investigation report for Los Angeles County (see listed citations therein) (Figure 4-6). We collected additional data throughout the USCR watershed in 2010 (see Appendix E of Stillwater Sciences 2011a for laboratory results). Historical aerial photographs and topographic data sources are discussed below in Sections 4.3.2 and 4.3.3.

The SCR today flows for approximately 132 km (83 miles) through Los Angeles and Ventura counties (Figure 1-1) to the Pacific Ocean. In planform, it is characterized by a wide, relatively straight floodway with one or more low-flow channels that are re-configured after each flood event (with the exception of the Soledad Canyon reaches along the USCR, which is discussed below). The overall mainstem channel is filled only during high-magnitude floods. Erosion of alternate outer banks of the active floodway in some reaches following large floods in January-February 2005 (Figure 4-13a, b) suggests that the entire floodway of the contemporary SCR behaves in a manner similar to a broad, single-thread meandering channel at very high flows. As floods recede, the river becomes more braided in character, with multiple flow courses. Perennial flow is insufficient to retain multiple flowing channels in a majority of the SCR and, in general, a single dominant channel defines the channel thalweg. In some reaches, however, residual flow continues to be carried by secondary channels.

The long profile is gently concave, with gradients along the LSCR ranging from approximately 0.0025 (near the mouth) to 0.0060 and along the USCR ranging from approximately 0.0050 (near the County line) to 0.0200 (near the headwaters). The SCR transports a mixed load of sediment ranging from fine sand to coarse gravel (see Section 4.1.4). Dominant sediment sizes sampled from the bed (i.e., stored sediments) have been recorded to range from medium sand up to coarse cobble. Reconnaissance following the January-February 2005 high-magnitude floods indicated that the river can transport coarse gravel to the Santa Clara River Estuary.

a)

b)

Figure 4-13. View of the SCR during the January 2005 flood, with a westward, downstream view of the LSCR near the Sespe Creek confluence (two channels entering from right) (a), and an eastward, upstream view of the USCR through the Santa Clarita Basin near the Bouquet Canyon confluence (channelized downstream extent entering from left) (courtesy of the California State Coastal Conservancy).

The morphology and dynamics of the present-day SCR channel likely differ quite significantly from the SCR prior to European settlement of the watershed. Overall, the entire SCR seems likely to have undergone a fundamental shift in its hydrology and sediment supply regime towards higher-magnitude flood flows carrying greater amounts of finer-textured sediment, and with less protection of the bed and banks from erosion. The various potential historical impacts serve as context in examining the morphology and river channel dynamics of the SCR since about 1930 (when detailed morphologic data started to become available). Significant river channel changes resulting from population growth in the watershed had already occurred, so that some of the post-1930 changes identified in the following sections may have been, at least in part, legacy responses to impacts caused by watershed changes prior to 1930.

4.3.1 Reach-level differences in channel form

The morphology and channel dynamics of the 132-km (83 mi) SCR do not vary consistently along the entire length of the channel. Instead, reach-level differences in the channel response have important implications for river management, including that management solutions may vary from reach to reach. As such, the SCR was sub-divided into 28 reaches, ranging from approximately 0.4 to 10 km in centerline length (0.2 to 6 mi) according to criteria that correspond to different morphological properties between reaches (Tables 4-10 and 4-11). These criteria include tributary junctions (where additional flow and sediment are received) and degree of channel confinement, whether by valley walls or by constructed levees. Using post-flood 2005 aerial photographs, the active channel width varied from approximately 13–570 m (43–1,870 ft), with the large 2005 flood scouring much of the channel bed clear of vegetation. These 28 reaches are the basis of all later analyses in this Chapter (see Figure 4-8 for reach locations).

Classification of the channel pattern into a distinct typology provides an important first step in understanding the morphodynamic behavior of river systems. However, channel pattern within the entire SCR is clearly stage-dependent and does not fit neatly into simple classification schemes (e.g., Rust's [1978] division into straight, meandering, braided or anastomosing channels). Using more complex graphical classifications, the SCR at various flow stages fits several of the 14 patterns identified by Schumm (1981, 1985, as developed by Knighton 1998, p. 206) and does not obviously fit any of the channel patterns in Shen et al.'s (1981) graphical matrix of possibilities, reinforcing the sense that the SCR does not operate like a "classic" alluvial channel. To explore the poorly predicted character of the SCR specifically, various "discriminant" analyses were performed (Figure 4-14 a–b) to evaluate channel typology by reach. All reaches conform to the "braided" category using Wolman and Leopold's (1957) slope-discharge-based distinction (Figure 4-14a). Additionally incorporating grain size, the river plots between the gravel-bed braided and sand-bed braided distinction implied in analyses by Ferguson (1987) and Knighton and Nanson (1993) (Figure 4-14b).

Using a pattern classification developed for dryland rivers with highly variable flows (Graf 1983, 1988a, and 1988b), or implied in regions with extended drought- and flood-dominated flow regimes (e.g., Warner 1987 and 1994, Erskine and Warner 1988), much of the SCR can be classified as a "compound" channel. The exception would be for the confined Soledad Canyon reaches where the channel is relatively steep and narrow. Graf's compound channel definition arises from research primarily in Arizona. He described compound channels as having two modes of operation: a single meandering channel at low flow and a braided channel at higher flows (1988b, p. 202). Compound channels are differentiated from braided channels by the existence of a dominant sub-channel and because the meandering channel fits within the overall braided channel form (Graf 1988b, p. 202). While the SCR shares several of these characteristics, especially the nested channel form and, usually, a dominant sub-channel, it is clearly

Table 4-10. LSCR reach characteristics.

Morphodynamic feature	1	2	3	4	5	6	7	8	9	10	11-A
	Santa Clara River Valley										
	Lower Santa Clara River Valley						*Upper Santa Clara River Valley*				
Reach boundaries (downstream to upstream)	*Harbor Blvd bridge Hwy 101 bridge*	*d/s Freeman Dam*	*u/s Freeman Dam Shell Rd.*	*Santa Paula Cr.*	*East flank South Mtn.*	*Sespe Cr.*	*E of Cham'burg Rd.*	*Hopper Cr.*	*Piru Cr.*	*E of Piru Cr.*	*County line*
Centerline reach length [a] (km)	6.4	10.0	4.7	3.5	2.5	6.8	5.3	5.7	4.7	4.4	6.1
Q_2 [a] (m^3 s^{-1})	185.9	185.9	185.9	185.9	185.9	185.9	89.5	60.6	60.6	54.2	52.9
Reach-average slope [a]	0.3%	0.3%	0.3%	0.4%	0.3%	0.4%	0.5%	0.6%	0.5%	0.6%	0.6%
D_{50} range [b] (mm)	0.2-5	0.6-15	1	1-5	1-4	0.8-3	0.6-1	1-5	2	1	2-67
Particle size type [c]	S–G_f	S–G_m	S	S–G_f	S–G_f	S–G_{vf}	S	S–G_f	S	S	S–C_v
Reach-average active width, 2005 [d] (m)	222	350	265	384	456	474	570	422	542	555	146
Local characteristics	Wide floodplain, part of natural distributary area for the river. Largely straight channel, levees on left bank, urban area behind.	Wide floodplain, part of natural distributary area for the river. Levee along most of left bank, and a short stretch of the right. Urban development to channel edge along most of the right bank, and downstream along the left bank. Gravel mining until 1988 in the lower and upper reach. Upstream extent bounded by Freeman Dam.	Left bank impinges on South Mountain. Gravel mining throughout the reach until 1988. Freeman Diversion Dam provides grade control at the downstream end.	Left bank close to South Mountain, urban development to edge of right bank. Some revetment on right bank. Gravel mining until 1986. Receives unregulated inflow from Santa Paula Creek.	Left bank impinges on South Mountain. Downstream end is confluence with Santa Paula Creek.	Wide floodplain, channel in center: sinuous and braided. Levee at upstream end opposite Sespe Creek confluence. Receives unregulated inflow from Sespe Creek.	Urban development to right bank edge in upper part of reach, right bank leveed in this area. Downstream end is confluence with Sespe Creek.	Wide floodplain floor. Upstream left bank close to mountains. Sinuous and braided. Inflow from Hopper Canyon.	Wide floodplain floor, channel veers towards towards left bank mountains. inuous and braided. Received highly regulated flow from Piru Creek.	Wide floodplain floor. Channel in center. Highly regulated flows.	Narrow valley segment. Highly regulated flows (downstream from Castaic Creek). Heavy agriculture use adjacent to floodway.

[a] From HEC-RAS output (modified from URS 2006).
[b] From compilation of bulk sediment size data (see Figure 4-6); values for Reach 5 were taken as the average of Reaches 4 and 6 because no bulk sediment sample data were available for that reach;
[c] Based on bulk sediment size data; size categories: S = sand (<2 mm), G_{vf} = very fine gravel (2–4 mm), G_f = fine gravel (4–8 mm), G_m = medium gravel (8–16 mm), G_c = coarse gravel (16–32 mm), G_{vc} = very coarse gravel (32–64 mm); C_v = fine cobble (64–128 mm); C_c = coarse cobble (128–256 mm).
[d] From active channel width analysis (1938, 1945, 1969, 1978, 1992, 1995, 2005) (see Table 4-12 and Figures 4-15 and 4-17).

Table 4-11. USCR reach characteristics.

Morphodynamic feature	11-B	12	13	14	15	16	17	18	19	20	21	22	23	24	25	26	27	28
	Santa Clarita Basin						Soledad Canyon									Acton Basin		
Reach boundaries (downstream to upstream)	***County line*** / ***SM Grande Cyn***	***Castaic Cr.***	***I-5 bridge*** / ***San Fran' Cyn So. Fk. SCR***	***Bouquet Cyn*** / ***Newhall Ranch Rd. br.***	***Mint Cyn*** / ***Sierra Hwy br.***	***Hwy 14 bridge***	***Tick Cyn*** / ***Lang Stn. Rd. crossing***				***Bear Cyn***	***Agua Dulce Cyn***	***Soledad Cyn Rd. bridge*** / ***Soledad Cyn Rd. bridge***			***Arrastre Rd. crossing***	***Acton Cyn***	***Aliso Cyn***
Centerline reach length, 2005 (km)	1.7	3.9	8.9	5.9	6.8	4.8	2.1	2.0	1.4	0.4	0.4	2.1	9.8	1.9	2.3	1.0	1.7	3.1
Q_2 [a] ($m^3 s^{-1}$)	69	65	52	36	29	26	26	21	21	21	21	20	17	13	13	12	12	8
Reach-average slope, 2005 [b]	0.5%	0.5%	0.6%	0.9%	0.9%	0.9%	0.7%	1.1%	1.3%	1.6%	1.7%	1.3%	1.3%	1.7%	1.5%	2.0%	1.3%	1.2%
D_{50} range [c] (mm)	0.8-3	0.7-2	0.3-4	2-4	4-12	3-8	4	2	4	15	200	9	1	2	2	4-32	2	3
Particle size type [d]	S–Gv_f	S–G_{vf}	S–G_{vf}	G_{vf}	G_f–G_m	G_{vf}–G_f	G_{vf}	G_{vf}	G_{vf}	G_m	C_c	G_m	S	G_{vf}	G_{vf}	G_f–G_c	G_{vf}	G_{vf}
Reach-average active width, 2005 [e] (m)	195	163	145	178	150	202	109	128	29	13	34	30	39	14	51	53	57	304
Local characteristics	Narrow valley segment. Highly regulated flows (downstream from Castaic Creek). Left bank close to Santa Susana Mtns front.	Narrow valley reach (broader than Reach 11-B) through planned Newhall Ranch develop-ment. Highly regulated flows immediately d/s from Castaic Creek.	Wide floodplain through densely urbanized Santa Clarita. Crossed by I-5, Hwy 126, and McBean Pkwy bridges. Receives unregulated inflow from San Francisquito Cyn and So. Fk. SCR.	Densely urbanized Santa Clarita. Narrow valley between Bouquet Canyon Rd. and Newhall Ranch Rd. bridges. Receives partially regulated inflow from Bouquet Canyon.	Wide floodplain, but highly constricted by levees and bank protection on both banks through Santa Clarita. Crossed by Soledad Cyn Rd., Whites Cyn Rd., Sierra Hwy, and Hwy 14 bridges. Receives unregulated inflow from Mint Cyn.	Eastern side of Santa Clarita Basin and urban develop-ments. Valley narrows to the east (u/s side). Crossed by Sand Cyn Rd. bridge.	Narrow valley reach immediately d/s of the Lang Stn. Rd. crossing and the active instream aggregate mining operation. Significant incision d/s of the crossing.	Narrow valley reach immediately u/s of the Lang Stn. Rd. crossing and d/s of the highly confined Soledad Canyon. River still exhibits a broad, braided planform before transitioning to a confined channel u/s.	Confined and sinuous canyon reach, crossed by railway line.	Confined canyon reach, further impinged on right bank by railway. Very coarse bed.	Confined canyon reach receiving very coarse sediment supply from Bear Canyon.	Confined canyon reach bordered along left side by San Gabriel Mtns front and along right side by railway line and Soledad Cyn Rd. Large rock quarry at d/s end. Receives unregulated flow and coarse sediment from Agua Dulce Cyn.	Confined, long canyon reach bordered closely by Soledad Cyn Rd. (left side) and railway line (right side), with some develop-ments and low-water road crossings within the active channel.	Confined canyon reach bordered closely by Soledad Cyn Rd. and railway line (right side), with some develop-ments and low-water crossings within the active channel.	Narrow floodplain floor within canyon. Bordered closely by Soledad Cyn Rd. and railway line (right side), with some developmen ts and low-water crossings within active channel.	Narrow floodplain floor at east end of canyon and west side of Acton Basin. Bordered closely by Soledad Canyon Rd. and other low density develop-ments. Immediatel y d/s of Arrastre Rd. crossing, with significant incision.	Narrow floodplain floor at west side of Acton Basin with agriculture and low density develop-ments on floodplain (left side). Downstrea m of Acton Canyon.	Wide floodplain flood with expansive braided, wash channel morph-ology. Receives unregulate d inflow from high relief Aliso Cyn.

[a] From HSPF model output (Aqua Terra 2009).
[b] From longitudinal profile generated in GIS with 2005 LiDAR data.
[c] From compilation of bulk sediment size data (see Figure 4-8);
[d] Based on bulk sediment size data; size categories: S = sand (<2 mm), G_{vf} = very fine gravel (2–4 mm), G_f = fine gravel (4–8 mm), G_m = medium gravel (8–16 mm), G_c = coarse gravel (16–32 mm), C_c = coarse cobble (128–256 mm).
[e] From active channel width analysis (1928, 1964, 1980/81, 1994, and 2005) (see Table 4-13 and Figures 4-16 and 4-18).

differentiated from Graf's examples because the floodway is retained within reasonably component channel banks (unlike Graf's) and so exhibits more of a single thread form at higher flows, while it is braided at lower flows. Compound channel morphology has also been described in southeast Australia where flood and drought cycles lasting on the order of decades result in a distinct "channel-in-channel" morphology for single thread channels during drought periods as the channel narrows, and subsequent widening during the flood-dominated periods (Warner 1987 and 1994, Erskine and Warner 1988). While the SCR is affected by multi-decade wet and dry periods, analyses of channel width changes in the less incised reaches (see Section 4.3.2) suggest that the active channel width is apparently correlated most strongly with the influence of individual flood events, primarily those resulting from ENSO oceanic conditions (see Section 4.1.3; Figure 4-5a), than any overall equilibrium "wet" and "dry" condition.

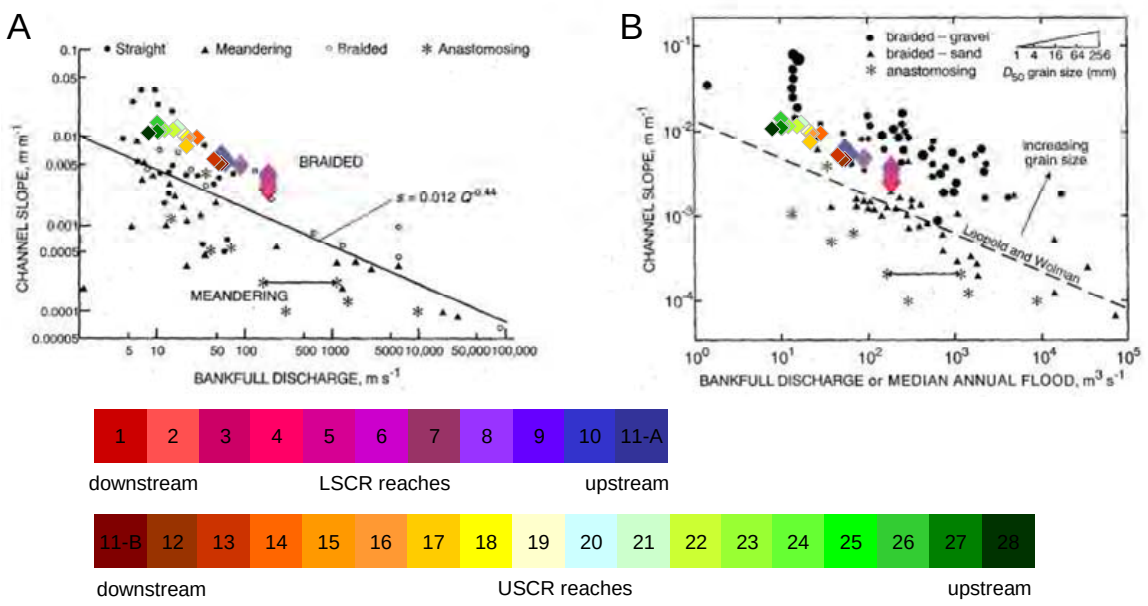

Figure 4-14. Predicted channel pattern for the SCR by reach. See text for details of data sources. Note that the pattern is classified variously as braided (A) between braided and meandering (B).

On balance, the contemporary planform of the SCR is unusual and does not fit neatly into any reviewed classification. Primarily because the river has two distinct functional regimes, it is a variation on a compound mixed-load channel. The low-flow regime exists for the majority of the time and consists of a dominant low flow channel and, occasionally, several minor channels, which meander across the sand and gravel bed of the active channel bed. During these periods, little sediment transport occurs. Summer flows are maintained by dam releases and urban effluent flows, where present upstream. In some areas, subsurface bedrock controls cause groundwater to flow towards the surface; elsewhere, flow is lost to the channel bed.

The SCR's high-flow regime occurs very intermittently in response to high-intensity rainfall events, usually occurring between December and March. Such flows are capable of inundating the majority of the channel floodway and cause the channel to function as a single-thread, low-sinuosity channel (see Figure 4-13a, b). Rates of sediment transport are very high and morphological change occurs primarily by bed level adjustments during flood events. Events can

result either in the net transport of material out of the SCR (i.e., channel incision), or into the SCR resulting in channel bed aggradation (see Section 4.3.3). In the largest events, alternate erosion of the outer banks of the active floodway can occur (observed along the LSCR following the January-February 2005 floods, see Figure 4-13a). It is possible that the river had more in common with Graf's dryland river examples prior to human impacts that have resulted in considerable channel incision (see Section 4.3.3).

Overall, this indeterminacy of channel form relative to "classic" channel typologies described elsewhere means that caution should be used in interpreting behavior of the SCR, and that management solutions must be drawn distinctly from the observed characteristics of the SCR rather than being imported from potentially dissimilar river elsewhere.

4.3.2 Changes in active width

As a predominantly braided but dryland river, the mainstem, alluvial channel flowing through the Santa Clara River Valley and Santa Clarita and Acton basins comprises a primary low-flow channel and various short-lived secondary channels (i.e., compound channel). The low-flow channel boundary changes rapidly and completely during flood events according to the magnitude of the event and other factors, whereas the boundary of the larger mainstem channel changes less frequently but carries greater importance in determining the relationship between the river's geomorphology and human activities on the adjacent floodplain.

Unlike single-thread meandering channels that generally have a well-defined edge that separates the mainstem channel from its floodplain, the lateral edges of the mainstem SCR channel is less well-defined. Because of intermittent flow, changeable morphology and thalweg location, and rapid colonization of the channel bed by riparian vegetation between flood events, the separation between the floodplain and channel is only evident following relatively large flood flows and is even then subject to interpretation according to the extent of apparent flow inundation and re-working of channel bed sediments achieved by the flood event. Prior empirical investigations of channel change have focused both on the position of the primary low-flow channel, to the extent it is discernable, and on the extent of the full width of flood flow (i.e., in the mainstem channel *and* over the floodplain) evident from aerial photographs of the SCR (e.g., the maps and supporting text in Section III of Simons, Li & Associates 1983 and in Section VI of Simons, Li & Associates 1987). Because large flood events physically affect more than just the low-flow channel(s), our analysis considers the "geomorphically active channel" in quantifying the change in the river's morphology over time.

The geomorphically active channel, or "active channel width," is considered here as that part of the mainstem channel bed that carried a significant part of the flood and sediment discharge during the recent flood event. Delineation of the active channel width was accomplished here in a GIS using an analysis of available large-scale aerial photographs where visible channel bed scour is visible. Because aerial photographs are typically taken of a particular landscape within political boundaries, the available photographs in Los Angeles and Ventura counties were, for the most part, not taken in the same year. Aerial photography in the LSCR has nearly always followed large flood events since the early 20th century, while post-flood photography in the USCR has occurred less often due to the lack of population until recently. For the LSCR analysis, we utilized photographs from 1938, 1945, 1969, 1978, 1992, 1995, and 2005. For the USCR, aerial photographic coverage was more sparse: 1928, 1964, 1980-81, 1994, and 2005. The aerial photograph analysis approach follows similar methods to studies in dryland rivers by Graf (1984, 2000), Tiegs and Pohl (2005), and Tiegs et al. (2005).

Both analyses performed for the LSCR and USCR employed identical methods. A technical account of the methods (Appendix C). The aerial photographic sets were chosen because they were the most comprehensive available for use in this study and they closely, or nearly closely, followed a moderate to large flood event where evidence of channel change was apparent. Aerial photographs from 1929 were available in the LSCR following the 1928 St. Francis Dam failure but were not used in the analysis because of their poor resolution. In the USCR analysis, photographic coverage for years immediately following two of the watershed's largest flood events—1938 and 1969—were unfortunately not available. Discrete polygons of the channel bed were digitized to define (1) clear-scoured channel bed without vegetation, and so clearly subjected to significant flow; (2) partially vegetated areas showing evidence of having been subjected to flow and erosion and/or deposition; and (3) densely vegetated areas on the channel bed without evidence for scour or deposition in the last flood. Hydrologically, the latter areas may have been inundated during the last flood event, but the effects related to geomorphic processes were minor. The extent of the active channel was designated to include all polygon types (1) and (2). The analyses was run for each set of aerial photographs over the entire SCR, or to the extent possible according to photographic coverage (Appendix C).

Dividing the total area of active channel by the length of each channel reach provided a measure of the average active channel width for each date, and a variety of associated statistics (Tables 4-12 and 4-13). Overall, a general narrowing trend is exhibited along much of the SCR. Also notable is the differences in active channel width in the four regions of the watershed, with the widths of the Santa Clara River Valley reaches generally larger than those in the Santa Clarita and Acton basins, and the widths in the Soledad Canyon reaches being much narrower due to the confinement by the canyon walls. The normalized standard deviation of active channel widths indicates two distinct reach groups: those reaches that have been more changeable over time (reaches 1, 5, 6, 7, 11-B, 12, 13, 20, 24, and 26: normalized standard deviation >0.40) and the remaining reaches that have been less changeable (normalized standard deviation $\leq$0.36).

Identification of the river's active channel position over time provides a useful means to predict where the river may continue to be located and where the river's course may eventually be located. To identify the spatial extent of the river's active channel in the past, we created two sets of maps, overlaying the active channel areas delineated using each of the historical aerial photograph sets. Initially, the channel bed was plotted as a proportion of time since the initial photograph year (i.e., LSCR: 1938; USCR: 1928) that the bed has occupied a given position (Figures 4-15 a–g and 4-16 a–g) to indicate the relative likelihood of channel courses. Second, the width of the bed in successive floods was overlaid with the most recent on top (Figures 4-17 a–g and 4-18 a–g) to indicate trends in active channel widths during floods. Also shown in Figures 4-17 a–g and 4-18 a–g are the areas of low channel disturbance for all years considered (i.e., polygon class 3, as described above).

Reach 1 is anomalous in that the active channel width is highly changeable and yet has narrowed in time. Whereas the reach was previously free to inundate and move sediment across a wide extent of floodplain (i.e., 1938; Figure 4-15a), levees have subsequently confined all subsequent floods except 1969, which broke through the levees and re-occupied the former flood extent. Reach 1 is the reach that has previously been described as losing more of its floodway than any other reach (Simons, Li & Associates 1983): the maps confirm this conclusion and indicate that, since the 1990s, the active channel width during floods has become narrower still (see Table 4-12).

Reaches 2, 3, and 4 have each become narrower over time, and they are not highly changeable in planform. Whereas the lack of adjustment in Reach 3 may be partly an attribute of the

confinement of the left bank by South Mountain, Reach 2 has been stabilized by levees and the course of Reach 4 may have been influenced by short lengths of bank protection. Although the flood in 2005 was the second largest on record, the flood outline occupied a relatively narrow trace through Reaches 2, 3, and 4. Significant extents of each of these reaches were permitted for aggregate mining, indicating that changes may have been partially related to channel incision that typically follows aggregate mining.

Reaches 5, 6, and 7 also display similar planform response attributes to the recent flood events. These three reaches are highly changeable and are largely free to adjust in accord with the magnitude of the flood event. Large areas along Reaches 5 and 6 have been inundated in the last flood events, and their changeability is highlighted in Figures 4-15 (d and e) by the lack of a contiguous course of channel occupation (i.e., breaks in the polygon recording a probability of occupation between 0.86–1.0). These reaches are both downstream of the confluence with Sespe Creek and thus may owe their behavior to the pattern of deposition of sediments emanating from Sespe Creek. Conversely, Reach 7 is upstream of the Sespe Creek confluence and it holds a more stable planform alignment even though the flood width varies in response to flood magnitude. This attribute is presumably a response to backwater effects of the mainstem in response to the frequently greater discharge emanating from Sespe Creek.

The active channel bed through Reaches 8, 9, and 10 is less changeable than that of the reaches downstream, and it has become narrower over time. Unlike Reaches 2, 3, and 4, these reaches are not confined by engineered levees, and have not been subject to instream aggregate mining. The reaches may be less changeable than those downstream because the reaches do not experience the extreme flows promoted downstream of the confluence of Sespe Creek. The estimated 1.5-year recurrence interval discharge in Reaches 8–10 is approximately 60 $m^3 s^{-1}$ (2,120 cfs) (URS 2006), whereas flow is estimated at 186 $m^3 s^{-1}$ downstream of Sespe Creek (Table 4-12). However, these reaches also show a consistent reduction in width over time, suggesting that other factors are influential. Chief among these may be flow regulation, especially of Piru Creek by Santa Felicia Dam. Using gauge information from above Lake Piru (USGS 11109600) indicates that, without regulation, large flows (>283 $m^3 s^{-1}$: 10,000 cfs) would have occurred also in 1962, 1969, 1978, 1983, 1992, 1998, 2001, and 2005. Therefore, the active channel width in Reaches 8 and 9 may have narrowed simply because of reductions in flood magnitudes since completion of Santa Felicia Dam. Reach 10 is situated above the Piru Creek confluence; although it is subject to regulation by Castaic Dam.

Reaches 11 to 13 in the Santa Clarita Basin have generally decreased in width since being heavily widened by the flood from the St. Francis Dam failure. The narrowing of these reaches is also likely due reduction in flow by Castaic Dam and development of the floodplain.

The widths of the upper reaches in this region (reaches 14 to 16) have fluctuated over time and in response to the individual floods. In many instances, the channel widths have been reduced due to channel encroachments by urban development, specifically in reaches 14 and 15 (Figures 4-18 b, c) where the city of Santa Clarita has grown considerably since the 1960s. In contrast, Reach 16, which is just east of the dense urban footprint of Santa Clarita, has progressively increased in width during this period.

Reaches 17 and 18 have exhibited progressive narrowing since the 1960s, particularly Reach 17 (now half its 1964 width, despite the 1969 and 1978 floods). This reach is situated immediately downstream of the Lang Station Road crossing where active instream aggregate mining has been occurring since the early 1960s. Therefore, it appears that the grade control structure (road

crossing) and aggregate mining have served to create an incised, inset, and narrower channel in Reach 17 (see Section 4.3.3 below).

The remaining reaches in confined sections of Soledad Canyon (i.e., reaches 20–25) have had varied changes in their respective active channel widths, but similar to reaches 17 and 18 they have generally exhibited channel narrowing since the 1960s and/or early 1980s. The specific causes of this condition are difficult to identify as there have been few new developments in the river corridor in these reaches during this period. The 2005 flood event, which was larger than all preceding events since 1969 (see Table 4-1), should have effectively scoured a relatively wider channel area than that formed following either the 1978 or 1992–1993 floods. However, one of the most significant differences in the long-term morphologic changes occurring in Reach 17 and in those upstream is the pattern of aggradation, rather than incision, occurring in the canyon reaches (see Section 4.3.3 below).

In the Acton Basin, reaches 28 and 29 constitute the historically broad channel areas of the depositional basin. Reach 28 has generally maintained its active large width while Reach 29 has narrowed considerably over time. The primary cause for this reduction in channel width is the encroachment of a residential development directly in the active channel area at the confluence of Aliso Canyon and the USCR. This development, positioned in and around the intersection of Aliso Canyon and Carson Mesa roads, appears to have been constructed over a period of a few years in the late 1980s and early 1990s (i.e., between the aerial photographs taken in 1980/81 and 1994).

Table 4-12. Width statistics for the LSCR for the period of record 1938–2005 by reach.

Aerial photo date	Follows flow [a]			Active channel width (m) [b]										
				Santa Clara River Valley										
				Lower Santa Clara River Valley						*Upper Santa Clara River Valley*				
	Flood date	($m^3 s^{-1}$)	(cfs)	1	2	3	4	5	6	7	8	9	10	11-A
2005	10 Jan 2005	3,851	136,000	222	350	265	384	456	474	570	422	542	555	146
1995	10 Jan 2005	3,115	111,000	209	331	277	223	391	402	463	305	473	470	99
1992	12 Feb 1992	2,945	104,000	229	357	204	265	279	528	465	297	515	521	112
1978	9-10 Feb 1978	2,890	98,610	347	405	294	431	508	677	584	586	519	487	
1969	25 Jan 1969	4,670	165,000	1,412	511	624	519	1,230	1,406	1,542	642	687	738	
1945	23 Jan 1943	2,265	80,000	497	662			330	519					
1938	2 Mar 1938	3,398	120,000	1,501		605	583	561	847			758	743	256
Weighted average (m)				603	493	473	458	502	660	745	480	623	617	
Standard deviation (m)				473	150	168	151	297	323	446	163	159	161	
Normalized standard deviation [c]				0.78	0.30	0.36	0.33	0.59	0.49	0.60	0.34	0.25	0.26	
Long-term morphologic trend				Narrowing										

[a] As measured at the Montalvo stream gauges (USGS 11114000), except for the 1943 events, which was estimated, and the 2005 event, which was estimated at the Freeman Diversion (source: VCWPD).
[b] Blank cells indicate that aerial photograph coverage in that reach was absent or incomplete.
[c] More changeable reaches have normalized standard deviations >0.40, while less changeable reaches have deviations ≤0.36.

Table 4-13. Width statistics for the USCR for the period of record 1928–2005 by reach.

Aerial photo date	Follows flow [a]			Active channel width (m) [b]																
				Santa Clarita Basin						Soledad Canyon									Acton Basin			
	Flood date	($m^3 s^{-1}$)	(cfs)	M11-B	M12	M13	M14	M15	M16	M17	M18	M19	M20	M21	M22	M23	M24	M25	M26	M27	M28	M29
2005	10 Jan 2005	906	32,000	195	163	145	178	150	202	109	128	29	13	34	30	39	14	51	53	57	304	54
1994	12 Jan 1992 18 Feb 1993	348 303	12,300 10,700	188	163	108	227	155	199	135	146	40	22	56	38	61	32	73	36	64	296	80
1980/81	9 Feb 1978 16 Feb 1980	646 394	22,800 13,900	194	282	98	263	171	183	149	152	49	22	70	41	75	58	80	68	60	322	213
1964	11 Feb 1962	258	9,100				261	184	189	208	163	32	21	53								
1928 [c]	13 Mar 1928	~$2x10^4$	~$7x10^5$	418	537	388	164	166	142	192	74	34	53	60	54	39	12	39	7	59	251	143
Weighted average (m)				313	389	260	209	168	170	174	118	37	35	58	46	50	25	54	29	60	278	139
Standard deviation (m)				113	166	140	45	10	25	31	39	6	16	9	9	15	18	18	25	2	30	49
Normalized standard deviation [d]				0.36	0.43	0.54	0.22	0.06	0.15	0.18	0.33	0.17	0.48	0.15	0.19	0.30	0.73	0.34	0.89	0.03	0.11	0.35
Long-term morphologic trend				Narrowing					Widening	Narrowing	Widening	Narrowing							Widening	Narrowing	Widening	Narrowing

[a] As measured at the County line stream gauges (USGS 11108500 and 11109000).
[b] Blank cells indicate that aerial photograph coverage in that reach was absent or incomplete.
[c] Peak discharge of St. Francis Dam failure flood predicted at the County line area by Begnudelli and Sanders (2007); applies only to reaches M11-B to M13 and the lower end of Reach M14. Last flood prior to 1928 above Reach M14 is unknown.
[d] More changeable reaches have normalized standard deviations >0.40, while less changeable reaches have deviations ≤0.36.

a)

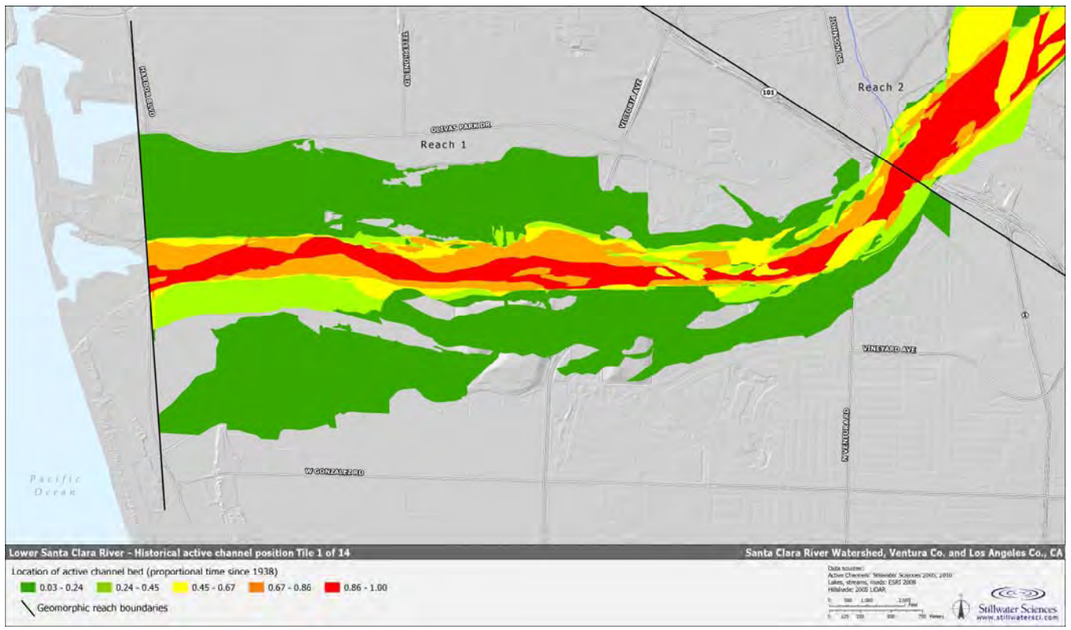

b)

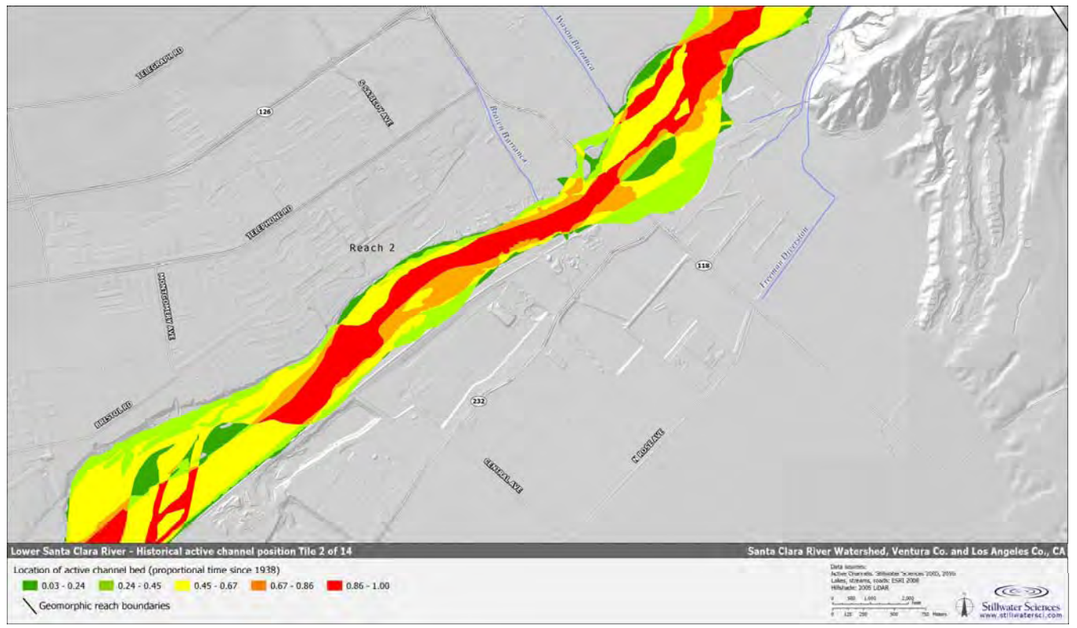

c)

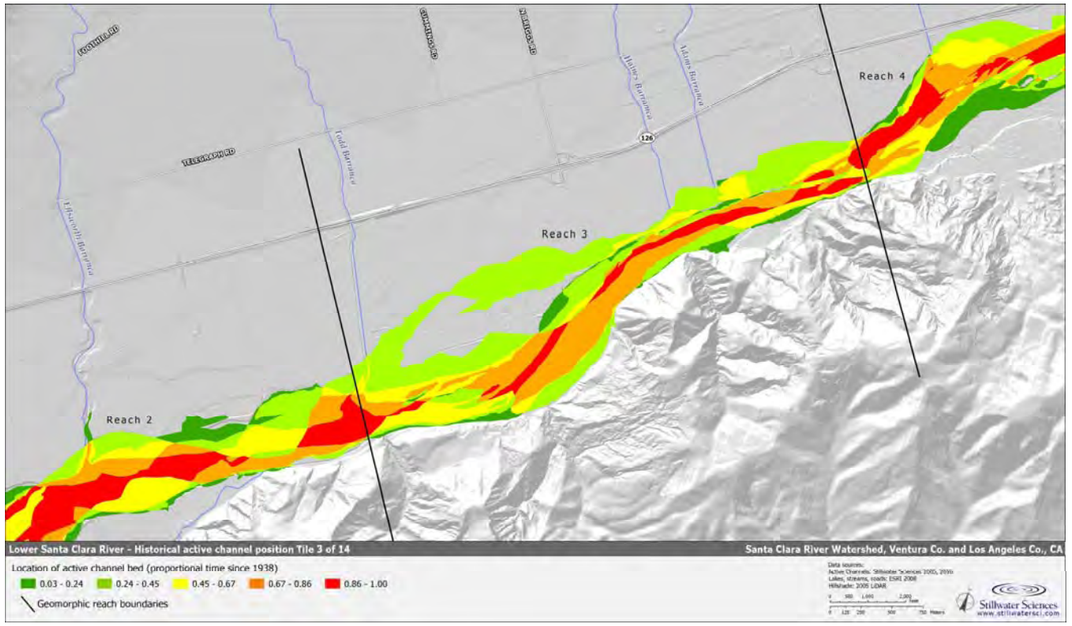

d)

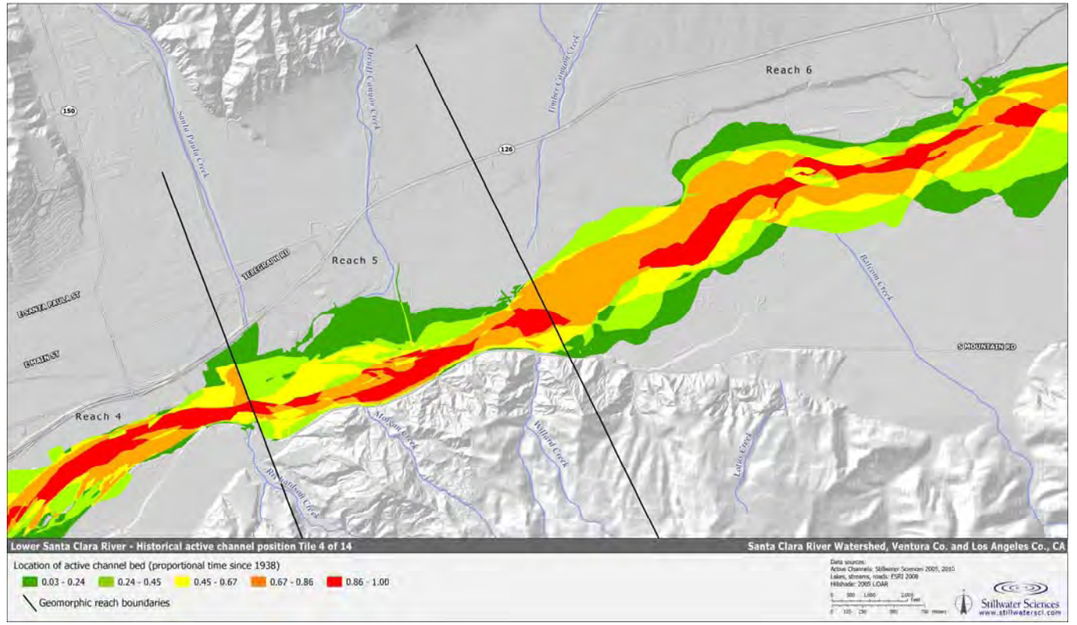

Figure 4-15 a, b, c, d. LSCR historical channel position: proportion of time since 1938 that the active channel bed has occupied a given location.

e)

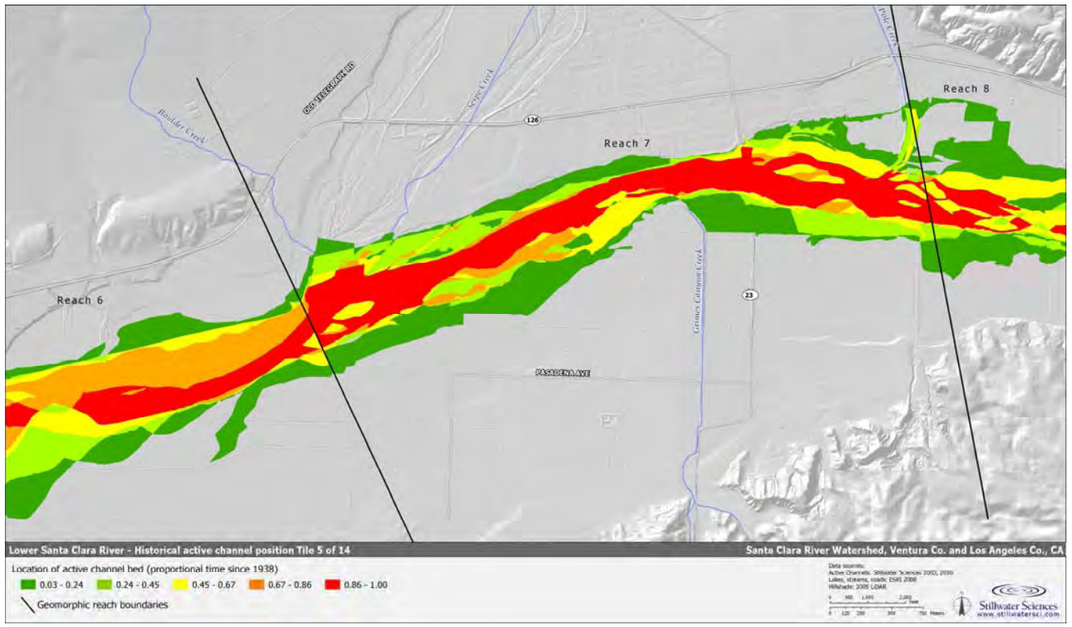

f)

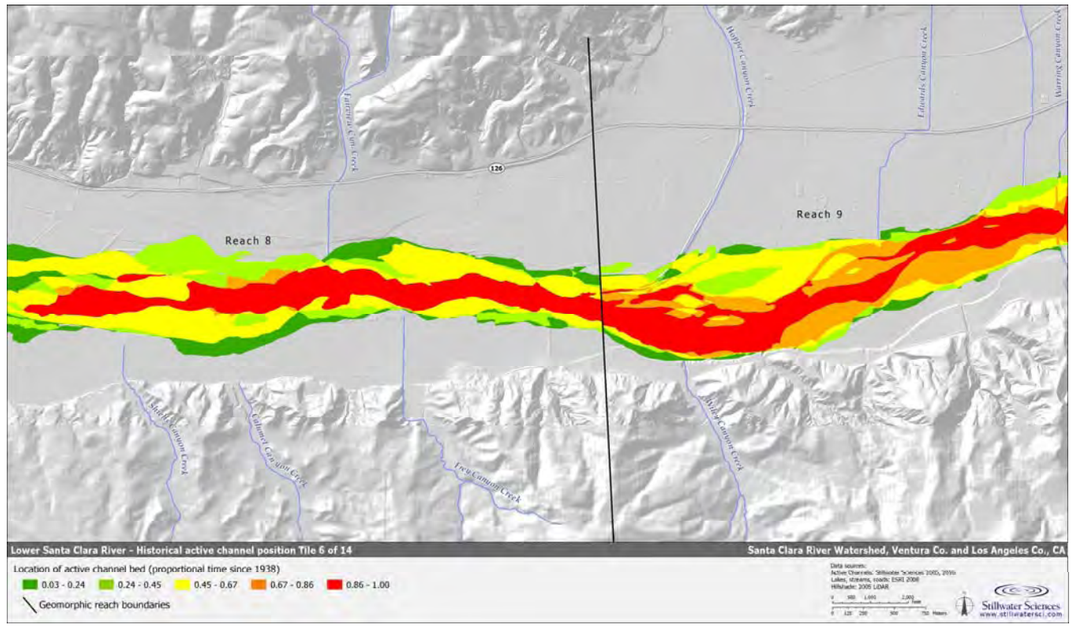

g)

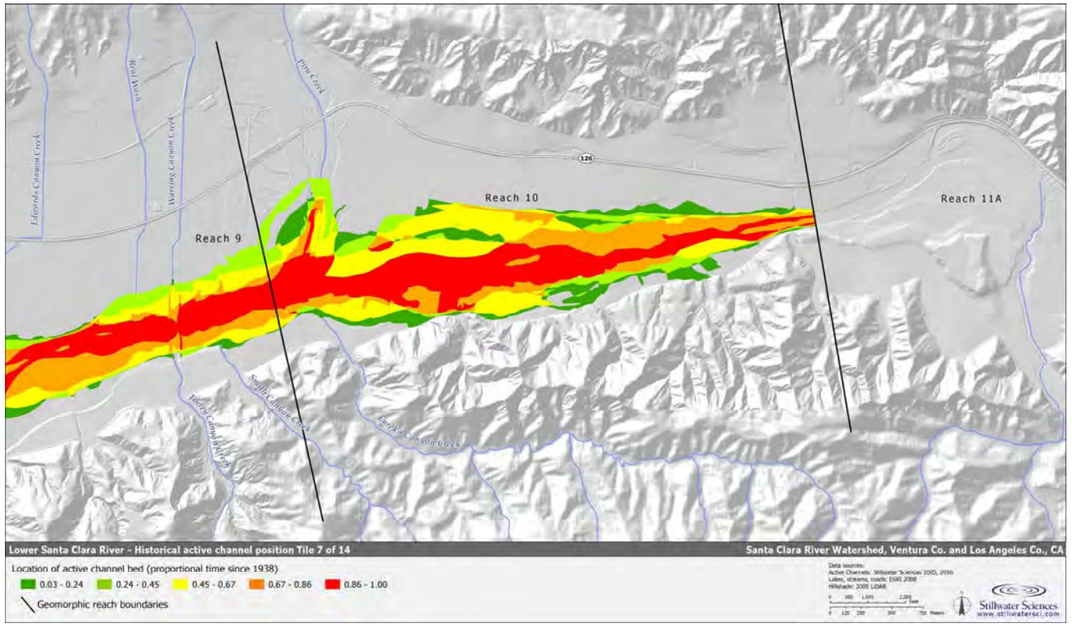

Figure 4-15 e, f, g. LSCR historical channel position: proportion of time since 1938 that the active channel bed has occupied a given location.

a)

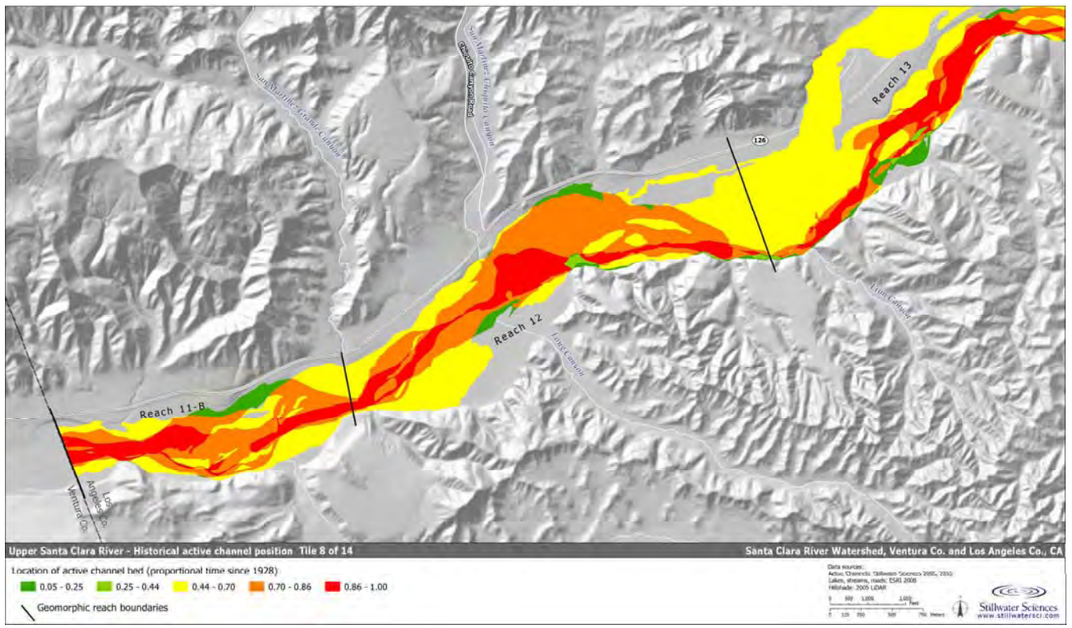

b)

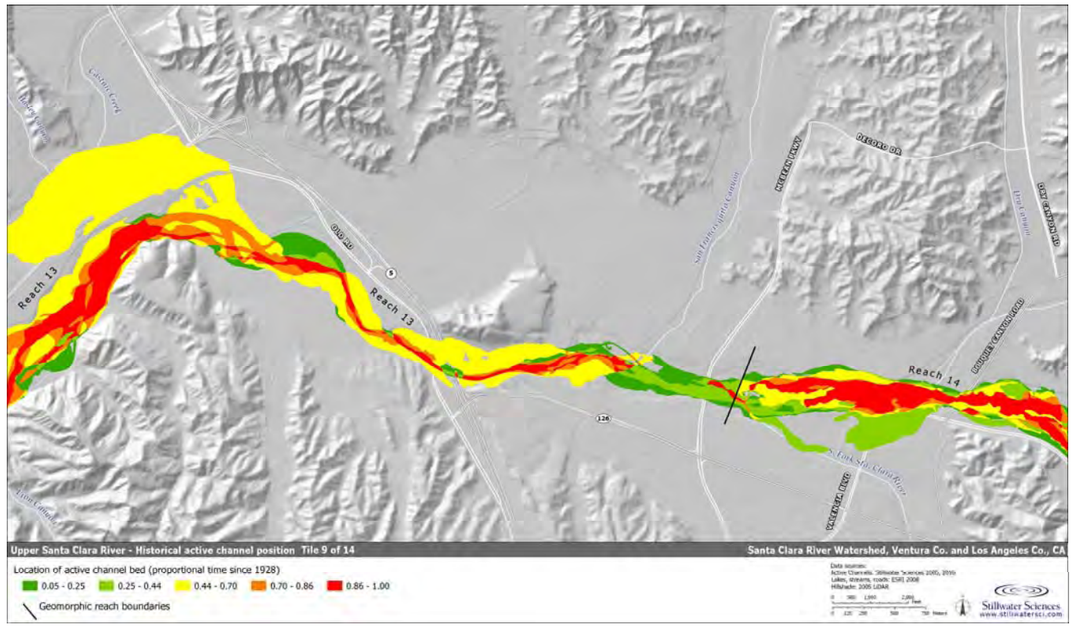

c)

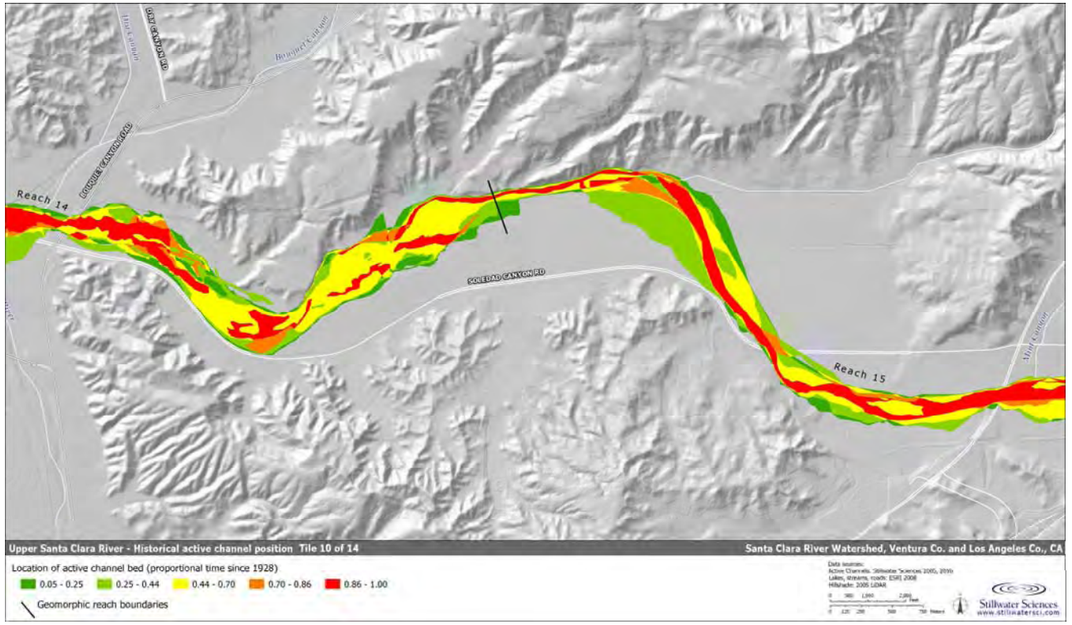

d)

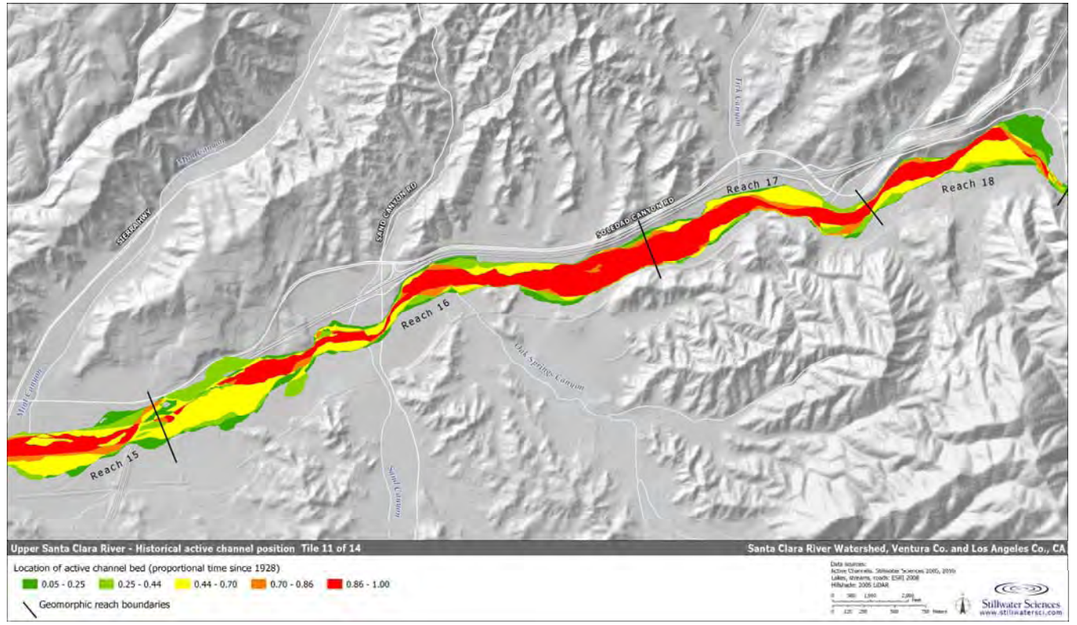

Figure 4-16 a, b, c, d. USCR historical channel position: proportion of time since 1928 that the active channel bed has occupied a given location.

e)

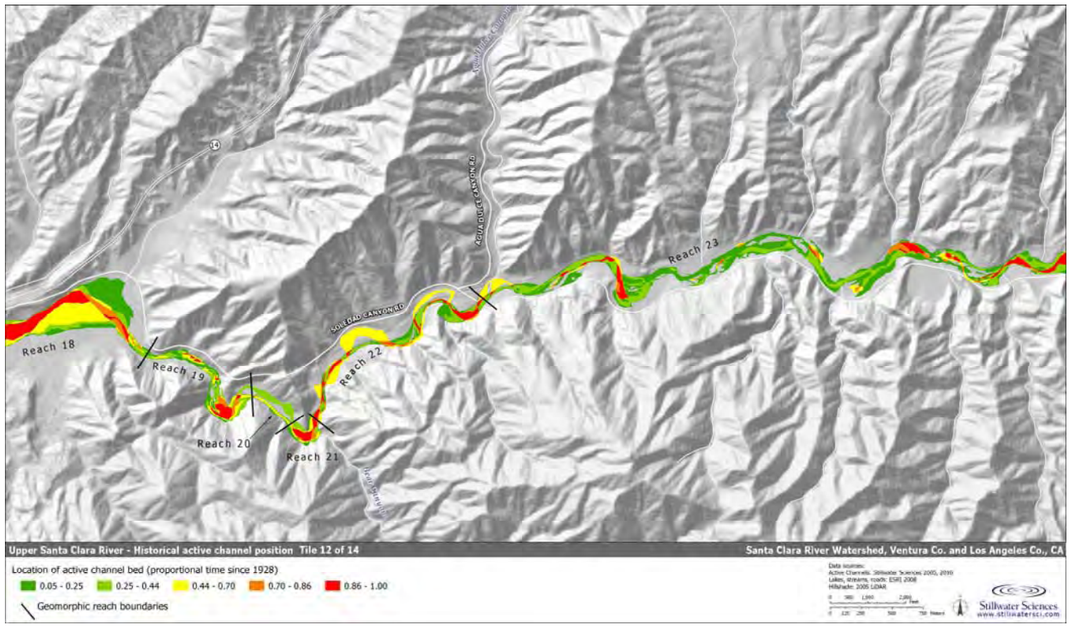

f)

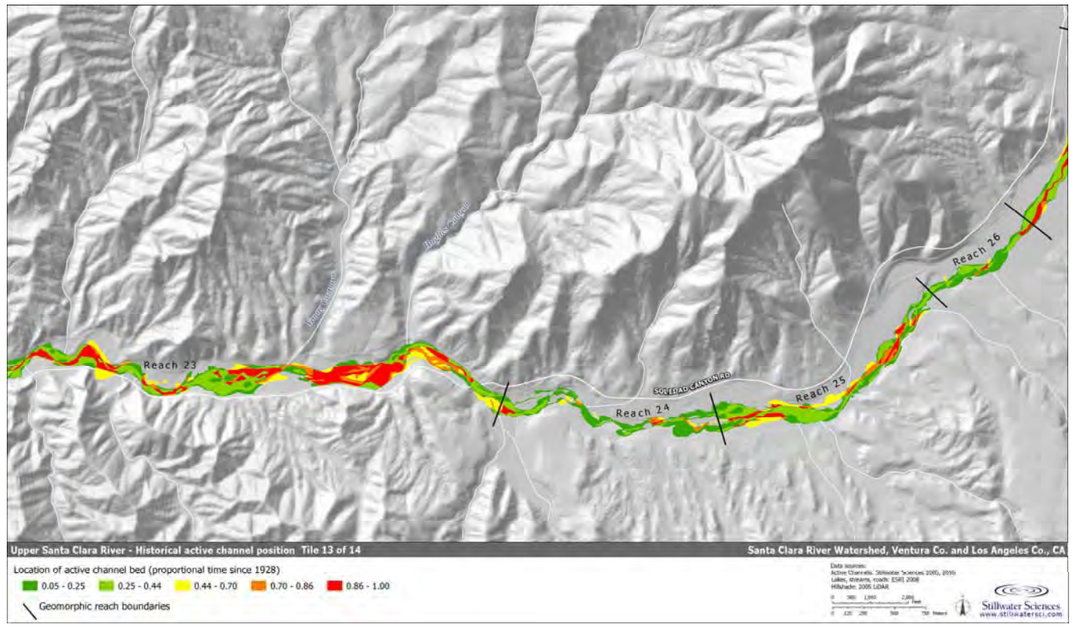

g)

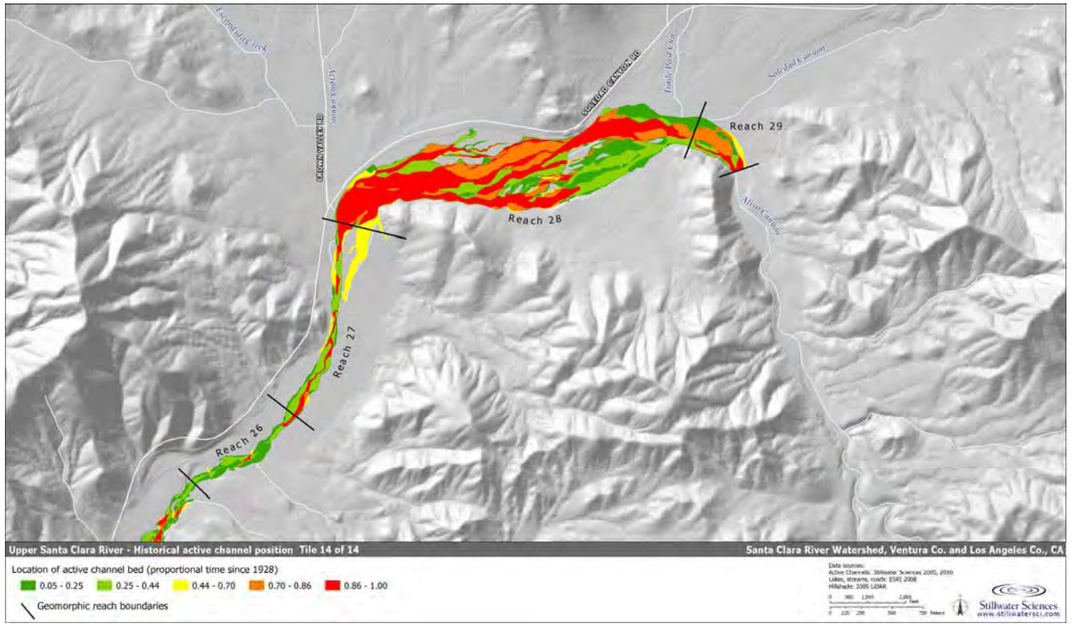

Figure 4-16 e, f, g. USCR historical channel position: proportion of time since 1928 that the active channel bed has occupied a given location.

a)

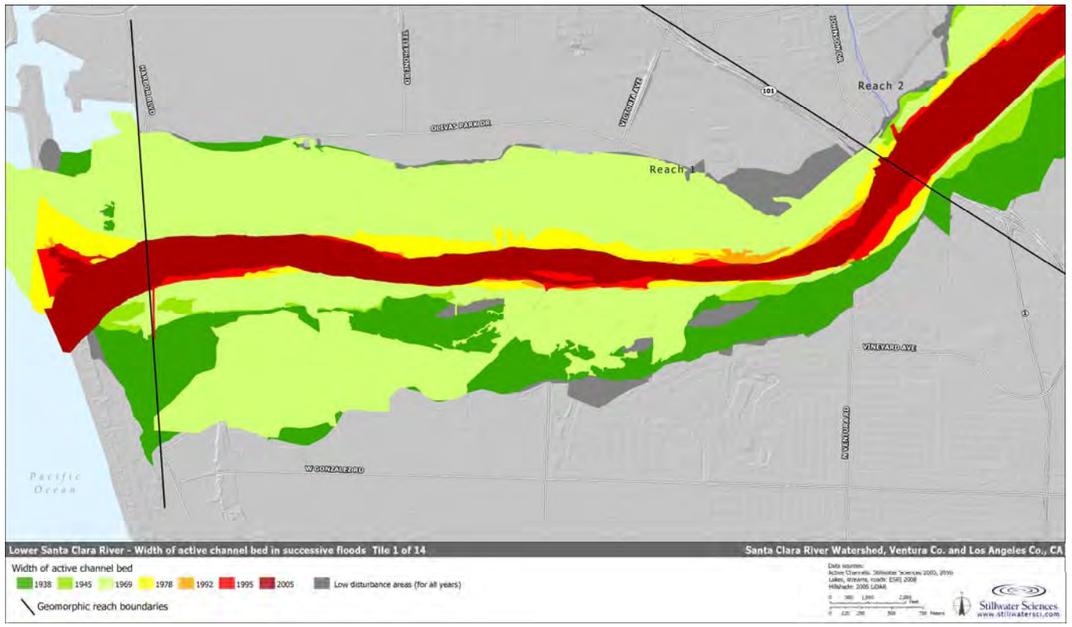

b)

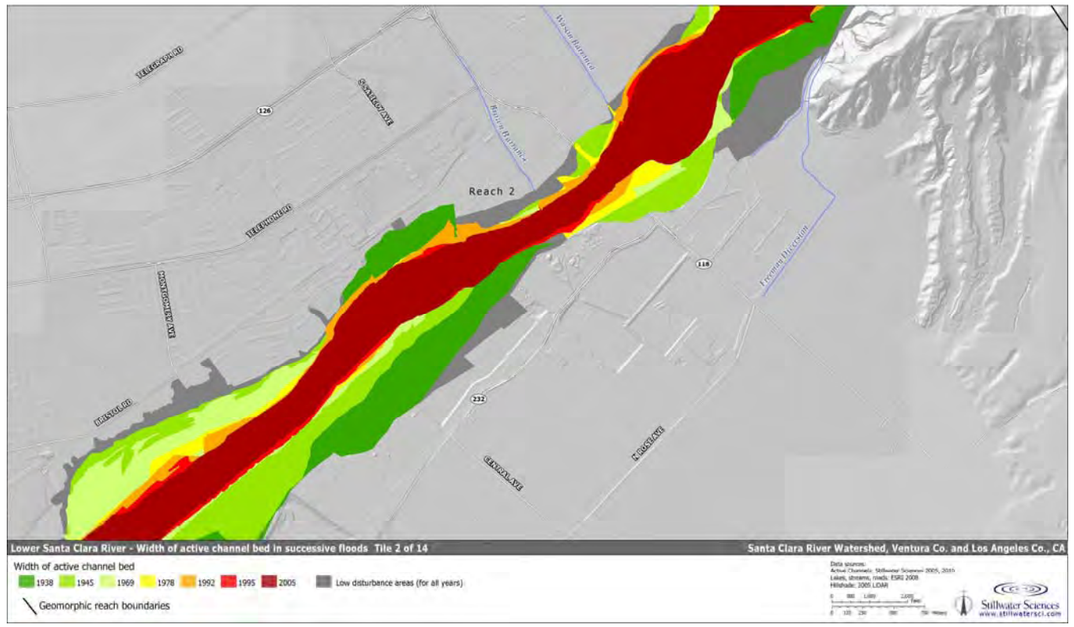

c)

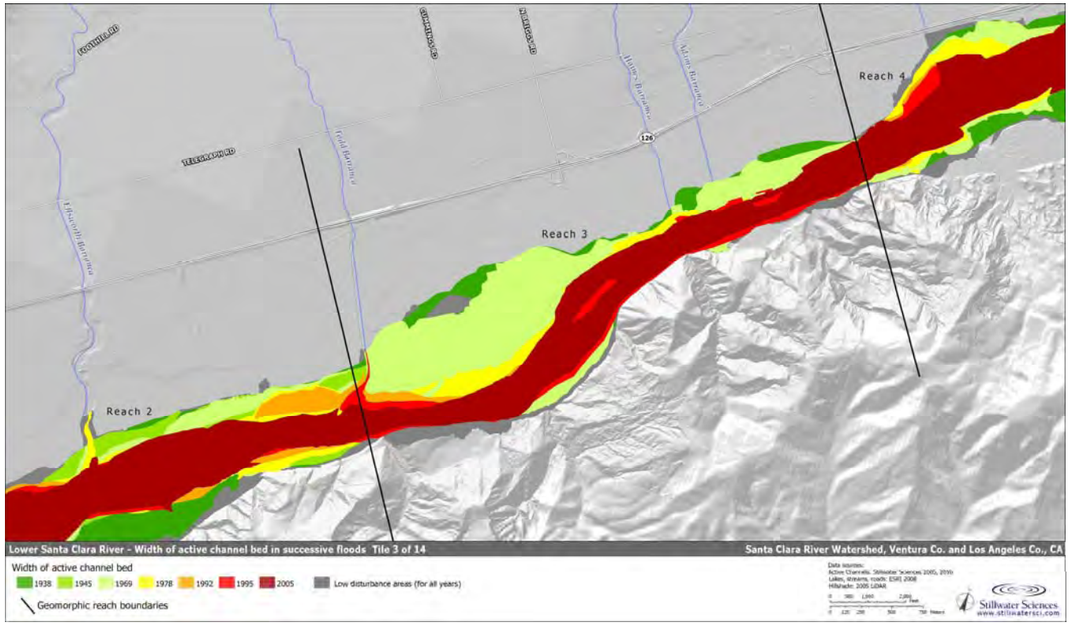

d)

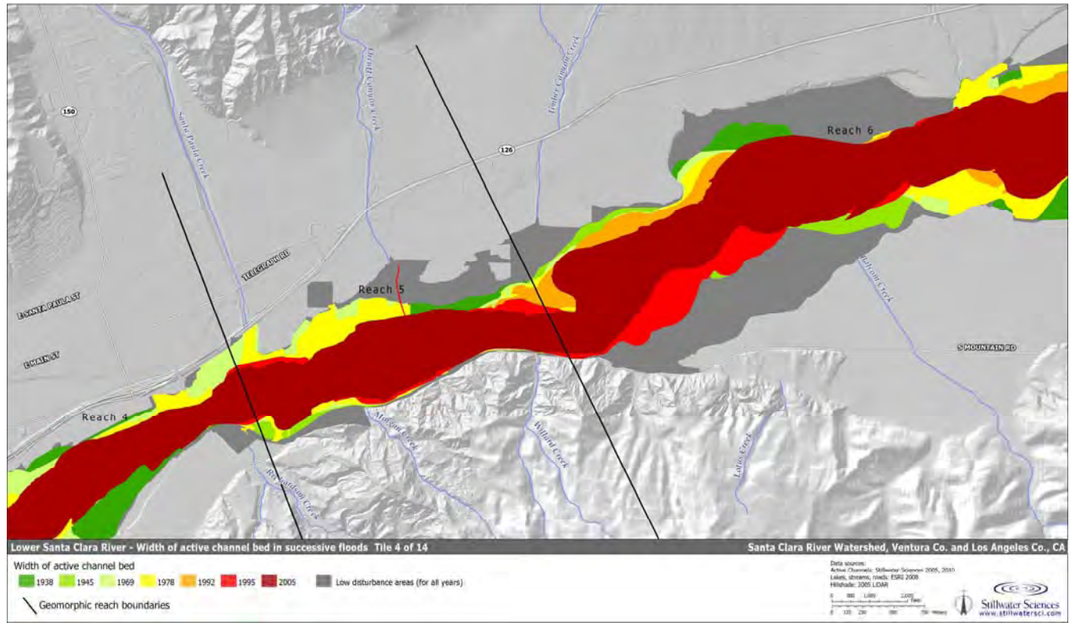

Figure 4-17 a, b, c, d. Active width of channel bed in successive floods since 1938 on the LSCR. The more recent floods are on top

e)

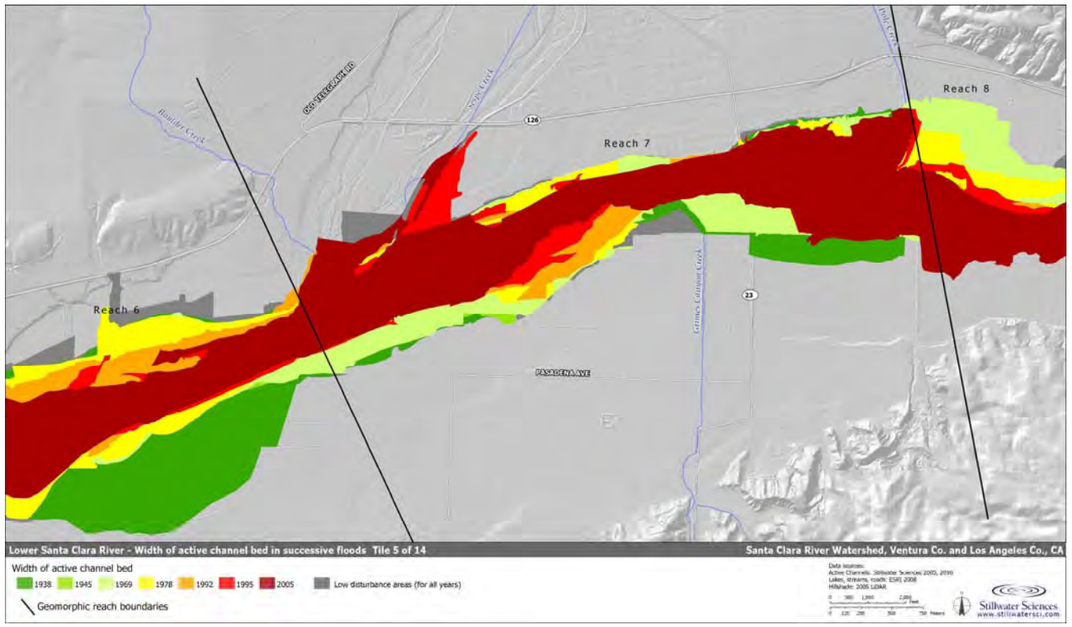

f)

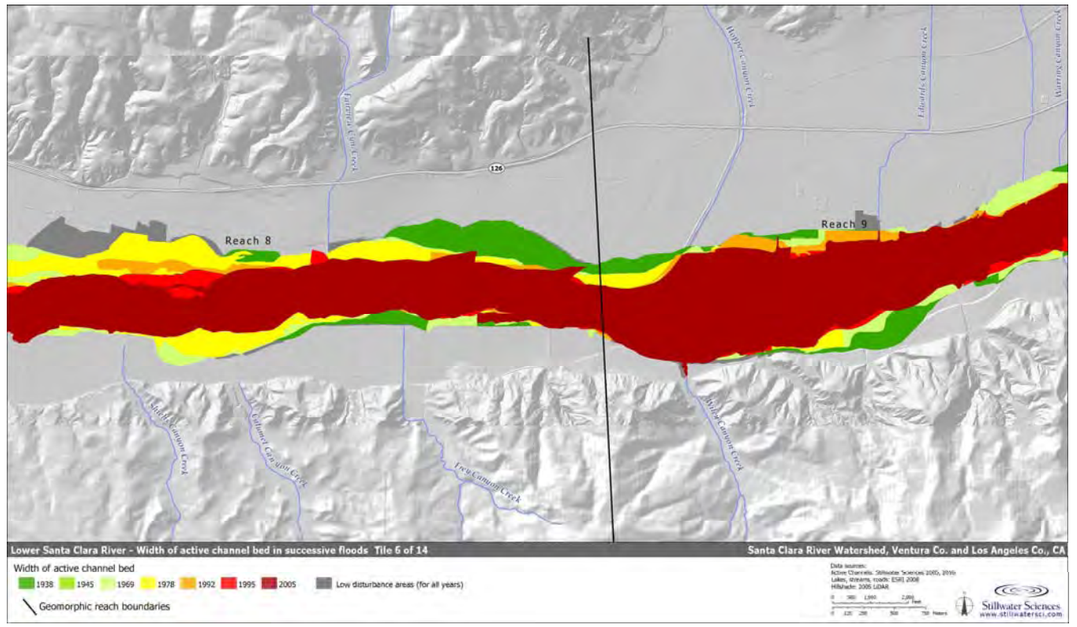

g)

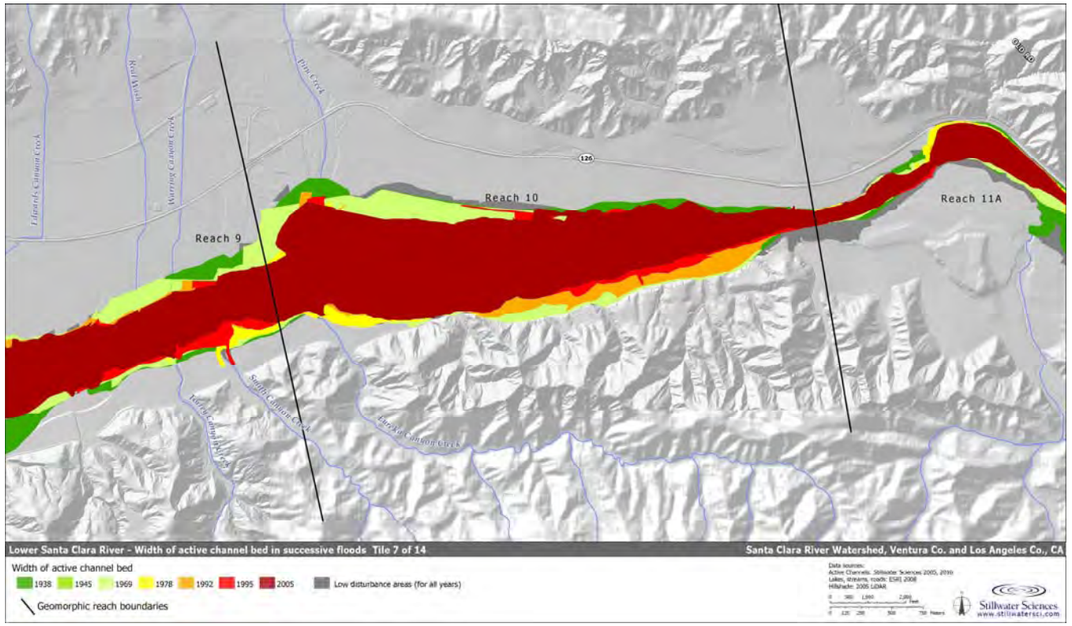

Figure 4-17 e, f, g. Active width of channel bed in successive floods since 1938 on the LSCR. The more recent floods are on top

a)

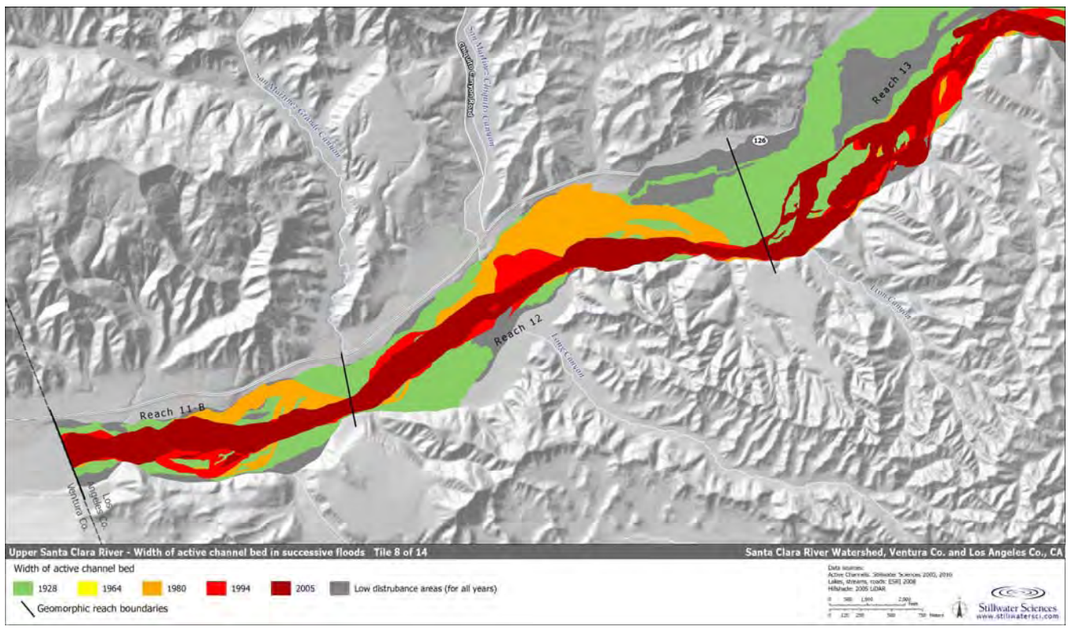

b)

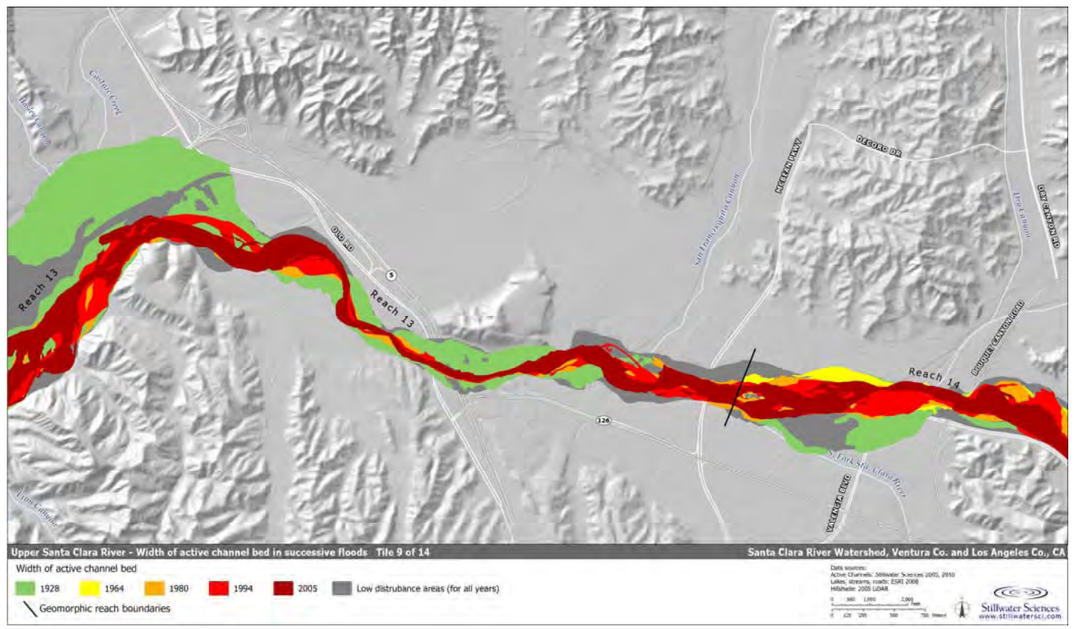

c)

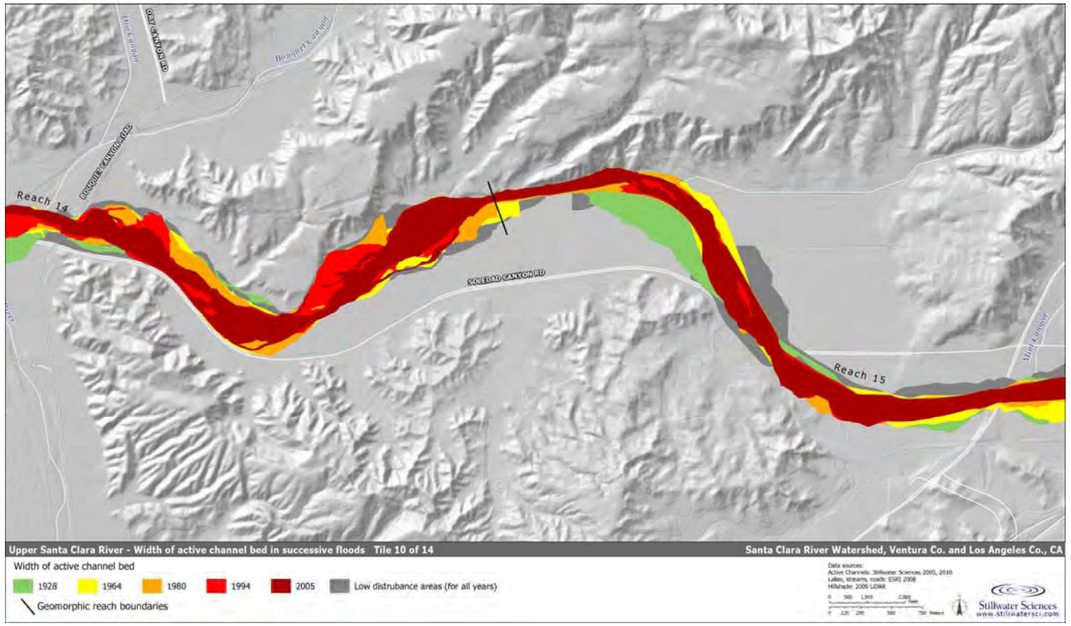

d)

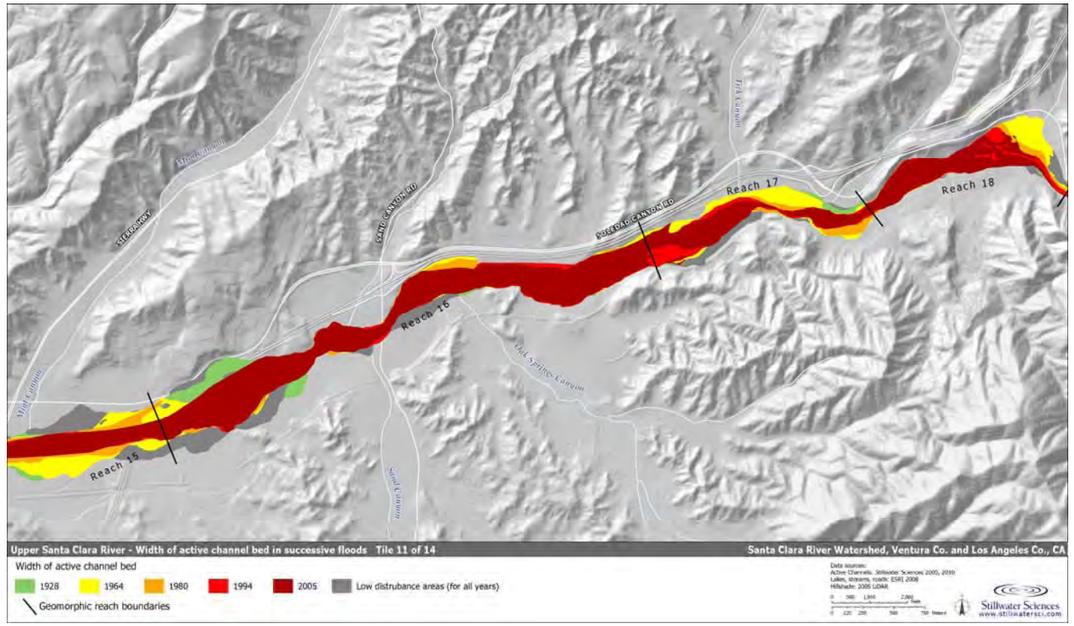

Figure 4-18 a, b, c, d. Active width of channel bed in successive floods since 1928 on the USCR. The more recent floods are on top

e)

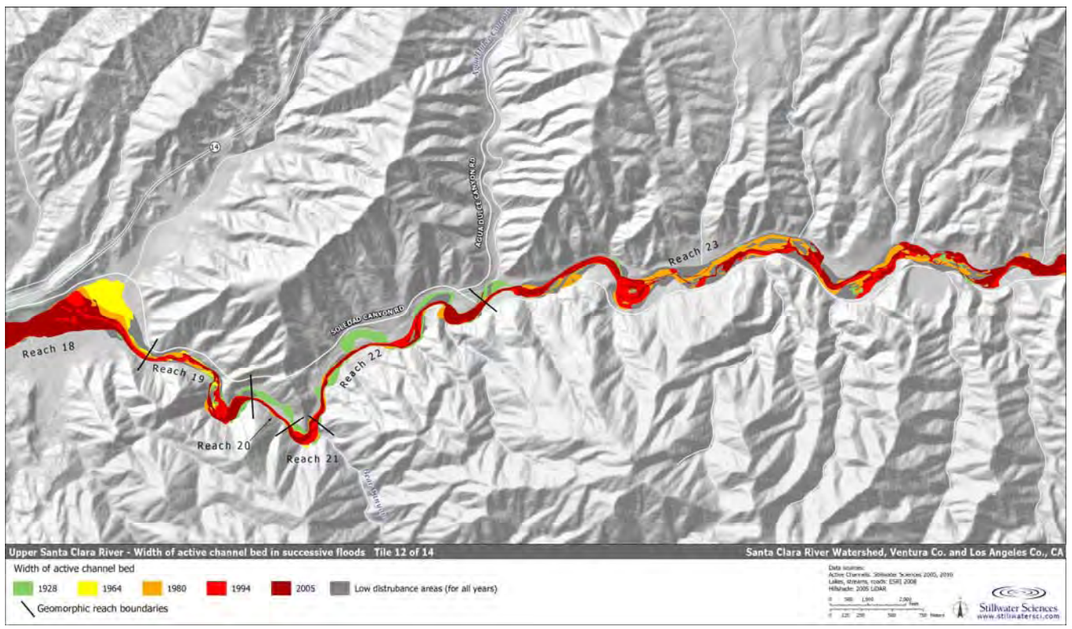

f)

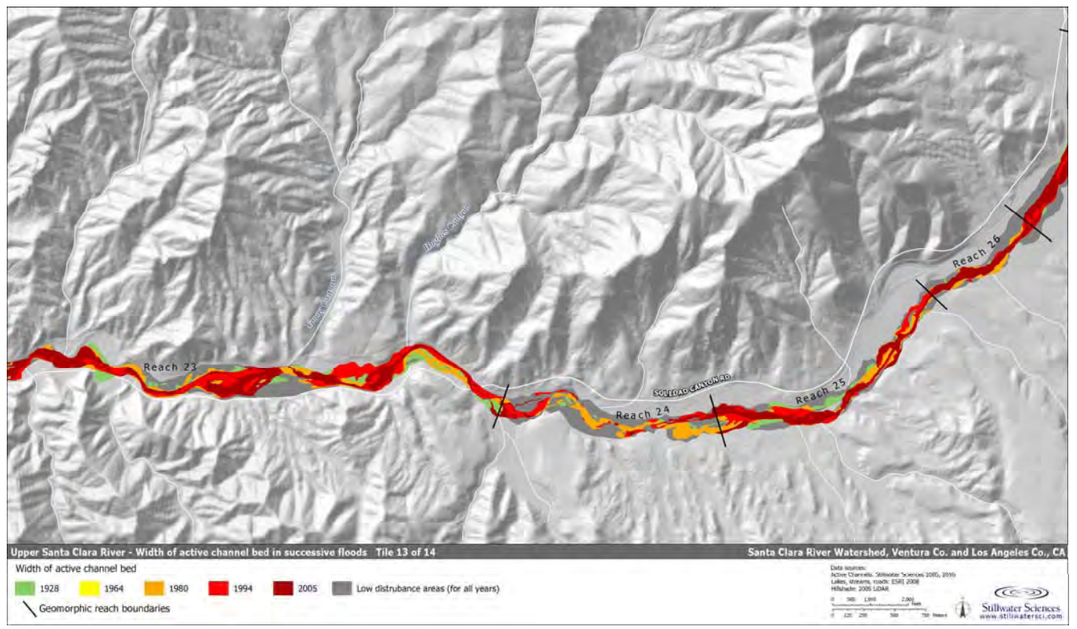

g)

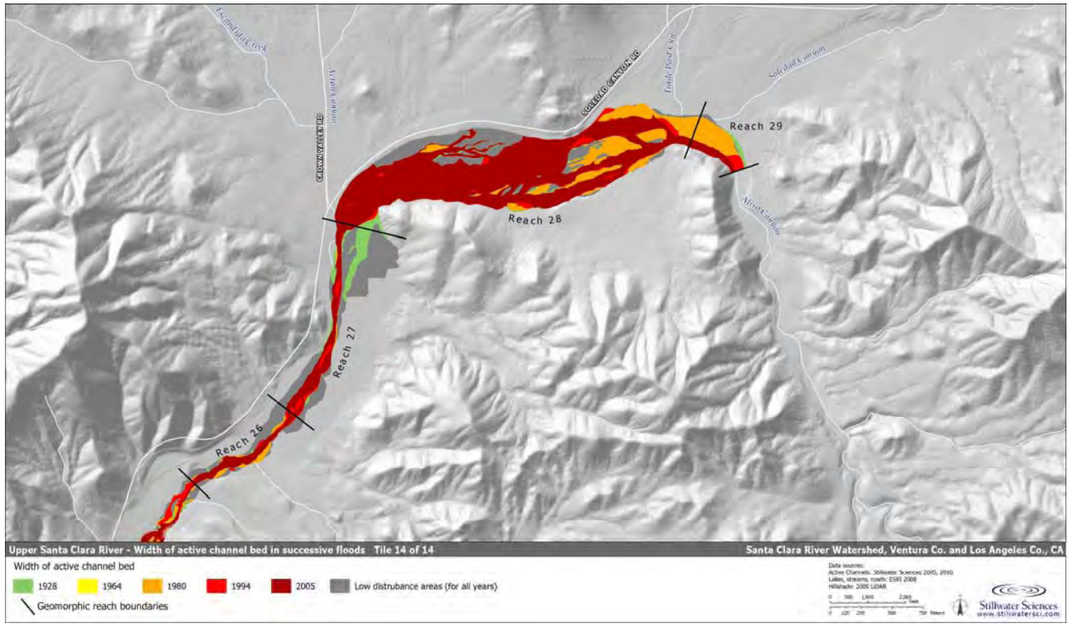

Figure 4-18 e, f, g. Active width of channel bed in successive floods since 1928 on the USCR. The more recent floods are on top

4.3.3 Long-term changes in channel bed elevation

Changes in channel bed elevation over time reveal trends of incision and aggradation for discrete reaches within the mainstem SCR. Changes in the active channel width are also very likely to be linked to changes in bed elevation. Combining these data with known impacts to the river channel and surrounding watershed can help reveal causes for past incision/aggradation trends, and they can contribute to the understanding of future trends in incision/aggradation.

For the LSCR reaches, repeat thalweg elevation surveys (i.e., surveys linking the deepest point of the channel bed) from the mouth to the County line are available from 1949 to 1993, and additional data exist from a survey undertaken in 1929 between the confluence of Piru Creek downstream to approximately the confluence of Santa Paula Creek. These data were collected as part of water abstraction planning. Data were extracted from graphical plots of thalweg elevation to the nearest 0.5 ft (the original unit of measurement). These data have been supplemented by information extracted from aerial LiDAR taken in 2005. Bed level changes in the LSCR can thus be established for the last 76 years (i.e., 1929–2005) in Reaches 6–10, and for the last 56 years (1949–2005) in reaches 1 to 5 and Reach 11-A. This synthesis report, however, presents only set of bed level comparison results: 1949–2005; additional results from intervening years may be referenced in the LSCR geomorphology report (Stillwater Sciences 2007a).

For the USCR, Simons, Li & Associates (1987) previously conducted a detailed geomorphic assessment of the fluctuations and long-term trends in the river's bed elevation using LADPW-provided topographic maps (2-ft contours generated photogrammetrically from 1964, 1977, and 1980/81 aerial photos). For the period between 1964 and 1981 and along the river between the County line and Bee Canyon at the downstream end of Soledad Canyon (our Reach 18), they found localized bed level changes, both rising and lowering, on the order of one to a few meters as averaged over each of their study reach lengths. Notable occurrences of aggradation were near the confluence with Castaic Creek, the Los Angeles Aqueduct crossing (halfway between Bouquet and Mint canyons), upstream of Highway 14, and Bee Canyon. Patterns of incision were found to be more common during this period, with much of it concentrated between Interstate 5 and Bouquet Canyon, between Mint Canyon and Highway 14, and between Sand Canyon and above Lang Station Road (see Table 6.1 of Simons, Li & Associates [1987]). This most upstream occurrence of incision exhibited the greatest amount of lowering (~15 m, which the authors attributed to being highly influenced by the instream aggregate mining activities near the Lang Station Road crossing.

To extend the study time period for the USCR both backward and forward in time, we utilized historic and current elevation data to construct additional longitudinal profiles of the river's thalweg. A total of four different datasets—1928, 1964, 2001, and 2005—were initially considered in this analysis. However, after discovering datum and projection inconsistencies within the 1964 and 2001 datasets, it was determined that only the 1928 and 2005 datasets could be used in this analysis, providing a low-resolution but long-term overview of bed level changes[5]. The 1928 dataset was based on USGS 1:24,000-scale topographic quadrangle sheets with 5-ft contour intervals created by the USGS just after the St. Francis Dam failure. However, the

[5] As part of the USCR geomorphology study, we conducted a comprehensive sediment transport capacity analysis for many reaches of the mainstem and several of the Feasibility Study tributaries. The details of this analysis are not presented in this synthesis report because a similar analysis was not undertaken as part of our LSCR geomorphology study. However, results related to aggradational, incisional, or stable trends determined by the transport capacity analysis to occur within each of the analyzed mainstem USCR reaches are referenced in the summary section below (see sections 4.3.4.2 through 4.3.4.4 and Table 4-15).

relatively good topographic resolution of this dataset only goes up through Reach 21, which prevents our bed level change analysis to continue upstream of this point. The 2005 dataset, representing the most recent elevation data available for use in this analysis, was the very high-resolution LiDAR (Light Detection and Ranging) collected across the entire USCR watershed within months after the 2005 flood event.

The elevation profiles depicted in Figure 4-19 are characterized by localized occurrences of thalweg rising and lowering, which is indicative of channel bed aggradation and incision, respectively. The change in bed elevations ranged between -8 m (-26 ft; incision) to +6 m (+20 ft; aggradation). The greatest degree of incision is associated with those reaches having experienced instream aggregate mining activities within the past several decades (i.e., reaches 2 and 17). Further, there is a broad trend of incision from 1949 to 2005 along the Lower Santa Clara River Valley reaches downstream of the Santa Paula Creek confluence (i.e., reaches 1 to 4), averaging 2.4 m (7.9 ft). In reaches 5 and 6, there is a variable trend of minor incision and aggradation from Santa Paula Creek to Sespe Creek. Within the Upper Santa Clara River Valley and much of the Santa Clarita Basin reaches (i.e., reaches 7 to 14), there is a moderate aggradation trend; the most aggradataion along the analyzed extent of the SCR occurs in Reach 15. Specifically, aggradation occurs between Castaic Creek and Interstate 5, between Bouquet and Mint canyons, and near the downstream end of the canyon; and incision occurs between Interstate 5 and Bouquet Canyon and near the Lang Station Road crossing.

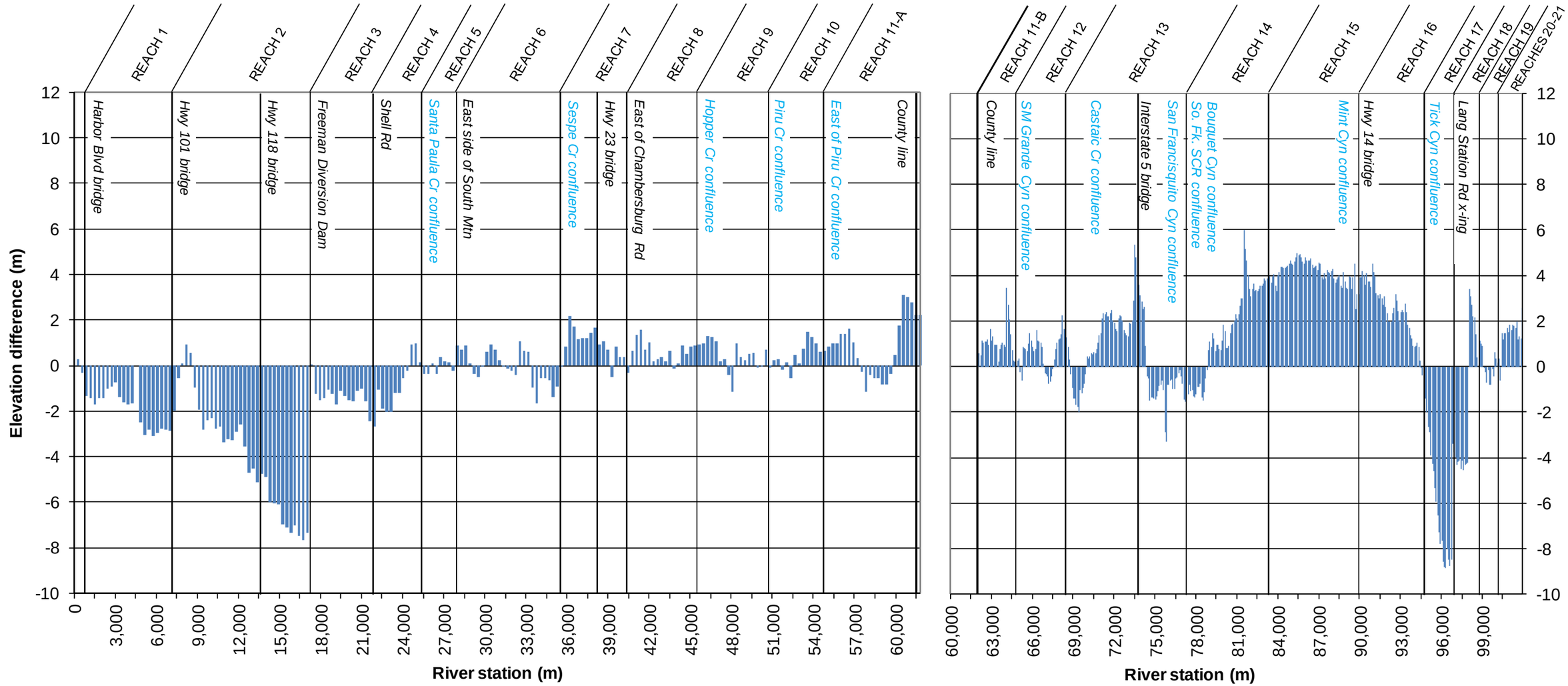

Figure 4-19. Net thalweg elevation change for the LSCR from 1949 to 2005 (left plot) and for the USCR from 1928 to 2005 (right plot).

4.3.4 Summary of reach-level dynamics

In summary, we assessed long-term trends in active channel width, bed elevation, and associated channel morphodynamics to reveal dominant channel form and evolution over time along the mainstem SCR (Tables 4-14 and 4-15). These results are discussed most readily by reference to our division of the SCR into several geomorphically-distinct reaches, numbered up from the river estuary. The reaches are grouped into four dominant regions that are characterized by the dominant morphological setting: the Santa Clara River Valley (which is further sub-divided into the "Lower" and "Upper" halves at the Sespe Creek confluence), includes the expansive, low gradient alluvial reaches; the Santa Clarita Basin includes the broad, low-gradient alluvial reaches through the densely developed city of Santa Clarita; the Soledad Canyon region includes the steeper, coarse-grained, and narrow reaches; and the Acton Basin includes the moderately expansive, more arid, alluvial reaches through the town of Acton. Through all alluvial reaches, a braided-channel morphology exists that adjusts in response to the largest floods on record (i.e., a compound, mixed-load channel). In the Soledad Canyon region, the river is considerably confined by the steep canyon walls and further narrowed by Soledad Canyon Road and the railroad).

Overall, the river planform and bed elevation have adjusted episodically over the past century. Although the entire river has experienced changes in response to regional influences, such as episodic storm events (e.g., 1969 and 2005) and sediment pulses following large wildfires, the changes have been most pronounced in the Santa Clara River Valley and Santa Clarita Basin reaches. These changes have also been strongly influenced by four main anthropogenic factors: (1) the flood wave released during the St. Francis Dam failure in 1928; (2) flow and sediment input reductions with the closure of Santa Felicia Dam in 1955 and Castaic Dam in 1972; (3) instream aggregate mining in the Lower Santa Clara River Valley and Soledad Canyon reaches (i.e., reaches 2, 3, 4, 17, and 18) over the past several decades; and (4) distributed land-use changes in the watershed over the past century and more localized urban encroachment into the floodplain and the active channel within the past few decades.

4.3.4.1 Summary of the Santa Clara River Valley reaches

Over the last 57 years, the reaches of the Santa Clara River Valley have experienced several notable changes to their morphologies in response to natural and anthropogenic influences. Reaches 1 to 4, below the confluence with Santa Paula Creek, have incised on average 2.4 m, have narrowed considerably, and have an active width that is no longer related to the magnitude of the last flood but instead to a legacy of instream aggregate mining and the existence of extensive levees (Table 4-14). The degree of thalweg incision within these reaches is the greatest anywhere along the LSCR (but is less than the incision in Reach 17 of the USCR [see below]). Reaches 5 and 6 are the least modified by anthropogenic influences along the LSCR, although upstream migrating knickpoints originating at instream aggregate mining operations in Reach 4 have extended into the lower end of Reach 5. Together, these two reaches have not appreciably changed bed elevation over the period of record, and they have a highly changeable active channel width related to the magnitude of the last flood rather than to constraints provided by human activity. Reaches 7 to 11-A (i.e., the mainstem SCR upstream of the Sespe Creek confluence) have aggraded 0.65 m since 1949, and they have narrowed in width over time but are still somewhat responsive to flood magnitude, possibly in response to flow regulation, to the passage of construction sediments or to sediments, deriving from episodically high natural supply rates (e.g., in response to wildfire or landslide activity).

The significant degree of channel bed incision within reaches 1 to 4 signifies that the channel in these reaches has been a net exporter of sediment. The formation of an inset channel here, caused by the incising thalweg, stands in contrast to the lack of a clearly defined channel in many of the upstream reaches (i.e., reaches 7 to 11-A and those of the Santa Clarita Basin and Acton basins). The current channel thus has a compound structure, with a highly changeable low-flow channel inset within a far larger channel that is largely straight in response to both regional tectonic controls and confinement caused by human activities such as levee construction and in-channel gravel mining. Whereas a subsequent process of (at least partial) bed elevation recovery might be expected following incision, it appears that the levee construction in combination with the flashy nature of large floods in the watershed have prevented recovery in reaches 1 and 2. It is important here to restate that episodic, high magnitude floods continue to occur in the Lower Santa Clara River Valley reaches despite the regulation of roughly one-third of the entire SCR watershed because of the significant step increase in discharge that occurs below the confluence with Sespe Creek.

Bed level aggradation has occurred in reaches 3 and 4 as a result of the construction of Freeman Diversion Dam (see Stillwater Sciences 2007a, Figure 5-19). Additional scour has occurred downstream of the dam, in the upper end of Reach 2, with aggradation in the lower end of the reach. Reach 1 has continued to incise mildly. Because of local hydraulic characteristics (e.g., high unit stream power at low-recurrence flows), reaches 1 to 4 continue to possess the energy to transport more sediment than supplied to them from upstream, indicating a possibility of further incision into the future.

4.3.4.2 Summary of the Santa Clarita Basin reaches

Moving upstream from the County line into the Santa Clarita Basin, our analyses reveal an overall trend of narrowing and aggradation (bedload deposition) from Reach 11-B upstream through Reach 15 over the past 80 years. This aggradational trend primarily reflects a broader river corridor as compared with the Soledad Canyon reaches (and thus increase in sediment deposition potential) coupled with high sediment delivery from adjacent tributary subwatersheds (e.g., San Martinez Grande, San Martinez Chiquito, and Lyon canyons and headwater tributaries to the South Fork SCR) (see Table 3-5 and Figure 3-8). On average, the bedload sediment yield from these tributaries outpaces the channel's ability to transport bedload, resulting in continued sediment deposition and bed aggradation. This trend is not ubiquitous, however, with some areas of localized mainstem bed incision (e.g., at the confluences with Bouquet and San Francisquito canyons and Castaic Creek).

The general aggradational trend observed within the mainstem of the Santa Clarita Basin reaches has also likely contributed to decreased channel gradient and aggradational trends within the lower reaches of several tributary subwatersheds that carry relatively high sediment loads (e.g., San Martinez Chiquito Canyon and South Fork SCR). Reach 16, the uppermost reach in this region similarly exhibits an aggradational trend, but its active width has been progressively increasing since 1928; the exact cause of this widening is not clear, particularly since Highway 14 represents a significant structural control on the river's ability to migrate in this reach.

The Santa Clarita Basin reaches likely once transported sediment in the same fashion as the reaches upstream; however, localized changes in water and sediment supply (perhaps the occurrence of the St. Francis Dam failure) appear to be the cause of the shift towards an aggradational, narrowing channel. Under undisturbed conditions, alluvial river channels tend to have little long-term net sediment accumulation or change in active channel width (i.e., the channel bed elevation and width are in quasi-equilibrium). It can be inferred from the results of

our analyses that the long-term aggradational and narrowing trends exhibited in the Santa Clarita Basin reaches may represent the river's response to the scouring floods released during the dam failure (i.e., recovery to an quasi-equilibrium bed elevation) and to the relatively high sediment inputs from historical land uses that occurred during the past century.

4.3.4.3 Summary of the Soledad Canyon reaches

In the Soledad Canyon reaches, the mainstem channel is confined and relatively steep with, accordingly, high bedload transport potential compared to downstream and upstream alluvial reaches (i.e., Santa Clarita and Acton basins, respectively). Reaches 17 and 18 have been impacted over the past several decades by the instream aggregate mining activities occurring at the Lang Station Road crossing. In Reach 17, below the crossing, the river exhibits its greatest degree of incision, attributed to the aggregate mining activities in the river channel and to the crossing itself, which functions as a grade control structure that hinders the passage of coarse-grained sediments to this reach (Simons, Li & Associates 1987 and this study). Continuing upstream, the remaining reaches in this region have a relatively high channel gradient and confinement that result in high transport capacity and a channel bed elevation that remains relatively fixed as a result of underlying bedrock, although with a modest narrowing downstream trend in the active channel width that is not well understood.

4.3.4.4 Summary of the Acton Basin reaches

The uppermost reaches of the mainstem SCR, in the relatively broad Acton Basin, have exhibited episodic adjustments when large, rare flood events occurred. Encroachment within the active channel includes low-water road crossings that hinder coarse sediment passage, particularly between reaches 26 and 27, which likely causes the observed incision below that particular crossing. Reach 27 exhibits a stable bed elevation trend, which is not surprising considering that the road crossing at the reach's downstream end acts to maintain the bed elevation. In Reach 28, the river is broad with numerous braid channels that are prone to adjustment during large flood events. As such, a large portion of the delivered bedload, primarily from the high-yielding Aliso Canyon tributary, is deposited in this reach.

Table 4-14. Summary of LSCR reach morphodynamics.

Morphodynamic feature	1	2	3	4	5	6	7	8	9	10	11-A
	Santa Clara River Valley										
	Lower Santa Clara River Valley						*Upper Santa Clara River Valley*				
Reach boundaries (downstream to upstream)	***Harbor Blvd bridge Hwy 101 bridge***	***d/s Freeman Dam***	***u/s Freeman Dam Shell Rd.***	***Santa Paula Cr.***	***East flank South Mtn.***	***Sespe Cr.***	***E of Cham'burg Rd.***	***Hopper Cr.***	***Piru Cr.***	***E of Piru Cr.***	***County line***
Centerline reach length [a] (km)	6.4	10.0	4.7	3.5	2.5	6.8	5.3	5.7	4.7	4.4	6.1
Q_2 [a] (m^3 s^{-1})	185.9	185.9	185.9	185.9	185.9	185.9	89.5	60.6	60.6	54.2	52.9
Reach-average slope [a]	0.3%	0.3%	0.3%	0.4%	0.3%	0.4%	0.5%	0.6%	0.5%	0.6%	0.6%
D_{50} range [b] (mm)	0.2-5	0.6-15	1	1-5	1-4	0.8-3	0.6-1	1-5	2	1	2-67
Particle size type [c]	$S–G_f$	$S–G_m$	S	$S–G_f$	$S–G_f$	$S–G_{vf}$	S	$S–G_f$	S	S	$S–C_v$
Reach-average active width, 2005 [d] (m)	222	350	265	384	456	474	570	422	542	555	146
Active width change trend [d]	Narrowing	Narrowing	Narrowing	Narrowing	Narrowing	Narrowing	Narrowing	Narrowing	Narrowing	Narrowing	Narrowing
Reach average bed elevation change, 1949-2005 [e] (m)	-2.0	-3.9	-1.2	-1.1	0.1	-0.1	0.9	0.6	0.4	0.4	0.8
General trend in bed level elevation [e]	Progressive mild incision	Incised and stabilizing, local scour upstream, aggradation downstream	Rapid incision prior to Freeman Dam. Recovered but slight incision recently	Recovered after Freeman Dam built. Slight incision recently	Recovered after Freeman Dam built. Slight incision recently	No trend	Slight aggradation, no trend	Slight aggradation, no trend	Slight aggradation, no trend	Slight aggradation, no trend	Slight aggradation, no trend
Local characteristics	Wide floodplain, part of natural distributary area for the river. Largely straight channel, levees on left bank, urban area behind.	Wide floodplain, part of natural distributary area for the river. Levee along most of left bank, and a short stretch of the right. Urban development to channel edge along most of the right bank, and downstream along the left bank. Gravel mining until 1988 in the lower and upper reach. Upstream extent bounded by Freeman Dam.	Left bank impinges on South Mountain. Gravel mining throughout the reach until 1988. Freeman Diversion Dam provides grade control at the downstream end.	Left bank close to South Mountain, urban development to edge of right bank. Some revetment on right bank. Gravel mining until 1986. Receives unregulated inflow from Santa Paula Creek.	Left bank impinges on South Mountain. Downstream end is confluence with Santa Paula Creek.	Wide floodplain, channel in center: sinuous and braided. Levee at upstream end opposite Sespe Creek confluence. Receives unregulated inflow from Sespe Creek.	Urban development to right bank edge in upper part of reach, right bank leveed in this area. Downstream end is confluence with Sespe Creek.	Wide floodplain floor. Upstream left bank close to mountains. Sinuous and braided. Inflow from Hopper Canyon.	Wide floodplain floor, channel veers towards towards left bank mountains. inuous and braided. Received highly regulated flow from Piru Creek.	Wide floodplain floor. Channel in center. Highly regulated flows.	Narrow valley segment. Highly regulated flows (downstream from Castaic Creek). Heavy agriculture use adjacent to floodway.

[a] From HEC-RAS output.
[b] From compilation of bulk sediment size data (see Figure 4-8); values for Reach 5 were taken as the average of Reaches 4 and 6 because no bulk sediment sample data was available for that reach;
[c] Based on bulk sediment size data; size categories: S = sand (<2 mm), G_{vf} = very fine gravel (2–4 mm), G_f = fine gravel (4–8 mm), G_m = medium gravel (8–16 mm), G_c = coarse gravel (16–32 mm), G_{vc} = very coarse gravel (32–64 mm); C_v = fine cobble (64–128 mm); C_c = coarse cobble (128–256 mm).
[d] From active channel width analysis (1938, 1945, 1969, 1978, 1992, 1995, 2005) (see Table 4-12 and Figures 4-15 and 4-17).
[e] From bed level changes analysis (see Figure 4-19).

Table 4-15. Summary of USCR reach morphodynamics.

Morphodynamic feature	11-B	12	13	14	15	16	17	18	19	20	21	22	23	24	25	26	27	28
	Santa Clarita Basin						Soledad Canyon									Acton Basin		
Reach boundaries (downstream to upstream)	*County line* / *SM Grande Cyn*	*Castaic Cr.*	*I-5 bridge* / *San Fran' Cyn* / *So. Fk. SCR*	*Bouquet Cyn* / *Newhall Ranch Rd. br.*	*Mint Cyn* / *Sierra Hwy br.*	*Hwy 14 bridge*	*Tick Cyn* / *Lang Stn. Rd. crossing*				*Bear Cyn*	*Agua Dulce Cyn*	*Soledad Cyn Rd. bridge* / *Soledad Cyn Rd. bridge*			*Arrastre Rd. crossing*	*Acton Cyn*	*Aliso Cyn*
Centerline reach length, 2005 (km)	1.7	3.9	8.9	5.9	6.8	4.8	2.1	2.0	1.4	0.4	0.4	2.1	9.8	1.9	2.3	1.0	1.7	3.1
Q_2 [a] (m^3 s^{-1})	69	65	52	36	29	26	26	21	21	21	21	20	17	13	13	12	12	8
Reach-average slope, 2005 [b]	0.5%	0.5%	0.6%	0.9%	0.9%	0.9%	0.7%	1.1%	1.3%	1.6%	1.7%	1.3%	1.3%	1.7%	1.5%	2.0%	1.3%	1.2%
D_{50} range [c] (mm)	0.8-3	0.7-2	0.3-4	2-4	4-12	3-8	4	2	4	15	200	9	1	2	2	4-32	2	3
Particle size type [d]	S–Gv_f	S–G_{vf}	S–G_{vf}	G_{vf}	G_f–G_m	G_{vf}–G_f	G_{vf}	G_{vf}	G_{vf}	G_m	C_c	G_m	S	G_{vf}	G_{vf}	G_f–G_c	G_{vf}	G_{vf}
Reach-average active width, 2005 [e] (m)	195	163	145	178	150	202	109	128	29	13	34	30	39	14	51	53	57	304
Active width change trend [e]	Narrowing	Narrowing	Narrowing	Narrowing	Narrowing	Widening	Narrowing	Widening	Narrowing	Narrowing	Narrowing	Narrowing	Narrowing	Narrowing	Narrowing	Widening	Narrowing	Widening
Reach average bed elevation change, 1928-2005 [f] (m)	1.1	0.6	0.5	1.5	4.2	2.5	-5.9	-1.7	0.1	0.6	1.5	--	--	--	--	--	--	--
General trend in bed level elevation [f]	Aggrading	Aggrading	Aggrading	Aggrading	Aggrading	Aggrading	Incising	Incising	Stable	Aggrading	Aggrading	*Stable*	*Stable*	*Stable*	--	--	*Stable*	*Aggrading*
Local characteristics	Narrow valley segment. Highly regulated flows (downstream from Castaic Creek). Left bank close to Santa Susana Mtns front.	Narrow valley reach (broader than Reach 11-B) through planned Newhall Ranch develop-ment. Highly regulated flows immediately d/s from Castaic Creek.	Wide floodplain through densely urbanized Santa Clarita. Crossed by I-5, Hwy 126, and McBean Pkwy bridges. Receives unregulated inflow from San Francisquito Cyn and So. Fk. SCR.	Densely urbanized Santa Clarita. Narrow valley between Bouquet Canyon Rd. and Newhall Ranch Rd. bridges. Receives partially regulated inflow from Bouquet Canyon.	Wide floodplain, but highly constricted by levees and bank protection on both banks through Santa Clarita. Crossed by Soledad Cyn Rd., Whites Cyn Rd., Sierra Hwy, and Hwy 14 bridges. Receives unregulated inflow from Mint Cyn.	Eastern side of Santa Clarita Basin and urban develop-ments. Valley narrows to the east (u/s side). Crossed by Sand Cyn Rd. bridge.	Narrow valley reach immediately d/s of the Lang Stn. Rd. crossing and the active instream aggregate mining operation. Significant incision d/s of the crossing.	Narrow valley reach immediately u/s of the Lang Stn. Rd. crossing and d/s of the highly confined Soledad Canyon. River still exhibits a broad, braided planform before transitioning to a confined channel u/s.	Confined and sinuous canyon reach, crossed by railway line.	Confined canyon reach, further impinged on right bank by railway. Very coarse bed.	Confined canyon reach receiving very coarse sediment supply from Bear Canyon.	Confined canyon reach bordered along left side by San Gabriel Mtns front and along right side by railway line and Soledad Cyn Rd. Large rock quarry at d/s end. Receives unregulated flow and coarse sediment from Agua Dulce Cyn.	Confined, long canyon reach bordered closely by Soledad Cyn Rd. (left side) and railway line (right side), with some develop-ments and low-water road crossings within the active channel.	Confined canyon reach bordered closely by Soledad Cyn Rd. and railway line (right side), with some develop-ments and low-water crossings within the active channel.	Narrow floodplain floor within canyon. Bordered closely by Soledad Cyn Rd. and railway line (right side), with some developments and low-water crossings within active channel.	Narrow floodplain floor at east end of canyon and west side of Acton Basin. Bordered closely by Soledad Canyon Rd. and other low density develop-ments. Immediately d/s of Arrastre Rd. crossing, with significant incision.	Narrow floodplain floor at west side of Acton Basin with agriculture and low density develop-ments on floodplain (left side). Downstream of Acton Canyon.	Wide floodplain flood with expansive braided, wash channel morph-ology. Receives unregulated inflow from high relief Aliso Cyn.

[a] From HSPF model output (Aqua Terra 2009).
[b] From longitudinal profile generated in GIS with 2005 LiDAR data.
[c] From compilation of bulk sediment size data (see Figure 4-8);
[d] Based on bulk sediment size data; size categories: S = sand (<2 mm), G_{vf} = very fine gravel (2–4 mm), G_f = fine gravel (4–8 mm), G_m = medium gravel (8–16 mm), G_c = coarse gravel (16–32 mm), C_c = coarse cobble (128–256 mm).
[e] From active channel width analysis (1928, 1964, 1980/81, 1994, and 2005) (see Table 4-13 and Figures 4-16 and 4-18).
[f] Results for reaches 11-B to 21 are from the bed level changes analysis (see Figure 4-19). Results for reaches 21–24, 27, 28 are from sediment transport capacity analysis (see Section 4.3.2 of Stillwater Sciences 2011a).
-- Results not available.

5 ESTUARINE AND COASTAL PROCESSES

This chapter focuses on morphodynamics and the primary influences to the Santa Clara River Estuary (SCRE), located at the mouth of the SCR between Reach 1 and the Pacific Ocean, and on general coastal processes operating along the coastline. Therefore, the information presented here serves to complement the prior chapters that focused on the "sources" of water and sediment in the SCR watershed by focusing on the export to the offshore basin, or "sink." Much of the material presented here was originally presented as Chapter 6 of the LSCR geomorphology report (Stillwater Sciences 2007a), but, where possible, certain elements have been updated and/or revised based on information produced from our ongoing work with the City of Ventura's estuary study (Stillwater Sciences 2011b).

5.1 Physical Characteristics

5.1.1 Morphology

The downstream end of the SCR forms an estuary composed of a main lagoon impounded by a seasonally closed-mouth berm. The total inundated area of the SCR Estuary (SCRE), defined by the maximum inundation extent within the river channel and main lagoon under closed-mouth, low-flow conditions, is currently 0.84 km^2 (0.33 ac) and extends approximately 750 m (2,500 ft) upstream of Harbor Boulevard bridge. The most current bathymetric survey (2005 LiDAR surveys by both Ventura County and the USGS) reveals that bed elevations range from 1.2 m (4.0 ft) in the current mouth channel location to 3.1 m (10.2 ft) at the upstream extent of inundation during low-flow, closed-mouth conditions, with a median bed elevation of approximately 1.9 m (6.5 ft) (Figure 5-1). The beach berm elevation currently varies between 4 m (14 ft) and 5 m (17 ft), which is approximately between 2.6 and 3.5 m (8.7 and 11.7 ft) above mean higher high water (MHHW). On average, the SCRE bed is currently approximately 1 m (3 ft) below the adjacent floodplain that defines the southern and northern boundaries. Swanson et al. (1990) reported a ground surface elevation range between 0.3 m (1 ft) above mean sea level (MSL) (1.1 m [3.7 ft]) on the bed at the SCRE mouth and 4 m (15 ft) MSL (5.3 m [17.7 ft]) on the mouth berm, indicating that the current elevation range is very similar to what existed over 20 years ago.

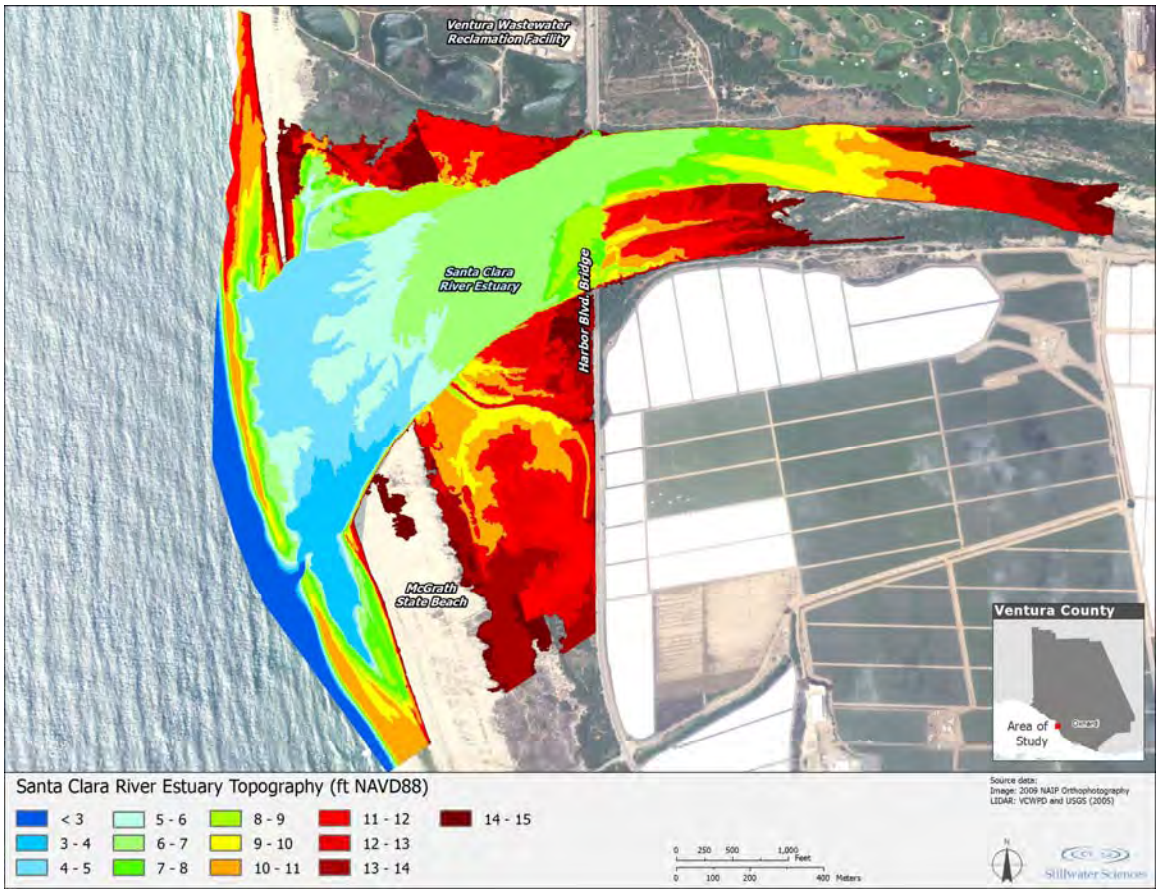

Figure 5-1. Santa Clara River Estuary (SCRE) and surrounding floodplain topography (from 2005 LiDAR).

5.1.2 Tidal and wave dynamics

Tidal inflow to the SCRE during open-mouth conditions can account for a large portion of the total SCRE water volume when the estuary has drained following a storm or other breaching event. The tides adjacent to the SCRE are mixed semidiurnal (O'Hirok 1985), meaning that in general there are two high tides (a lower high and a higher high) and two low tides (a higher low and a lower low) per day, although there are days in which there is only one high tide and one low tide. The closest continuously operating tide gauge that can be used to reflect conditions adjacent to the SCRE is in Santa Barbara (NOAA Station 9411340). At this tide gauge, mean tide range (the difference between mean high water [MHW] and mean low water [MLW]) is 1.11 m (3.65 ft) and mean diurnal range (the difference between mean higher high water [MHHW] and mean lower low water [MLLW]) is 1.64 m (5.39 ft) (Table 5-1). In general, storm-induced increases in tidal elevation are relatively small (less than 0.3 m [1 ft]) in comparison with normal tidal fluctuations (Noble Consultants 1989). Mean sea level (MSL) adjacent to the SCRE has increased approximately 30 cm (12 in) since the onset of European colonization over 150 years ago (see Cayan et al. 2008 and references therein).

Using MHHW (water surface elevation of 1.6 m [5.3 ft]) as the maximum tidally-induced water surface elevation in the SCRE, the tide can currently extend approximately 400 m (1,300 ft) inland from the mouth berm and inundate approximately 22% of the SCRE area and fill

approximately 7% of the total SCRE volume. Tidal flow into and out of the SCRE can last for days to weeks until the tide's ability to maintain an open channel is counteracted by strong wave action bringing sediment onshore, thereby causing mouth closure.

Table 5-1. Tidal elevations for Santa Barbara, CA (1990–2010).

Tidal datum	Elevation (m NAVD88)	Elevation (ft NAVD88)
Extreme high (observed January 1992)	+2.21	+7.26
Mean higher high water (MHHW)	+1.62	+5.30
Mean high water (MHW)	+1.38	+4.54
Mean diurnal tide level (MDTL)	+0.79	+2.60
Mean tide level (MTL)	+0.83	+2.71
Mean sea level (MSL)	+0.82	+2.69
Mean low water (MLW)	+0.27	+0.89
Mean lower low water (MLLW)	-0.03	-0.09

Source: NOAA Center for Operational and Oceanographic Products and Services website (www.co-ops.nos.noaa.gov)

The effective wave energy modifying the coast is a function of wave direction, height, and period. Waves breaking onshore at the SCR mouth often approach from due west and are generated in the winter by low pressure systems over the Gulf of Alaska, and during the remainder of the year by the Hawaiian high pressure cell driving winds and swells to the east. Late summer tropical storms and Southern Hemisphere cyclones generate large swells from the south and south-southwest (O'Hirok 1985). The average wave height along this shoreline is 1 m but ranges from 0.3 m to 7 m (Orme 1982, as cited in O'Hirok 1985).

Breaking wave type (plunging, spilling, or surging) influences the relative onshore movement of beach material. The most common wave type at the mouth of the SCR is a mixed plunge-spill breaker (O'Hirok 1985). Owing to predominant deposition along this short segment of the coast, the foreshore is rarely steepened enough to generate surging waves. The width of the surf zone is a function of the slope of the near-shore bottom, wave height, tidal stage, and discharge. The submerged delta formed off the SCR can create surf zones greater than 250 m wide. Surf zones measured during high spring tides are narrower, as waves break closer to the steeper foreshore. When river discharge is low and sediment moved onshore by wave action forms a barrier that closes the SCR mouth, the surf zone can decrease to less than 100 m with waves breaking only once (O'Hirok 1985).

5.1.3 Estuary hydrology and hydraulics

Water in the SCRE is supplied predominantly by flow from the SCR and effluent from the City of Ventura waste water treatment plant, with local agricultural runoff and wave overwash also contributing to the overall supply (Swanson et al. 1990). Water surface elevations within the SCRE can range from approximately 1.5 m (5 ft) when the estuary is essentially empty to over 4.3 m (14 ft) when the estuary fills with river discharge during storm events (Stillwater Sciences 2011b) . The SCR discharge is very low most of the year (less than 0.03 m^3s^{-1} [1 cfs]), but winter and spring storms can increase discharge by several orders of magnitude within just a few hours. At the mouth of the SCR, the City of Ventura Water Reclamation Facility (VWRF) discharges an average of approximately 32,000 m^3 day^{-1} (8.4 million gallons day^{-1}) of treated freshwater into the SCRE (City of Ventura 1999), which is equivalent to an average year-round stream flow of approximately 0.4 m^3s^{-1} (14 cfs). During the winter months when river flows dominate and

generally maintain an open mouth, effluent discharge is a relatively small portion of total discharge volume. However, the average daily effluent discharge is far more than the average summer and fall streamflow that would be expected from an unregulated southern California river when the mouth is closed (ESA 2003). Discharge of treated effluent from the VWRF while the mouth is closed can cause the water level of the SCRE to rise above the sand barrier and cause the barrier at the mouth to breach at a time of year when this would not occur under natural conditions (Swanson et al. 1990 as cited in ESA 2003).

In addition to the SCR mouth breaching as a result of impounded discharge causing erosion of the barrier beach, the mouth has been mechanically breached in the past to alleviate the risk of flooding adjacent to the estuary. Known recent authorized breaches include an emergency breach as part of the 1994 McGrath Lake oil spill and occasional breaches associated with the Ventura Port District annual winter dredging disposal operations (ESA 2003). The McGrath Beach State Park 1979 General Plan indicated that park personnel would routinely breach the estuary barrier to prevent flooding of the campground caused by high groundwater. Due to natural resource considerations, this practice ended by 1985 (ESA 2003).

5.1.4 Sediment particle sizes

Bed sediments within the SCRE are characterized by stratified layers of coarse sand and range in size from clay- to boulder-sized particles. In general, the SCRE exhibits a pattern similar to most river-mouth lagoons where the surface bed particle size decreases moving downstream from the river-lagoon transition (i.e., zone where flow velocity decreases and larger sediment drops out of the transported load) to the lagoon-ocean interface. Estuary-wide and localized particle size distribution is strongly influenced by both storm-induced river flows and deposition during tidal exchange. During most storm flows, sediment ranging in size from silt/sand to gravel is delivered to the SCRE. During the peak discharge of larger storm events, flow velocity and associated shear stress in the dominant channel can be high enough to transport cobble and boulder-sized sediment far into the SCRE or through the estuary completely and out to the Santa Barbara Channel (O'Hirok 1985). Deposition of very fine sediment (i.e., silt and clay-sized material) on the surface above coarser sediment then occurs as storm flows recede (USFWS 1999) and also as a result of flocculation (aggregation of fine sediment) induced by river and ocean water mixing during open-mouth conditions (O'Hirok 1985). Therefore, between larger floods that cause significant bed scour and coarse sediment transport, lesser flood events result in transport and deposition of finer sediment above a coarser substrate.

Recent bed sediment data collected from fall 2009 through spring 2010 illustrate the current conditions (i.e., period between large storms that includes lesser, depositional storm events) within the SCRE (Stillwater Sciences 2011b). In general, the SCRE bed surface is composed predominantly of sand throughout, with coarser sediment being present primarily towards the upstream estuary extent and within and adjacent to the main lagoon channel. Upstream of Harbor Boulevard bridge, the main lagoon channel currently has large patches of coarse gravel (gravel with sand and cobbles) and coarse sand (sand with gravel and cobble) with adjacent high depositional bars containing coarse sediment (gravel and cobble). Approximately 100 m (330 ft) upstream of the bridge, there is a distinct break in the main channel slope and associated transition from coarser to finer bed sediment going upstream to downstream. Downstream of Harbor Blvd. bridge, the main lagoon channel currently flows towards the south, resulting in coarser surface sediment in the southern portion of the SCRE and finer surface sediment towards the northern portion. Towards the mouth berm and in the VWRF outfall channel, surface sediment is predominantly sand.

5.2 Sedimentation Dynamics

Sediment deposition dynamics at the mouth of the SCR and within the SCRE are driven by both fluvial and littoral sediment transport processes. Understanding how these processes interact to mediate deposition and subsequent SCR mouth closure dynamics is fundamental to understanding: (1) the fate of sediment within this fluvial-littoral interface, (2) the current and future geomorphic state of this mouth/estuary complex, and (3) the current and projected future ecological state of this system with respect to vegetation dynamics and fish passage. The following is a compilation of the current understanding of historical and present fluvial process and delta-building dynamics, longshore transport and shoreline dynamics, and barrier deposition and closure dynamics associated with the SCR mouth and estuary.

5.2.1 Fluvial processes and delta dynamics

The SCR discharges a considerable amount of sediment primarily during high intensity, low recurrence storm events. Estimates of sediment discharge from the SCR by mass (tonnes yr^{-1}) and by volume (m^3 yr^{-1}) are shown in Table 5-2. In general, the coarser sediment (>0.0625 mm) that is delivered from the SCR during storm events contributes to the building of near-shore and offshore deltas, which in turn provides sediment for littoral transport (and down-coast beach deposition) and supplies sediment that builds the barrier beach and causes mouth closure during periods of low river discharge.

Table 5-2. Summary of sediment discharge estimates for the SCR.

Sediment discharge class	Sediment discharge ($t\ yr^{-1}$)	Sediment discharge ($m^3\ yr^{-1}$)
Suspended Sediment	3.5 million *[for 1950 to 1999]* (Warrick and Milliman 2003)	
Sand		0.14 million (Noble Consultants 1989)
		0.57 million (PRC Toups 1980)
Sand & Gravel	0.96 million *[for 1928–1975]* (Brownlie and Taylor 1981)	0.91 million *[for 1971–1999]* (Willis and Griggs 2003)
Total Sediment	3.3 million *[for 1928–1975]* (Williams 1979)	
	3.5 million *[for 1928–1999]* (Warrick 2002)	

The high discharge events in the SCR that deposit sediment to the offshore delta are dominated by hyperpycnal flows (Warrick 2002, Warrick and Milliman 2003). Hyperpycnal flows are flows in which the river discharge is denser than ocean water due to high suspended sediment concentration. Buoyancy theory suggests a hyperpycnal threshold for suspended sediment concentration of approximately 40 grams per liter ($g\ L^{-1}$) (approximate total flow density of 1,040 $kg\ m^{-3}$) for southern California rivers (ocean density = 1,025 $kg\ m^{-3}$) (Warrick 2002). During the 1969 flood events, SCR suspended sediment concentrations exceeded the hyperpycnal threshold of 40 $g\ L^{-1}$ for periods of hours to days. Warrick and Milliman (2003) suggest that the hyperpycnal threshold is surpassed during SCR flows less than 1 to 3 times the value of the mean annual flow (recurrence interval of approximately 1–4 yr) and that approximately 75% of the estimated 170 million tonnes of sediment delivered from the SCR between 1950 and 1999 was delivered during hyperpycnal events. The density and velocity associated with hyperpycnal flows

from the SCR cause the suspended sediment to pass through the estuary and nearshore zone, and be deposited on the offshore delta. This deposited sediment is then stored in the offshore delta and can be considered a potential loss of immediate beach sand supply (Warrick and Milliman 2003). Hyperpycnal events with a low exceedance probability (>100-yr recurrence interval) have the potential to deposit sediment out of the littoral cell in offshore basins, essentially resulting in a net loss of sediment within the system (Warrick and Milliman 2003). This sediment routing can lead to local erosion by evacuating bed sediment that is deposited within the estuary.

The offshore delta of the SCR varies temporally with respect to volume due to variability in sediment input from the river and sediment erosion and subsequent down-coast deposition. The offshore delta had an estimated volume of 191 million m^3 (250 million yd^3) in 1989 (Noble Consultants 1989). The largest recorded input of sediment from the SCR to the offshore delta occurred during the floods of 1969, where approximately 9.9 million m^3 (13 million yd^3) of sediment was deposited (Noble Consultants 1989), and in 2005 where approximately 4.6 million m^3 (6 million yd^3) of sediment was transported out of the SCRE (Barnard et al. 2009). Drake (1972) determined that approximately 75% to 95% of the total load from the 1969 flood was deposited within 20 km from the SCR mouth, and that sand delivered from the river during the 1969 flood was initially deposited in a nearshore river mouth delta and was subsequently transported 1 to 1.5 km offshore onto the SCR delta. Following the 1969 flood events, bathymetric surveys conducted by the VCWPD and the USACE between December 1975 and May 1978 show a maximum seasonal gain in delta volume of approximately 3.1 million m^3 during fall/winter of 1977/1978 (~3x gain observed in two previous fall/winter surveys) as a result of deposition from a flooded SCR, and a loss of approximately 1.2 million m^3 of sediment from the delta during winter 1975/1976 (USACE 1980) due to lack of storms and subsequent sediment supply from the SCR. These data collectively suggest that the delta can be a significant source of sediment due to replenishment from the SCR during storm events, but prolonged periods between major storms can cause delta depletion which can lead to down-coast beach erosion. The mechanism of down-coast sediment delivery (longshore transport) and down-coast shoreline dynamics are discussed in Section 5.2.2.

Near-shore deltas form at the mouth of the SCR during more frequently occurring hypopycnal (river discharge is less dense than ocean water) storm events. O'Hirok (1985) suggested that near-shore delta formation and evolution at the mouth of the river can be described by application of jet theory (Bates 1953), in which three zones exist: zone of flow establishment (constant velocity), zone of transportation (constant rate of velocity decrease), and zone of established flow (residual velocity decays rapidly through turbulence) (Figure 5-2). Deceleration in the transition zone results in sediment deposition and delta building. Decelerations can be induced by density differences between incoming river water and ocean water. During hypopycnal flow events such as the flood event of March 1983, O'Hirok (1985) suggests that there is deposition of buoyant deltas (deposition as a function of flood water mixing with more dense sea water) and friction deltas (deposition as a function of decreased discharge resulting in accelerated sediment deposition and delta bifurcation) at the mouth of the SCR. Near-shore delta deposits from hypopycnal flows are ephemeral features subject to immediate wave impact and longshore transport, as well as local deposition at the mouth of the SCR which leads to barrier formation and subsequent mouth closure. The details of SCR mouth closure dynamics are discussed in Section 5.2.3.

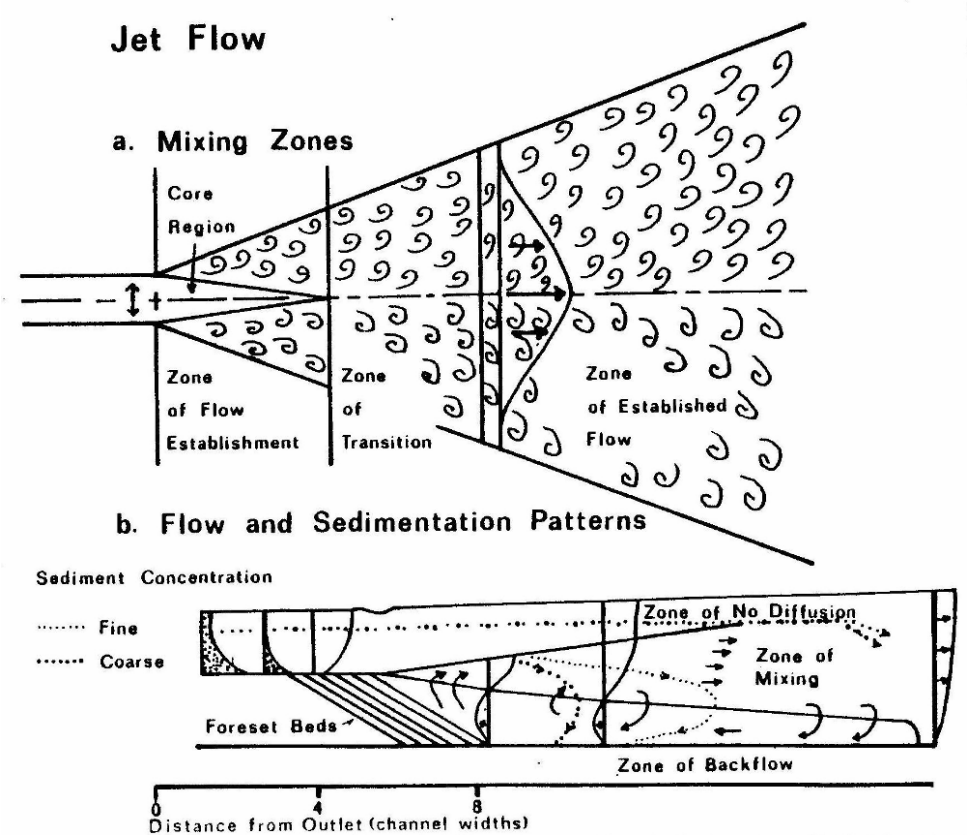

Figure 5-2. Conceptual description of sediment deposition from jet flow (O'Hirok 1985 after Bates 1953).

5.2.2 Longshore transport processes and shoreline dynamics

The sediment discharged from the SCR is transported down-coast via longshore transport as a part of the Santa Barbara Littoral Cell. Littoral cells are discrete coastal regions that can be considered closed systems within which sediment is transported. The Santa Barbara Littoral Cell, which is associated with the Santa Barbara Channel, is adjacent to the Santa Maria Littoral Cell and extends from Point Conception to Mugu submarine canyon (Figure 5-3). The portion of the littoral cell (subcell) for which the SCR specifically contributes sediment extends from Ventura Harbor at the northern extent to Channel Islands Harbor at the southern extent. Although Ventura River north of Ventura Harbor does contribute sediment to this subcell, Ventura Harbor is considered the northern subcell extent. The strength and direction of the longshore current is a function of incoming wave height, direction of wave approach, and beach slope. In response to prevailing wind direction of 247° in the area of the SCR mouth and wave shelter from offshore islands, the longshore current generally flows down-coast in a southeasterly direction (O'Hirok 1985, Noble Consultants 1989). Longshore velocity can reach 2 m s^{-1} (Orme 1982 as cited in O'Hirok 1985). The direction of the current is subject to reversal during the summer months when occasional tropical storms generate large swells from the south (Orme 1982 as cited in O'Hirok 1985). Although longshore current reversals are frequent, sediment transported during these conditions represent a small portion of average total annual volume (Noble Consultants 1989). Estimates by PRC Toups (1980) suggest that the SCR delivers approximately 65% of all sediment transport down-coast within the Santa Barbara Littoral Cell (O'Hirok 1985).

Figure 5-3. Location and extent of the Santa Barbara Littoral Cell (Noble Consultants 1989).

Historical surveys show that the shoreline has changed considerably over the past 150 years immediately around the SCR mouth. From 1855 until artificially stabilized in the 1950s, the shoreline north of the SCR experienced a net seaward advance of several hundred meters while at the same time large retreats and advances down-coast occurred in response to fluctuations of the SCR offshore delta. Stabilization was affected by emplacement of a groin field (1962–1967), construction of Ventura Harbor (1963) in Pierpoint Beach, and establishment of a sand bypassing program for Ventura Harbor (Thompson 1994). The shoreline directly adjacent to the SCR advanced seaward approximately 100 m (330 ft) between surveys made in 1933 and 1948, retreated approximately 80 m (250 ft) from 1948 to 1961, and advanced approximately 100 m (330 ft) from 1961 to 1987 (during the 1969 flood a temporary delta extended seaward of the existing shoreline approximately 600 m [2,000 ft]) (Thompson 1994). Pronounced accretion between 1947 and 1955 was a result of the sediment made available in the offshore delta from the 1938 flood (Inman 1950; Oceanographic Services, Inc., 1977, as cited in O'Hirok 1985). In the period directly after the 1969 flood events, there was considerable beach erosion at Oxnard Shores south of the SCR mouth, with subsequent shoreline advance in the early 1980s that yielded the approximate 150 m wide beach that currently exists (Orme, pers. comm., 2005a). The overall net accretion that has occurred at the SCR mouth from 1855 to 1987 is approximately 270 m (900 ft) (Thompson 1994).

In an effort to better quantify the relationship between observed beach erosion/deposition dynamics and sediment availability, Noble Consultants (1989) developed a sediment budget for

the Santa Barbara Littoral Cell. The sediment budget analysis included numerical modeling of fluvial inputs from the SCR, analysis of net changes in sediment volume as computed by beach profile data, and estimates of annual longshore transport rates from dredging records from the Santa Barbara Harbor, Ventura Harbor, and Channel Islands Harbor. The sediment budget results indicate a yearly net loss of sand (as calculated from beach profile data) of approximately 300,000 m^3 (390,000 yd^3) between 1948 and 1966. The period between 1948 and 1963 represents pre-harbor conditions and was interpreted to be indicative of 'natural' conditions. An annual average net gain of sand of approximately 765,000 m^3 (1.00 million yd^3) was experienced between 1966 and 1970, which essentially records the effects of the 1969 flood. From 1970 to 1987, the average net gain was reduced to about 55,000 m^3 yr^{-1} (72,000 yd^3 yr^{-1}). Dredging records between 1970 and 1987 indicate that approximately 490,000 m^3 yr^{-1} (640,000 yd^3 yr^{-1}) on average is dredged from the Ventura Marina (up-coast of the SCR) and approximately 910,000 m^3 yr^{-1} (1.2 million yd^3 yr^{-1}) on average is dredged from Channel Islands Harbor (down-coast of the SCR) (Noble Consultants 1989). The dredged spoils are deposited down-coast of the harbor entrances on the beach and in the near-shore zone, and the sediment is subsequently entrained within the longshore current.

O'Hirok (1985) suggested that small symmetrical sand deposits lying between the dunes and the foreshore are remnants of spoil dredged from the Ventura Marina. Taking into account annual longshore transport reversals, the average annual net littoral transport rate near Ventura Harbor was determined to be approximately 380,000 m^3 (500,000 yd^3) and the average annual net littoral transport rate near the Channel Islands Harbor was determined to be approximately 840,000 m^3 (1.1 million yd^3) (Noble Consultants 1989). Combining this littoral transport rate in the vicinity of Ventura Harbor with a modeled average annual sand delivery rate from the SCR of approximately 134,000 m^3 (175,000 yd^3) (i.e., sand from the SCR that is transported down-coast) yields an estimated average annual littoral transport rate of approximately 516,000 m^3 (675,000 yd^3) (Noble Consultants 1989).

5.2.3 Barrier deposition and mouth closure dynamics

Typical of southern California rivers, barrier formation causes periodic closure of the mouth of the SCR. High-energy winter storms cause the mouth to remain open by both onshore wave action and increased offshore river discharge. Lower-intensity wave action and sediment deposition, and lower river discharges in the summer months facilitate onshore sediment transport and sediment deposition at the mouth, increasing mouth closure frequency and duration compared with the rest of the year (Swanson et al. 1990; Smith 1990, as cited in ESA 2003). When tidal range decreases during periods of low river discharge, the sediment transport capacity decreases due to a decrease in tidal prism, resulting in mouth closure. Specific mechanisms shown to be important in mediating barrier closure and morphology in southern California lagoons include onshore migration of shore-parallel bars and longshore migration and eventual closure of the lagoon outlet (O'Hirok 1985). In general, the combination of river discharge dynamics, sediment availability from the near-shore river delta, sediment availability from longshore transport, and tidal dynamics contribute to barrier formation and mouth closure at the SCR. The closure dynamics of the SCR mouth can be a key component in determining the salinity regime of the system and subsequent vegetation establishment dynamics, as well a key component in controlling the migration of fish in and out of the watershed.

Data on the status of the mouth of the SCR suggest that the mouth is open more often than it is closed. Data collected daily by the City of Ventura from 1984 to 2009 indicate that SCR mouth was open approximately 61% of the total time, with 2009 having the lowest daily frequency of an open mouth (16% of the year) and 1993 and 1995 having the highest daily frequency of an open

mouth (96% of year) (Figure 5-4). On a seasonal basis, these daily observations show that the mouth has been open with the highest daily frequency during March (84% of time) and the lowest daily frequency during September (44% of time), and is open on average less than 50% of time from summer into the fall (July through October) (Figure 5-5). The variability in the amount of time the mouth is open is the lowest for February and March and highest for July and October, indicating that late winter months have a more consistently open mouth than the summer and fall months have a consistently closed mouth. The influence of ENSO-induced flows on the status of SCR mouth has also been documented within this record, with extended open mouth periods during winter and spring being recorded during several ENSO years (e.g., WY 1993 and 1998).

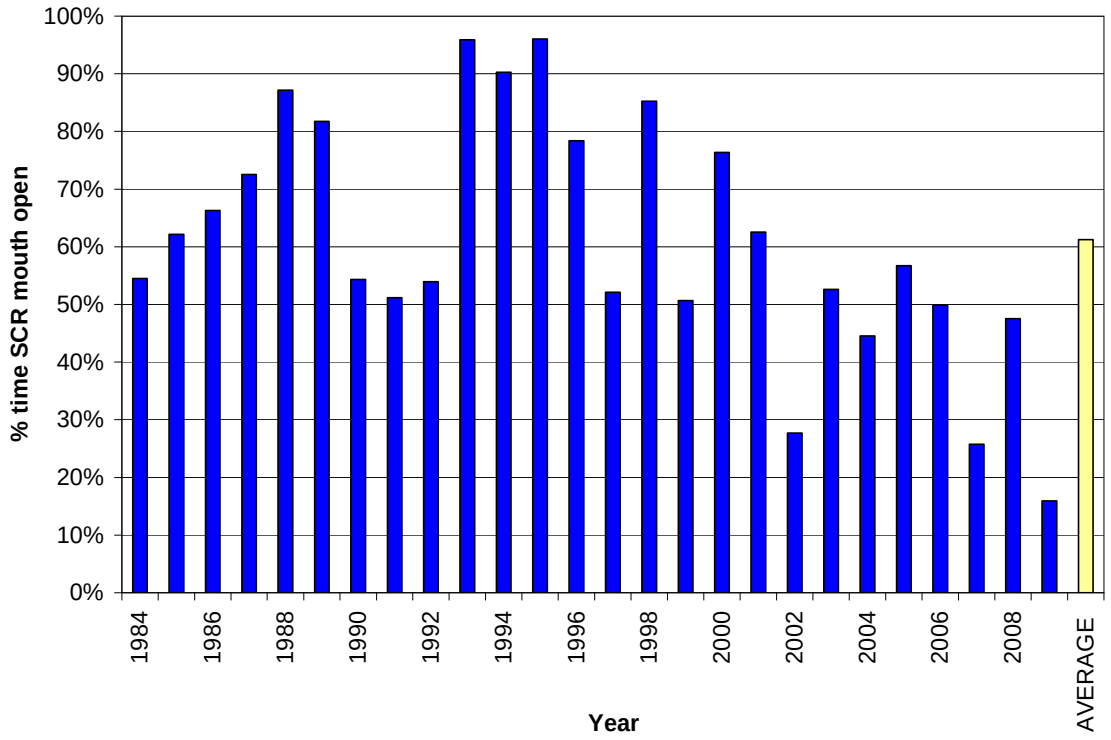

Figure 5-4. Percentage of time that the SCR mouth was open on an annual basis (1984–2009) (City of Ventura).

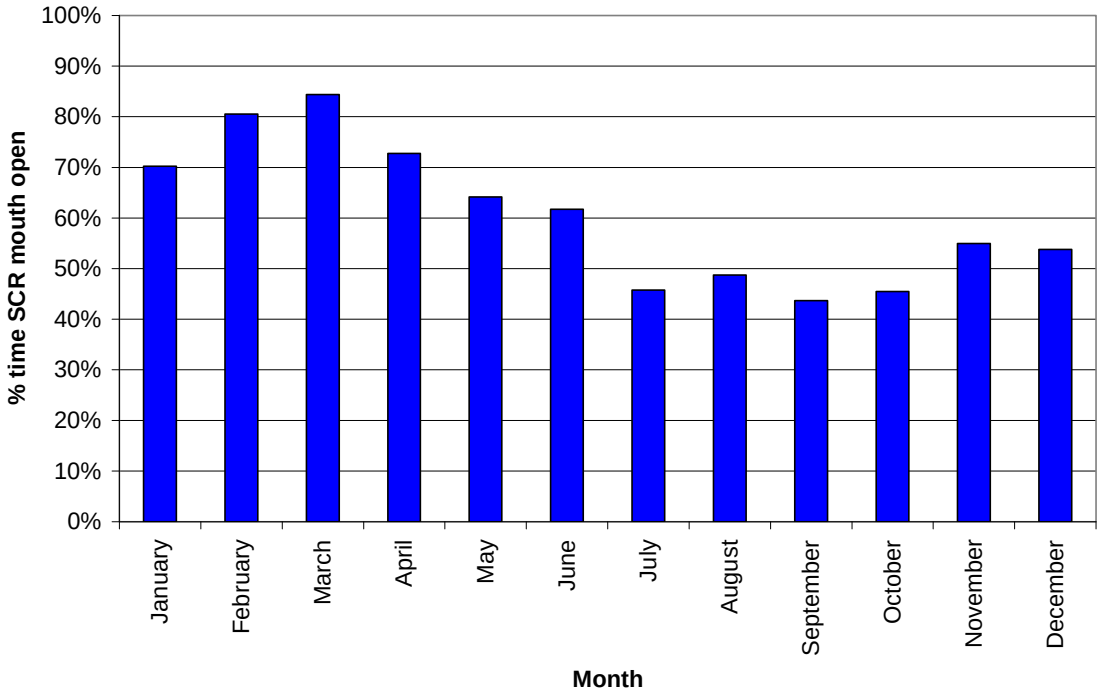

Figure 5-5. Percentage of time that the SCR mouth was open on a monthly basis (1984–2009) (City of Ventura).

The mechanics of a single barrier formation (mouth closure) and barrier erosion (breaching) at the mouth of the SCR following a single spring storm event have been documented, providing an insight into the processes and rates of barrier construction. O'Hirok (1985) examined a closure at the SCR mouth that occurred from April 16 to May 19, 1982 and breaching/resealing that occurred from May 20 to June 25, 1982 (Figure 5-6a-f and 5-7a-f). Following a series of storms in April 1982, secondary barrier building began around the breached primary barrier and an offshore bar formed at the interface between river discharge and the ocean (Figure 5-6a). This accumulated bar caused breaking waves to then refract in many directions as they broke onshore. Continued onshore bar migration was facilitated by decreasing river discharge, increasing tidal range, decreasing wave height, and decreasing wave steepness. Decreased river discharge caused building of the secondary bar (Figure 5-6b). Secondary bar material was made up of silt over sand at the surface and gravel on the margins. As the bar continued to migrate onshore, river flow was divided into two channels (termed "middle-formed bar") until the bar fused to the secondary barriers approximately 7 days after the closure began, creating a single outlet for river flow (Figure 5-6c).

Longshore transport (including a weak current reversal) and overwash by tidal action caused extension and increased the elevation of the secondary barriers, until a period of increased wave height and steepness caused increased onshore sediment movement and closure of the SCR mouth (approximately 34 days after closure began) (Figure 5-6d-f). As water elevation increased from a continuous low discharge (0.33 m^3s^{-1}) into the lagoon, the barrier was breached by overspill and the resulting high velocities in the channel (3 ms^{-1}) caused sediment approximately 300 mm in diameter to be transported within the downcutting and widening (to 20 m) lagoon channel (Figure 5-7a,b). Longshore transport and overwash built up sediment around the breach (Figure 5-7c-e). Increasing tidal range and low intensity waves caused barrier sealing approximately 30 days after breaching (Figure 5-7f) (O'Hirok 1985). O'Hirok (1985) concluded

that mouth closure occurs at the SCR during "tidal dominance" when wave energy is low, longshore current is slow, and river power is minimal. O'Hirok (1985) further concluded that tidal delta morphology (large flood-tidal delta and smaller ebb tide delta), which can contribute to mouth closure dynamics, was controlled by the magnitude of tidal prism, lagoon geometry, wave energy, longshore current, and quantity of longshore drift.

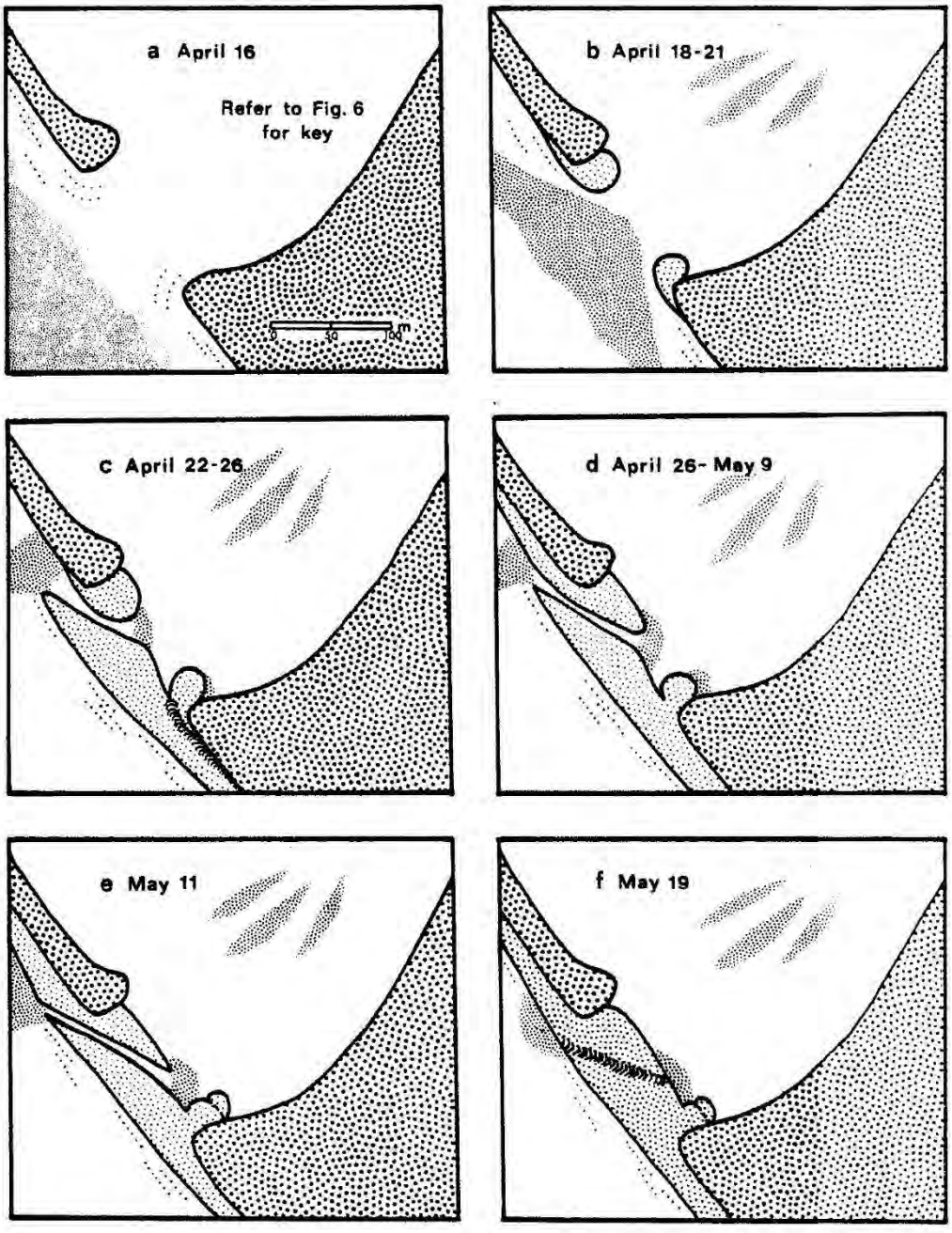

Figure 5-6. Time series of SCR mouth closure (April 16–May 19, 1982) (O'Hirok 1985).

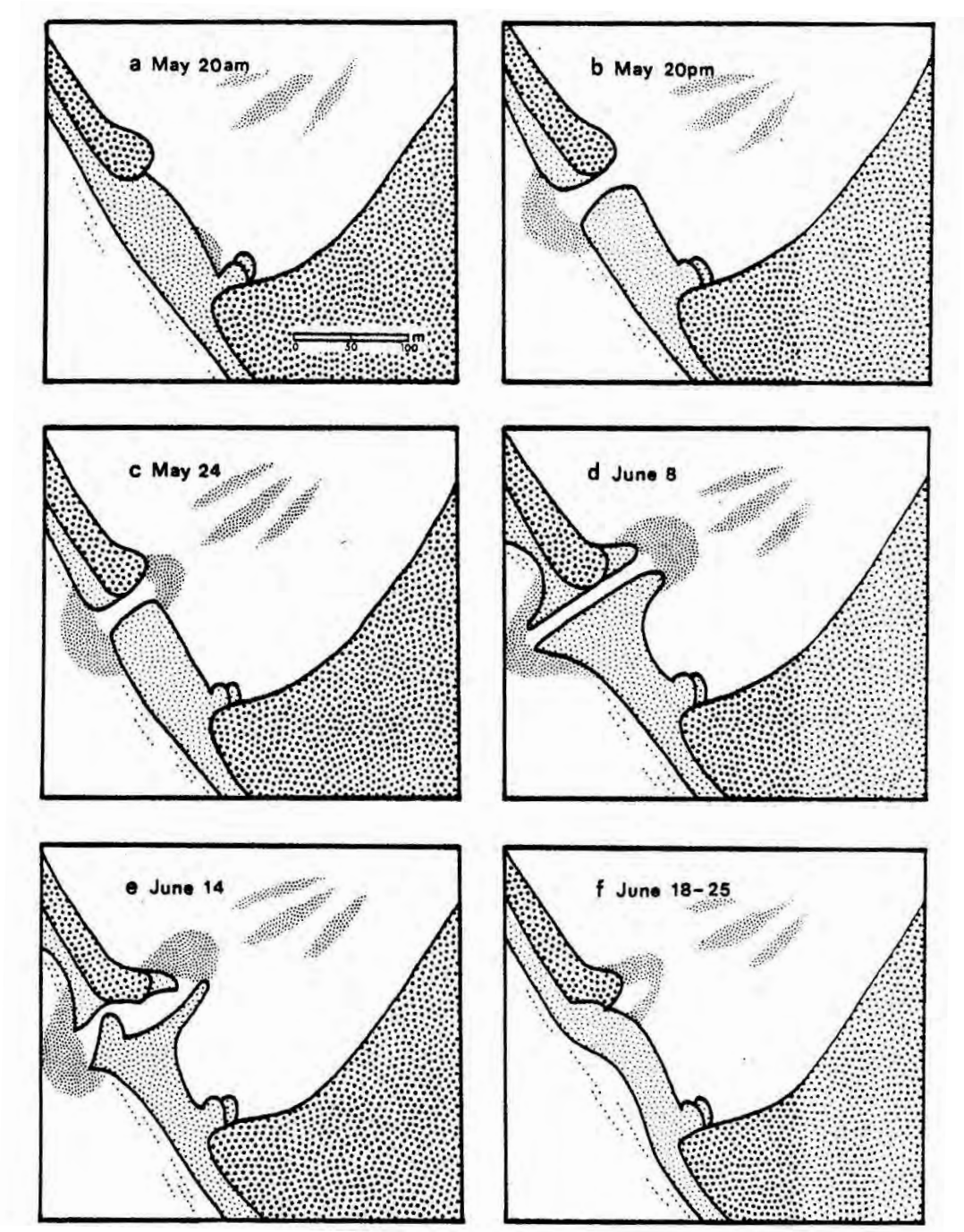

Figure 5-7. Time series of Santa Clara River mouth breach and closure (May 20–June 25, 1982) (O'Hirok, 1985).

5.3 Estuary Historical Change Analysis (1855–2009)

The entire SCR and SCRE have undergone considerable geomorphic change over the past 150 years since European-American settlement due to a combination of land-use practices and climatic conditions. Historically, the SCRE was an expansive ecosystem that included an open-water lagoon and a series of channels that supported intertidal vegetation. Land development since the mid-19th century has resulted in a 75% (Swanson et al. 1990, ESA 2003) to 90% (Nautilus Environmental 2005) decrease in overall SCRE area and available habitat, and the confinement of flood flows by levees. Following the period of intensive development, a shift in precipitation patterns associated with the ENSO has resulted in a wet-period ENSO cycle in southern California over the past 40 years, resulting in a higher frequency and duration of large storms.

Here, we describe changes in the LSCR and SCRE extent since the mid-19th century to highlight the drivers for morphologic change. Data sources used included pre-existing descriptions of morphologic change in and around the SCRE (e.g., Swanson et al. 1990, Schwartzberg and Moore 1995, ESA 2003, Nautilus Environmental 2005, Barnard et al. 2009), and orthorectified topographic maps and aerial photographs from 1855 through 2007. These data were compiled and then used to assess morphologic changes approximately every few decades since 1855. This analysis is then used in the next section as the foundation for developing a conceptual model of the dominant processes controlling SCRE morphologic evolution (see Section 5.4).

The goal of the analysis presented here is to provide a brief overview. A more thorough narrative describing morphologic changes caused by both anthropogenic and climatic influences since the mid-19th century is given in reports by Swanson et al. (1990) and Stillwater Sciences (2011b).

5.3.1 Historical map and photographic interpretation

1855 The map of the SCR mouth from 1855 shows a meandering river channel with a broad floodplain and an extensive estuary/lagoon complex with a distributary channel network at the southern extent of the mouth complex (Figure 5-8). The shoreline and the river mouth (and associated estuary) were inland and the mouth/estuary complex was farther north compared with the 2007 location. The extent of the SCRE was approximately 3.5 km^2 (870 ac) (Swanson et al. 1990).

1927 The shoreline and river mouth shown in the 1927 photograph advanced in comparison with the 1855 position (Figure 5-8). The river meandered through an active channel that extended an additional 762 m (2,500 ft) to the north and 305 m (1,000 ft) to the south in comparison with current conditions. A significant portion of the historical estuary to the north appears to have been filled in and the mouth/estuary complex appears to have moved to the south (to approximate present location). Agriculture encroachment at the southern extent appears to have caused infilling of the distributary's channel network. Vegetation establishment within the active channel was not prevalent.

1945 The shoreline and river mouth shown in the October 1945 photograph advanced to the north and remained relatively stable to the south in comparison with the 1927 position (Figure 5-9). The sediment deposited from the St. Francis Dam failure (1928) and following 1938 floods (approximate 50-year event) is evident in the 1945 photograph. Vegetation within the main channel was still absent, presumably from scour associated with the 1938 flood event. The distributary channel network at the southern extent appears in-filled due to agricultural encroachment. Although the mouth/estuary complex

appears to have expanded with shoreline advance, the area to the north appears to have been filled in more relative to the 1927 photograph.

1958 The shoreline and river mouth shown in the April 1958 photograph eroded landward at both the north and south ends in comparison with the 1947 photograph (Figure 5-9). A decade without a major discharge event from the SCR (i.e., instantaneous discharge was less than 1,416 $m^3 s^{-1}$ [50,000 cfs] between 1947 and 1958) led to considerable vegetation development within the active channel. Riparian forest development at the southern portion of the active channel extent within the mouth/estuary complex led to a quasi-stable channel exiting to the north.

1969 The shoreline and river mouth shown in the February 1969 photograph appear relatively unchanged when compared with the 1958 photograph (Figure 5-10). Levees on both banks established upstream of the Harbor Boulevard bridge had been established by 1969. The effects of the January and February 1969 floods within and around the SCR mouth are apparent in the photograph: a scoured channel network evident is evident on north side of the channel (upstream of Harbor Boulevard bridge) where the flow overtopped the levee; the impact of levee overtopping on the destruction of Ventura Marina is evident; and considerable deposition of sediment on the south side of channel upstream of Harbor Boulevard is apparent. The location of the channel within the mouth/estuary complex was still to the north, but bank erosion induced by the 1969 flood is evident on riparian forest terrace to the south.

1978 The shoreline and river mouth shown in the May 1978 photograph migrated landward compared to the 1969 photograph (Figure 5-10). The March 1978 storm event caused the main channel through the SCRE to move south towards its current location and resulted in the establishment of depositional bars with side channels along the main SCRE channel downstream of Harbor Boulevard and in the mainstem channel upstream of Harbor Boulevard. There is very little in-channel and tidal vegetation shown in the photograph, which is presumably caused by scour during March 1978 storm event.

2005 The shoreline and river mouth shown in the September 2005 photograph extended seaward compared to the 1978 photograph due to sediment deposition associated with the January and February 2005 flood events (two of the largest floods of record) (Figure 5-11). Topographic surveys show that the shoreline adjacent to the SCRE extended seaward approximately 130 m (430 ft) due to the large amount of sediment delivered from the 2005 flood events (Barnard et al. 2009). In addition to causing the formation of a nearshore delta, these floods scoured all bar vegetation in the channel upstream of the Harbor Boulevard bridge, scoured and widened the main SCRE channel downstream of Harbor Boulevard bridge. Unlike the 1969 floods, the levees in the LSCR were capable of containing the 2005 flood flows. Although the 2005 floods did cause considerable vegetation scour, vegetation established in the northern portion of the SCRE since 1978 remained.

2007 The shoreline and river mouth shown in the September 2007 photograph eroded landward compared to the 2005 photograph (Figure 5-11). By 2007, vegetation re-established on depositional bars within the LSCR and SCRE, a southern backwater area had developed, and the mouth berm position stabilized. The southern backwater area currently extends approximately 600 m (2,000 ft) south of the pre-2005 southeast corner of the main lagoon. This morphology appears generally stable and will likely remain until the next large storm event.

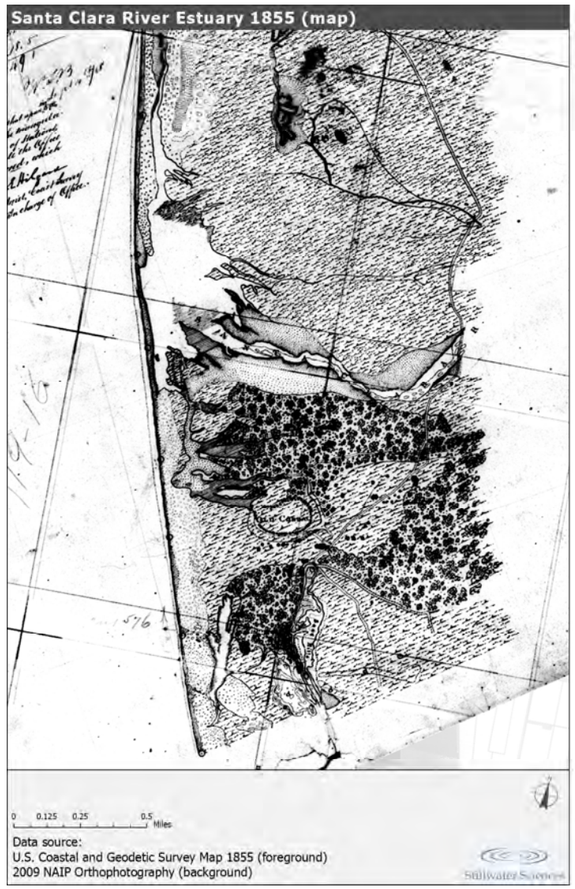

Figure 5-8. SCRE and surrounding floodplain (1855 and 1927).

Figure 5-9. SCRE and surrounding floodplain (1945 and 1958).

Figure 5-10. SCRE and surrounding floodplain (1969 and 1978).

Figure 5-11. SCRE and surrounding floodplain (2005 and 2007).

5.4 Conceptual Model and Projected Trajectory of the SCRE

In order to understand the anticipated trajectory of the SCRE morphology and help inform future watershed management decisions, a simple conceptual model of geomorphic processes currently operating within and acting upon the SCRE was developed. The model was developed from the historical SCRE morphologic change described in the previous section combined with data pertaining to SCRE morphology and SCR discharge and sediment transport dynamics presented in Sections 5.1 and 5.2. Table 5-3 lists the system variables that were identified as potentially affecting the geomorphic state of the SCRE and used to construct the model. The model is intended to provide a general picture of the dominant processes affecting SCRE morphology; a more detailed description of current SCRE geomorphic processes their relationship to undisturbed conditions can be found in Stillwater Sciences (2011b).

Table 5-3. Elements of conceptual understanding of SCRE morphology.

Potential impact on estuary morphology	Description
Sediment loading to the mouth has decreased due to dam and mining effects	Less sediment is available to the off-shore delta compared with historical conditions Potential for decrease in mouth closure frequency and decrease in down-coast beach replenishment
Magnitude of flows have decreased for given storm events due to dam effects	Potential for more frequent mouth closure compared with historical conditions Potential for increased sediment deposition in estuary
Levees have constrained flows	Levees have caused position of estuary on the larger Oxnard Plain to remain stable relative to historical conditions Constraining of flows causes local bed scour and channel migration relative to historical conditions.
ENSO impacts	Current ENSO wet period has increased magnitude and frequency of large storm events Increase in large storm events results in more dynamic morphologic state
Sea level rise	Potential for drowning of mouth, causing landward migration Potential for increased sediment deposition

The conceptual model for SCRE morphologic dynamics is illustrated in Figure 5-12. Currently, storm flows within the much of the SCR are constrained compared with historical conditions due to the network of flood-control levees. The discharge from the Santa Clara River watershed to the Santa Clara River mouth during lower intensity (more frequent) storm events is less dense than the adjacent ocean water (hypopycnal), whereas discharge from higher intensity (less frequent) storm events is dense with sediment in comparison with the adjacent ocean water (hyperpycnal). Hypopycnal events result in near-shore delta deposits that supply sediment for down-coast littoral transport and deposition, and supply sediment for barrier formation that occurs periods of low river discharge. Hyperpycnal events result in sediment deposition on the offshore delta and have the potential to deposit sediment in offshore basins during infrequent high-magnitude events. Sediment deposited in the offshore delta has the potential to be re-suspended during storm events and transported down-coast. The current ENSO wet period has resulted in many large storm events that have caused considerable sediment transport and deposition dynamics and have the greatest potential to modify SCRE morphology. Prior to 1969 (around the start of current ENSO wet-period cycle), a flow of at least 100,000 cfs (or a 10-year flood event) came through the LSCR and SCRE approximately once every 20 to 25 years. Since the start of this current wet-

period, a flow of this magnitude has occurred within an ENSO year approximately once every 5 to 10 years.

In summary, the conditions described above result in high, episodic storm flows that will maintain a river mouth and estuary that will: (1) remain in a fixed location on the Oxnard Plain in comparison with historical conditions; (2) migrate within the current constrained active channel during high discharge events; and (3) supply sediment for mouth closure (near-shore deposition) and down-coast beach building (near-shore and offshore deposition). Although sediment loading to the SCR mouth is reduced compared with historical levels and sea level will continue to rise, hyperpycnal events still occur with sufficient frequency to maintain the mouth/estuary. The current ENSO wet period is characterized by higher storm magnitude and frequency, which in turn has potentially caused substantial geomorphic change within the SCRE, as compared to historical conditions. Although it is not known exactly how long this wet period will persist, it will likely continue into the foreseeable future, causing this current dynamic morphologic state to continue in the near future.

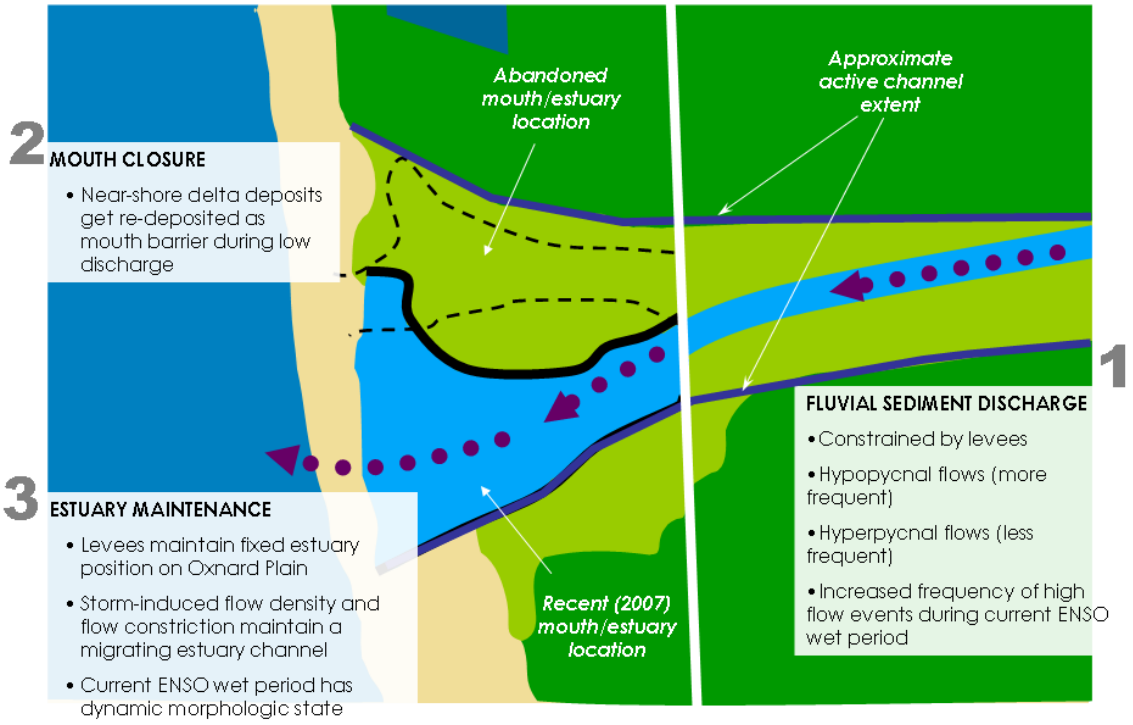

Figure 5-12. Conceptual model of the current and future maintenance of the SCR mouth/estuary complex.

6 SYNTHESIS

This report has presented a geomorphic assessment of key natural and anthropogenically driven processes that have physically shaped and continue to influence the entire SCR and its watershed; it represents a synthesis of the USCR and LSCR studies recently conducted (Stillwater Sciences 2007a and 2011a), in addition to more geographically-focused studies (Stillwater Sciences 2007b, 2009, 2010, and 2011b). In those studies, and re-presented here, the overlying forces controlling geomorphic processes and resulting conditions in the river and watershed are examined over past, present, and future time frames, and at watershed-wide through sub-reach spatial scales. This concluding chapter begins by summarizing the key findings and concludes with a list of remaining information gaps that have the potential to affect management decision-making throughout the SCR watershed.

6.1 Key Findings of the Watershed Geomorphic Assessment

The Santa Clara River functions in a relatively natural state along much of its entire length, in marked contrast to many other coastal rivers of southern California, particularly those in more urbanized basins such as the Los Angeles and Santa Ana rivers—where entire reaches have been channelized with concrete, the majority of their floodplains have been paved, and water and sediment originating from adjacent uplands have been intercepted. In contrast, the Santa Clara River, including the LSCR and USCR halves, remains part of an active, dynamic system that supports a relatively rich ecosystem, subject to episodic, sediment-mobilizing events that create and renew this ecosystem but which also represent hazards to existing human developments, particularly in the densely urbanized centers of Ventura and Santa Clarita. These hazards include episodic occurrences of high-intensity storms with associated flash floods and debris flows, earthquake-induced landslides, and wildfire-induced sediment pulses. The inherently unpredictable nature of hillslope erosion processes results in substantial year-to-year variability in tributary and river sediment loads. This behavior also makes the SCR unlike humid-region rivers, where moderate discharges of intermediate recurrence carries the majority of the sediment load—in contrast, the "dominant discharge" for the SCR is the largest discharge on record. As a consequence of the periodically intense delivery of water and sediment, the SCR exhibits a highly dynamic morphology subject to significant vertical and lateral adjustments, with localized migration into adjacent floodplain areas.

Future planning in the SCR watershed therefore requires informed consideration of these geomorphic processes, along with their associated area of influence and episodicity, in any planning effort in order to avoid: (1) placing projects at risk from nature and/or human-induced hazards; (2) further degrading the ecological functions and benefits of the system; and (3) creating unintended consequences that further destabilize local conditions. Continued expansion of the urban footprints of Ventura, Oxnard, Santa Paula, Fillmore, and Santa Clarita (particularly in steep upland areas or along active margins of the SCR) has great potential to place a greater proportion of the population and infrastructure closer to both the sources and the consequences of the watershed's major hazards. Continuing such urbanization while implementing measures to limit risks from these hazards will further degrade the watershed's ecologic quality, through alteration or loss of existing habitat and disruption of the geomorphic processes that (re)create new habitat. Such measures already implemented and likely to be expanded to protect the growing urban footprint include levee construction, bank stabilization, channelization, and flow and sediment routing structure (e.g., storm drains and debris basins). These hazard-prevention measures provide a degree of safety, but they also can cause understandable (though not precisely

predictable) responses by the river during large flood events that can raise the risk to human safety and damage ecological functions.

6.2 Information Gaps Affecting Watershed Management Decision-making

The reports on the LSCR (Stillwater Sciences 2007a) and the USCR (Stillwater Sciences 2011a) identified several key information gaps in the general understanding of geomorphic processes in the two halves of the watershed. We present here a comprehensive list of information gaps in the understanding of the entire SCR watershed that we have identified over the course of this study. When acquired and analyzed, these data could further assist watershed managers with their assessment and planning endeavors. One primary overarching recommendation related to each of the following information gaps is the need for inter-county coordination during watershed-wide data collection efforts in order to provide the most seamless and effective datasets as possible.

- **Repeat channel survey data:** following the 2005 floods, an airborne LiDAR survey was flown in both Ventura and Los Angeles counties. It provides the highest resolution elevation dataset of the river bed to date. Previous bed elevation surveys in the LSCR and USCR, as discussed above in Section 4.3.4, included several different sources, each with unique resolution quality. Further, all available historic datasets lack the detail to accurately determine river bed elevation changes finer than their respective resolutions can reasonably afford when compared to each other or to the higher resolution LiDAR dataset. In order to more rigorously detect changes in the river's morphology in the future, additional elevation surveys that employ high-resolution data collection techniques, such as LiDAR, are needed. These surveys should be coupled with high-resolution aerial photography taken with the elevation surveys to provide another layer of critical information on watershed conditions.
- **Additional sediment transport measurements:** few bedload samples have been taken during high flows in the SCR, making sediment transport modeling problematic because coarse material transport is estimated from sediment transport equations that have uncertain applicability in the SCR. The sediment loads in the river are so high, and such an important component of planning for river management, that resources should be committed for regular sampling of both bedload and suspended load in major tributaries and the mainstem during high flow events.
- **Inventory of flood management structures:** there is currently no comprehensive spatial database that contains information on all existing levees (both federal and non-federal), bank protection (e.g., rock or concrete revetment), and channelized structures (concrete banks with or without concrete stream beds) throughout the watershed, especially within the more densely populated areas of Santa Clarita. The California Department of Water Resources is presently digitizing federal and non-federal levees from available maps as part of their flood management efforts (CDWR 2009) and both VCWPD and LADPW possess numerous maps containing bridge, levee, debris basin, storm drain, and other flood management-related infrastructure locations. However, compilation of a single, easily referable spatial database containing the locations and attributes of all of these structures, particularly those that are located within a stream channel's active width, would greatly assist those attempting to assess (and model) the impacts of these existing structures and future structures on the hydrology, sediment transport capacity, and morphology of the river corridor and its tributaries.

- **Reservoir sedimentation measurements:** presently, there are no known measurements of sedimentation in Pyramid and Castaic lakes and sedimentation measurements in Lake Piru and Bouquet Canyon Reservoir have not occurred since shortly after they were constructed decades ago. These four reservoirs capture sediment being produced in nearly one-third of the total SCR watershed area. Measuring sedimentation rates in these reservoirs via bathymetric surveys, in addition to performing particle-size analysis of the accumulated sediments, would potentially provide much needed insight into watershed sediment production rates and processes. Because Castaic Lake is effectively split in two parts—Elderberry Forebay captures upper Castaic Creek and Castaic Lake proper captures Elizabeth Lake Canyon—sediment production rates and the processes that control them could be further studied at a slightly finer scale when measuring sedimentation rates and patterns in those two parts.
- **Investigation of the 1928 failure of the St. Francis Dam on geomorphic and sediment transport effects:** the impacts of the massive flood from the dam failure to the river and valley morphology within and downstream of San Francisquito Canyon are not wholly understood. Our analysis of historical changes in the river's active width and bed elevation indicate that narrowing and aggradation has generally occurred since this event. However, it is not known whether these adjustments have finally achieved a state of relative equilibrium (i.e., the river has recovered from the scouring flood), or whether the river is still adjusting in response to this catastrophic event. Future topographic surveys and aerial photography of both the SCR and lower San Francisquito Canyon would allow river managers a means to continue tracking the evolution of these channel corridors, which are becoming progressively more developed, that may still be adjusting to the dam failure event.
- **Estimation of long-term coarse sediment yield:** while reasonably reliable estimates of hillslope sediment production are available, there is only limited information about how much coarse sediment is transported downstream to the river corridor. Coarse sediment is arguably the most important part of the load in this case because it is most relevant to channel- and floodplain- forming processes and to littoral transport and beach replenishment. The high hillslope sediment production rates reported here suggest that the coarse load may be far higher than implied by previous sediment yield data. Quantifying the rate of coarse sediment delivery to the river corridor is a major challenge but might be achieved by comparing estimates of total load with estimates of suspended sediment yield to derive a residual coarse load, or by bathymetric surveys of reservoir sedimentation (see above).
- **Develop a better understanding of the relationship between historical sediment supply changes and channel morphological change:** most of our data regarding channel change post-dates 1930. However, significant increases in sediment load caused by ranching on hillslopes in the mid-19th century, together with reductions in riparian vegetation caused by irrigation, diversions, and clearances in the early 20th century may have had profound morphological impacts on the river that are currently undocumented. A dedicated scientific study of early phase human impacts on the SCR would help elucidate the extent to which these pre-1930 impacts affected channel form, and the extent to which their legacy must be accommodated in future river management strategies.

Pursuing these types of information to fill data gaps will allow for a better understanding of the dynamics of the SCR, and provide managers with useful tools to predict how the river will change and the likely outcomes of management, development, and restoration scenarios.

7 REFERENCES

Printed Sources

AMEC (AMEC Earth and Environmental). 2005. Santa Clara River Enhancement and Management Plan (SCREMP). Public review document. Prepared for the Ventura County Watershed Protection District, Los Angeles County Department of Public Works, and the SCREMP Project Steering Committee.

Andrews, E. D., R. C. Antweiler, P. J. Neiman, and F. M. Ralph. 2004. Influence of ENSO on flood frequency along the California Coast. Journal of Climate 17:337-348.

Aqua Terra (Aqua Terra Consultants). 2009. Hydrologic Modeling of the Santa Clara River Watershed with the U.S. EPA Hydrologic Simulation Program - FORTRAN (HSPF). Revised Final Draft submitted to the Ventura County Watershed Protection District. July.

Barnard, P. L., Revell, D. L., Hoover, D., Warrick, J., Brocatus, J., Draut, A.E., Dartnell, P., Elias, E., Mustain, N., Hart, P. E., and Ryan, H. F. 2009. Coastal processes study of Santa Barbara and Ventura counties, California. U.S. Geological Survey Open-File Report 2009-1029. http://pubs.usgs.gov/of/2009/1029/.

Bates, C. C. 1953. Rational theory of delta formation. American Association of Petroleum Geologists Bulletin 37: 2119-2161.

Begnudelli, L. and B. F. Sanders. 2007. Simulation of the St. Francis Dam-break flood. Journal of Engineering Mechanics 133: 1200–1212.

Benda, L., and T. Dunne. 1997. Stochastic forcing of sediment supply to channel networks from landsliding and debris flow. Water Resources Research 33: 2,849–2,863.

Bendix, J., and C. M. Cowell. 2010. Impacts of wildfire on the composition and structure of riparian forests in southern California. Ecosystems 13: 99–107.

Bierman, P. R. 2004. Rock to sediment-Slope to sea with Be-10 - Rates of landscape change. Annual Review of Earth and Planetary Sciences 32: 215–255.

Blakley, E. R., and K. Barnette. 1985. Historical overview of Los Padres National Forest.

Blythe, A. E., D. W. Burbank, K. A. Farley, and E. J. Fielding. 2000. Structural and topographic evolution of the central Transverse Ranges, California, from apatite fissiontrack, (U/Th)/He and digital elevation model analyses. Basin Research 12: 97–114.

Boughten, D. A., P. B. Adams, E. Anderson, C. Fusaro, E. Keller, E. Kelley, L. Lentsch, J. Nielsen, K. Perry, H. Regan, J. Smith, C. Swift, L. Thompson, and F. Watson. 2006. Steelhead of the south-central/southern California coast: population characterization for recovery planning. NOAA Technical Memorandum NMFS. October 2006.

Brownlie W. R., and B. D. Taylor. 1981. Coastal sediment delivery by major rivers in Southern California. Sediment management of southern California mountains, coastal plains, and

shorelines. Environmental Quality Laboratory Report 17-C, 314. Part C, California Institute of Technology, Pasadena.

Brozovic, N., F. A. Booker, and W. E. Dietrich. 1997. A seventy year record of erosion and sedimentation from the San Gabriel Mountains, southern California. American Geophysical Union, 1997 Fall Meeting 78.

Burbank, D. W., J. Leland, E. Fielding, R. S. Anderson, N. Brozovic, R. Reid-Mary, and C. Duncan. 1996. Bedrock incision, rock uplift and threshold hillslopes in the northwestern Himalayas. Nature 379: 505–510.

Cayan, D. E., P. D. Bromirski, K. Hayhoe, M. Tyree, M. D. Dettinger, and R. E. Flick. 2008. Climate change projections of sea level extremes along the California coast. Climatic Change 87 (Suppl. 1): S57–S73.

Cayan, D. E., K. T. Redmond, and L. G. Riddle. 1999. ENSO and hydrologic extremes in the Western United States. Journal of Climate 12:2881–2893.

CDF (California Department of Finance). 2010. January 2010 cities and counties ranked by size, numeric, and percent change. Prepared by CDF, Sacramento, California.

CDF FRAP (California Department of Forestry and Fire, Fire and Resource Assessment Program). 2010. Statewide fire history electronic database. Website. http://frap.cdf.ca.gov/data/frapgisdata/download.asp?rec=fire [Accessed 25 May 2010].

CDMG (California Division of Mines and Geology). 1993. Update of mineral land classification of Portland cement concrete aggregate in Ventura, Los Angeles, and Orange Counties, California. DMG Open File Report 93-10. Sacramento, California, California Division of Mines and Geology.

CDSD (California Division of Safety of Dams). 2005. Website: http://damsafety.water.ca.gov/about.htm

CDWR (California Department of Water Resources). 2009. 100-year floodplains based upon best available data (Los Angeles County). Website. http://www.water.ca.gov/floodmgmt/lrafmo/fmb/fes/best_available_maps/los_angeles/ [Accessed 30 November 2010].

Chang, H. H. 1990. Fluvial study of Santa Clara River for Curtis Sand and Gravel Mining. Prepared for Curtis Sand and Gravel, Canyon Country, CA through Manee Consulting, Yucaipa, California.

CLWA (Castaic Lake Water Agency). 2003. Groundwater management plan, Santa Clara River Valley groundwater basin, east subbasin, Los Angeles, California. Prepared by Luhdorff & Scalmanini, Woodland, California for CLWA, Santa Clarita, California.

County of Ventura. 2008. Ventura County General Plan, Land Use Appendix. Prepared by the County of Ventura, Resource Management Agency, Planning Division, Ventura, California. http://www.ventura.org/rma/planning/pdf/plans/GP_Land_Use_12-16-08.pdf [Accessed 15 December 2010].

CNRA (California Natural Resources Agency). 2010. Statewide general plan map for California, GIS database. Prepared by the University of California at Davis.

Collins, B. D., and T. Dunne. 1990. Assessing the effects of gravel harvesting on sediment transport and channel morphology: a guide for planners. State of California Division of Mines and Geology, Sacramento, California. 26pp.

Davis, F., E. Keller, A. Parikh, and J. Florsheim. 1989. Recovery of the chaparral riparian zone after wildfire. General Technical Report PSW-110. USDA Forest Service, Pacific Southwest Research Station, Albany, California.

De Koff, J. P., R. C. Graham, K. R. Hubbert, and P. M. Wohlgemuth. 2006. Prefire and postfire erosion of soil nutrients within a chaparral watershed. Soil Science 171: 915–928.

Deser, C., A. Capotondi, R. Saravanan, and A. Phillips. 2004. Tropical Pacific and Atlantic climate variability in CCSM3. Submitted to J. Climate CCSM# Special Issue.

Dibblee, T. W. 1997. Geologic map of the Green Valley quadrangle, Los Angeles County, California. Scale 1:24,000. Dibblee Geological Foundation, Santa Barbara, California.

Doerr, S. H., R. A. Shakesby, and R. P. D. Walsh. 2000. Soil water repellency, its characteristics, causes and hydro-geomorphological consequences. Earth-Science Reviews 51: 33–65.

Downs, P. W., and K. J. Gregory. 2004. River Channel Management: towards sustainable catchment hydrosystems. Arnold, London.

Drake, D. E. 1972. Distribution and transport of suspended matter, Santa Barbara Channel, California, University of California, Santa Barbara, Santa Barbara, California.

Duvall, A., E. Kirby, and D. Burbank. 2004. Tectonic and lithologic controls on bedrock channel profiles and processes in coastal California. Journal of Geophysical Research 109: F03002, doi:10.1029/2003JF000086.

Emmett, W. W. and G. M. Wolman. 2001. Effective discharge and gravel-bed rivers. Earth Surface Processes and Landforms 26:1,269–1,380.
Engstrom, W. N. 1995. The California storm of January 1862. Quaternary Research 46: 141–148.

Erskine, W., and R. F. Warner. 1988. Further assessment of flood- and drought-dominated regimes in south eastern Australia. Australian Geographer 29:257-261.

ESA (Environmental Science Associates). 2003. McGrath State Beach natural resources management plan (final). Los Angeles, California, Prepared for the California Department of Parks and Recreation, Channel Coast District.

Ferguson, R. I. 1987. Hydraulic and sedimentary controls of channel pattern. In Richards, K. S. ed., River channels: environment and process. Blackwell, Oxford, 129-158.

Florsheim, J. L., E. A. Keller, and D. W. Best. 1991. Fluvial sediment transport in response to moderated storm flows following chaparral wildfire, Ventura County, southern California. Geological Society of America 103: 504–511.

Freeman, V. M. 1968. People-land-water: Santa Clara Valley and Oxnard Plain, Ventura County, California. Lorrin L. Morrison, Los Angeles.

Gabet, E. J. 2003. Sediment transport by dry ravel. Journal of Geophysical Research. doi:10.1029/2001JB001686.

Gabet, E. J. and T. Dunne. 2002. Landslides on coastal sage-scrub and grassland hillslopes in a severe El Niño winter: the effects of vegetation conversion on sediment delivery. Geological Society of America Bulletin 114: 983–990.

Gabet, E. J. and T. Dunne. 2003. A stochastic sediment delivery model for a steep Mediterranean landscape. Water Resources Research 39: 1237, doi:1210.1029/2003WR002341.

Graf, W. L. 1983. Flood-related change in an arid region river. Earth Surface Processes and Landforms 8: 125-139.

Graf, W. L. 1984. Flood-related change in an arid region river. Earth Surface Processes and Landforms 8: 125–139.

Graf, W. L. 1988a. Fluvial processes in dryland rivers. Springer-Verlag, Berlin.

Graf, W. L. 1988b. Applications of catastrophe theory in fluvial geomorphology. In Anderson, M. G. ed., Modeling geomorphological systems. J. Wiley and Sons, Chichester, 33-47.

Graf, W. L. 2000. Locational probability for a dammed, urbanizing stream: Salt River, Arizona, USA. Environmental Management 25: 321–335.

Harp, E. L., and R. W. Jibson. 1996. Landslides triggered by the 1994 Northridge, California earthquake. Bulletin of the Seismological Society of America 86: 319-332.

Harvey, M. D., and C. C. Watson. 1986. Fluvial processes and morphological thresholds in incised channel restoration. Water Resources Bulletin 22: 359-368.

Heimsath, A. M. 1998. The soil production function. Doctoral dissertation/ University of California, Berkeley.

Homer, C., C. Huang, L. Yang, B. Wylie, and M. Coan. 2004. Development of a 2001 national landcover database for the United States. Photogrammetric Engineering and Remote Sensing 70: 829–840. http://www.mrlc.gov/.

Inman, D.L. 1950. Report on beach study in the vicinity of Mugu Lagoon, California. Beach Erosion Board, Technical Memo 14: 1-47.

Inman, D.L. and S.A. Jenkins. 1999. Climate change and the episodicity of sediment flux of small California rivers. Journal of Geology 107:251-270.

Joseph, S. E., R. V. Miller, S. S. Tan, and R. W. Goodman. 1987. Mineral land classification of the greater Los Angeles area: classification of sand and gravel resource areas, Saugus-Newhall Production-Consumption Region, and Palmdale Production-Consumption Region. California Division of Mines and Geology, Special Report 143, Part V.

Keeley, J. E. 1987. Role of fire in seed germination of woody taxa in California chaparral. Ecology 68: 434–443.

Keeley, J. E. and P. H. Zedler. 2009. Large, high-intensity fire events in southern California shrublands: debunking the fine-grain age patch model. Ecological applications 19: 69–94.

Keeley, S. C., J. E. Keeley, S. M. Hutchinson, and A. W. Johnson. 1981. Postfire succession of the herbaceous flora in southern California chaparral. Ecology 62: 1,608–1,621.

Kennedy/Jenks (Kennedy/Jenks Consultants). 2008. Upper Santa Clara River Integrated Regional Water Management Plan (IRWMP).

Kirchner, J. W., R. C. Finkel, C. S. Riebe, D. E. Granger, J. L. Clayton, and J. G. King. 2001. Mountain erosion over 10 yr, 10 k.y., and 10 m.y. time scales. Geology 29: 591–594.

Knighton, A. D. 1998. Fluvial forms and processes. Arnold, London.

Knighton, A. D., and G. C. Nanson. 1993. Anastomosis and the continuum of channel pattern. Earth Surface Processes and Landforms 18: 613–625.

Kondolf, G. M. 1994a. Geomorphic and environmental effects of instream gravel mining. Landscape and Urban Planning 28: 225-243.

Kondolf, G. M. 1994b. Environmental planning in regulation and management of instream gravel mining in California. Landscape and Urban planning 29: 185-199.

Krammes, J. S. and J. F. Osborne. 1969. Water repellent soils and wetting agents as factors influencing erosion. Pages 177–186 *in* L. F. DeBano and J. Letey, editors. Proceedings of the symposium on water-repellent soils. Riverside, California.

LACDRP (Los Angeles County Department of Regional Planning). 2009. Draft Santa Clarita Valley area plan: one valley one vision. http://planning.lacounty.gov/ovov.

LACFCD (Los Angeles County Flood Control District). 1959. Report on debris reduction studies for mountain watersheds of Los Angeles County. Los Angeles, California.

LADPW (Los Angeles County Department of Public Works). 2006. Sedimentation manual, 2nd Edition. Prepared by LADPW, Water Resources Division.

LADPW. 2008. Santa Clara River fluvial study: field investigation report. Volume 1: Los Angeles County. Prepared by LADPW, Water Resources Division.

Larsen, I. J. and L. H. MacDonald. 2007. Predicting postfire sediment yields at the hillslope scale: testing RUSLE and Disturbed WEPP. Water Resources Research 43: W11412, doi:10.1029/2006WR005560.

Lavé, J. and D. Burbank. 2004. Denudation processes and rates in the Transverse Ranges, southern California: erosional response of a transitional landscape to external and anthropogenic forcing. Journal of Geophysical Research 109: F01006, doi:01010.01029/02003JF000023.

Leopold, L. B. 1968. Hydrology for urban planning—a guidebook on the hydrologic effects of urban land use. U.S. Geological Survey Circular 554. Washington, D.C.

Lustig, L. K. 1965. Sediment yield of the Castaic watershed, western Los Angeles County, California—A quantitative geomorphic approach. U.S. Geological Survey Professional Paper 422-F.

Manzer, D. 2006. Evolution of the local rancho. Online archives and repository of the Gazette, Santa Clarita, California. http://www.oldtownnewhall.com/gazette/gazette1202-manzer.htm [Accessed 30 August 2010].

Meigs, A., D. Yuleb, A. Blythec, and D. Burbank. 2003. Implications of distributed crustal deformation for exhumation in a portion of a transpressional plate boundary, Western Transverse Ranges, Southern California. Quaternary International 101-102: 169–177.

Mensing, S. A., J. Michaelsen, and R. Byrne. 1999. A 560-year record of Santa Ana fires reconstructed from charcoal deposited in the Santa Barbara Basin, California. Quaternary Research 51: 295–305.

Metcalf, J. G. 1994. Morphology, chronology, and deformation of Pleistocene marine terraces, southwestern Santa Barbara County, California. Master's thesis. University of California, Santa Barbara.

Minnich R. A. 1983. Fire mosaics in Southern-California and Northern Baja California. Science 219, 4590: 1287–1294.

Minear, T. and G. M. Kondolf. 2009. Estimating reservoir sedimentation rates at large spatial and temporal scales: a case study of California. Water Resources Research, doi: 10.1029/2007WR006703.

Nautilus Environmental. 2005. Comprehensive analysis of enhancements and impacts related with discharge of treated effluent from the Ventura Water Reclamation Facility to the Santa Clara River Estuary: Toxicology, Ecology, and Hydrology. Prepared by Nautilus Environmental, Gardena, California, with assistance from Kamman Hydrology & Engineering, Inc., San Rafael, California, for City of San Buenaventura Ventura Water Reclamation Facility, California.

Noble Consultants. 1989. Coastal Sand Management Plan, Santa Barbara, Ventura County Coastline. Irvine, California, Prepared for BEACON (Beach Erosion Authority for Control Operations and Nourishment).

NWS CPC (National Weather Service Climate Prediction Center). 2010. Cold and warm episodes by season. Website. http://www.cpc.ncep.noaa.gov/products/analysis_monitoring/ensostuff/ensoyears.shtml [Accessed 27 Dec 2010].

Oceanographic Services, Inc. 1977. Stability on the beaches in the Hollywood beach area, prepared for Howorth, Anderson and Lafer.

O' Hirok, L.S. 1985. Barrier beach formation and breaching, Santa Clara River mouth, California. Masters thesis, University of California, Los Angeles.

Orme, A. R. 1982. Temporal variability of a summer shorezone. In Thorne, C.E. ed., Space and time in geomorphology, Allen and Unwin, London, 285-313.

Orme, A. R. 1998. Late Quaternary tectonism along the Pacific coast of the Californias: a contrast in style. Pages 179–197 i*n* R. L. Stewart and C. Vita-Finzi, editors. Coastal tectonics, special publication 146. Geological Society, London.

Orme, A. R. and R. G. Bailey. 1971. Vegetation conversion and channel geometry in Monroe Canyon, Southern California. Yearbook - Association of Pacific Coast Geographers 33: 65–82.

Parker, G., and D. Andres. 1976. Detrimental effects of river channelization. Proceedings of Conference Rivers 76: 1248-1266.

Peterson, M. D. and S. G. Wesnousky. 1994. Fault slip rates and earthquake histories for active faults in southern California. Bulletin of Seismological Society of America 84: 1,608–1,649.

Peterson, M. D., W. A. Bryant, C. H. Cramer, T. Cao, M. Reichle, A. D. Frankel, J. J. Lienkaemper, M. A. McCrory, and D. P. Schwartz. 1996. Probabilistic seismic hazard assessment for the state of California. USGS Open-File Report 96-706.

PRC Toups Corp. 1980. Vern Freeman diversion project, final environmental impact report. Prepared for United Water Conservation District.

Prosser, I. P. and L. Williams. 1998. The effect of wildfire on runoff and erosion in native eucalyptus forest. Hydrological Processes 12: 251–265.

Pulling, H. A. 1944. A history of California's Range-Cattle Industry, 1770–1912. Doctoral dissertation. University of Southern California.

Reid, L. M. and T. Dunne. 1984. Sediment production from forest road surfaces. Water Resources Research 20: 1,753–1,761.

Reid, L. M., and T. Dunne. 1996. Rapid construction of sediment budgets for drainage basins. Catena-Verlag, Cremlingen, Germany.

Reneau, S. L., D. Katzman, G. A. Kuyumjian, A. Lavine, and D. V. Malmon. 2007. Sediment delivery after a wildfire. Geology 35: 151–154.

Rice, R.M., and G.T. Foggin. 1971. Effect of high intensity storms on soil slippage on mountainous watersheds in southern California. Water Resources Research 7: 1485-1496.

Rice, R. M., E. S. Corbett, and R. G. Bailey. 1969. Soil slips related to vegetation, topography, and soil in southern California. Water Resources Research 5: 647–659.

Rockwell, T. 1988. Neotectonics of the San Cayetano fault, Transverse Ranges, California. Geological Society of America Bulletin 100: 500–513.

Rockwell, T. K., E. A. Keller, M. N. Clark, and D. L. Johnson. 1984. Chronology and rates of faulting of the Ventura terraces, California. Geological Society of America Bulletin 95: 1466–1474.

Roering, J. J., K.M. Schmidt, J. D. Stock, W. E. Dietrich, and D. R. Montgomery. 2003. Shallow landsliding, root reinforcement, and the spatial distribution of trees in the Oregon Coast Range. Canadian Geotechnical Journal 40: 237–253.

Roering, J. J., J. W. Kirchner, and W. E. Dietrich. 2005. Characterizing structural and lithologic controls on deep-seated landsliding: Implications for topographic relief and landscape evolution in the Oregon Coast Range. USA. Geological Society of America Bulletin 117: 654–668.

Rowe, P. B., C. M. Countryman, and H. C. Storey. 1954. Hydrological analysis used to determine effects of fire on peak discharge and erosion rates in southern California watersheds. U.S. Forest Service, Forest and Range Experiment Station, Berkeley, California.

Schumm, S.A. 1981. Evolution and response of the fluvial system, sedimentologic implications. Society of Economic Paleontologists and Mineralogists Special Publication 31: 19–29.

Schumm, S.A. 1985. Patterns of alluvial rivers. Annual Review of Earth and Planetary Sciences 13: 5–27.

Schwartzberg, B. and P. Moore. 1995. A history of the Santa Clara River, Santa Clara River enhancement and management plan.

Scott, K., and R.P. Williams. 1978. Erosion and sediment yields in the Transverse Ranges, Southern California. Geological Survey Professional Paper 1030.

Scott, K. M., J. R. Ritter, and J. M. Knott. 1968. Sedimentation in the Piru Creek watershed, southern California. U.S. Geological Survey Water-Supply Paper 1798-E.

SCREMP (Santa Clara River Enhancement Management Plan). 1996. Flood Protection Report (Final Draft). Aggregate Subcommittee.

Selby, M. J. 1993. Hillslope materials and processes. Oxford University Press, New York.

Shakesby, R. A. and S. H. Doerr. 2006. Wildfire as a hydrological and geomorphological agent. Earth-Science Reviews 74: 269–307.

Shen, H. W., S. A. Schumm, J. D. Nelson, D.O . Doehring, M. M. Skinner, and G. L. Smith. 1981. Methods for assessment of stream-related hazards to highways and bridges. Technical Report for US Department of Transportation FHWA/RD-80/160, Colorado State University, Fort Collins, Colorado.

Shen, Z. K., D. D. Jackson, and B. X. Ge. 1996. Crustal deformation across and beyond the Los Angeles basin from geodetic measurements. Journal of Geophysical Research 101: 27957–27980.

Simon, A. 1989. A model of channel response in disturbed alluvial channels. Earth Surface Processes and Landforms 14: 11-26.

Simons, Li & Associates. 1983. Hydraulic, erosion and sedimentation study of the Santa Clara River Ventura County, California. Prepared for Ventura County Flood Control District, Ventura, California.

Simons, Li & Associates. 1987. Fluvial study of the Santa Clara River and its tributaries, Los Angeles County, California. Data collection, field reconnaissance, and qualitative geomorphic analysis of existing conditions. Prepared for Los Angeles County Department of Public Works, Los Angeles, California.

Smith, J. J. 1990. The effects of sandbar formation and inflows on aquatic habitat and fish utilization in Pescadero, San Gregorio, Waddell, and Pomponio Creek estuary/lagoon systems, 1985-1989. Prepared by San Jose State University, Department of Biological Sciences, San Jose, California for California Department of Parks and Recreation.

Sommerfield, C. K., and H. J. Lee. 2003. Magnitude and variability of Holocene sediment accumulation in Santa Monica Bay, California. Marine Environmental Research 56: 151–176.

Spotila, J. A., M. A. House, A. E. Blythe, N. A. Niemi, and G. C. Blank. 2002. Controls on the erosion and geomorphic evolution of the San Bernardino and San Gabriel mountains, southern California. Pages 205–230 in A. Barth, editor. Contributions to crustal evolution of the southwestern United States. Special Paper 365. The Geological Society of America, Boulder, Colorado.

Stillwater Sciences. 2007a. Santa Clara River Parkway floodplain restoration feasibility study: assessment of geomorphic processes for the Santa Clara River watershed, Ventura and Los Angeles counties, California. Prepared by Stillwater Sciences, Berkeley, California for the California State Coastal Conservancy, Oakland, California.

Stillwater Sciences. 2007b. Santa Paula Creek watershed planning project: geomorphology and channel stability assessment. Prepared by Stillwater Sciences, Berkeley, California for California Fish and Game, Santa Paula Creek Fish Ladder Joint Power Authority.

Stillwater Sciences. 2009. Hydrogeomorphic analysis of San Francisquito Creek at USFS Road 5N27 Crossing. Draft Report. Prepared by Stillwater Sciences, Berkeley, California for Power Engineers, Inc., and Los Angeles Department of Water and Power.

Stillwater Sciences. 2010. Sespe Creek hydrology, hydraulics, and sedimentation analysis: watershed assessment of hillslope and river geomorphic processes. Final Report. Prepared by Stillwater Sciences, Berkeley, California for Ventura County Watershed Protection District, Ventura, California.

Stillwater Sciences. 2011a. Assessment of geomorphic processes for the upper Santa Clara River watershed, Los Angeles County, California. Final report. Prepared by Stillwater Sciences, Berkeley, California for Ventura County Watershed Protection District, Los Angeles County Department of Public Works, and the U.S. Army Corps of Engineers-L.A. District.

Stillwater Sciences. 2011b. City of Ventura special studies: Estuary Subwatershed Study assessment of the physical and biological condition of the Santa Clara River Estuary, Ventura County, California. Synthesis Report – Administrative Draft. Prepared by Stillwater Sciences, Berkeley, California for City of Ventura, California.

Swanson, M.L., M. Josselyn, and J. McIver. 1990. McGrath State Beach Santa Clara River Estuary Natural Preserve: restoration and management plan, Page 75. Ventura County, California, California Department of Parks and Recreation.

Szabolcsi, K. 2000. Searching for Tataviam answers. Online archives and repository of the Santa Clarita Valley Historical Society, Santa Clarita, California. http://www.scvhistory.com/scvhistory/sg081898.htm [Accessed 30 August 2010].

Thompson, W.C. 1994. Shoreline geomorphology of the Oxnard Plain from early U.S. Coast Survey Maps. Shore and Beach, July 1994: 39-50.

Tiegs, S. D. and M. Pohl. 2005. Planform channel dynamics of the lower Colorado River: 1976-2000. Geomorphology 69: 14–27.

Tiegs, S. D., J. F. O'Leary, M. M. Pohl, and C. L. Munill. 2005. Flood disturbance and riparian diversity on the Colorado River Delta. Biodiversity and Conservation 14: 1175–1194.

Trecker, M. A., L. D. Gurrola, and E. A. Keller. 1998. Oxygen-isotope correlation of marine terraces and uplift of the Mesa Hills, Santa Barbara, California, USA. Geological Society Special Publication 146: 57–69.

University of Southern California. 2004. William Mulholland and the collapse of the St. Francis Dam. http://www.usc.edu/isd/archives/la/scandals/st_francis_dam.html.

URS (URS Corporation). 2005. Santa Clara River Parkway Floodplain Restoration Feasibility Study—Water Resources Investigations. Prepared for the California Coastal Conservancy. April.

URS. 2006. Re: Revised set-up and verification of hydraulic model of Santa Clara River, memorandum. Letter to Bill Sears, Stillwater Sciences. 13 September 2006.

USACE (United States Army Corp of Engineers). 1980. Survey report for beach erosion control, main report. Prepared for Ventura County.

USACE and CDFG (U.S. Army Corps of Engineers and California Department of Fish and Game). 2009. Newhall Ranch resource management and development plan and the spineflower conservation plan draft EIS/EIR. http://www.dfg.ca.gov/regions/5/newhall/docs/.

USFS (USDA Forest Service). 1954. Fire-flood sequences on the San Dimas Experimental Forest. USDA Forest Service, California Forest and Range Experiment Station 6.

USFS. 1997. Sespe Watershed analysis: Ojai Ranger District, Los Padres National Forest.

USFS. 2010. Angeles National Forest cultural history. http://www.fs.usda.gov/wps/portal/fsinternet/!ut/p/c4/04_SB8K8xLLM9MSSzPy8xBz9CP0os3gjAwhwtDDw9_AI8zPyhQoY6BdkOyoCAGixyPg!/?ss=110501&navtype=BROWSEBYSUBJECT&cid=STELPRDB5161139&navid=150140000000000&pnavid=150000000000000&position=Feature*&ttype=detail&pname=Angeles%20National%20Forest-%20History%20&%20Culture [Accessed 30 December 2010].

USFWS (U.S. Fish and Wildlife Service). 1999. Santa Clara River Estuary, Ecological Monitoring Program. In G. M. Prepared by Greewald, L.S. Snell, G.S. Sanders, and S.D. Pratt, eds., Ventura, California, USFWS.

UWCD (United Water Conservation District). 2010. Study plan to characterize geomorphic effects of Santa Felicia Dam on lower Piru Creek. Santa Felicia Project FERC Licence No. 2153-012.

VCWPD and LADPW (Ventura Watershed Protection District Los Angeles County Department of Public Works). 1996. Flood protection report, June 1996. Prepared by the Ventura County Watershed Protection District (formerly Ventura County Flood Control District) and the Los Angeles County Department of Public Works, California.

W&S Consultants (Whitley and Simon Consultants). 1995. Archival records search. Prepared for Newhall Ranch.

Warner, R.F. 1987. Spatial adjustments to temporal variations in flood regime in some Australian rivers. In Richards, K. S. ed., River channels: environment and process. Blackwell, Oxford, 14-40.

Warner, R.F. 1994. A theory of channel and floodplain responses to alternating regimes and its application to actual adjustments in the Hawkesbury River, Australia. *In* Kirkby, M. J. ed., Process models and theoretical geomorphology. J. Wiley and Sons, Chichester, 173-200.

Warrick, J.A. 2002. Short-term (1997–2000) and long-term (1928–2000) observations of river water and sediment discharge to the Santa Barbara channel, California. Ph.D. dissertation, University of California, Santa Barbara.

Warrick, J. A. and D. M. Rubin. 2007. Suspended-sediment rating-curve response to urbanization and wildfire, Santa Ana River, California. Journal of Geophysical Research 112, F02018, doi:10.1029/2006JF000662.

Warrick, J. A., and J. D. Milliman. 2003. Hyperpycnal sediment discharge from semiarid southern California rivers: implications for coastal sediment budgets. Geological Society of America Bulletin 31: 781-784.

Warrick, J. A., and K. L. Farnsworth. 2009. Sources of sediment to the coastal waters of the Southern California Bight. Pages 39-52 *in* H. J. Lee and W. R. Normark, editors. Earth sciences in the urban ocean: the southern California continental borderland. Geological Society of America Special Paper 454, Boulder, Colorado.

Warrick, J. A., and L. A. K. Mertes. 2009. Sediment yield from the tectonically active semiarid western Transverse Ranges of California. Geological Society of America Bulletin 121: 1054–1070.

Warrick, J. A., J. Hatten, G. B. Pasternak, A. Gray, M. Goni, and R. Wheatcroft. In preparation. The effects of wildfire on the sediment yield of a coastal California watershed. Geological Society of America Bulletin.

Wells, W. G., II. 1981. Some effects of brushfires on erosion processes in coastal Southern California. Pages 305–342 i*n* T. Davies, and A. Pearce, editors. Erosion and sediment transport in Pacific Rim Steeplands. Proceedings of the Christchurch Symposium, 25-31 January 1981, Christchurch, New Zealand.

Wells, W.G., II. 1987. The effects of fire on the generation of debris flows in southern California. In Costa J.E. and G.F. Wiezorek, eds., Debris flows/avalanches: Processes, recognition and mitigation: Reviews in Engineering Geology 7: 105-114.

Wells, W. G., II, P. M. Wohlgemuth, and A. G. Campbell. 1987. Postfire sediment movement by debris flows in the Santa Ynez Mountains, California. Pages 275–276 i*n* R. L. Beschta, editor. Erosion and sedimentation in the Pacific Rim. College of Forestry, Oregon State University,. Corvallis, Oregon.

Williams, G. P., and M. G. Wolman. 1984. Downstream effects of dams on alluvial rivers. Professional Paper 1286. U.S. Geological Survey, Washington D.C.

Williams, R. P. 1979. Sediment discharge in the Santa Clara River basin, Ventura and Los Angeles counties, California. U.S. Geological Survey, Menlo Park, California.

Willis, C. M., and G. B. Griggs. 2003. Reductions in fluvial sediment discharge by coastal dams in California and implications for beach sustainability. Journal of Geology 111: 167-182.

Wills, C. J., R. J. Weldon II, and W. A. Bryant. 2008. Appendix A: California fault parameters for the National Seismic Hazard Maps and working group on California earthquake probabilities 2007. USGS Open File Report 2007-1437A.

Wohlgemuth, P. M. 2003. Hillslope erosion following the Williams fire on the San Dimas experimental forest, southern California. Second international wildland fire ecology and fire management congress. American Meteorological Society.

Wohlgemuth, P., J. Beyers, C. Wakeman, and S. Conard. 1998. Effects of fire on grass seedling and soil erosion in southern California chaparral. 19th Forest Vegetation Management Conference.

Wolman, M. G., and J. P. Miller. 1960. Magnitude and frequency of forces in geomorphic processes. Journal of Geology 68: 54–74.

Wolman, M.G., and L.B. Leopold. 1957. River flood plains: some observations on their formation. Professional Paper 271. U.S. Geological Survey, Washington D.C.

Wolman, M. G., and R. Gerson. 1978. Relative scales of time and effectiveness of climate in watershed geomorphology. Earth Surface Processes 3: 189–208.

Yeats, R. S. 1981. Quaternary flake tectonics of the California Transverse Ranges. Geology 9: 16–20.

Personal Communications

Allen, A. 2010. Chief, USACE, North Coast Branch. E-mail correspondence with G. Leverich, Stillwater Sciences, providing historical aggregate mining information.

Araiza, M. 2010. Engineer, LADPW. E-mail correspondence with B. Amerson, Stillwater Sciences, providing debris basin data.

Orme, A. R. 2005. Professor, University of California, Los Angeles. Phone conversation with P. Downs, Stillwater Sciences, providing information on the Santa Clara River watershed.

Romans, B. 2011. Research geologist, Chevron Energy Technology Company. In person correspondence with G. Leverich, Stillwater Sciences, providing cosmogenic nuclide sediment dating results from the lower Santa Clara River.

Wu, G. 2010. Staff, LADWP, Power System. E-mail correspondence with G. Leverich, Stillwater Sciences, providing sedimentation records for Castaic Powerplant debris basins.

Appendices

Appendix A

Watershed Impacts Chronology
Supporting Materials

WATERSHED IMPACTS CHRONOLOGY SUPPORTING MATERIALS

This appendix provides supplementary information that was used in the development of the impacts assessments of the lower Santa Clara River (LSCR) and upper Santa Clara River (USCR) watersheds (Stillwater Sciences 2007, 2011). These assessments were synthesized in Chapter 2 and Section 4.2 of the main report to this appendix. The watershed impacts chronology is summarized in detail in Table A-1. Compilation of available historic and forecasted population data for the watershed, including its major urban centers, was conducted as part of this assessment and is summarized in Table A-2.

The methods employed to determine the "wet" and "dry" periods in the SCR watershed, as depicted in Figure 2-1 in the main report, are also described here. Determining when wet and dry periods have occurred in the past provides valuable context of the watershed's historical hydrological conditions, which have had strong influences on the watershed and, particularly, the river's morphologic history and likely future trajectory. That is, the largest floods have typically occurred during wet years and, further, have typically been concentrated during wet periods (i.e., grouping of years). It is during these large floods when the vast majority of sediment transport (i.e., geomorphic activity) has occurred in the watershed and the river. For this analysis, two of the longest precipitation gauge records in the entire Santa Clara River (SCR) watershed were utilized:

- LSCR: the Santa Paula station (#245A) operated by the Ventura County Watershed Protection District (VCWPD) was used to represent the LSCR watershed conditions. The station began measuring precipitation in water year 1873 and continues to present day. Data for this station can be accessed from VCWPD's website: http://www.vcwatershed.net/hydrodata/. Seasonal precipitation values prior to this period were estimated by Freeman (1968) for water years 1770–1872 based on information first published by Lynch (1931).
- USCR: the San Franciscquito Canyon station (Powerhouse #1) operated by the Los Angeles Department Water and Power (LADWP) was used to represent the USCR watershed. Available data from this station are from water years 1918–2009.

The methodology used was initially developed by Lynch (1931), as described and refined by Freeman (1968). For our analysis, designation of wet and dry periods was determined by first calculating the departure of the total annual precipitation for each water year from the average annual precipitation over the entire period of record. The cumulative departure was then calculated for each water year and wet periods and dry periods were determined as a function of the trend in cumulative departure values. Wet periods were those periods of time when the cumulative departure values were consistently increasing with time (i.e., there was a positive trend in the plot of cumulative value versus water year) and dry periods were those periods of time when the cumulative departure values were consistently decreasing with time (i.e., there was a negative trend in the plot of departure values versus water year). Freeman (1968) described wet periods as "accumulation" periods and dry periods as "depletion" periods. The plots we generated from the Santa Paula and San Francisquito Canyon precipitation gauge data are presented in Figure A-1. Both plots show very similar patterns, with only two notable differences in their overall trends: the San Francisquito Canyon gauge location (i.e., USCR watershed) experienced dry periods during 1970–1977 and 1999–2004 while the Santa Paula gauge location (i.e., LSCR watershed) maintained wet characteristics during these time periods. This result highlights the subtle hydrological differences between these two halves of the SCR watershed, where the USCR portion is more arid than the LSCR portion. Our plot for Santa Paula is similar to the plot Freeman (1968) created for the water years he had available: 1770–1965 (Figure A-2).

Using a long-term record of wildfire data held by the state (CDF FRAP 2010), we applied a similar analysis as described above for the long-term precipitation records to determine periods since 1911 when a relatively high or low proportion of the SCR watershed has burned, termed here as "high burn" and "low burn" periods, respectively (Figure A-3).

Table A-1. Chronology of impacts to geomorphic processes in the USCR watershed.

Factor	Pre-1850	1851–1870	1871–1890	1891–1900	1901–1910	1910–1920	1921–1930	1931–1940	1941–1950	1951–1960	1961–1970	1971–1980	1981–1990	1991–2000	2001–2010 (present)	2010–2050 (future)
Climate																
El Nino Southern Oscillation (ENSO) Cycle (WY 1950-2010) [A]										**WY 1952** **WY 1958**	**WY 1964** **WY 1966** **WY 1969** **WY 1970**	**WY 1973** **WY 1977** **WY 1978**	**WY 1983** **WY 1987** **WY 1988**	**WY 1992** **WY 1995** **WY 1998**	**WY 2003** **WY 2005** **WY 2007** **WY 2010**	Expect contemporary ENSO cycle recurrence interval of 3-8 years to continue
Major Floods & Dam Failure (WY 1928 – 2010) [B, C, D, E, F]	**1811** **1815** **1820-21** **1824-25** **1840**	**Jan 1862:** worst in 19th century, made an inland sea in Ventura Co.; eroded land; numerous landslides throughout watershed **1867:** Flood discharge unknown	**1884:** Flood discharge unknown in SCR, but ~15 in. of rain in 34 hours; flood waters "swept down Soledad Canyon and… spread out over the valley"; river banks stripped bare of riparian trees	**1893 and 1895:** Flood discharges unknown	**1905:** Reportedly contained the "greatest rainstorm since 1884" **1906, 1907, 1909:** Flood discharges unknown, but river flowed through Santa Paula and damaged Saticoy Bridge and farmland	**1911, 1914, 1916:** Flood discharges unknown, but reports of substantial damages in 1914 (e.g., State 23 bridge) and all of the US southwest was impacted in 1916	**March 12–13, 1928:** St. Francis Dam failure (est. 500,000–1,000,000 cfs); peak of wall of water at 78 ft; water 25 ft deep at Santa Paula (42 mi d/s); parts of Ventura Co. under 70 ft of debris; 385 killed; 1,250 homes lost; 23,700 ac of orchards lost; ~$5.5M damage	**1932:** Montalvo gauge initiated **Mar 2, 1938:** Montalvo: 120,000 cfs; Saugus: 24,000 cfs Comparable to 1914, but <1862 & 1884 Extensive damages: farmland, and Saticoy, Newhall Ranch, and Sta. Paula STW bridges	**Jan 23, 1943:** Saugus: 15,000 cfs **Feb 22, 1944:** Saugus: 22,200 cfs	**Apr 3, 1958**: Montalvo: 52,200 cfs	**Dec 29, 1965**: Montalvo: 51,900 cfs Co-line: 32,000 cfs Saugus: 11,600 cfs **Jan 25, 1969**: largest recorded flood Montalvo: 165,000 cfs Co-line: 68,800 cfs **Feb 26, 1969:** caused more damage than Jan flood Saugus: 31,800 cfs	**Feb 11, 1973**: Montalvo: 58,200 cfs Co-line: 12,800 cfs **Feb 9, 1978**: Co-line: 22,800 cfs **Mar 4, 1978** Montalvo: 102,200 cfs **Feb 16, 1980**: Montalvo: 81,400 cfs Co-line: 13,900 cfs	**Mar 1, 1983**: Montalvo: 100,000 cfs Co-line: 30,600 cfs Saugus: 14,925 cfs **Feb 15, 1986**: Co-line: 12,300 cfs	**Jan 12, 1992:** Montalvo: 104,000 cfs Co-line: 12,300 cfs **Feb 18, 1993:** Co-line: 10,700 cfs **Jan 10, 1995:** Montalvo: 110,000 cfs Co-line: 17,100 cfs **Feb 23, 1998:** Montalvo: 84,000 cfs Co-line: 10,000 cfs Saugus: 19,000 cfs	**Jan 9-11, 2005:** Montalvo: 136,000 cfs Co-line: 32,000 cfs Saugus: 20,900 cfs **Jan 2, 2006:** Co-line: 12,500 cfs	Expect contemporary 3–5 year recurrence interval of floods >40,000 cfs at the former Montalvo stream gauge location (i.e., the LSCR) and of floods >10,000 cfs at the Co-line stream gauge (i.e., the USCR) to continue
Wildfires (10 largest fires in the watershed, 1878-2009) [G] **(See Figure A-3)**						**1917 Unnamed Fire:** 178 km^2 (44,009 ac) Sespe and Piru creeks	**1928 Ridge Fire #98:** 176 km^2 (43,472 ac) Piru Creek	**1932 Matilija Fire:** 548 km^2 (135,358 ac) Sespe and upper Santa Paula creeks			**1968 Liebre Fire:** 196 km^2 (48,523 ac) Upper Castaic Creek		**1985 Ferndale Fire:** 174 km^2 (42,980 ac) Santa Paula Creek		**2003 Simi Fire:** 178 km^2 (44,064 ac) Santa Susana Mtns **2003 Piru Fire:** 258 km^2 (63,726 ac) Piru Creek **2006 Day Fire:** 652 km^2 (161,148 ac) Sespe Creek **2007 Buckweed Fire:** 155.2 km^2 (38,347 ac) Bouquet Canyon **2007 Ranch Fire:** 236 km^2 (58,410 ac) Piru Creek	Expect historical ~40-yr recurrence of "high burn" periods to continue

Factor	Pre-1850	1851–1870	1871–1890	1891–1900	1901–1910	1910–1920	1921–1930	1931–1940	1941–1950	1951–1960	1961–1970	1971–1980	1981–1990	1991–2000	2001–2010 (present)	2010–2050 (future)
Channel Management																
Channelization & Bank Protection [F, H]							St. Francis Dam disaster prompts start of channelization on tributaries and bank protection on the river			**1950s – present:** Urban developments encroach on floodplain and prompt construction of hardened banks of river, some levees along the river channel, and highly channelized sections of the lower reaches of several tributaries, mostly near the more urbanized areas of Ventura and Santa Clarita.						Expect increased need for flood and debris protection infrastructure as population and urban footprint increases, particularly in the Santa Clarita Valley
Regulation [F, H]						**1912:** Dry Canyon Reservoir on Dry Canyon (trib. to Bouquet Canyon): 12 km^2 (4.5 mi^2); taken out of operation in 1966 due to seepage problems, but dam remains in place	**1926-1928:** San Francisquito Reservoir (St. Francis Dam) on San Francsiquito Canyon: 98 km^2 (38 mi^2); dam collapsed Mar 12-13, 1928	**1934:** Bouquet Canyon Reservoir on Bouquet Canyon: 35 km^2 (13.6 mi^2)		**1955:** Lake Piru (Santa Felicia Dam) on Piru Creek: 1,091 km^2 (421 mi^2)		**1972:** Castaic Lake on Castaic Creek:398 km^2 (154 mi^2); and Pyramid Lake on upper Piru Creek: 759 km^2 (293 mi^2)			No new reservoirs planned
Abstraction [E, F, I]							**1930:** SCVWD began Piru Creek diversions									No new diversion structures planned, but modifications to the Harvey and Freeman diversion dams and to usage changes of certain spreading grounds have been proposed
								1931: SCVWD began Santa Paula Creek diversions								
									1954-56: Lower River Project improved diversion at Saticoy and elsewhere							
										1991: Freeman Diversion Dam completed on the LSCR						
Instream Aggregate Mining [B, F, J, K]					Start of small-scale aggregate mining in river					**1950s:** Instream aggregate mining begins in Soledad Canyon (USCR) at Lang Station Road						Instream operations (SMP #86357) in Soledad Canyon expected to continue, but unknown when operations may cease and/or when new operations elsewhere along the SCR may initiate
											1960s: Earliest SCR mining permits issued		**1986-92:** Mining activity along lower Sespe Creek			
													1980s: VC created red line for mining depth in river **1989:** most agg. mining in LSCR finished	**1996:** one active instream operation remaining in LAC; 3 out-of-river in LAC and VC		
Management Policy [F, H, L]						**1912:** Los Angeles County Flood Control District formed	**1925:** Santa Clara River Protective Assoc. formed to retain control of SCR **1927:** SCWCD formed from SCRPA		**1944:** Ventura County Flood Control District (now VCWPD) **1950:** SCWCD and City of Oxnard form UWCD	**1950s:** LA County begins taxing property based on housing and commercial potential, initiating large-scale urban development			**1985:** LADPW forms as consolidation of the Flood Control District, County Engineer, and Road Department	**1992:** 51 km (32 mi) of upper Sespe Creek designated as Wild and Scenic	**Sept 29, 2004:** USACE, LADPW, and VCWPD initiated the Santa Clara River Feasibility Study	Watershed management agencies and actions would continue

Factor	Pre-1850	1851–1870	1871–1890	1891–1900	1901–1910	1910–1920	1921–1930	1931–1940	1941–1950	1951–1960	1961–1970	1971–1980	1981–1990	1991–2000	2001–2010 (present)	2010–2050 (future)
Irrigation Infrastructure & Groundwater Extraction [E, F, H, I, M]			**By 1870s:** water demands high enough to need pumped water supplies in watershed	**By 1890s:** Water demands high enough to need pumped water supplies	**Early 1900s:** 16,000 ac irrigated in Ventura County	**1912:** 17,000 ac irrigated in VC by surface flows of SCR **1913:** First public water utility in the Santa Clarita Valley est: Newhall Water System (now NCWD) **1919:** 31,700 ac irrigated in VC	**1925:** 35,000 ac irrigated in VC		**1947–1960s:** Santa Clarita Valley (USCR) groundwater pumping for agriculture: 27,000 – 42,000 AFY **1949:** 107,689 ac irrigated in VC	**1960:** Santa Clarita Valley groundwater pumping for municipal: 5,000 AFY	**1960s:** Santa Clarita Valley groundwater pumping for municipal use: 10,000 AFY **1969:** 101,140 ac irrigated in VC **1960s–1980s:** Santa Clarita Valley groundwater pumping for agriculture: ~12,500 AFY	**1980:** State Water Project via Castaic Lake Water Agency begins to augment Santa Clarita Valley groundwater supply **1980:** Santa Clarita Valley groundwater pumping for municipal uses: 22,000 AFY **1980:** 106,480 ac irrigated in VC	**1981–1990:** State Water Project delivers ~15,000 AFY **1980s–1990s:** Santa Clarita Valley groundwater pumping for agriculture: 9,000 AFY	**1990s:** Groundwater production in Santa Clarita Valley: 43,500 AFY; Acton basin: ~1,500 AFY **1991–2000:** State Water Project delivers ~19,000 AFY **1990s–2000s:** Santa Clarita groundwater pumping for agriculture: 13,500 AFY	**2000s:** Recycled water use begins in Santa Clarita Valley **2000s:** Groundwater production in Santa Clarita Valley and Acton basin: ~30,000 – 35,000 AFY **2001–2005:** State Water Project delivers ~44,000 AFY	Groundwater extraction rates expected to be similar to contemporary levels; Up to 95,200 AFY of State Water Project supply is available to Castaic Lake Water Agency

Factor	Pre-1850	1851–1870	1871–1890	1891–1900	1901–1910	1910–1920	1921–1930	1931–1940	1941–1950	1951–1960	1961–1970	1971–1980	1981–1990	1991–2000	2001–2010 (present)	2010–2050 (future)
Land Use Changes																
Agriculture [B, E, F, M, N, O]	**Early 1800s:** Ranching and farming begins with est. of Spanish Mission and Rancho Removal of riparian and scrub/shrub vegetation cover to grazing and farm land	**1863-1864:** drought decimates cattle industry, replaced initially by sheep, followed by recovery of cattle industry in USCR; shifted focus to ag. in Ventura Co.	**1880s:** 15,000 acres of wheat in Santa Clarita Valley—largest exported of wheat in state Continued conversion of native vegetation areas to agricultural lands throughout SCR	**1892:** Angeles National Forest est.—federal control over land use in semi-protected area		**Post-WWI:** citrus becomes main crop in VC **1917:** 29,000 ac of orchards along LSCR		**1936:** Los Padres National Forest est., assembled from several smaller National Forests (e.g., Santa Barbara NF, San Gabriel NF [portion], Pine Mtn and Zaca Lake reserves, and Santa Ynez Reserve)		**1950:** 66,000 ac of orchards along LSCR	**1960s–1990s:** agriculture in Santa Clarita Valley diminishes as urban developments expand				**2000s–present:** Crop cultivation remains active mostly in LSCR and some ranching practices remain active mostly in USCR (e.g., Acton basin)	Currently zoned agriculture (crops, ranching, etc.) lands remain in general plan maps of Ventura and LA counties
Urbanization (See Table A-2)	**1770:** Portola Expedition encounters ~1,000 Native Americans living in the Santa Clarita Valley **1782:** Mission San Buena-ventura est. **1797:** Mission San Fernando est. **1850:** California gains US statehood	**1866:** City of Ventura incorporated **1870:** town of Santa Paula est. **1870:** Watershed population: 628	**1878:** towns of Newhall and Saugus est. **1887:** towns of Acton and Piru est. **1888:** town of Fillmore est. **1890:** Watershed population: 9,707	**1900:** Watershed population: 8,361 **1903:** City of Oxnard 1903 est.	**1910:** Watershed population: 12,424	**1920:** Watershed population: 19,013	**Mid-1920s:** town of Val Verde est. **1930:** Watershed population: 39,256	**1940:** Watershed population 46,487	**1950:** Watershed population 61,342	**1960:** Watershed population 63,651	**1965:** town of Valencia est. **1970:** Watershed population 134,806	**1980:** Watershed population 193.832	**1987:** City of Santa Clarita incorporated with merging of the towns Canyon Country, Newhall, Saugus, and Valencia **1990:** Watershed population 242,899	**2000:** Watershed population 380,879	**2010:** Watershed population 486,899	Watershed population expected to increase at current growth rates: **2020:** ~570,000 **2030:** ~660,000 **2040:** ~760,000 **2050:** ~880,000

Factor	Pre-1850	1851–1870	1871–1890	1891–1900	1901–1910	1910–1920	1921–1930	1931–1940	1941–1950	1951–1960	1961–1970	1971–1980	1981–1990	1991–2000	2001–2010 (present)	2010–2050 (future)
Linear Features Construction (road and rail) [B, F, P]			**1870s:** So. Pacific Railroad constructed line from Newhall through Soledad Canyon **1880s:** Railway line constructed west to Ventura			**1910s–1920s:** Extensive development of paved roads and construction of more permanent bridges				**1963:** Highway 101 completed through VC	**1960s:** Interstate 5 and State Highway 14 constructed, bisecting drainages and re-routing water and sediment		**1980s-present:** Numerous roads and bridges constructed along floodplain and across USCR through the Santa Clarita Valley			Numerous city and county roads are planned and/or expected to be constructed according to general plans of Ventura and LA counties, with a greater concentration in the Santa Clarita Valley

Abbreviations:
ac = acres cfs = cubic feet per second km^2 = square kilometers SCV = Santa Clarita Valley USCR = Upper Santa Clara River WY = water year
AFY = acre-feet per year est. = established LADPW = Los Angeles County Department of Public Works USACE = U.S. Army Corps of Engineers VCWPD = Ventura County Watershed Protection District

Sources:
A NWS CPC. 2010.
B Historical accounts from the Santa Clarita Valley Historical Society webpage: http://www.scvhistory.com, accessed 30 August 2010.
C Discharge records from the former Montalvo gauge (USGS 11114000), County line gauge (USGS 11108500, 11109000), Santa Clara River near Saugus (USGS 11107922), and Santa Clara River at Old Road Bridge (LADPW F-92).
D Magnitude of St. Francis Dam flood: Begnudelli and Sanders (2007).
E Historical flood events: Freeman (1968), Schwartzberg and Moore (1995), Engstrom (1995), Paulson et al. (1991).
F General historical information: AMEC (2005).
G Wildfire name, date, and total area: CDF FRAP (2010); areal extent within the SCR watershed determined in GIS for this study.
H General historical information on water resources: Kennedy/Jenks Consultants (2008).
I General abstraction information on groundwater resources: UWCD 2007 and Fox Canyon GMA 2007
J In- and off-channel extraction rates estimated: Joseph et al. (1987); In-channel extraction rates by USACE (A. Allen, pers. comm., 2010);
K Aggregate mining activity information for lower Sespe Creek: Stillwater Sciences 2010.
L County tax policy: Worden (1995).
M Groundwater use history and pumping data: Hamilton (1999); NCWD (2010); CLWA (2003); Slade and Associates (2002, as cited in CDWR 2006); Slade (1990, as cited in CDWR 2004).
N Historical agriculture practices information: Manzer (2006).
O Future agriculture land zoning information: County of Ventura (2008), LACDRP (2009), and CNRA (2010).
P History of California highways: California Highways website (2010).

Table A-2. Historical and forecasted populations in the SCR watershed.

Year	Ventura Co. population within the LSCR watershed						Los Angeles Co. population within the USCR watershed									Total for entire SCR watershed
							Santa Clarita Valley									
	Ventura [a]	Saticoy	Santa Paula	Fillmore	Piru	Total for LSCR	Val Verde	Valencia	Newhall	Canyon Country	Saugus (Bouquet Canyon)	Santa Clarita [b]	Total SCV	Acton	Total for USCR	
1850																
1860	628 [c]					628 [f]										628
1870													265 [m]		265 [f]	265
1880	1,370 [c]		188 [c]			3,943 [e]			61 [c]				412 [k]		412 [f]	4,355
1890	2,320 [c]	218 [c]	1,047 [c]			6,996 [e]							2,711 [k]		2,711 [f]	9,707
1900	2,470 [c]					7,377 [e]							984 [k]		984 [f]	8,361
1910	2,901 [c]		2,216 [c]			10,537 [e]							1,887 [k]		1,887 [f]	12,424
1920	4,156 [c]		3,967 [c]	1,597 [c]		16,822 [e]							2,191 [k]		2,191 [f]	19,013
1930	11,603 [c]		7,452 [c]	2,893 [c]		36,230 [e]							3,026 [k]		3,026 [f]	39,256
1940	13,264 [c]		8,986 [c]	3,252 [c]	733 [e]	40,849 [g]			1,666 [k]				5,638 [k]		5,638 [g]	46,487
1950	16,534 [c]	2,216 [c]	11,049 [c]	3,884 [c]		51,341 [g]			2,527 [c]				10,001 [k]		10,001 [g]	61,342
1960	29,114 [c]	2,283 [c]	13,279 [c]	4,808 [c]		51,148 [h]			4,705 [c]						12,503 [o]	63,651
1970	57,964 [c]		18,001 [c]	6,285 [c]		86,217 [h]		4,243 [c]	9,651 [c]						48,589 [p]	134,806
1980	73,774 [c]		20,658 [c]	9,602 [c]	1,284 [c]	120,672 [h]		12,163 [c]	12,029 [c]	15,728 [c]	16,283 [c]	66,730 [c]	73,160 [h]		73,160 [f]	193,832
1990	92,575 [c]		25,062 [c]	11,992 [c]	1,157 [c]	130,786 [f]	1,689 [c]					110,642 [c]		1,471 [c]	112,113 [f]	242,899
2000	100,916 [c]		28,598 [c]	13,643 [c]	1,196 [c]	155,276 [i]	1,472 [c]					151,088 [c]	212,611 [l]	2,390 [c]	225,603 [l]	380,879
2010	109,946 [d]		30,048 [d]	15,787 [d]		175,950 [i]						177,641 [d]	301,774 [l]	9,175 [n]	310,949 [f]	486,899
2020						201,565 [i]						222,290 [l]	368,691 [l]		368,691 [f]	570,256
2030						230,909 [j]						242,620 [l]	428,209 [l]		428,209 [f]	659,118
2040						264,525 [j]							497,335 [j]		497,335 [f]	761,860
2050						303,035 [j]							577,620 [j]		577,620 [f]	880,655

Blank cells = no data available and/or projections were not made

Sources:

a. Often referred to in census reports as San Buenaventura.
b. Incorporated in 1987 with the union of Canyon Country, Newhall, Saugus, and Valencia.
c. CDF 2010a
d. CDF 2010b
e. CDF 2010c; Derivation of Ventura Co. total from sum of township data from Fillmore (1910-1950), Piru (1890-1950), Santa Paula (1900-1950), Saticoy (1880-1900), and Ventura (1880-1950; included only San Buenaventura and Saticoy, excluded Chrisman and Nordhoff which are not in the SCR watershed boundaries).
f. Value estimated by Stillwater Sciences using all available population data in the absence of available watershed-wide data.
g. U.S. Census Bureau 1952; majority of the USCR watershed was referred to as Soledad Township in the 1940 and 1950 census data.
h. U.S. Census Bureau 1982; for the USCR—Newhall Division included: Canyon Country (CDP), part of Los Angeles city, Newhall (CDP), Saugus-Bouquet Canyon (CDP), and Valencia (CDP); for the LSCR—included Divisions of Fillmore-Piru, Santa Paula, and Ventura.
i. County of Ventura 2008; included zoning areas of Fillmore, Piru, San Buenaventura, and Santa Paula; 2000 value based on 2000 census data; 2010-2020 values are forecasts made by County of Ventura (average annual growth rate = 1.5%).
j. Population projected by Stillwater Sciences using average annual growth rates for the LSCR watershed estimated by Ventura County (2008; 1.5%, see footnote i) and for the USCR watershed estimated by Kennedy/Jenks (2008; 1.6%, see footnote l).
k. CDF 2010d; included Soledad Township (includes Newhall CDP).
l. Kennedy/Jenks 2008
m. Earle 2003
n. City of Acton 2010
o. Value from sum of Newhall CDP population (CDF 2010a) and populations from unincorporated census tracts identified by Kennedy/Jenks (2008) to be situated within the USCR watershed (U.S. Census Bureau 1962; tracts: 9012, 9108, and 9201).
p. U.S. Census Bureau 1973

a)

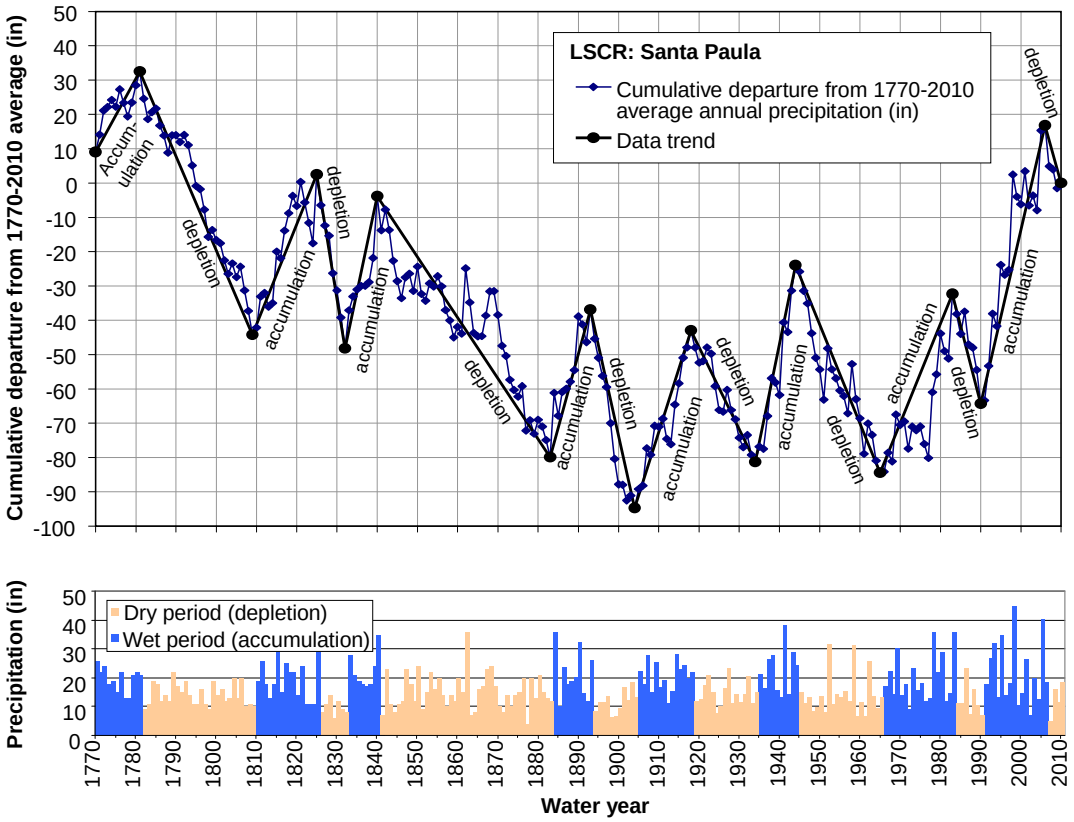

b)

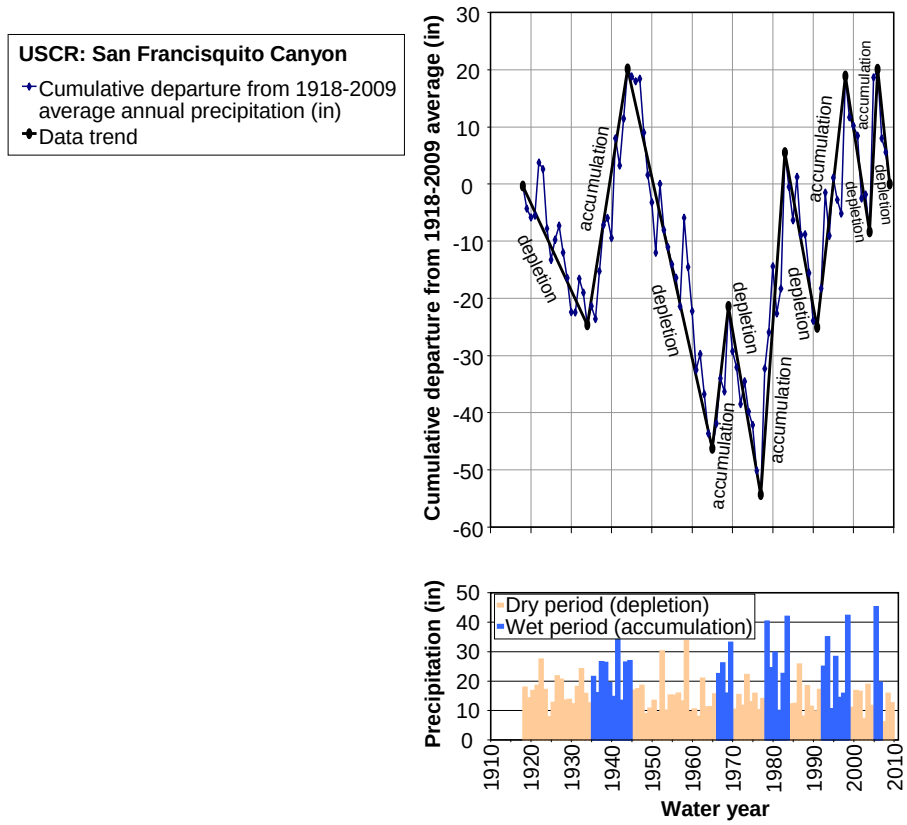

Figure A-1. Wet and dry periods at Santa Paula (a) and San Francisquito Canyon (b).

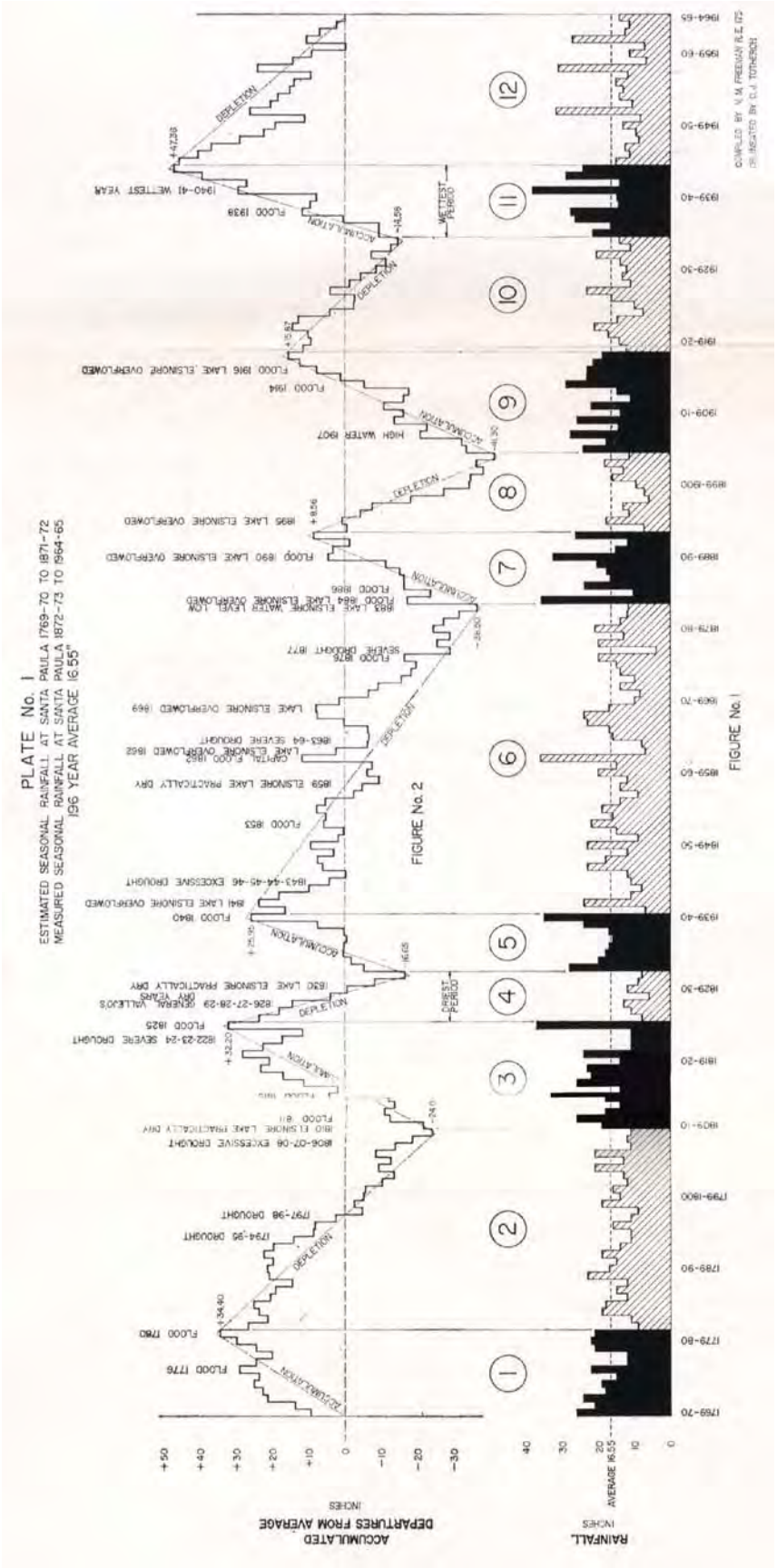

Figure A-2. Estimated and measured annual precipitation at Santa Paula 1770–1872 and 1873–1965, respectively, with delineations of periods of accumulation (wet) and depletion (dry) (from Freeman 1968, courtesy of Lorrin L. Morrison printer and publisher).

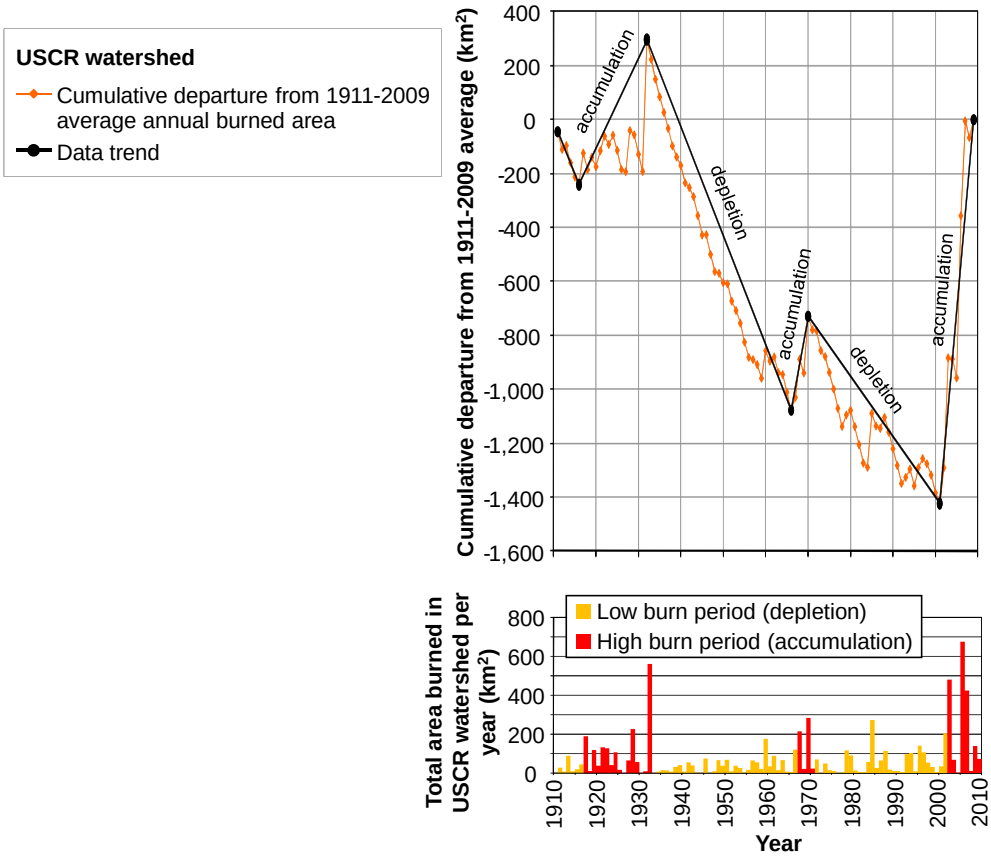

Figure A-3. High and low burn periods in the SCR watershed.

REFERENCES

Allen, A. 2010. Chief, USACE, North Coast Branch. E-mail correspondence with G. Leverich, Stillwater Sciences, providing historical aggregate mining information.

AMEC (AMEC Earth & Environmental). 2005. Santa Clara River Enhancement and Management Plan (SCREMP). Prepared by AMEC, Santa Barbara, California for VCWPD, Ventura, California, LADPW, Alhambra, California, and SCREMP Project Steering Committee.

Begnudelli, L. and B. F. Sanders. 2007. Simulation of the St. Francis Dam-break flood. Journal of Engineering Mechanics 133: 1200–1212.

California Highways. 2010. Online archives and repository of California Highways. http://www.cahighways.org/ [Accessed 15 December 2010].

CDF (California Department of Finance). 2010a. Historical Census Populations of Places, Towns, and Cities in California, 1850-2000. Website: http://www.dof.ca.gov/research/demographic/reports/census-surveys/historical_1850-2000/ [Accessed 15 December 2010].

CDF. 2010b. E-4 Population Estimates for Cities, Counties and the State, 2001-2010, with 2000 Benchmark. Sacramento, California. May. Website: http://www.dof.ca.gov/research/demographic/reports/estimates/e-4/2001-09/ [Accessed 15 December 2010].

CDF. 2010c. Population totals by township and place for California counties: 1860 - 1950: Table 57. Ventura County. Website: http://www.dof.ca.gov/research/demographic/reports/census-surveys/totals_1860-1950/documents/Pop-Twnshp-Ventura_County.xls [Accessed 15 December 2010].

CDF). 2010d. Population totals by township and place for California counties: 1860 - 1950: Table 20. Los Angeles County. Website: http://www.dof.ca.gov/research/demographic/reports/census-surveys/totals_1860-1950/documents/Pop-Twnshp-Los_Angeles_County.xls [Accessed 15 December 2010].

CDF FRAP (California Department of Forestry and Fire, Fire and Resource Assessment Program). 2010. Statewide fire history electronic database. Website. http://frap.cdf.ca.gov/data/frapgisdata/download.asp?rec=fire [Accessed 25 May 2010].

CDWR (California Department of Water Resources). 2004. California's groundwater, Bulletin 188: Acton Valley groundwater basin. http://www.dpla2.water.ca.gov/publications/groundwater/bulletin118/basins/pdfs_desc/4-5.pdf [Accessed 30 August 2010].

CDWR. 2006. California's groundwater, Bulletin 188: Santa Clara River Valley groundwater basin, Santa Clara River Valley east subbasin. http://www.water.ca.gov/pubs/groundwater/bulletin_118/basindescriptions/4-4.07.pdf [Accessed 30 August 2010].

City of Acton. 2010. Acton, California. Website: http://www.cityofacton.org/ [Accessed 26 August 2010].

CLWA (Castaic Lake Water Agency). 2003. Groundwater management plan, Santa Clara River Valley groundwater basin, east subbasin, Los Angeles, California. Prepared by Luhdorff & Scalmanini, Woodland, California for CLWA, Santa Clarita, California.

CNRA (California Natural Resources Agency). 2010. Statewide general plan map for California, GIS database. Prepared by the University of California at Davis.

County of Ventura. 2008. Ventura County General Plan, Land Use Appendix. Prepared by the County of Ventura, Resource Management Agency, Planning Division, Ventura, California. http://www.ventura.org/rma/planning/pdf/plans/GP_Land_Use_12-16-08.pdf [Accessed 15 December 2010].

Earle, D. 2003. Mining and ranching in Soledad Canyon and Antelope Valley. Online archives and repository of the Santa Clarita Valley Historical Society, Santa Clarita, California. http://www.scvhistory.com/scvhistory/earle-mining-0103.htm [Accessed 30 August 2010].

Engstrom, W. N. 1995. The California storm of January 1862. Quaternary Research 46: 141–148.

Fox Canyon GMA (Fox Canyon Groundwater Management Agency). 2007. 2007 update to the Fox Canyon Groundwater Management Agency Groundwater Management Plan. Prepared by Fox Canyon GMA, United Water Conservation District, and Callegues Municipal Water District.

Freeman, V. M. 1968. People-land-water: Santa Clara Valley and Oxnard Plain, Ventura County, California. Lorrin L. Morrison, Los Angeles.

Hamilton, J. 1999. Newhall County Water District: an historical perspective. Online archives and repository of the Santa Clarita Valley Historical Society, Santa Clarita, California. http://www.scvhistory.com/scvhistory/ncwd.html [Accessed 30 August 2010].

Joseph, S. E., R. V. Miller, S. S. Tan, and R. W. Goodman. 1987. Mineral land classification of the greater Los Angeles area: classification of sand and gravel resource areas, Saugus-Newhall Production-Consumption Region, and Palmdale Production-Consumption Region. California Division of Mines and Geology, Special Report 143, Part V.

Kennedy/Jenks (Kennedy/Jenks Consultants). 2008. Upper Santa Clara River Integrated Regional Water Management Plan (IRWMP).

LACDRP (Los Angeles County Department of Regional Planning). 2009. Draft Santa Clarita Valley area plan: one valley one vision. http://planning.lacounty.gov/ovov.

Lynch, H. B. 1931. Rainfall and stream run-off in southern California since 1769. Prepared for the Metropolitan Water District of Southern California, Los Angeles, CA.

Manzer, D. 2006. Evolution of the local rancho. Online archives and repository of the Gazette, Santa Clarita, California. http://www.oldtownnewhall.com/gazette/gazette1202-manzer.htm [Accessed 30 August 2010].

NCWD (Newhall County Water District). 2010. Online history. http://www.ncwd.org/history.htm [Accessed 30 August 2010].

NWS CPC (National Weather Service Climate Prediction Center). 2010. Cold and warm episodes by season. Website: http://www.cpc.ncep.noaa.gov/products/analysis_monitoring/ensostuff/ensoyears.shtml [Accessed 30 August 2010].

Paulson, R. W., E. B. Chase, R. S. Roberts, and D. W. Moody. 1991. National water summary 1988–1989.

Schwartzberg, B. and P. Moore. 1995. A history of the Santa Clara River, Santa Clara River enhancement and management plan.

Slade, R. C. 1990. Assessment of hydrogeologic conditions within alluvial and stream terrace deposits, Acton area, Los Angeles County. Prepared for County of Los Angeles, Department of Public Works, and ASL Consulting Engineers.

Slade, R. C. and Associates. 2002. Hydrogeologic conditions in the alluvial and Saugus Formation aquifer systems. Volume I. Prepared for Santa Clarita Valley Water Purveyors.

Stillwater Sciences. 2007. Santa Clara River Parkway floodplain restoration feasibility study: assessment of geomorphic processes for the Santa Clara River watershed, Ventura and Los Angeles counties, California. Prepared by Stillwater Sciences, Berkeley, California for the California State Coastal Conservancy, Oakland, California.

Stillwater Sciences. 2010. Sespe Creek hydrology, hydraulics, and sedimentation analysis: watershed assessment of hillslope and river geomorphic processes. Final Report. Prepared by Stillwater Sciences, Berkeley, California for Ventura County Watershed Protection District, Ventura, California.

Stillwater Sciences. 2011. Assessment of geomorphic processes for the upper Santa Clara River watershed, Los Angeles County, California. Final report. Prepared by Stillwater Sciences, Berkeley, California for Ventura County Watershed Protection District, Los Angeles County Department of Public Works, and the U.S. Army Corps of Engineers-L.A. District.

U.S. Census Bureau. 1952. Census of population: 1950, volume II: characteristics of the population, part 5: California. http://www2.census.gov/prod2/decennial/documents/37778768v2p5ch2.pdf [Accessed 26 August 2010].

U.S. Census Bureau. 1962. U.S. census of population and housing: 1960. Census tracts. Final report PHC(1)-82. U.S. Government Printing Office, Washington, D. C. http://www.census.gov/prod/www/abs/decennial/1960.html [Accessed 15 December 2010]

U.S. Census Bureau. 1973. U.S. census of population and housing: 1970, volume 1: characteristics of the population, part 6: California, section 1. http://www2.census.gov/prod2/decennial/documents/1970a_ca1-01.pdf [Accessed 15 December 2010].

U.S. Census Bureau. 1982. 1980 census of population, volume 1: characteristics of the population, chapter A: number of inhabitants, part 6: California. Website: http://www.census.gov/prod/www/abs/decennial/1980cenpopv1.html [Accessed 26 August 2010].

UWCD (United Water Conservation District). 2007. Water Management Plan, summary report. Report No. UWCD-RP-2007-01, version 1.0.

Worden, L. 1995. Prime Valencia real estate, $2 an acre. Online archives and repository of the Santa Clarita Valley Historical Society, Santa Clarita, California. http://www.scvhistory.com/scvhistory/signal/worden/lw060795.htm [Accessed 30 August 2010].

Appendix B

Debris Basin and Reservoir Sedimentation Records

DEBRIS BASIN AND RESERVOIR SEDIMENTATION RECORDS

This appendix provides the source data of sedimentation rates recorded in Ventura County Watershed Protection District (VCWPD) and Los Angeles County Department of Public Works (LADPW) operated debris basins in the SCR watershed, Los Angeles County Department of Water and Power (LADWP) operated debris basins at Castaic Powerplant, and Lake Piru and Bouquet Canyon reservoirs. All data were provided to us in 2010 and represent the most current information available. Data from the VCWPD debris basins for records up through WY 2005 were based on information published by VCWPD in their Debris and Detention Basins report (2005) (re-presented here as Figures B-1 through B-8). More recent cleanout data from WY 2005–2008 were provided by Dr. Yunsheng Su, engineer with VCWPD (Table B-1). Data from the LADPW debris basins were provided by Mr. Martin Araiza, engineer with LADPW (Table B-2). Data from the LADWP Castaic Powerplant debris basins were provided by Ms. Gloria Wu, technical staff member with LADWP (Table B-3). Finally, data from Lake Piru and Bouquet Canyon reservoirs were provided by WICP ACWI (2010) (Figures B-9 and B-10).

These sedimentation data were used in our analysis of sediment yields in the SCR watershed (see Section 3.3.2 of the main report), with the exception of debris basins "Franklin Barranca", "Knoll" and "Line 'A'" which were not used because their periods of record were less than one year. The sedimentation data from Lake Piru and Bouquet Canyon reservoirs were subsequently refined by Minear and Kondolf (2009) in order to better account for reservoir trapping efficiencies and more appropriate sediment density conversions.

The locations of the debris basins and reservoir structures are shown in Figure 3-6 of the main report. Additional information on the VCWPD and LADPW debris basins is provided in VCWPD 2005 and LADPW 2006, respectively.

VCWPD- Zone 2 ***Debris and Detention Basins***

EXPECTED DEBRIS PRODUCTION (cy):		
Storm Frequency	**Design Condition**	**100% Burn**
100-YEAR	149,000	221,650
50-YEAR	114,320	168,960
25-YEAR	50,410	74,500

BASIN HISTORY: **ADAMS BARRANCA DEBRIS BASIN**

DATE	ACTION	REMAINING CAPACITY (cy)	REMOVED (cy)	AADP* (cy)
09-94	Aerial Survey	84,200		
01-95	Disaster Declaration			5,940
06-95	Aerial Survey	24,200		
12-95	Cleanout		61,505	
12-95	Aerial Survey	85,705		
07-96	Aerial Survey	Not Digitized		
07-97	Aerial Survey	78,080		
02-98	Disaster Declaration			3,510
07-98	Aerial Survey	4,330		
12-98	Cleanout		75,806	
12-98	Aerial Survey	80,135		
05-99	Cleanout		56	
12-99	Aerial survey	Not Digitized		
08-01	Aerial survey	Not Digitized		
11-02	Cleanout		448	
12-02	Aerial survey	Not Digitized		
11-03	Aerial survey	Not Digitized		
01-05	Disaster Declaration			982
07-05	Cleanout		112,089	

NOTES
* AADP (Average Annual Debris Production) Computed Excluding Disaster Debris
NA= Not Available / Not Applicable

Figure B-1. Sedimentation records of the VCWPD-operated Adams Barranca debris basin located in the LSCR watershed (reprinted from VCWPD 2005).

VCWPD- Zone 2 ***Debris and Detention Basins***

EXPECTED DEBRIS PRODUCTION (cy); Sexton Canyon Only, Assumes Lake Canyon Dam in Place		
Storm Frequency	**Design Condition**	**100% Burn**
100-YEAR	22,576	32,745
50-YEAR	17,259	25,033
25-YEAR	12,403	17,990

Designed to be in series with Lake Canyon Dam (not yet constructed) to operate as intended; (Elevations NGVD29)

BASIN HISTORY: **ARUNDELL BARRANCA DETENTION BASIN**

DATE	ACTION	REMAINING CAPACITY (cy)	REMOVED (cy)	AADP* (cy)
01-96	New Dam Completed			5,308**
01-96	Aerial Survey	64,800		
06-96	Aerial Survey	49,523		
07-96	Aerial Survey	Not Digitized		
07-97	Aerial Survey	48,420		
02-98	Disaster Declaration			5,308
07-98	Aerial Survey	45,570		
05-99	Cleanout		101,450	
05-99	Aerial Survey	64,800		
12-99	Aerial Survey	Not Digitized		
08-01	Aerial Survey	Not Digitized		
12-02	Aerial Survey	Not Digitized		
11-03	Aerial Survey	Not Digitized		
01-05	Disaster Declaration			6,419
	OLD BASIN DATA DB2-06			
02-69	Disaster Declaration			
10-70	Aerial Survey	36,100		
09-71	Cleanout		20,000	
01-72	Aerial Survey	35,900		
07-72	Cleanout		4,100	
05-73	Aerial Survey	26,225		
09-73	Cleanout		15,400	
11-73	Aerial Survey	39,650		
06-74	Aerial Survey	33,200		
10-75	Aerial Survey	25,606		
10-76	Aerial Survey	21,900		

Page 49

Figure B-2a. Sedimentation records of the VCWPD-operated Arrundell Barranca debris basin located in the LSCR watershed (Page 1 of 2; reprinted from VCWPD 2005).

VCWPD- Zone 2 ***Debris and Detention Basins***

BASIN HISTORY: **ARUNDELL BARRANCA DETENTION BASIN**

DATE	ACTION	REMAINING CAPACITY (cy)	REMOVED (cy)	AADP* (cy)
12-77	Aerial Survey	18,600		
03-78	Disaster Declaration			
11-78	Aerial Survey	3,905		
05-79	Cleanout		19,100	
06-79	Aerial Survey	20,100		
02-80	Disaster Declaration			5,643**
06-80	Aerial Survey	2,610		
12-80	Cleanout		21,000	
11-82	Aerial Survey	16,400		
03-83	Disaster Declaration			4,882**
04-83	Aerial Survey	8,960		
12-85	Cleanout		61,000	
12-85	Aerial Survey	58,380		
11-87	Aerial Survey	53,899		
02-89	Cleanout		4,200	
10-89	Aerial Survey	58,115		
03-90	Cleanout		5,000	5,260
10-90	Aerial Survey	64,800		
06-91	Aerial Survey	36,300		
12-91	Cleanout		36,000	
12-91	Aerial Survey	64,900		
02-92	Disaster Declaration			5,403**
05-92	Aerial Survey	37,400		
05-92	Cleanout		30,700	
12-92	Aerial Survey	68,100		
07-93	Aerial Survey	31,700		
01-94	Cleanout		33,800	
01-94	Aerial Survey	65,500		
01-95	Disaster Declaration			5,308
03-95	Disaster Declaration			5,308
05-95	Aerial Survey	Not Digitized		
06-95	Cleanout & Excavation		76,334	
06-95	Aerial Survey	76,330		
01-96	**New Dam Completed**			

Notes

* AADP (Average Annual Debris Production) Computed Excluding Disaster Debris

** From historical record of DB2-06

NA= Not Available / Not Applicable

Page 50

Figure B-2b. Sedimentation records of the VCWPD-operated Arrundell Barranca debris basin located in the LSCR watershed (Page 2 of 2; reprinted from VCWPD 2005).

VCWPD- Zone 2 ***Debris and Detention Basins***

EXPECTED DEBRIS PRODUCTION (cy):		
StormFrequency	DesignCondition	100% Burn
100-YEAR	13,413	19,456
50-YEAR	7,062	10,244
25-YEAR	4,992	7,238

BASIN HISTORY: **CAVIN ROAD DEBRIS BASIN**

DATE	ACTION	REMAINING CAPACITY (cy)	REMOVED (cy)	AADP* (cy)
02-69	Disaster Declaration			
10-71	Aerial Survey	7,379		
03-78	Disaster Declaration			
10-81	Aerial Survey	Not Digitized		
03-83	Disaster Declaration			
04-83	Aerial Survey	2,886		
04-84	Cleanout		5,640	470**
09-84	Aerial Survey	8,690		
12-85	Aerial Survey	8,681		
07-86	Aerial Survey	8,540		
11-87	Aerial Survey	8,716		
11-88	Aerial Survey	Not Digitized		
09-90	Aerial Survey	Not Digitized		
05-91	Aerial Survey	7,339		
02-92	Disaster Declaration			362**
05-92	Aerial Survey	Not Digitized		
06-92	Cleanout		4,283	
01-95	Disaster Declaration			
07-96	Aerial Survey	Not Digitized		
05-97	Aerial Survey	8,841		
07-97	Aerial Survey	Not Digitized		
02-98	Disaster Declaration			362
07-98	Aerial Survey	4,100		
12-99	Aerial Survey	Not Digitized		
08-01	Aerial Survey	Not Digitized		
12-02	Aerial Survey	Not Digitized		
11-03	Aerial Survey	Not Digitized		
11-03	Cleanout		1,736	
12-04	Cleanout		458	
01-05	Disaster Declaration			209

Notes

* AADP (Average Annual Debris Production) Computed Excluding Disaster Debris

** FEMA Accepted Value for Disaster Declaration

*** Theoretical Value from Kevin Scott Formula

NA= Not Available / Not Applicable

Page 56

Figure B-3. Sedimentation records of the VCWPD-operated Cavin Road debris basin located in the LSCR watershed (reprinted from VCWPD 2005).

VCWPD- Zone 2 ***Debris and Detention Basins***

EXPECTED DEBRIS PRODUCTION (cy):		
Storm Frequency	Design Condition	100% Burn
100-YEAR	104,600	154,000
50-YEAR	79,300	116,750
10-YEAR	21,300	31,400

BASIN HISTORY: **FAGAN CANYON DEBRIS BASIN**

DATE	ACTION	REMAINING CAPACITY (cy)	REMOVED (cy)	AADP* (cy)
08-94	Basin Constructed			
09-94	Aerial Survey	88,400		
01-95	Cleanout		128	
01-95	Disaster Declaration			5,874
06-95	Aerial Survey	42,100		
10-95	Cleanout		42,950	
12-95	Aerial Survey	84,950		
07-96	Aerial Survey	Not Digitized		
07-97	Aerial Survey	81,470		
02-98	Disaster Declaration			2,203
07-98	Aerial Survey	38,170		
12-98	Cleanout		48,460	
12-98	Aerial Survey	86,630		
12-99	Aerial Survey	Not Digitized		
08-01	Aerial Survey	Not Digitized		
12-02	Aerial Survey	Not Digitized		
11-03	Aerial Survey	Not Digitized		
02-04	Cleanout		582	
01-05	Disaster Declaration			2,200
07-05	Cleanout		53,812-Survey	

Notes

* AADP (Average Annual Debris Production) Computed Excluding Disaster Debris

NA= Not Available / Not Applicable

Page 61

Figure B-4. Sedimentation records of the VCWPD-operated Fagan Canyon debris basin located in the LSCR watershed (reprinted from VCWPD 2005).

VCWPD- Zone 2 **Debris and Detention Basins**

EXPECTED DEBRIS PRODUCTION (cy):		
Storm Frequency	Design Condition	100% Burn
100-YEAR	11,507	16,685
50-YEAR	8,856	12,845
25-YEAR	6,247	9,058

BASIN HISTORY: **FRANKLIN BARRANCA DEBRIS BASIN**

DATE	ACTION	REMAINING CAPACITY (cy)	REMOVED (cy)	AADP* (cy)
02-69	Disaster Declaration			
01-70	Aerial Survey	Not Digitized		
02-70	Aerial Survey	8,328		
11-70	Aerial Survey	8,128		
05-71	Aerial Survey	7,422		
05-72	Aerial Survey	Not Digitized		
05-73	Aerial Survey	Not Digitized		
03-78	Disaster Declaration			
06-78	Aerial Survey	1,402		
10-81	Aerial Survey	Not Digitized		
03-83	Disaster Declaration			890***
10-90	Aerial Survey	Not Digitized		
06-91	Aerial Survey	Not Digitized		
02-92	Disaster Declaration			890
05-92	Aerial Survey	Not Digitized		
01-95	Disaster Declaration			890
05-96	Outlet repaired/modified			
02-98	Disaster Declaration			890
01-05	Disaster Declaration			

Notes
* AADP (Average Annual Debris Production) Computed Excluding Disaster Debris
*** Theoretical Value from Kevin Scott Formula
NA= Not Available / Not Applicable

Page 66

Figure B-5. Sedimentation records of the VCWPD-operated Franklin Barranca debris basin located in the LSCR watershed (reprinted from VCWPD 2005).

VCWPD- Zone 2 **Debris and Detention Basins**

EXPECTED DEBRIS PRODUCTION (cy):		
Storm Frequency	Design Condition	100% Burn
100-YEAR	55,800	80,100
50-YEAR	42,000	60,400
25-YEAR	29,900	43,000

BASIN HISTORY: **JEPSON WASH DEBRIS BASIN**

DATE	ACTION	REMAINING CAPACITY (cy)	REMOVED (cy)	AADP* (cy)
02-69	Disaster Declaration			
09-69	Cleanout		41,000	
02-70	Aerial Survey	43,088		
11-70	Aerial Survey	Not Digitized		
11-70	Aerial Survey	42,074		
12-70	Aerial Survey	40,337		
05-71	Aerial Survey	33,751		
08-71	Cleanout		1,800	
10-71	Aerial Survey	36,499		
01-72	Aerial Survey	33,101		
10-72	Cleanout		9,100	
11-72	Aerial Survey	42,059		
05-73	Aerial Survey	22,798		
08-73	Cleanout		27,000	
11-73	Aerial Survey	49,371		
06-74	Aerial Survey	43,204		
06-75	Aerial Survey	37,082		
10-75	Aerial Survey	38,460		
09-76	Cleanout		5,000	
10-76	Aerial Survey	44,087		
07-77	Cleanout		1,700	
12-77	Aerial Survey	44,174		
01-78	Aerial Survey	Not Digitized		
03-78	Disaster Declaration			
06-78	Aerial Survey	11,137		
10-78	Cleanout		33,400	
10-78	Aerial Survey	45,582		
11-78	Aerial Survey	Not Digitized		
06-80	Aerial Survey	13,520		
02-80	Disaster Declaration			
12-80	Cleanout		41,720	

Page 71

Figure B-6a. Sedimentation records of the VCWPD-operated Jepson Wash debris basin located in the LSCR watershed (Page 1 of 3; reprinted from VCWPD 2005).

VCWPD- Zone 2 **Debris and Detention Basins**

BASIN HISTORY: **JEPSON WASH DEBRIS BASIN**

DATE	ACTION	REMAINING CAPACITY (cy)	REMOVED (cy)	AADP* (cy)
12-80	Aerial Survey	53,010		6,664**
10-81	Aerial Survey	Not Digitized		
11-82	Aerial Survey	49,810		
03-83	Disaster Declaration			5,880**
04-83	Aerial Survey	17,781		
02-84	1st Cleanout		26,000	
02-84	Aerial Survey	43,803		
03-84	2nd Cleanout		7,400	
03-84	Aerial Survey	51,178		
07-85	Cleanout		4,291	
12-85	Aerial Survey	53,198		
07-86	Aerial Survey	39,955		
10-86	Cleanout		15,654	
10-86	Aerial Survey	55,027		
10-87	Aerial Survey	54,700		
10-88	Aerial Survey	Not Digitized		
10-89	Aerial Survey	53,858		4,034
09-90	Aerial Survey	Not Digitized		
05-91	Aerial Survey	49,865		4,031
02-92	Disaster Declaration			3,953**
05-92	Aerial Survey	38,880		
11-92	Cleanout		15,867	
11-92	Aerial Survey	54,750		
07-93	Aerial Survey	26,400		
10-93	Cleanout		28,700	
01-94	Aerial Survey	55,100		
01-95	Disaster Declaration			4,355
06-95	Aerial Survey	21,350		
09-95	Cleanout		33,250	
12-95	Aerial Survey	54,750		
07-96	Aerial Survey	Not Digitized		
08-96	Cleanout		3,540	
07-97	Aerial Survey	43,660		
02-98	Disaster Declaration			4,239
03-98	Field Survey	18,800		
07-98	Aerial Survey	16,400		
12-98	Cleanout		37,580	
12-98	Aerial Survey	53,980		
12-99	Aerial Survey	Not Digitized		

Page 72

Figure B-6b. Sedimentation records of the VCWPD-operated Jepson Wash debris basin located in the LSCR watershed (Page 2 of 3; reprinted from VCWPD 2005).

VCWPD- Zone 2 ***Debris and Detention Basins***

BASIN HISTORY: **JEPSON WASH DEBRIS BASIN**

DATE	ACTION	REMAINING CAPACITY (cy)	REMOVED (cy)	AADP* (cy)
08-01	Aerial Survey	Not Digitized		
12-02	Aerial Survey	Not Digitized		
11-03	Aerial Survey	Not Digitized		
02-04	Cleanout		872	
08-04	Cleanout		6,768	
01-05	Disaster Declaration			3,556
07-05	Cleanout		42,918	
07-05	Cleanout		14,034-Survey	

Notes

* AADP (Average Annual Debris Production) Computed Excluding Disaster Debris

** FEMA Accepted Value for Disaster Declaration

NA= Not Available / Not Applicable

Page 73

Figure B-6c. Sedimentation records of the VCWPD-operated Jepson Wash debris basin located in the LSCR watershed (Page 3 of 3; reprinted from VCWPD 2005).

VCWPD- Zone 2 ***Debris and Detention Basins***

EXPECTED DEBRIS PRODUCTION (cy):		
Storm Frequency	Design Condition	100% Burn
100-YEAR	11,500	16,400
50-YEAR	8,500	12,200
25-YEAR	6,000	8,600

BASIN HISTORY: **REAL WASH DEBRIS BASIN**

DATE	ACTION	REMAINING CAPACITY (cy)	REMOVED (cy)	AADP* (cy)
10-67	Aerial Survey	Not Digitized		
02-69	Disaster Declaration			
09-69	Cleanout		19,300	
01-70	Aerial Survey	Not Digitized		
11-70	Aerial Survey	19,878		
12-70	Aerial Survey	17,175		
05-71	Aerial Survey	15,503		
05-72	Aerial Survey	11,875		
08-72	Cleanout		6,000	
11-72	Aerial Survey	19,926		
05-73	Aerial Survey	14,499		
09-73	Cleanout		6,500	
11-73	Aerial Survey	20,606		
06-74	Aerial Survey	19,755		
06-75	Aerial Survey	18,385		
10-75	Aerial Survey	18,260		
09-76	Cleanout		3,300	
10-76	Aerial Survey	22,251		
12-77	Aerial Survey	20,720		
01-78	Aerial Survey	Not Digitized		
03-78	Disaster Declaration			
06-78	Aerial Survey	2,276		
11-78	Cleanout		18,400	
12-78	Aerial Survey	21,187		
02-80	Disaster Declaration			
06-80	Aerial Survey	7,026		
11-80	Cleanout		17,100	2,514**
11-80	Aerial Survey	23,920		
10-81	Aerial Survey	Not Digitized		
11-82	Aerial Survey	21,315		

Page 78

Figure B-7a. Sedimentation records of the VCWPD-operated Real Wash debris basin located in the LSCR watershed (Page 1 of 3; reprinted from VCWPD 2005).

VCWPD- Zone 2 **Debris and Detention Basins**

BASIN HISTORY: **REAL WASH DEBRIS BASIN**

DATE	ACTION	REMAINING CAPACITY (cy)	REMOVED (cy)	AADP* (cy)
03-83	Disaster Declaration			
04-83	Aerial Survey	13,834		
09-84	Cleanout		25,070	2,507**
09-84	Aerial Survey	25,886		
12-85	Aerial Survey	25,947		
07-86	Aerial Survey	19,864		
10-86	Cleanout		13,500	
10-86	Aerial Survey	29,958		
12-87	Aerial Survey	29,402		
10-88	Aerial Survey	Not Digitized		
07-89	Cleanout		6,224	2,014
10-89	Aerial Survey	31,576		
09-90	Aerial Survey	Not Digitized		
05-91	Aerial Survey	26,877		
11-91	Cleanout		6,742	
11-91	Aerial Survey	32,106		
02-92	Disaster Declaration			2,573**
05-92	Aerial Survey	19,140		
11-92	Cleanout		13,500	
11-92	Aerial Survey	31,112		
06-94	Aerial Survey	11,488		
10-94	Aerial Survey	11,330		
12-94	Cleanout		23,580	
12-94	Aerial Survey	30,750		
01-95	Disaster Declaration			5,225**
02-95	Cleanout		22,160	
05-95	Aerial Survey	3,000		
12-95	Cleanout		28,250	
12-95	Aerial Survey	31,250		
07-96	Aerial Survey			
08-96	Aerial Survey	11,050		
01-97	Field Survey	2,950		
01-97	Cleanout		19,580	
04-97	Aerial Survey	22,530		
07-97	Aerial Survey	Not Digitized		
02-98	Disaster Declaration			3,709***
03-98	Field Survey	5,240		
06-98	Cleanout		25,470	
06-98	Aerial Survey	28,150		

Page 79

Figure B-7b. Sedimentation records of the VCWPD-operated Real Wash debris basin located in the LSCR watershed (Page 2 of 3; reprinted from VCWPD 2005).

VCWPD- Zone 2 ***Debris and Detention Basins***

BASIN HISTORY: **REAL WASH DEBRIS BASIN**

DATE	ACTION	REMAINING CAPACITY (cy)	REMOVED (cy)	AADP* (cy)
12-99	Aerial Survey	Not Digitized		
09-00	Cleanout		1,300	
08-01	Aerial Survey	Not Digitized		
10-02	Cleanout		8,916	
12-02	Aerial Survey	Not Digitized		
08-03	Cleanout		152	
09-03	Cleanout		5,962	
11-03	Aerial Survey	Not Digitized		
08-04	Cleanout		3,864	
09-04	Cleanout		5,177	
01-05	Disaster Declaration			4,124
07-05	Cleanout		**44,674**	
07-05	Cleanout		**2,644- Survey**	

Notes

* AADP (Average Annual Debris Production) Computed Excluding Disaster Debris

** FEMA Accepted Value for Disaster Declaration

*** Theoretical Value from Kevin Scott Formula

NA= Not Available / Not Applicable

Page 80

Figure B-7c. Sedimentation records of the VCWPD-operated Real Wash debris basin located in the LSCR watershed (Page 3 of 3; reprinted from VCWPD 2005).

VCWPD- Zone 2 **Debris and Detention Basins**

EXPECTED DEBRIS PRODUCTION (cy):		
Storm Frequency	Design Condition	100% Burn
100-YEAR	52,400	75,000
50-YEAR	38,800	55,600
25-YEAR	27,200	39,000

BASIN HISTORY: **WARRING CANYON DEBRIS BASIN**

DATE	ACTION	REMAINING CAPACITY (cy)	REMOVED (cy)	AADP* (cy)
10-67	Aerial Survey	Not Digitized		
02-69	Disaster Declaration			
06-6	Cleanout		27,100	
01-70	Cleanout		18,000	
02-70	Aerial Survey	Not Digitized		
10-70	Cleanout		11,300	
11-70	Aerial Survey	36,054		
12-70	Aerial Survey	32,054		
05-71	Cleanout		125	
05-71	Aerial Survey	32,174		
01-72	Aerial Survey	28,000		
09-72	Cleanout		9,400	
11-72	Aerial Survey	37,300		
05-73	Aerial Survey	23,406		
09-73	Cleanout		14,200	
10-73	Aerial Survey	37,034		
06-74	Aerial Survey	35,969		
10-75	Aerial Survey	33,247		
10-76	Cleanout		6,250	
10-76	Aerial Survey	39,288		
12-77	Aerial Survey	35,046		
01-78	Aerial Survey	Not Digitized		
03-78	Disaster Declaration			
06-78	Aerial Survey	3,884		
11-78	Cleanout		30,700	8,143**
11-78	Aerial Survey	34,562		
06-80	Aerial Survey	2,628		
11-80	Cleanout		27,100	8,829**
11-80	Aerial Survey	32,196		
10-81	Aerial Survey	Not Digitized		

Page 85

Figure B-8a. Sedimentation records of the VCWPD-operated Warring Canyon debris basin located in the LSCR watershed (Page 1 of 3; reprinted from VCWPD 2005).

VCWPD- Zone 2 **Debris and Detention Basins**

BASIN HISTORY: **WARRING CANYON DEBRIS BASIN**

DATE	ACTION	REMAINING CAPACITY (cy)	REMOVED (cy)	AADP* (cy)
08-82	Cleanout		7,200	
11-82	Aerial Survey	39,89		
03-83	Disaster Declaration			
04-83	Aerial Survey	16,478		
11-83	Aerial Survey	12,762		
01-84	Cleanout		24,940	
01-84	Aerial Survey	40,174		
09-84	Cleanout		12,904	
09-84	Aerial Survey	51,878		
12-85	Aerial Survey	49,922		
07-86	Aerial Survey	31,639		
10-86	Cleanout		27,036	
10-86	Aerial Survey	59,456		
10-87	Aerial Survey	Not Digitized		
12-87	Aerial Survey	53,952		
12-88	Aerial Survey	Not Digitized		
07-89	Cleanout		6,188	5,100
10-89	Aerial Survey	57,099		
09-90	Aerial Survey	58,326		
05-91	Aerial Survey	56,125		
06-91	Cleanout		5,664	
11-91	Aerial Survey	61,080		
02-92	Disaster Declaration			5,611**
05-92	Aerial Survey	30,890		
09-92	Cleanout		31,300	
09-92	Aerial Survey	62,820		
12-92	Aerial Survey	Not Digitized		
09-93	Aerial Survey	40,130		
02-94	Cleanout		22,200	
03-94	Aerial Survey	62,770		
01-95	Disaster Declaration			6,022
06-95	Aerial Survey	11,570		
11-95	Cleanout		50,650	
11-95	Aerial Survey	62,220		
07-96	Aerial Survey	Not Digitized		
07-97	Aerial Survey	52,500		
02-98	Disaster Declaration			5,049***
07-98	Aerial Survey	8,440		

Page 86

Figure B-8b. Sedimentation records of the VCWPD-operated Warring Canyon debris basin located in the LSCR watershed (Page 2 of 3; reprinted from VCWPD 2005).

VCWPD- Zone 2 **Debris and Detention Basins**

BASIN HISTORY: **WARRING CANYON DEBRIS BASIN**

DATE	ACTION	REMAINING CAPACITY (cy)	REMOVED (cy)	AADP* (cy)
12-98	Cleanout		50,244	
12-98	Aerial Survey	58,690		
12-99	Aerial Survey	Not Digitized		
08-01	Aerial Survey	Not Digitized		
12-02	Aerial Survey	Not Digitized		
04-02	Aerial Survey	53,375		
NA	Cleanout	Volume Unknown	NA	
03-03	Aerial Survey	62,314		
12-04	Cleanout		17,450	
01-05	Disaster Declaration			4,927
07-05	Cleanout		**85,687**	
07-05	Cleanout		**21,965-Survey**	

Notes

* AADP (Average Annual Debris Production) Computed Excluding Disaster Debris

** FEMA Accepted Value for Disaster Declaration

*** Theoretical Value from Kevin Scott Formula

NA= Not Available / Not Applicable

Page 87

Figure B-8c. Sedimentation records of the VCWPD-operated Warring Canyon debris basin located in the LSCR watershed (Page 3 of 3; reprinted from VCWPD 2005).

Table B-1. Sedimentation records of the VCWPD-operated debris basins located in the LSCR watershed for the period of WY 2004–2008.

Debris basin name	Volume of sediment removed, cubic yards (cubic meters)				
	WY 2004	WY 2005	WY 2006	WY 2007	WY 2008
Adams Barranca		110,227 (84,275)			30,626 (23,415)
Arundell Barranca					
Cavin Road		9,545 (9,298)			
Fagan Canyon		98,012 (74936)			
Franklin Barranca					
Jepson Wash		66,239 (50,643)			10,033 (7,671)
Real Wash		108,617 (83,044)	21,291 (16,278)	3,186 (2,436)	17,541 (13,411)
Warring Canyon	17,578 (13,439)	107,652 (82,306)	6,890 (5,268)		

Empty cells indicate no cleanout was performed.
Source: VCWPD (Y. Su, pers. comm., 2010), data presented as received with an addition of the extraction volume also reported in cubic meters per year.

Table B-2. Sedimentation records of the LADPW-operated debris basins located in the USCR watershed.

Debris basin name	Season	Water year	Cubic yards removed	Cubic meters removed
CROCKER	1982–83	1983	0.0	0.0
CROCKER	1983–84	1984	0.0	0.0
CROCKER	1984–85	1985	0.0	0.0
CROCKER	1985–86	1986	0.0	0.0
CROCKER	1986–87	1987	0.0	0.0
CROCKER	1987–88	1988	0.0	0.0
CROCKER	1988–89	1989	0.0	0.0
CROCKER	1989–90	1990	0.0	0.0
CROCKER	1990–91	1991	0.0	0.0
CROCKER	1991–92	1992	5865.0	4486.7
CROCKER	1992–93	1993	2707.0	2070.9
CROCKER	1993–94	1994	0.0	0.0
CROCKER	1994–95	1995	4864.0	3721.0
CROCKER	1995–96	1996	0.0	0.0
CROCKER	1996–97	1997	0.0	0.0
CROCKER	1997–98	1998	300.0	229.5
CROCKER	1998–99	1999	0.0	0.0
CROCKER	1999–00	2000	0.0	0.0
CROCKER	2000–01	2001	90.0	68.9
CROCKER	2001–02	2002	0.0	0.0
CROCKER	2002–03	2003	0.0	0.0
CROCKER	2003–04	2004	0.0	0.0
CROCKER	2004–05	2005	0.0	0.0

Debris basin name	Season	Water year	Cubic yards removed	Cubic meters removed
CROCKER	2005–06	2006	0.0	0.0
CROCKER	2006–07	2007	0.0	0.0
CROCKER	2007–08	2008	0.0	0.0
KNOLL	2004–05	2005	10250.0	7841.3
LINE "A"	2004–05	2005	683.0	522.5
MARSTON/PARAGON	1988–89	1989	0.0	0.0
MARSTON/PARAGON	1989–90	1990	879.0	672.4
MARSTON/PARAGON	1990–91	1991	0.0	0.0
MARSTON/PARAGON	1991–92	1992	0.0	0.0
MARSTON/PARAGON	1992–93	1993	0.0	0.0
MARSTON/PARAGON	1993–94	1994	130.0	99.5
MARSTON/PARAGON	1994–95	1995	140.0	107.1
MARSTON/PARAGON	1995–96	1996	0.0	0.0
MARSTON/PARAGON	1996–97	1997	0.0	0.0
MARSTON/PARAGON	1997–98	1998	0.0	0.0
MARSTON/PARAGON	1998–99	1999	0.0	0.0
MARSTON/PARAGON	1999–00	2000	0.0	0.0
MARSTON/PARAGON	2000–01	2001	0.0	0.0
MARSTON/PARAGON	2001–02	2002	800.0	612.0
MARSTON/PARAGON	2002–03	2003	0.0	0.0
MARSTON/PARAGON	2003–04	2004	0.0	0.0
MARSTON/PARAGON	2004–05	2005	0.0	0.0
MARSTON/PARAGON	2005–06	2006	0.0	0.0
MARSTON/PARAGON	2006–07	2007	0.0	0.0
MARSTON/PARAGON	2007–08	2008	0.0	0.0
OAKDALE	2004–05	2005	72744.0	55649.2
OAKDALE	2005–06	2006	0.0	0.0
OAKDALE	2006–07	2007	0.0	0.0
OAKDALE	2007–08	2008	0.0	0.0
OAKDALE	2008–09	2009	7600.0	5814.0
SADDLEBACK	1990–91	1991	0.0	0.0
SADDLEBACK	1991–92	1992	0.0	0.0
SADDLEBACK	1992–93	1993	20.0	15.3
SADDLEBACK	1993–94	1994	0.0	0.0
SADDLEBACK	1994–95	1995	2440.0	1866.6
SADDLEBACK	1995–96	1996	1060.0	810.9
SADDLEBACK	1996–97	1997	0.0	0.0
SADDLEBACK	1997–98	1998	0.0	0.0
SADDLEBACK	1998–99	1999	0.0	0.0
SADDLEBACK	1999–00	2000	0.0	0.0
SADDLEBACK	2000–01	2001	990.0	757.4
SADDLEBACK	2001–02	2002	0.0	0.0
SADDLEBACK	2002–03	2003	0.0	0.0
SADDLEBACK	2003–04	2004	0.0	0.0
SADDLEBACK	2004–05	2005	0.0	0.0
SADDLEBACK	2005–06	2006	0.0	0.0
SADDLEBACK	2006–07	2007	0.0	0.0
SADDLEBACK	2007–08	2008	0.0	0.0
SHADOW	1994–95	1995	0.0	0.0
SHADOW	1995–96	1996	0.0	0.0

Debris basin name	Season	Water year	Cubic yards removed	Cubic meters removed
SHADOW	1996–97	1997	0.0	0.0
SHADOW	1997–98	1998	0.0	0.0
SHADOW	1998–99	1999	0.0	0.0
SHADOW	1999–00	2000	0.0	0.0
SHADOW	2000–01	2001	0.0	0.0
SHADOW	2001–02	2002	0.0	0.0
SHADOW	2002–03	2003	5370.0	4108.1
SHADOW	2003–04	2004	0.0	0.0
SHADOW	2004–05	2005	12120.0	9271.8
VICTORIA	2002–03	2003	0.0	0.0
VICTORIA	2003–04	2004	0.0	0.0
VICTORIA	2004–05	2005	32208.0	24639.1
VICTORIA	2005–06	2006	0.0	0.0
VICTORIA	2006–07	2007	0.0	0.0
VICTORIA	2007–08	2008	0.0	0.0
VICTORIA	2008–09	2009	2670.0	2042.6
WEDGEWOOD	2001–02	2002	0.0	0.0
WEDGEWOOD	2002–03	2003	0.0	0.0
WEDGEWOOD	2003–04	2004	0.0	0.0
WEDGEWOOD	2004–05	2005	0.0	0.0
WEDGEWOOD	2004–06	2006	1611.0	1232.4
WHITNEY	2000–01	2001	0.0	0.0
WHITNEY	2001–02	2002	0.0	0.0
WHITNEY	2002–03	2003	0.0	0.0
WHITNEY	2003–04	2004	0.0	0.0
WHITNEY	2004–05	2005	1540.0	1178.1
WILDWOOD	1967–68	1968	2092.0	1600.4
WILDWOOD	1968–69	1969	15986.0	12229.3
WILDWOOD	1969–70	1970	1199.0	917.2
WILDWOOD	1970–71	1971	4830.0	3695.0
WILDWOOD	1971–72	1972	201.0	153.8
WILDWOOD	1972–73	1973	4013.0	3069.9
WILDWOOD	1973–74	1974	1422.0	1087.8
WILDWOOD	1974–75	1975	286.0	218.8
WILDWOOD	1975–76	1976	0.0	0.0
WILDWOOD	1976–77	1977	1020.0	780.3
WILDWOOD	1977–78	1978	16699.0	12774.7
WILDWOOD	1978–79	1979	4433.0	3391.2
WILDWOOD	1979–80	1980	13558.0	10371.9
WILDWOOD	1980–81	1981	933.0	713.7
WILDWOOD	1981–82	1982	549.0	420.0
WILDWOOD	1982–83	1983	5527.0	4228.2
WILDWOOD	1983–84	1984	0.0	0.0
WILDWOOD	1984–85	1985	0.0	0.0
WILDWOOD	1985–86	1986	0.0	0.0
WILDWOOD	1986–87	1987	0.0	0.0
WILDWOOD	1987–88	1988	911.0	696.9
WILDWOOD	1988–89	1989	0.0	0.0
WILDWOOD	1989–90	1990	0.0	0.0
WILDWOOD	1990–91	1991	0.0	0.0

Debris basin name	Season	Water year	Cubic yards removed	Cubic meters removed
WILDWOOD	1991–92	1992	13185.0	10086.5
WILDWOOD	1992–93	1993	4706.0	3600.1
WILDWOOD	1993–94	1994	0.0	0.0
WILDWOOD	1994–95	1995	5560.0	4253.4
WILDWOOD	1995–96	1996	0.0	0.0
WILDWOOD	1996–97	1997	0.0	0.0
WILDWOOD	1997–98	1998	13500.0	10327.5
WILDWOOD	1998–99	1999	0.0	0.0
WILDWOOD	1999–00	2000	0.0	0.0
WILDWOOD	2000–01	2001	1260.0	963.9
WILDWOOD	2001–02	2002	0.0	0.0
WILDWOOD	2002–03	2003	0.0	0.0
WILDWOOD	2003–04	2004	0.0	0.0
WILDWOOD	2004–05	2005	0.0	0.0
WILDWOOD	2005–06	2006	11983.0	9167.0
WILDWOOD	2006–07	2007	0.0	0.0
WILDWOOD	2007–08	2008	0.0	0.0
WILLAM S HART	1983–84	1984	0.0	0.0
WILLAM S HART	1984–85	1985	0.0	0.0
WILLAM S HART	1985–86	1986	321.0	245.6
WILLAM S HART	1986–87	1987	0.0	0.0
WILLAM S HART	1987–88	1988	0.0	0.0
WILLAM S HART	1988–89	1989	0.0	0.0
WILLAM S HART	1989–90	1990	0.0	0.0
WILLAM S HART	1990–91	1991	0.0	0.0
WILLAM S HART	1991–92	1992	0.0	0.0
WILLAM S HART	1992–93	1993	0.0	0.0
WILLAM S HART	1993–94	1994	0.0	0.0
WILLAM S HART	1994–95	1995	97.0	74.2
WILLAM S HART	1995–96	1996	0.0	0.0
WILLAM S HART	1996–97	1997	0.0	0.0
WILLAM S HART	1997–98	1998	0.0	0.0
WILLAM S HART	1998–99	1999	0.0	0.0
WILLAM S HART	1999–00	2000	0.0	0.0
WILLAM S HART	2000–01	2001	72.0	55.1
WILLAM S HART	2001–02	2002	0.0	0.0
WILLAM S HART	2002–03	2003	0.0	0.0
WILLAM S HART	2003–04	2004	0.0	0.0
WILLAM S HART	2004–05	2005	0.0	0.0
WILLAM S HART	2005–06	2006	0.0	0.0
WILLAM S HART	2006–07	2007	0.0	0.0
WILLAM S HART	2007–08	2008	0.0	0.0
YUCCA	1996–97	1997	0.0	0.0
YUCCA	1997–98	1998	0.0	0.0
YUCCA	1998–99	1999	0.0	0.0
YUCCA	1999–00	2000	2447.0	1872.0
YUCCA	2000–01	2001	0.0	0.0
YUCCA	2001–02	2002	0.0	0.0
YUCCA	2002–03	2003	0.0	0.0
YUCCA	2003–04	2004	0.0	0.0

Debris basin name	Season	Water year	Cubic yards removed	Cubic meters removed
YUCCA	2004–05	2005	4661.0	3565.7

Source: LADPW (M. Araiza, pers. comm., 2010), data presented as received with an addition of the extraction volume also reported in cubic meters per year.

Table B-3. Sedimentation records of the LADWP-operated debris basins located at the Castaic Powerplant.

Rainfall Year	Rainfall (inch)	FY	#	Basin 1	Basin 2	Basin 3	Below CD3	Tailrace	Reservoir	Unspecified Location	TOTAL (CY)	Comments
74-75		75-76									0	
75-76		76-77									0	
76-77		77-78									0	
77-78	25.00	78-79	1								0	
78-79	25.96	79-80	1								0	
79-80	23.27	80-81	1						326,926		326,926	
80-81	0.00	81-82	1								0	No Rainfall info
81-82	10.78	82-83	1								0	
82-83	28.28	83-84	1		95,000						95,000	
83-84	11.30	84-85	1								0	
84-85	8.92	85-86	1				20,049	232,878			252,927	
85-86	22.91	86-87	1								0	
86-87	8.23	87-88	1								0	
87-88	15.33	88-89	1							83,000	83,000	
88-89	6.31	89-90	1								0	
89-90	8.26	90-91	1								0	
90-91	15.45	91-92	1								0	
91-92	33.13	92-93	1							40,000	40,000	
92-93	45.61	93-94	1								0	
93-94	14.67	94-95	1	54,100	54,260	53,900				25,000	187,260	
94-95	45.45	95-96	1				x	x		166,450	166,450	
95-96	15.01	96-97	1	74,175	53,250	113,775					241,200	
96-97	19.84	97-98	1	44,410	12,600	0					57,010	
97-98	43.55	98-99	1	65,162	56,469	96,819					218,450	
98-99	10.98	99-00	1								0	
99-00	15.49	00-01	1								0	Rev. on 7/26/2010
00-01	22.09	01-02	1								0	
01-02	6.79	02-03	1								0	
02-03	16.06	03-04	1								0	
03-04	11.60	04-05	1								0	
04-05	55.15	05-06	1	56,500	120,325	119,225					296,050	
05-06	16.84	06-07	1					208,350		Tailbay	208,350	There is ~1M CY of sedimentation near the edge of reservoir at the conflence of Bypass Channel & Tailrace Channel
06-07	6.24		1								0	
07-08	17.75		1								0	
08-09	14.18	09-10	1	134,450	70,345	40,370					245,165	
09-10	22.43		1								0	No work plan this year

Source: LADWP (G. Wu, pers. comm., 2010), table image from original .pdf

RESERVOIR SEDIMENT
DATA SUMMARY
SCS-34 Rev. 6-66

Santa Felicia
NAME OF RESERVOIR

U. S. DEPARTMENT OF AGRICULTURE
SOIL CONSERVATION SERVICE

71-40
DATA SHEET NO.

DAM

1. OWNER United Water Consery. Dist.	2. STREAM Piru Creek	3. STATE California
4. SEC. 3 TWP. 4N RANGE 18W	5. NEAREST P.O. Piru	6. COUNTY Ventura
7. LAT. ° ' " LONG. ° ' "	8. TOP OF DAM ELEVATION 1,075	9. SPILLWAY CREST ELEV. 1,055

RESERVOIR

10. STORAGE ALLOCATION	11. ELEVATION TOP OF POOL	12. ORIGINAL SURFACE AREA, ACRES	13. ORIGINAL CAPACITY, ACRE-FEET	14. GROSS STORAGE, ACRE-FEET	15. DATE STORAGE BEGAN
a. FLOOD CONTROL					Oct. 1955
b. MULTIPLE USE					
c. POWER					16. DATE NORMAL OPER. BEGAN
d. WATER SUPPLY					
e. IRRIGATION	1,055	1,240	101,200	101,200	
f. CONSERVATION					
g. INACTIVE					

WATERSHED

17. LENGTH OF RESERVOIR 4.3 MILES		22. AV. WIDTH OF RESERVOIR	MILES
18. TOTAL DRAINAGE AREA 425 SQ. MI.		22. MEAN ANNUAL PRECIPITATION 12 to 24+	INCHES
19. NET SEDIMENT CONTRIBUTING AREA 425 SQ. MI.		23. MEAN ANNUAL RUNOFF	INCHES
20. LENGTH MILES	AV. WIDTH MILES	24. MEAN ANNUAL RUNOFF	AC.-F T.
21. MAX. ELEV. 8,831	MIN. ELEV. 870	25. ANNUAL TEMP: MEAN	RANGE

SURVEY DATA

26. DATE OF SURVEY	27. PERIOD YEARS	28. ACCL. YEARS	29. TYPE OF SURVEY	30. NO. OF RANGES OR CONTOUR INT.	31. SURFACE AREA, ACRES	32. CAPACITY, ACRE-FEET	33. C/I. RATIO, AC.-FT. PER AC.-FT.
Oct. 1955		--	--	--	1,240	101,200	
Oct. 1965	10.0	10.0	Range	15	1,240	98,730	

26. DATE OF SURVEY	34. PERIOD ANNUAL PRECIPITATION	35. PERIOD WATER INFLOW, ACRE-FEET			36. WATER INFL. TO DATE, AC.-FT.	
		a. MEAN ANNUAL	b. MAX. ANNUAL	c. PERIOD TOTAL	a. MEAN ANNUAL	b. TOTAL TO DATE

26. DATE OF SURVEY	37. PERIOD CAPACITY LOSS, ACRE-FEET			38. TOTAL SED. DEPOSITS TO DATE, ACRE-FEET		
	a. PERIOD TOTAL	b. AV. ANNUAL	c. PER SQ. MI.-YEAR	a. TOTAL TO DATE	b. AV. ANNUAL	c. PER SQ. MI.-YEAR
Oct. 1965	2,470	247	0.58	2,470	247	0.58

26. DATE OF SURVEY	39. AV. DRY WGT., LBS. PER CU. FT.	40. SED. DEP., TONS PER SQ. MI.-YR.		41. STORAGE LOSS, PCT.		42. SED. INFLOW, PPM	
		a. PERIOD	b. TOTAL TO DATE	a. AV. ANN.	b. TOT. TO DATE	a. PERIOD	b. TOT. TO DATE
Oct. 1965	52	658	658	0.24	2.44	--	--

Figure B-9a. Sedimentation record of Lake Piru Reservoir (Santa Felicia Dam). (Page 1 of 2; Source: Water Information Coordination Program, Advisory Committee on Water Information, http://ida.water.usgs.gov/ressed/datasheets/71-40.pdf)

26. DATE OF SURVEY	43. DEPTH DESIGNATION RANGE IN FEET BELOW, AND ABOVE, CREST ELEVATION											
	PERCENT OF TOTAL SEDIMENT LOCATED WITHIN DEPTH DESIGNATION											

26. DATE OF SURVEY	44. REACH DESIGNATION PERCENT OF TOTAL ORIGINAL LENGTH OF RESERVOIR													
	0-10	10-20	20-30	30-40	40-50	50-60	60-70	70-80	80-90	90-100	-105	-110	-115	-120	-125
	PERCENT OF TOTAL SEDIMENT LOCATED WITHIN REACH DESIGNATION														

45. RANGE IN RESERVOIR OPERATION

WATER YEAR	MAX. ELEV.	MIN. ELEV.	INFLOW, AC.-FT.	WATER YEAR	MAX. ELEV.	MIN. ELEV.	INFLOW, AC.-FT.

46. ELEVATION-AREA-CAPACITY DATA

ELEVATION	AREA	CAPACITY	ELEVATION	AREA	CAPACITY	ELEVATION	AREA	CAPACITY

47. REMARKS AND REFERENCES

Scott, K. M., Ritter, J. R., and Knott, J. M., 1968, Sedimentation in the Piru Creek watershed, southern California: U.S. Geol. Survey Water-Supply Paper 1798-E, 48 p.

48. AGENCY MAKING SURVEY

49. AGENCY SUPPLYING DATA U.S. Geol.Survey,Water Resources Div. 50. DATE August 1971

April 1966

Figure B-9b. Sedimentation record of Lake Piru Reservoir (Santa Felicia Dam). (Page 2 of 2; Source: Water Information Coordination Program, Advisory Committee on Water Information, http://ida.water.usgs.gov/ressed/datasheets/71-40.pdf)

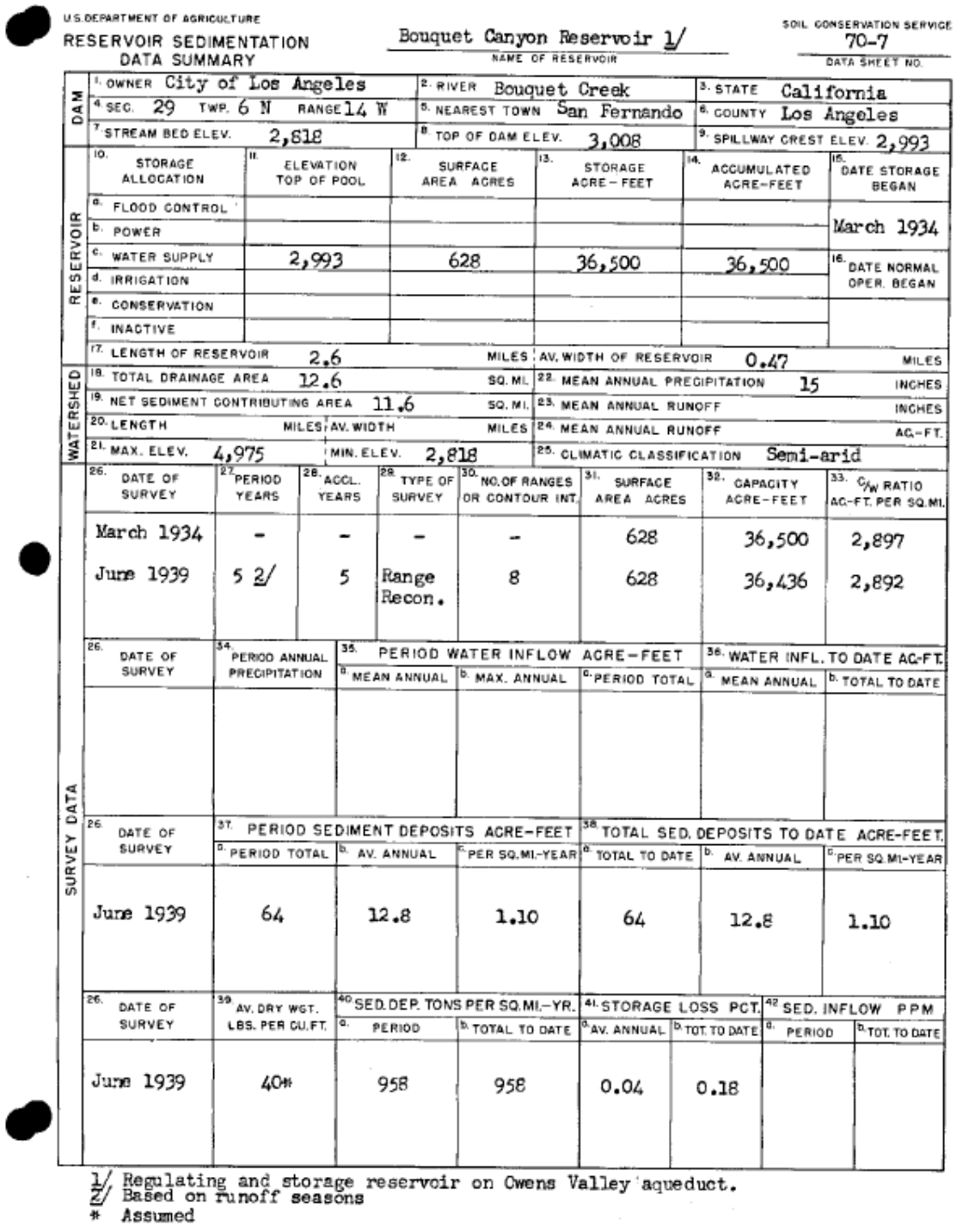

U.S. DEPARTMENT OF AGRICULTURE
SOIL CONSERVATION SERVICE

RESERVOIR SEDIMENTATION DATA SUMMARY

Bouquet Canyon Reservoir 1/ — NAME OF RESERVOIR

70-7 — DATA SHEET NO.

DAM

1. OWNER City of Los Angeles	2. RIVER Bouquet Creek	3. STATE California
4. SEC. 29 TWP. 6 N RANGE 14 W	5. NEAREST TOWN San Fernando	6. COUNTY Los Angeles
7. STREAM BED ELEV. 2,818	8. TOP OF DAM ELEV. 3,008	9. SPILLWAY CREST ELEV. 2,993

RESERVOIR

10. STORAGE ALLOCATION	11. ELEVATION TOP OF POOL	12. SURFACE AREA ACRES	13. STORAGE ACRE-FEET	14. ACCUMULATED ACRE-FEET	15. DATE STORAGE BEGAN
a. FLOOD CONTROL					
b. POWER					March 1934
c. WATER SUPPLY	2,993	628	36,500	36,500	16. DATE NORMAL OPER. BEGAN
d. IRRIGATION					
e. CONSERVATION					
f. INACTIVE					

17. LENGTH OF RESERVOIR 2.6 MILES | AV. WIDTH OF RESERVOIR 0.47 MILES

WATERSHED

18. TOTAL DRAINAGE AREA 12.6 SQ. MI.		22. MEAN ANNUAL PRECIPITATION 15	INCHES
19. NET SEDIMENT CONTRIBUTING AREA 11.6 SQ. MI.		23. MEAN ANNUAL RUNOFF	INCHES
20. LENGTH MILES	AV. WIDTH MILES	24. MEAN ANNUAL RUNOFF	AC.-FT.
21. MAX. ELEV. 4,975	MIN. ELEV. 2,818	25. CLIMATIC CLASSIFICATION Semi-arid	

SURVEY DATA

26. DATE OF SURVEY	27. PERIOD YEARS	28. ACCL. YEARS	29. TYPE OF SURVEY	30. NO. OF RANGES OR CONTOUR INT.	31. SURFACE AREA ACRES	32. CAPACITY ACRE-FEET	33. $C_{/W}$ RATIO AC.-FT. PER SQ. MI.
March 1934	-	-	-	-	628	36,500	2,897
June 1939	5 2/	5	Range Recon.	8	628	36,436	2,892

26. DATE OF SURVEY	34. PERIOD ANNUAL PRECIPITATION	35. PERIOD WATER INFLOW ACRE-FEET			36. WATER INFL. TO DATE AC-FT.	
		a. MEAN ANNUAL	b. MAX. ANNUAL	c. PERIOD TOTAL	a. MEAN ANNUAL	b. TOTAL TO DATE

26. DATE OF SURVEY	37. PERIOD SEDIMENT DEPOSITS ACRE-FEET			38. TOTAL SED. DEPOSITS TO DATE ACRE-FEET		
	a. PERIOD TOTAL	b. AV. ANNUAL	c. PER SQ. MI.-YEAR	a. TOTAL TO DATE	b. AV. ANNUAL	c. PER SQ. MI-YEAR
June 1939	64	12.8	1.10	64	12.8	1.10

26. DATE OF SURVEY	39. AV. DRY WGT. LBS. PER CU. FT.	40. SED. DEP. TONS PER SQ. MI.-YR.		41. STORAGE LOSS PCT.		42. SED. INFLOW PPM	
		a. PERIOD	b. TOTAL TO DATE	a. AV. ANNUAL	b. TOT. TO DATE	a. PERIOD	b. TOT. TO DATE
June 1939	40*	958	958	0.04	0.18		

1/ Regulating and storage reservoir on Owens Valley aqueduct.
2/ Based on runoff seasons
* Assumed

Figure B-10a. Sedimentation record of Bouquet Canyon Reservoir. (Page 1 of 2; Source: Water Information Coordination Program, Advisory Committee on Water Information, http://ida.water.usgs.gov/ressed/datasheets/70-7.pdf)

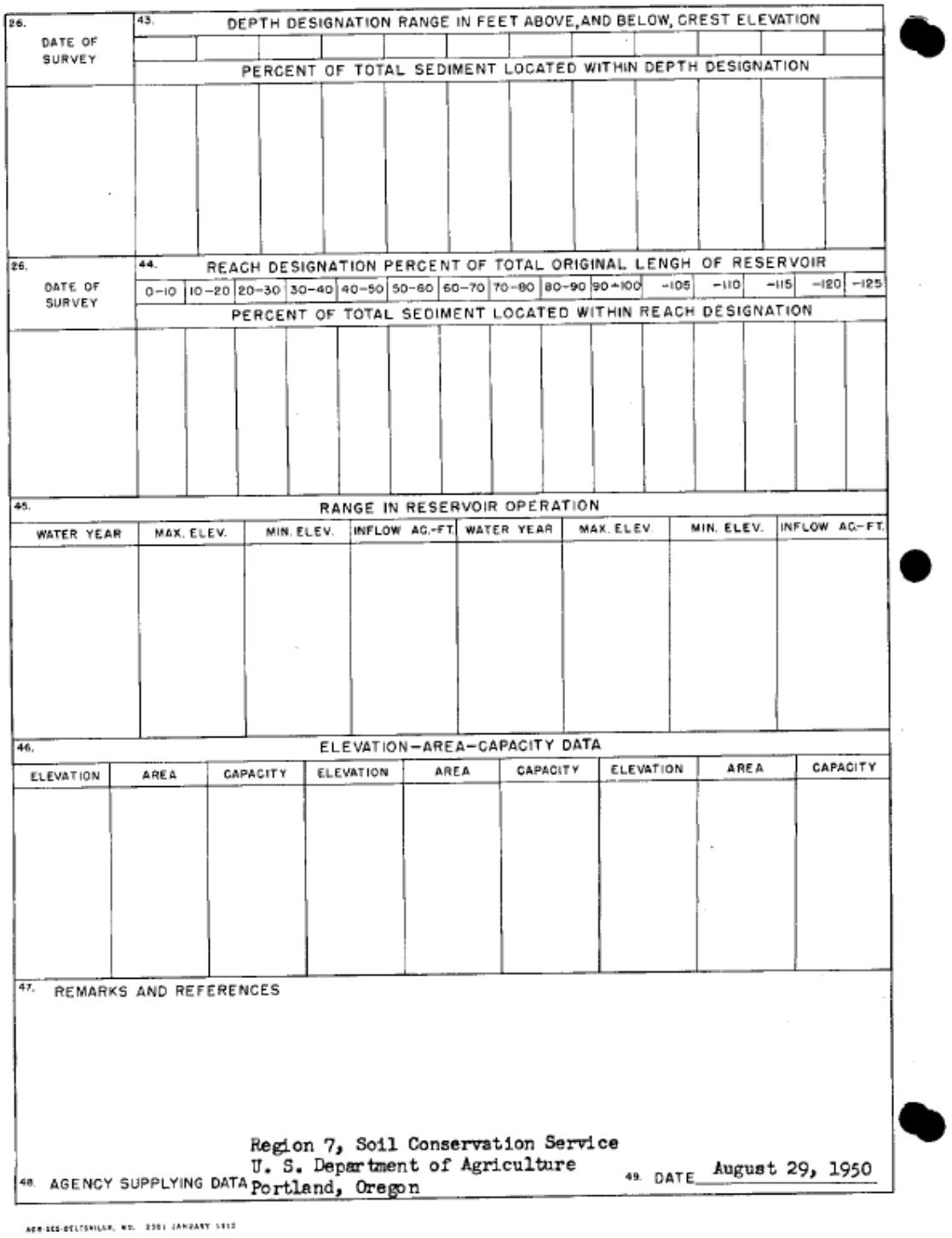

26. DATE OF SURVEY

43. DEPTH DESIGNATION RANGE IN FEET ABOVE, AND BELOW, CREST ELEVATION

PERCENT OF TOTAL SEDIMENT LOCATED WITHIN DEPTH DESIGNATION

26. DATE OF SURVEY

44. REACH DESIGNATION PERCENT OF TOTAL ORIGINAL LENGH OF RESERVOIR

0-10	10-20	20-30	30-40	40-50	50-60	60-70	70-80	80-90	90-100	-105	-110	-115	-120	-125

PERCENT OF TOTAL SEDIMENT LOCATED WITHIN REACH DESIGNATION

45. RANGE IN RESERVOIR OPERATION

WATER YEAR	MAX. ELEV.	MIN. ELEV.	INFLOW AC.-FT.	WATER YEAR	MAX. ELEV.	MIN. ELEV.	INFLOW AC.-FT.

46. ELEVATION-AREA-CAPACITY DATA

ELEVATION	AREA	CAPACITY	ELEVATION	AREA	CAPACITY	ELEVATION	AREA	CAPACITY

47. REMARKS AND REFERENCES

48. AGENCY SUPPLYING DATA Region 7, Soil Conservation Service
U. S. Department of Agriculture
Portland, Oregon

49. DATE August 29, 1950

Figure B-10b. Sedimentation record of Bouquet Canyon Reservoir. (Page 2 of 2; Source: Water Information Coordination Program, Advisory Committee on Water Information, http://ida.water.usgs.gov/ressed/datasheets/70-7.pdf)

REFERENCES

Araiza, M. 2010. Engineer, LADPW. E-mail correspondence with B. Amerson, Stillwater Sciences, providing debris basin data.

LADPW (Los Angeles County Department of Public Works). 2006. Sedimentation manual, 2nd Edition. Prepared by LADPW, Water Resources Division.

Minear, T., and G. M. Kondolf. 2009. Estimating reservoir sedimentation rates at large spatial and temporal scales: a case study of California. Water Resources Research, doi: 10.1029/2007WR006703.

Su, Y. 2010. Engineer, VCWPD. E-mail correspondence with G. Leverich, Stillwater Sciences, providing debris basin data.

VCWPD (Ventura County Watershed Protection District). 2005. Debris and detention basins. September.

WICP ACWI (Water Information Coordination Program, Advisory Committee on Water Information, Subcommittee on Sedimentation). 2010. Reservoir Sedimentation (RESSED) Database. Website. http://ida.water.usgs.gov/ressed/index.cfm [Accessed 11 Nov 2009].

Wu, G. 2010. Staff, LADWP, Power System. E-mail correspondence with G. Leverich, Stillwater Sciences, providing sedimentation records for Castaic Powerplant debris basins.

Appendix C

Methods for Assessing Planform Channel Dynamics of the Santa Clara River

INTRODUCTION

This appendix briefly summarizes the methods employed in the aerial photograph analyses of the LSCR and USCR watersheds. The combined results of these two analyses are presented in Section 4.3.2 of the main report. Additional details are contained within Appendix E of the LSCR geomorphology study report (Stillwater Sciences 2007) and Appendix H of the USCR geomorphology study report (Stillwater Sciences 2011).

Historical aerial photography was utilized in a geographic information system (GIS) to delineate areas of flood disturbance for selected historical floods along the length of the Santa Clara River (SCR). Because aerial photographs for the lower SCR (LSCR) in Ventura County and upper SCR (USCR) in Los Angeles County were not taken during the same years, except for 2005, our analysis examined different aerial photographic sets for the LSCR and USCR watersheds. For the LSCR, seven photosets were utilized: 1938, 1945, 1969, 1978, 1992, 1995, and 2005. For the USCR, five photosets were utilized: 1928, 1964, 1980/81, 1994, and 2005. Many aspects of this analysis were modeled on similar work done by Graf (2000), Tiegs et al. (2005), and Tiegs and Pohl (2005).

PHOTO ACQUISITION

Imagery for the LSCR and USCR analyses was acquired from a number of sources, including government agencies, state universities, and private vendors (Tables C-1 and C-2). Aerial photography was acquired in one of two different formats, depending upon availability and age: non-georeferenced digital images or orthorectified imagery[1]. The non-georeferenced photography was typically scanned by the supplier at resolutions ranging from 600 dots per square inch (dpi) to 1200 dpi. For both analyses, photo sets were chosen to represent the effects of several major floods of interest (see Table C-1 and C-2 and Figures C-1 and C-2).

[1] Georeferencing refers to the process of "rubber-sheeting" or matching features in an image to a "real-world" coordinate system. Georeferencing typically only considers horizontal referencing, whereas an orthorectified image will be referenced using both horizontal and vertical components, resulting in a more accurate representation of earth's surface.

Table B-1. Aerial photography sets used in the mainstem LSCR channel processes analysis. [a, b]

Photography date(s)	Most recent significant flood date(s)	Estimated peak discharge (cfs) at Montalvo [a]	Original scale	Pixel resolution	Photo source[a]
9/1/05	2/21/05	82,200 [d]		1.0 feet	APUSA
2/1-4/05	1/10/05 1/9/05	136,000 [d] 129,000 [d]		0.5 feet	APUSA/VCWPD
1/31/95	1/10/95	110,000		1 meter	APUSA
11/1/92	2/12/95	104,000	1:24000	1 meter	PWAS
5/16/78	3/4/78	102,200	1:24000	1 meter	PWAS
3/2/69 2/26/69	2/25/69 1/25/69	152,000 165,000	1:12000	1 meter	VCWPD
11/2/45 10/25/45	1/23/43	80,000 [e]		1 meter	VCWPD
7/1/38 **5/25/38** **5/10/38**	3/2/38	120,000		1 meter	VCSO

[a] Montalvo stream gauge represented by USGS 11114000 (Santa Clara River at Montalvo; 1952-1996) and USGS 11109000 (Santa Clara River near Piru; 1997-present).
[b] SCR = Santa Clara River mainstem.
[c] APUSA = AirPhoto USA, VCWPD = Ventura County Watershed Protection District, PWAS = Pacific Western Aerial Surveys, IKC = IK Curtis, VCSO = Ventura County Surveyors Office
[d] Discharge estimated at the Freeman Diversion Dam
[e] Discharge from USACE 1968 (cited in Simons, Li & Associates 1983)

Table C-2. Aerial photography sets used in the mainstem USCR channel processes analyses. [a, b]

Photography year(s)	Most recent significant flood date(s)	Estimated peak discharge (cfs) at County Line gauge [a]	Coverage extent [b]	Resolution/ scale	Photo source [c]	Use in analysis
1928	N/A [d]	N/A	SCR – County line to Acton	1:18,000	UCSB	Digitize active channel areas and facies
1964	2/11/62	9,100	SCR – County line to Soledad Canyon	1:1,200 (from matching topographic maps)	LADPW	
1980/1981	2/9/78 2/16/80	22,800 13,900	SCR – County line to Soledad Canyon	1:6,000	LADPW	
1994	1/12/92 2/18/83	12,300 10,700	Entire watershed	0.3 m (1-ft) resolution	USGS	
2005	1/10/05	32,000	Entire watershed	0.3 m (1-ft) resolution	LADPW	
2009	1/2/06 1/25/08	12,500 3,130	Entire watershed	1 m (3.3 ft) resolution	NAIP	Used this high-resolution aerial photograph set to guide active channel areas in other aerial photograph years

[a] County line stream gauge represented by USGS 11108500 (Santa Clara River at L.A.-Ventura Co. Line; 1928-2004).
[b] SCR = Santa Clara River mainstem.
[c] UCSB = U.C. Santa Barbara M.I.L. Davidson Library, LADPW = L.A. County Department of Public Works, USGS = U.S. Geological Survey, NAIP = National Agriculture Imagery Program.
[d] No flow records in USCR watershed prior to 1930. The 1928 aerial photos are potentially useful to the analysis by providing the oldest condition of the active channel area. Prior to 1928, two recorded high rainfall events occurred: 1914 precipitation at Santa Paula rain gauge of 28 inches was same as precipitation during known flood year of 1938; and 1917 precipitation at Santa Paula rain gauge of 23 inches.

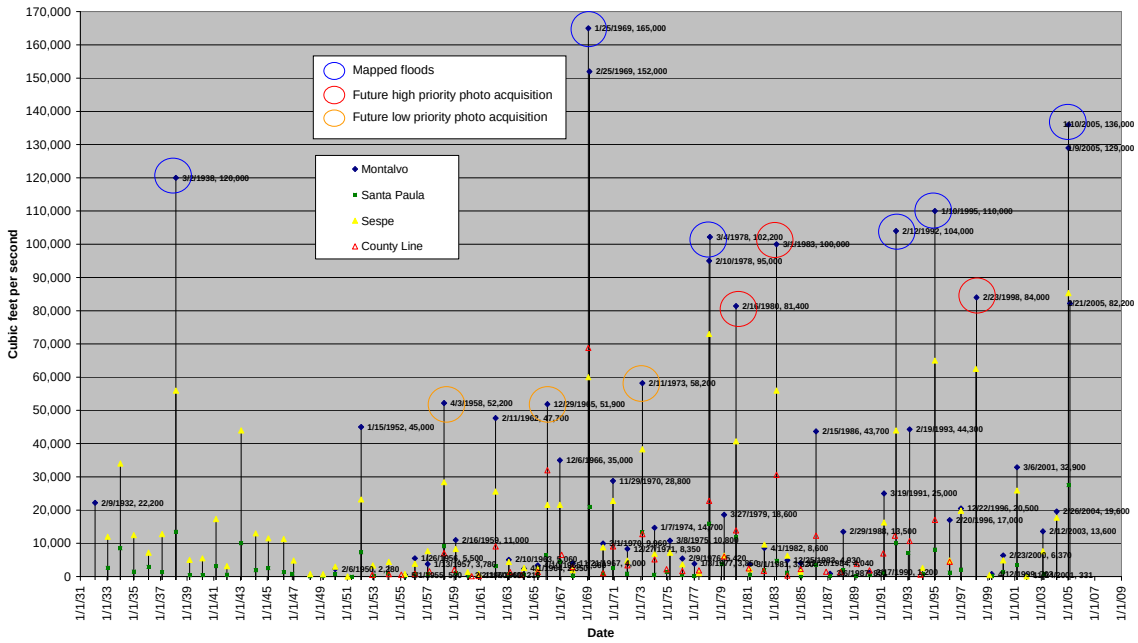

Figure C-1. Historical peak flows at stream gauges on LSCR shown in comparison to known air photo imagery acquisition dates.

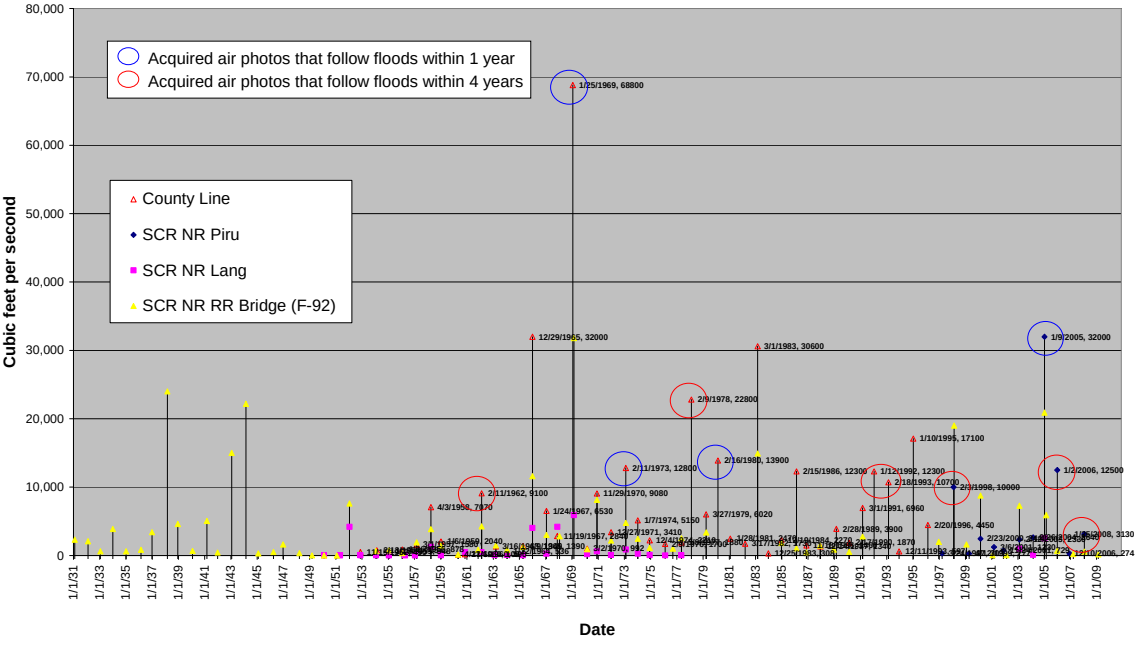

Figure C-2. Historical peak flows at stream gauges on USCR shown in comparison to known air photo imagery acquisition dates.

GEOREFERENCING

In order to extract and accurately compare river planform data from the acquired aerial photography, a common spatial context was necessary. The methodologies employed for the LSCR and USCR analyses were similar, with subtle differences due to inherent differences between data quality (e.g., photo resolution and density of reference points). Using a GIS, all imagery was georeferenced to a single spatial projection (UTM Zone 11N, NAD 83). Aerial photographs taken following significant flood events were obtained for several years (Tables C-1 and C-2). The ESRI ArcGIS georeferencing toolset was utilized to georeference the scanned hardcopy contact prints and digital imagery to either the high-resolution 2005 (LSCR) or 2009 (USCR) orthophotography, thus providing a highly accurate standard control point source for the entire photographic record. Control points were typically located using old buildings, bridges, intersections, and other features that appeared unchanged between photos sets. Georeferencing methods utilized at least 10 control points per photograph; thin plate splines were used to produce a smooth (continuous and differentiable) surface. Orthorectified imagery was acquired at pixel resolutions ranging from about 0.5 to 1 m.

Spatial error in certain portions of photo sets due to imagery registration errors were occasionally significant, as high as 35 m. These errors were typically associated with image distortion at the outer edges of older photos, due to sub-standard aerial photography techniques, standard lens distortion, or oblique camera angles. However, spatial errors between most photo sets generally ranged between 3 and 15 m, and sometimes as low as 1 m.

FLOOD SCOUR DIGITIZING

Each set of spatially referenced photography (each representing a particular flood) was used in a GIS to interpret two levels of flood-caused disturbance in the channel and floodplain areas. In addition, areas of low-disturbance or areas apparently retaining natural riparian vegetation coverage[2] after the flood were also mapped. For purposes of photo interpretation, these areas were defined as follows:

High disturbance: These areas are characterized by distinct channel and floodplain areas severely disturbed by flow (i.e. scoured to bare substrate), typically with 10% or less apparent remaining riparian vegetative cover. This category may include agricultural or developed lands with a high level of apparent disturbance by flood flows, thus identification of this type is not always based upon vegetative cover, sometimes relying on patterns of obvious scour. Additionally, certain channel-adjacent areas surrounded by scour were classified as high disturbance, despite having high coverage of herbaceous or nascent vegetation; this characterization was assigned when vegetation appeared to have grown post-flood and prior to the aerial photograph date.

Medium disturbance: This class is characterized by distinct areas of low to moderate apparent disturbance by flow, typically defined as areas with more than 10% but less than 80% apparent riparian vegetative cover. This type includes agricultural or developed lands with low to moderate

[2] In the context of the floodplain vegetation communities of the SCR, "riparian vegetation" may include types more typical of upland communities, such as coastal sage scrub, or non-native plant species which in some cases includes non-native species. Agricultural lands within the river's floodplain/terraces were also included as Low Disturbance, but were excluded from the active channel area.

apparent disturbance by flood flows, thus identification of this type is not always based upon vegetative cover, as with the high disturbance class.

Low disturbance (riparian vegetation): These areas were characterized by distinct zones of apparently natural riparian vegetation with little to no apparent disturbance by flood, typically containing more than 80% riparian vegetation. Areas in this class may have been inundated by floodwaters, but did not show significant signs of scouring or other disturbance that removed vegetation.

In addition to flood disturbance level, all polygons were classified as being either within or outside of the active channel. Polygons within the active channel were those that appeared to have been directly affected by the river during the prior flood event and/or subsequent flows (i.e., most areas of medium to high disturbance). Areas of riparian or non-riparian vegetation with no apparent disturbance were excluded, unless bounded by the active channel on three or more sides. Particular areas of medium to high disturbance were nonetheless excluded from the active channel when these areas appeared to have been affected by flows from tributaries at their confluence with the river, or by runoff from surrounding land, rather than the river itself.

To record these areas, polygons were delineated around features within each flood year photo set using heads-up digitizing at a scale of 1:4500 in the GIS; in certain upstream canyon areas, shadow or dense vegetation made it necessary to sometimes digitize at scales of 1:2500 or, in cases of extremely low visibility, 1:1500. For the 2005 dataset, orthophotographs and associated 2005 LiDAR data were used to delineate the active channel and classify areas of disturbance. While methods for digitizing generally followed those described by Tiegs and Pohl (2005), the data generated in this study were not converted to a raster format for analysis, but rather kept as polygons in an ESRI shapefile format (.shp), as originally digitized. All subsequent analyses were conducted using the polygon representation, which allowed for a finer scale of resolution in analysis output.

In addition to spatial error related to georeferencing, polygon delineation likely resulted in unknown spatial errors due to difficulties in interpreting features of interest. These types of error are most likely to occur with older images (e.g., LSCR: 1938 and 1945; USCR: 1928, 1964, 1980/81) used in this study. Older photographic film typically had a coarser grain than more modern films resulting in lower feature resolution once the image was scanned and georeferenced, making interpretation of floodplain features more difficult. The grayscale color spectrum of older imagery (e.g., LSCR: 1938, 1945, and 1969; USCR: 1928, 1964, 1980/81, and 1994) made interpretation of residual riparian vegetation more difficult in certain cases as well.

QUALITY CONTROL

Each flood year polygon data set was checked for spatial and interpretive accuracy by a GIS analyst that was not associated with the digitization process for that particular year. This process ensured that the data sets were consistent and accurate between and across years. Assessments of spatial error were conducted by a GIS analyst not directly involved in georeferencing or digitization processes.

ANALYSES

The planform data digitized from the aerial photography sets were used to conduct a number of spatial analyses to support understanding of fluvial dynamics in the LSCR and USCR. These analyses included calculation of historical flood disturbance probability, "last flood" spatial analyses, and average reach width calculations for each historical flood.

Locational Probability Model

The methods and nomenclature discussed below have been modeled on those of Graf (2000) and Tiegs et al. (2005). For this analysis, we define a locational probability model as a graphical representation of the historical probability that any particular area within the floodplain and channel of the river was scoured (i.e. the "high disturbance" and "medium disturbance" categories described above) by a major flood. As discussed above, aerial photographs chosen for use in this study were taken after major floods (see Tables C-1 and C-2) and thus represent the post-flood channel configuration for a particular flood.

Because the SCR is a flood event dominated system (see Chapter 4 of the main report) and each set of photography was taken shortly after a major flood event, it can be assumed that each photo set represents the dominant planform configuration of the channel until the next large flood documented by aerial photography. This approach differs from that of Graf (2000), Tiegs et al. (2005), and Tiegs and Pohl (2005), who assume that each photo set is representative of general channel conditions for a period of time from one photo set to the previous photo set. Thus, their approach does not appear to explicitly consider whether the photo is representative of the effects of particular floods, but rather describes general channel conditions over time.

There are numerous caveats to our assumption discussed above, the most important being that smaller floods occur between the photograph sets and likely result in reworking of the channel; however, it remains that major changes to the channel and floodplain of the SCR are accomplished by large floods. Another significant caveat for the USCR analysis is the lack of aerial photographic coverage for two major floods in 1938 and 1969; although partial aerial photography exists to document these floods, funding limited the number of aerial photograph sets that could be processed.

To derive a disturbance probability model, the LSCR and USCR study areas were divided into 11 and 19 reaches, respectively, which were distinguished primarily by differences dominant morphologic character (see Chapter 4 of the main report for further discussion). A separate disturbance probability model was calculated for each of reaches. In order to build the disturbance probability model, the photo sets needed to be weighted based on the amount of time each represented in the overall study period[3] (i.e., LSCR: 1938-2007; USCR: 1928-2010), on a reach basis. The weighting values were calculated for each flood year and reach using the following equation:

[3] Photography was acquired for selected floods between 1938 and 2005 for the LSCR analysis and between 1928 and 2005 for the USCR analysis, thus these periods represent the photographic records for each analysis. For the purposes of calculating probability of disturbance, the "study periods" were 1938–2007 for the LSCR and 1928–2010 for the USCR, since no major floods had occurred between 2005 and the year each study was completed.

$$\text{Weighting value } (W_n) = \frac{\text{years represented by given photograph } (t_n)}{\text{total number of years in photographic record (m)}}$$

The value of t_n is the number of years between the documented flood of interest and the next photo documented flood. The value of m is the total number of years documented by aerial photography for a particular reach, from earliest photography set to most recent. Working through the equation for each flood year and reach gave the results displayed in Tables C-3 through C-6 below.

Table C-3. Years represented by individual flood photography and total number of years in the photographic record, by reach of the LSCR.

Reach	Number of years represented by given flood photography (t_n)							Number of years in photographic record (m)
	1938	1945	1969	1978	1992	1995	2005	
1	7	24	9	14	3	10	2	69
2	-	24	9	14	3	10	2	62
3	31	-	9	14	3	10	2	69
4	31	-	9	14	3	10	2	69
5	7	24	9	14	3	10	2	69
6	7	24	9	14	3	10	2	69
7	-	-	9	14	3	10	2	38
8	-	-	9	14	3	10	2	38
9	31	-	9	14	3	10	2	69
10	31	-	9	14	3	10	2	69

Table C-4. Weighting values for individual floods photography and reaches of the LSCR.

Reach	Weighting value (W_n)						
	1938	1945	1969	1978	1992	1995	2005
1	0.10	0.35	0.13	0.20	0.04	0.14	0.03
2	-	0.39	0.15	0.23	0.05	0.16	0.03
3	0.45	-	0.13	0.20	0.04	0.14	0.03
4	0.45	-	0.13	0.20	0.04	0.14	0.03
5	0.10	0.35	0.13	0.20	0.04	0.14	0.03
6	0.10	0.35	0.13	0.20	0.04	0.14	0.03
7	-	-	0.24	0.37	0.08	0.26	0.05
8	-	-	0.24	0.37	0.08	0.26	0.05
9	0.45	-	0.13	0.20	0.04	0.14	0.03
10	0.45	-	0.13	0.20	0.04	0.14	0.03

Table C-5. Years represented by individual flood photography and total number of years in the photographic record, by reach of the USCR.

Reach	Number of years represented by given flood photography (t_n)					Number of years in photographic record (m)
	1928	1964	1980/81	1994	2005	
11-B	36	16/17	14/13	11	4	81
12	36	16/17	14/13	11	4	81
13	36	16/17	14/13	11	4	81
14	36	16/17	14/13	11	4	81
15	36	16/17	14/13	11	4	81
16	36	16/17	14/13	11	4	81
17	36	16/17	14/13	11	4	81
18	36	16/17	14/13	11	4	81
19	36	16/17	14/13	11	4	81
20	36	16/17	14/13	11	4	81
21	36	16/17	14/13	11	4	81
22	36	16/17	14/13	11	4	81
23	36	16/17	14/13	11	4	81
24	36	16/17	14/13	11	4	81
25	36	16/17	14/13	11	4	81
26	36	16/17	14/13	11	4	81
27	36	16/17	14/13	11	4	81
28	36	16/17	14/13	11	4	81
29	36	16/17	14/13	11	4	81

Table C-6. Weighting values for individual floods photography and reaches of the USCR.

Reach	Weighting value (W_n)				
	1928	1964	1980/81	1994	2005
11-B	0.44	0.20/0.21	0.17/0.16	0.14	0.05
12	0.44	0.20/0.21	0.17/0.16	0.14	0.05
13	0.44	0.20/0.21	0.17/0.16	0.14	0.05
14	0.44	0.20/0.21	0.17/0.16	0.14	0.05
15	0.44	0.20/0.21	0.17/0.16	0.14	0.05
16	0.44	0.20/0.21	0.17/0.16	0.14	0.05
17	0.44	0.20/0.21	0.17/0.16	0.14	0.05
18	0.44	0.20/0.21	0.17/0.16	0.14	0.05
19	0.44	0.20/0.21	0.17/0.16	0.14	0.05
20	0.44	0.20/0.21	0.17/0.16	0.14	0.05
21	0.44	0.20/0.21	0.17/0.16	0.14	0.05
22	0.44	0.20/0.21	0.17/0.16	0.14	0.05
23	0.44	0.20/0.21	0.17/0.16	0.14	0.05
24	0.44	0.20/0.21	0.17/0.16	0.14	0.05

Reach	Weighting value (W_n)				
	1928	**1964**	**1980/81**	**1994**	**2005**
25	0.44	0.20/0.21	0.17/0.16	0.14	0.05
26	0.44	0.20/0.21	0.17/0.16	0.14	0.05
27	0.44	0.20/0.21	0.17/0.16	0.14	0.05
28	0.44	0.20/0.21	0.17/0.16	0.14	0.05
29	0.44	0.20/0.21	0.17/0.16	0.14	0.05

Weighting values were assigned to flood year and reach polygon layers in the GIS. All of the flood year layers for each analysis were then combined in the GIS (using the "union" function), resulting in numerous smaller polygons, all of which retained their original assigned probability for each year and reach. For each individual polygon, all the years weighting values were summed, resulting in a probability of scour for each (Tables C-7 and C-8). The probability field was then used to illustrate locational probability in a map (see Figures 4-23 a–i in the main report) for each reach.

Table C-7. Example of GIS data table with summed weighting values or probability of scour ("SumProb") for each polygon.

Polygon	1938	1969	1978	1992	1995	2005	SumProb	Shape_Area
1	0.45	0	0	0	0	0	0.45	1459947.254
2	0	0.13	0	0	0	0	0.13	1710181.258
3	0	0.13	0	0	0	0	0.13	825.8837909
4	0	0.13	0	0	0	0	0.13	321.74415
5	0.45	0.13	0	0	0	0	0.58	1037.485881
6	0	0.13	0	0	0	0	0.13	1777.786451
7	0	0.13	0.2	0	0	0	0.53	181.1416506
8	0	0.13	0.2	0	0	0	0.53	113.8613641
9	0	0.13	0.2	0	0	0	0.53	5636.241047
10	0	0	0	0.04	0	0	0.04	46170.7421
11	0	0	0	0.04	0	0	0.04	435.8034547
12	0	0	0	0.04	0	0	0.04	2020.878413
13	0	0	0	0	0.14	0	0.14	327800.4409
14	0	0	0	0	0.14	0	0.14	40539.56361
15	0	0	0	0	0	0.03	0.03	222838.8706
16	0	0	0	0	0	0.03	0.03	66320.23549

Table C-8. Example of GIS data table with summed weighting values or probability of scour ("SumProb") for each polygon of the USCR analysis.

Polygon	1938	1969	1978	1992	1995	2005	Sum prob	Shape area
1	0.45	0	0	0	0	0	0.45	1459947.254
2	0	0.13	0	0	0	0	0.13	1710181.258
3	0	0.13	0	0	0	0	0.13	825.8837909
4	0	0.13	0	0	0	0	0.13	321.74415
5	0.45	0.13	0	0	0	0	0.58	1037.485881
6	0	0.13	0	0	0	0	0.13	1777.786451
7	0	0.13	0.2	0	0	0	0.53	181.1416506
8	0	0.13	0.2	0	0	0	0.53	113.8613641
9	0	0.13	0.2	0	0	0	0.53	5636.241047
10	0	0	0	0.04	0	0	0.04	46170.7421
11	0	0	0	0.04	0	0	0.04	435.8034547
12	0	0	0	0.04	0	0	0.04	2020.878413
13	0	0	0	0	0.14	0	0.14	327800.4409
14	0	0	0	0	0.14	0	0.14	40539.56361
15	0	0	0	0	0	0.03	0.03	222838.8706
16	0	0	0	0	0	0.03	0.03	66320.23549

Width of Active Channel Bed in Successive Floods

Knowledge of the last known flood disturbance for any particular area of the floodplain is critical to understanding the age of geomorphic surfaces and thus the approximate age of riparian vegetation growing there. For each analysis, the flood scour layers were manipulated in the GIS to derive a map of "last flood" scour areas for the entire study reach. All flood year layers were combined in a GIS using the "union" command, resulting in numerous smaller polygons each retaining information on the years in which the particular polygon was inundated. Using a "max number" algorithm, the most recent year was chosen from the GIS data and copied to a new field; the value in the new field (the "last flood" field) now contained the date of the most recent scour event for any particular polygon. The value of the "last flood" field was then used to produce a map of last flood scour for the entire study reach (see Figures 4-16 and 4-17 in the main report).

Reach Width Analysis

In order to help inform an understanding of the behavior of the USCR, a geomorphological analysis was undertaken using the "active channel width" (i.e. the scoured area or "high disturbance" and "medium disturbance" classifications) of each documented flood (see Chapter 4). In order to facilitate the analysis, reach average widths were calculated for each documented flood based upon the area of scour documented for each flood (as calculated in the GIS). A channel centerline was established as the basis for reach length, then width was derived from the simple relationship between length, width and area: Width = Area/Length.

Reach-based areas for each documented flood were exported from the GIS and imported to Microsoft Excel, where the calculations were completed using the Pivot Tables function.

REFERENCES

Graf, W. L. 2000. Locational probability for a dammed, urbanizing stream: Salt River, Arizona, USA. Environmental Management 25: 321–335.

Simons, Li & Associates. 1983. Hydraulic, erosion and sedimentation study of the Santa Clara River Ventura County, California. Prepared for Ventura County Flood Control District, Ventura, California.

Stillwater Sciences. 2007. Santa Clara River Parkway floodplain restoration feasibility study: assessment of geomorphic processes for the Santa Clara River watershed, Ventura and Los Angeles counties, California. Prepared by Stillwater Sciences, Berkeley, California for the California State Coastal Conservancy, Oakland, California.

Stillwater Sciences. 2011. Assessment of geomorphic processes for the upper Santa Clara River watershed, Los Angeles County, California. Final report. Prepared by Stillwater Sciences, Berkeley, California for Ventura County Watershed Protection District, Los Angeles County Department of Public Works, and the U.S. Army Corps of Engineers-L.A. District.

Tiegs, S. D., and M. Pohl. 2005. Planform channel dynamics of the lower Colorado River: 1976-2000. Geomorphology 69: 14–27.

Tiegs, S. D., J. F. O'Leary, M. M. Pohl, and C. L. Munill. 2005. Flood disturbance and riparian diversity on the Colorado River Delta. Biodiversity and Conservation 14: 1175–1194.